# SPATIALLY AND TEMPORALLY CONTROLLED MECHANICAL SIGNALS TO DIRECT HUMAN MESENCYHMAL STEM CELL BEHAVIOR

Ross A. Marklein

A DISSERTATION

in

Bioengineering

Presented to the Faculties of the University of Pennsylvania

in

Partial Fulfillment of the Requirements for the

Degree of Doctor of Philosophy

2012

_____

**Supervisor of Dissertation**
Dr. Jason A. Burdick
Associate Professor of Bioengineering

_____

**Graduate Group Chairperson**
Dr. Beth Winkelstein
Professor of Bioengineering

**Dissertation Committee**
Dr. Daniel A. Hammer (chair), Professor of Bioengineering
Dr. Kurt D. Hankenson, Associate Professor of Cell Biology
Dr. Paul A. Janmey, Professor of Physiology

## ACKNOWLEDGMENTS

It is difficult to fully credit everyone that has impacted my life and the completion of this dissertation. From California, to Georgia (round one), to Michigan, to Vermont, to Georgia (round two), and finally to Philly I have been surrounded by incredible people in both my personal and professional life. These people have provided exceptional guidance, support, and criticism that I will never forget and will always cherish.

First and foremost I would like to thank my advisor Jason Burdick for providing me an opportunity to advance myself as a scientist and an independent thinker. It's incredible to see how consistently and reliably he churns out great scientific researchers, and I fully expect to see this trend continue for many years to come! Furthermore, I'd like to thank Drs. Daniel Hammer, Kurt Hankenson, and Paul Janmey for serving as my dissertation committee and offering excellent guidance and assistance during the proposal and defense processes.

It is going to be difficult finding coworkers that can proverbially "hold a candle" to the JABLAB folks. Not only does Jason provide assistance in the form of his advisement, but he also surrounds everyone in lab with great scientific thinkers that are friendly, encouraging, and supportive. Thanks to the warm welcome from the JABLAB "First Class" (Jamie Ifkovits, Darren Brey, Josh Katz, and Cindy Chung), transitioning to a new lab was effortless and I learned so much in my first couple years. Murat Guvendiren's scientific passion and enthusiasm, as well as his willingness to simply drop what he's doing and help anyone, is rivaled by no one and I will sorely miss all our

discussions and times spent together trying to understand stem cells! Sudhir Khetan, it was truly an honor working with you for five years.

While I have moved around quite a bit and been exposed to many different people and surroundings, the love and support of my family has been constant. My parents have always been there to provide encouragement and perspective and I dedicate this work to them. To my brother Eric and sister Katy, I am so thankful to have you both in my life and appreciate all the thoughtfulness, friendship, rivalries, annoyances, and love we have provided each other over the years.

And finally to my best friend/partner/fiancé/coworker/consultant/motivator/love-of-my-life, Iris. Trying to put into words the positive effect you've had on my life would double the size of this dissertation. So I'll simply say that with you I am the best person I can possibly be and I love you so much for everything we've done together and will accomplish in the future!

# ABSTRACT

## SPATIALLY AND TEMPORALLY CONTROLLED MECHANICAL SIGNALS TO DIRECT HUMAN MESENCYHMAL STEM CELL BEHAVIOR

Ross A. Marklein

Jason A. Burdick, PhD.

In order to effectively incorporate stem cells into tissue engineering solutions, a deeper understanding of the microenvironment factors that influence their behaviors is necessary. Specifically, the inherent mechanics of the extracellular matrix (ECM) have been shown to profoundly effect multiple stem cell behaviors such as their morphology, proliferation, differentiation, and secretion of factors. The effect of matrix mechanics on stem cells has been investigated using a wide range of material systems; however, many of these systems lack the mechanical complexity that native tissues possess in terms of their spatial and temporal properties, as well as context (2D vs. 3D). In order to determine the effect of heterogeneous and dynamic mechanical signals on stem cells, a sequential crosslinking technique was developed that allowed for formation of hydrogels with a wide range in mechanical properties in terms of magnitude, context, and spatiotemporal presentation. Hydrogels with tunable mechanics were synthesized using methacrylate hyaluronic acid (MeHA) in a sequential process: 1) Michael-type 'addition' crosslinking using dithiothreitol to consume a fraction of the methacrylate groups, and 2)

UV-initiated ‘radical’ crosslinking using controlled UV light exposure in the presence of a photoinitiator to consume unreacted methacrylates.

Using this approach, we demonstrated local control of stem cell morphology, proliferation, and differentiation (adipogenesis and osteogenesis) in both patterned and gradient systems on 2D hydrogels. We further investigated the effects of mechanics in a 3D context using non-porous and porous presentations of controlled mechanics. In the non-porous system, cell behavior was shown to be dependent on mechanics as threshold responses were observed related to the ability of hMSCs to adopt a spread or rounded morphology within the hydrogel. In the 3D macroporous system, mechanics were spatially and temporally modulated and hMSC morphology, proliferation, differentiation, and secretion of angiogenic and cytokine factors were shown to be dependent on the local and temporal presentation of mechanical signals.

This dissertation work emphasizes the importance of the magnitude, context, and presentation of mechanical signals and highlights this sequential crosslinking process as a model system for future investigations into heterogeneous, dynamic microenvironments, as well as a novel platform for developing future tissue engineering strategies.

# TABLE OF CONTENTS

**CHAPTER 3-**

# LIST OF FIGURES

# CHAPTER 1

*Stem Cells Sense and Respond to Matrix Mechanics*

## 1.1 Introduction

Stem cells have become an attractive option for tissue engineering applications due to their proliferative capacity, differentiation potential, and their ability to promote tissue repair through trophic mechanisms.[1-3] However, a significantly greater understanding of stem cell responses to their microenvironment (both *in vitro and in vivo*) is needed before the lofty expectations of tissue engineering are satisfied and stem cells are incorporated into clinically effective therapies. Human mesenchymal stem cells (hMSCs) have particularly received significant attention from this field due to their ease of isolation (even from the patient), as well as their ability to differentiate into numerous cell types[4] and facilitate tissue regeneration.[5] However, there is still a fundamental need to further understand what factors influence stem cell behaviour and how cells effectively interpret their environments and respond accordingly.

Ever since the realization that cells do indeed exert forces and are able to sense the mechanics of their substrate,[6] matrix mechanics have not only been investigated in fundamental cell biology studies, but also as a design variable for tissue engineered scaffolds. Within this field, it has become apparent that mechanics direct a number of cell responses including, but not limited to, cell morphology, proliferation, migration, differentiation, and the secretion of factors.[7-11] Therefore, in order to effectively incorporate stem cells into tissue engineering strategies, it is necessary to understand how stem cells respond to matrix mechanics in the context of the application, as distinct

mechanical properties are evident in different tissues.[12] With this, techniques to then manipulate mechanics within engineered systems will help drive the use of mechanics as a design variable for tissue engineering therapies.

## 1.2 Stem Cell Mechanotransduction

### *1.2.1 Role of acto-myosin complex*

While the specific mechanism by which stem cells transduce a mechanical signal into a response is still being elucidated, major components of this system have been discovered and characterized. Sensing the substrate requires the ability of a cell pull and probe the surroundings and this is achieved through a complex cytoskeleton network. This is best exemplified by stem cells grown on soft and stiff substrates as the cells on stiffer substrates are able to exert greater tension and develop a more organized actin cytoskeleton (evidenced by stress fibers, see **Figure 1.1A**) as opposed to cells on softer substrates, which exert less tension and possess a more diffuse, less organized actin cytoskeleton.[12, 13] Quantification of this force generation is also possible using traction force microscopy, where fluorescent beads are incorporated within substrates in order to measure bead displacement and generate force maps, as shown in **Figure 1.1B**.[14] Along with the actin cytoskeleton, several other components of this mechanosensing machinery have been identified using inhibition assays. For example, non-muscle myosin II (NMMII) has been shown to have a profound effect on hMSC differentiation in response to mechanics as inhibition of this protein (using blebbistain) completely abrogates the differentiation response observed on polyacrylamide substrates over a physiologic range of mechanics.[7] It was also shown that NMMII expression levels varied across the range

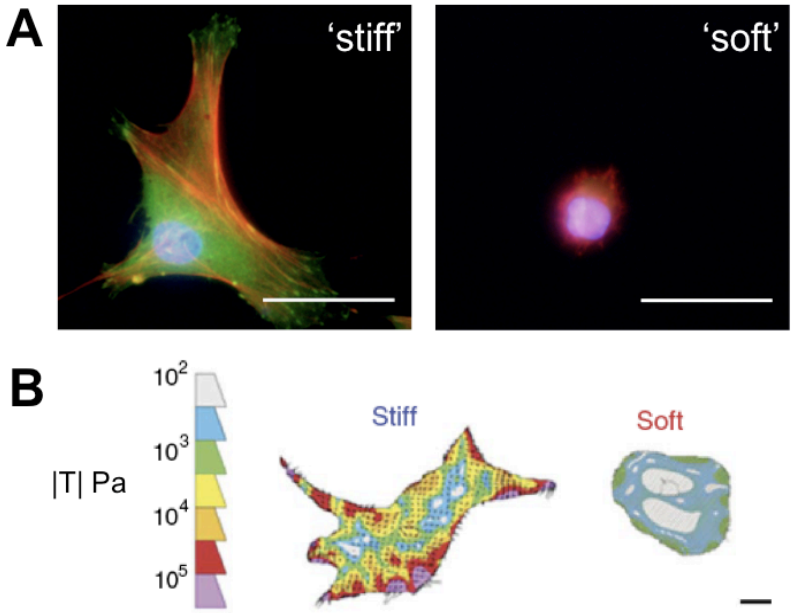


**Figure 1.1** (A) hMSCs on 'stiff' (~100 kPa) and 'soft' (~3 kPa) substrates with staining for actin (red), nuclei (blue), and vinculin (green). Marklein et al. *unpublished*. (B) Representative traction maps of hMSCs cultured on stiff (30 kPa) and soft (3 kPa) hydrogels. Color scale indicates spatial traction force |T|, scale bar = 25 μm. Adapted from Guvendiren et al.[14]

of mechanics as cells on stiffer substrates expressed higher levels of NMMII, which agreed well with the observation of a more organized acto-myosin cytoskeleton.

### *1.2.2 Role of Cell Adhesive Complex*

In order to exert tension and sense the matrix mechanics, the cytoskeleton must be coupled to proteins that interact with adhesive ligands such as fibronectin or vitronectin.[15] Cell adhesion complexes consist of a multitude of proteins known collectively as focal adhesions, which are involved in regulation of cell behavior in response to mechanics.[16] Vinculin is one well-studied member of this complex that exhibits differential expression

based on the stiffness of the material. Expression of vinculin has been shown to increase in quantity and exhibit greater association with the cytoskeleton on stiffer substrates.[17]

At the interface of the focal adhesion and matrix-binding site are integrins, which are a family of heterodimeric proteins involved in many cell functions such as cell motility, proliferation, and differentiation.[18, 19] The binding of integrins (such as $\alpha_5\beta_1$) is tension-dependent, as increased tension results in conformational changes in the protein and exposure of cryptic binding sites that allow for recognition of synergy sequences on fibronectin.[18] Integrin binding can then result in phosphorylation of other focal adhesion proteins such as focal adhesion kinase (FAK) and Rho kinase (ROCK).[13, 20] These two mechanosensory proteins serve as downstream regulators of stem cell functions, such as differentiation, and inhibition can result in impaired osteogenic differentiation of MSCs as the signal transduction cascade originating from integrin $\alpha_2\beta_1$ binding can not effectively reach the nucleus and initiate the differentiation program.[21]

## 1.3 Stem Cell Responses to Matrix Mechanics

### *1.3.1 Effect of mechanics on stem cell morphology and proliferation*

As cytoskeletal tension is regulated by matrix mechanics, it follows that the ability of a cell to spread and adopt a given morphology is highly dependent on this matrix property. Cell morphology has been identified as not only a consequence, but also a cause,[22] of cell fate specification and mechanics have been shown to have a significant impact on the adoption of a given cell shape. hMSCs seeded on matrices of variable stiffness exhibit the general trend of increased cell spread area with increasing mechanics.[7, 9] As mentioned above, cells on stiffer substrates exert greater force and they

are able to spread to a greater degree as increased contraction correlates well with subsequent increases in cell area.[14] Not only do cells follow an observed trend of increased spreading on stiffer substrates, they also adopt distinct morphologies reminiscent of the cells associated with the tissue from which the mechanics are being mimicked. For example, hMSCs cultured on soft 1 kPa hydrogels mimicking neural tissue developed extensive neurite networks similar to those of primary neurons. In the same study, hMSCs cultured on hydrogels of elasticity similar to muscle (~11 kPa) became highly elongated like fully differentiated myoblasts and cardiomyocytes, which also exhibit morphologies dependent on matrix mechanics.[7, 23, 24]

Cell proliferation is another cell response that is highly dependent on the ability of dividing cells to exert tension and effectively "pull" on their substrate. As cells exert greater tension on stiffer matrices, phosphorylated FAK levels increase, which further activates the Extracellular signal-regulated protein kinase (ERK) cascade and allows for progression through the cell cycle.[13] Much like the cell morphological response to mechanics (**Figure 1.2A**), cell proliferation exhibits the trend of higher rates of proliferation on stiffer substrates while lower rates of proliferation are observed on softer substrates (**Figure 1.2B**). This has been exemplified by hMSCs cultured on substrates covering a physiologic range of mechanics (1-100 kPa) with a threshold mechanics (>3 kPa) necessary for not only increased cell spreading, but also proliferation.[9, 11, 25] In these systems, cells were either unspread and non-proliferating or spread and proliferating. This further agrees with morphology-dependent responses observed for cells grown on micropatterned substrates with varying cell adhesive areas. As cell adhesive area was increased, cells spread to fill the area and increased DNA synthesis while cells cultured

on smaller islands had lower levels of DNA synthesis and subsequent increases in markers for apoptosis.[26]

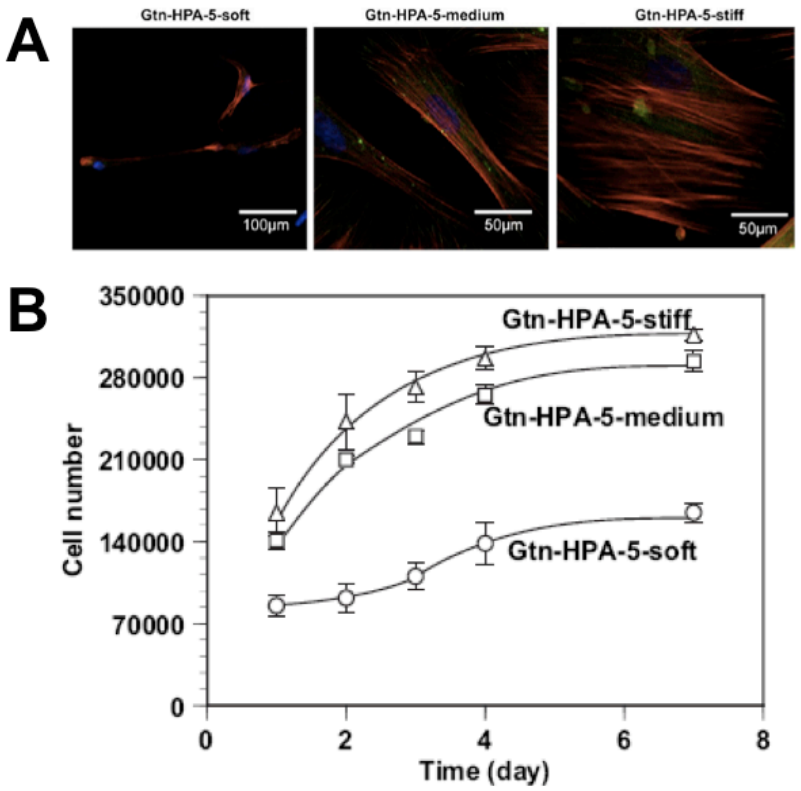


**Figure 1.2** (A) hMSCs cultured on gelatin-hydroxyphenylpropionic acid (Gtn-HPA) hydrogels of varied mechanics (soft-0.6 kPa, medium-2.5 kPa, stiff-8.2 kPa) nuclei (blue), actin (red). (B) hMSC proliferation on Gtn-HPA hydrogels with time. Adapted from Wang et al. [11]

*1.3.2 Effects of mechanics on stem cell differentiation and secretion*

The distinct mechanical properties of a given tissue have implications not only at the macroscale (i.e., bones providing support and muscles' ability to contract), but also at the microscale as the local mechanics can guide differentiation to cells of that tissue.[24, 27] In a seminal study performed by Engler et al., stem cell differentiation was found to be

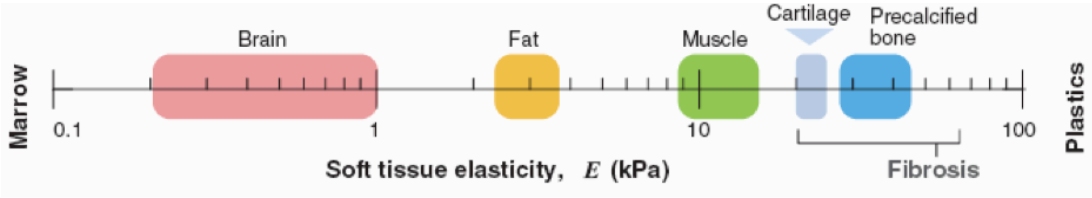


**Figure 1.3** Scale illustrating range of mechanics present in native tissues, adapted from Discher et al.[12]

dependent on the mechanics of the substrate.[7] Specifically, cells cultured on soft matrices (1 kPa) expressed neurogenic markers, cells on intermediate stiffness matrices (11 kPa) expressed myogenic markers, and cells on stiff matrices (34 kPa) expressed osteogenic markers. These 1 kPa, 11 kPa, and 34 kPa hydrogels closely mimicked the moduli present in native brain, muscle, and pre-calcified bone, respectively (**Figure 1.3**).[12] More committed pre-osteoblast cells also exhibited mechanodependence as increased osteocalcin and alkaline phosphatase expression (indicative of osteogenesis) was observed on stiffer substrates as compared to softer substrates (**Figure 1.4**).[28]

Although much of the focus on stem cell application for tissue regeneration has focused on the ability of these cells to differentiate into desired cell types and replace damaged tissue, an increasing amount of work is being performed to understand how stem cells can facilitate tissue repair through the secretion of trophic factors.[29-32] This new paradigm of tissue engineering focuses on stem cells as stimulators and facilitators of endogenous tissue repair compared to the replacement tissue engineering strategy initially proposed by the field.[33] Stem cell tropism is influenced by matrix mechanics, as the secretion of various angiogenic and inflammatory factors are differentially regulated on distinct mechanical environments. In one study,[10] hMSCs exhibited distinct

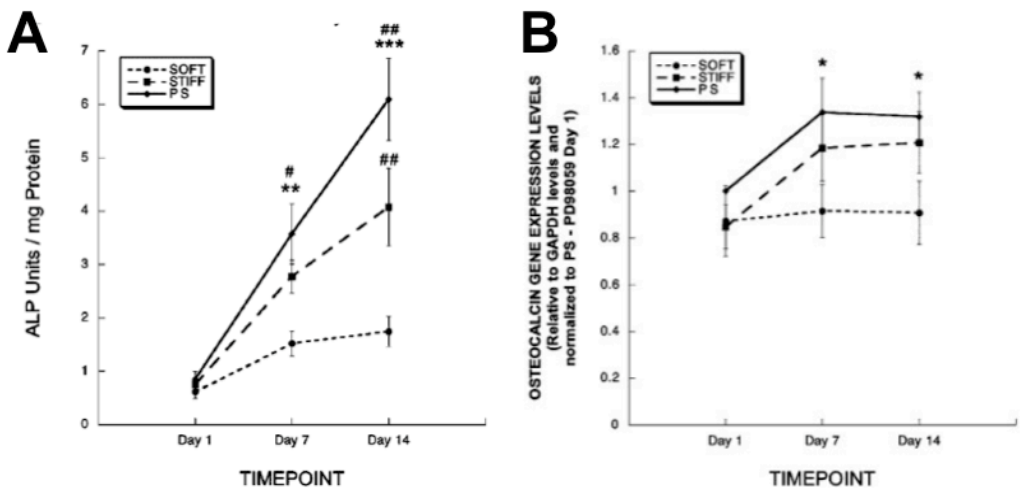


**Figure 1.4** MC3T3-E1 cells cultured on soft (13.7 kPa) and stiff (424 kPa) PEGDA hydrogels and tissue culture polystyrene (PS). (A) Alkaline Phosphatase (ALP) activity revealed significant differences between the 3 groups at day 7 (**p<0.01) and day 14 (***p<0.001). (B) Osteocalcin expression on stiff and PS substrates showed significantly higher expression at both day 7 and 14 (*p<0.05). Adapted from Khatiwala et al. [28]

expression profiles for an array of angiogenic and cytokine factors on soft (2 kPa) and stiff (20 kPa) hydrogels at early and late timepoints (**Figure 1.5A**). Secretion of VEGF, IL-8, and urokinase plasminogen activator (uPA) were also quantified and shown to be dependent on matrix mechanics not only in terms of the magnitude of secretion, but also in terms of temporal expression (**Figure 1.5B**). In another study using adipose-derived stem cells, mechanics were shown to simultaneously influence both stem cell differentiation (in this case adipogenesis) and secretion of the potent angiogenic stimulator VEGF.[34] As expected, cells readily differentiated into adipocytes in more compliant hydrogels (3.3 kPa) while VEGF secretion and stimulation of HUVEC network formation was favored by cells grown in stiffer hydrogels (12.4 kPa).

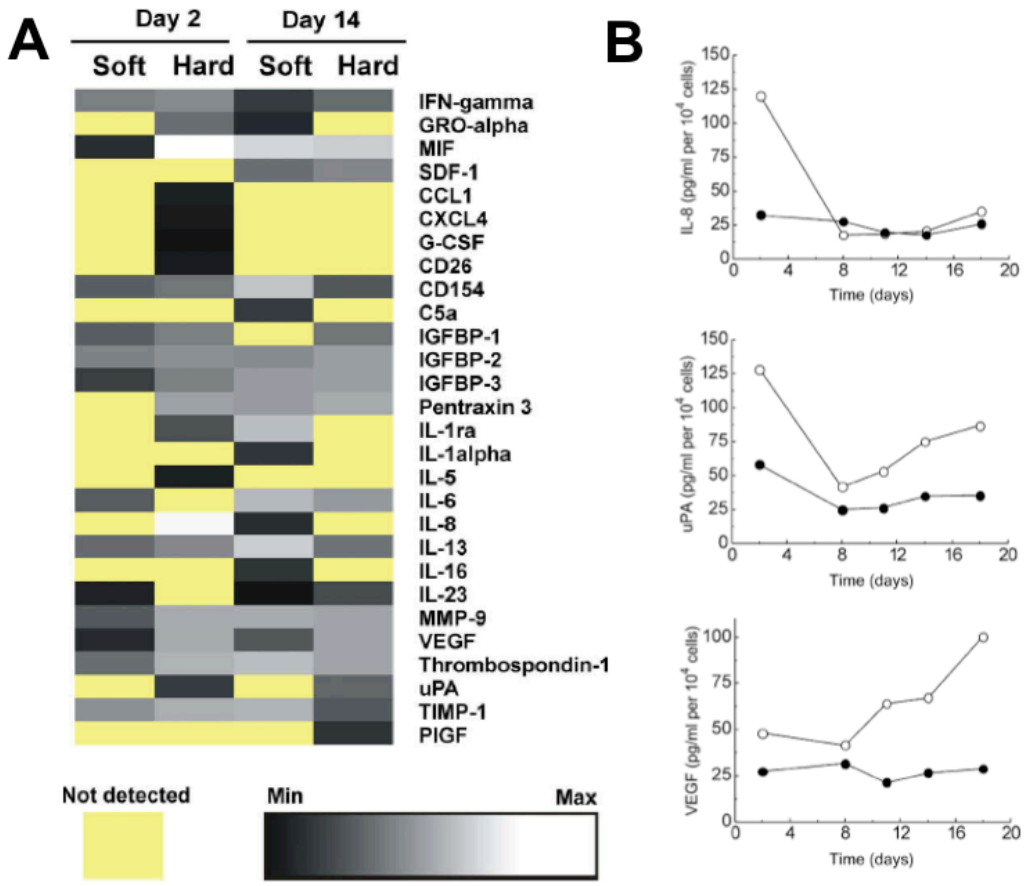


**Figure 1.5** Secretory response of hMSCs on soft (2 kPa) and stiff (20 kPa) hydrogels. (A) Secretory profiles of cells on soft and hard hydrogels characterized using proteome profile arrays at day 2 and 14. Protein levels normalized to cell number at each time point. (B) Temporal expression of IL-8, uPA, and VEGF over duration of culture on soft (closed circles) and hard (closed circles) hydrogels using ELISA. Adapted from Seib et al.[10]

### *1.3.3 Stem cell responses to mechanics in vivo*

Although difficult to experimentally validate, the effect of *in vivo* mechanics on stem cell behavior has been implicated as one of the reasons for the observed undesirable outcomes of certain stem cell therapies. Due to their ability to stimulate angiogenesis,[35]

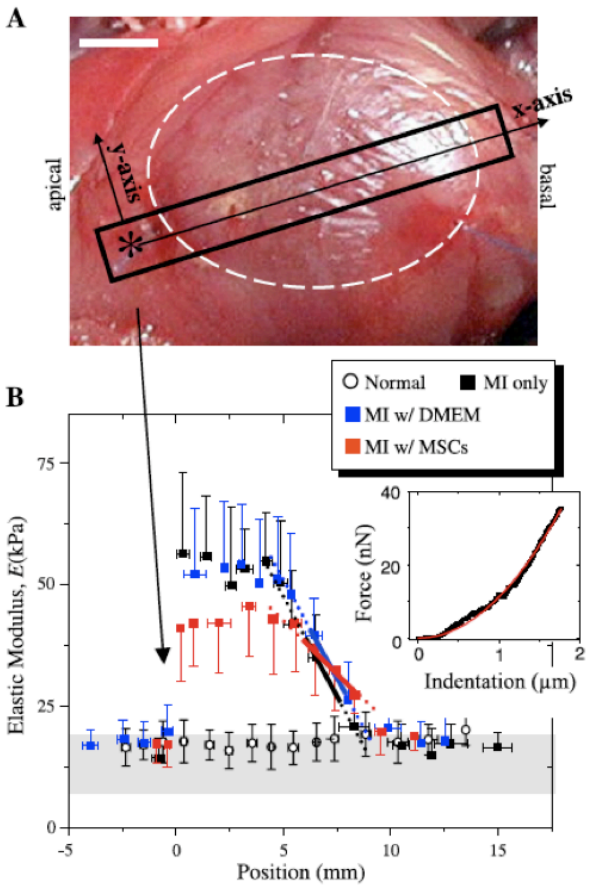


**Figure 1.6** Mechanical characterization of rat heart mechanics pre- and post-myocardial infarction. A) Dotted white line denotes area of infarction with axis drawn to indicate location along which elastic moduli were calculated (using AFM). Scale bar = 2 mm. B) Local elastic moduli plotted along axis for non-infarcted (Normal), infarct control (MI only), as well as two treatment methods post-infarct (MI w/ DMEM and w/ MSCs). Adapted from Berry et al.[43]

reduce inflammation,[36] promote survival of cardiomyocytes,[37] and differentiate into cardiomyocytes,[38, 39] MSCs have been investigated as a potential cell therapy source for regenerative strategies post-myocardial infarction. However, in several studies utilizing this multipotential cell source to aid in cardiac repair, maladaptive responses were observed typically associated with calcification.[40, 41] Considering the effects of stiffer microenvironments on MSC osteogenesis, this is not unexpected as cardiac tissue post-

infarct is typified by an increase in mechanics (both spatially and temporally)[42] and quantitatively evaluated by Berry et al. (**Figure 1.6)**.[43] In order to effectively overcome these aberrant responses and achieve more desirable functional repair of cardiac tissue, the timing and exposure of stem cells to the appropriate microenvironmental cues (i.e. mechanics) must be realized and incorporated into tissue engineering strategies.

Stem cells have also been explored as a means to modulate and inhibit tumor progression *in vivo* due to their innate ability to home to sites of tumorigenesis.[44] However, due to the secretion of various pro-angiogenic and pro-survival factors, MSCs can potentially promote tumorigenesis and metastasis.[1, 45] This response has been attributed to tumor cell-MSC crosstalk[46] and, more importantly, the mechanosensitive response of stem cells to the pathologically stiffer matrix associated with tumor formation.[47, 48] As shown *in vitro*, stem cells migrate from softer to stiffer substrates in a process called durotaxis, which has been observed in many systems employing gradients of mechanics.[49-51] Once at the site of the tumor, observed increases in angiogenesis[52] can occur as the stiffer environments have been previously described to promote the secretion of angiogenic factors (such as VEGF[10, 34]) *in vitro*. Although stem cells have been shown to preferentially localize at tumor sites, this response could also be exploited in order to deliver anti-cancer therapies by genetically modifying the targeting cells.[53]

## 1.4 Systems for Studying Stem Cell Responses to Mechanics

### *1.4.1 Hydrogels with Tunable Mechanical Properties*

In order to better understand stem cell responses to mechanics, advanced material systems are necessary that afford the ability to recapitulate aspects of the native tissue

environment. Typically, these systems consist of a single component hydrogel with a range of mechanics achieved by varying the crosslinking density either through the number of reactive sites or crosslinking molecules or by varying the amount of material. The most widely used mechanically-tunable platform consists of polyacrylamide hydrogels due to their ease of formation and ability to possess mechanics that span several orders of magnitude (0.1-100 kPa) and thus encompass a wide range of native tissues.[54] This system, while able to effectively replicate native tissue mechanics, has only been used to investigate 2D mechanical signals and due to the cytotoxicity of acrylamide cannot be used for 3D studies. Calcium-crosslinked alginate has also been widely used to investigate mechanosensitive responses as it is a bioinert polymer that can be easily tuned to possess a range of mechanics by varying both the composition of alginate and amount of $Ca^{2+}$ ions.[55, 56] This system does allow for 3D encapsulation of cells, but often results in a somewhat restricted morphology[56] and requires degradation in order to promote adequate cell spreading and infiltration.[57] Incorporation of a cell adhesion site (such as RGD or collagen) is necessary for both of these systems as both polyacrylamide and alginate alone do not support stem cell adhesion and mechanosensing.

While some natural materials (such as fibrin and collagen) have been investigated as mechanically-tunable systems[58, 59], issues arise due to the manner in which mechanics are varied in these systems. Altering the concentration of a given material in order to modulate mechanics can result in confounding variables in terms of differences in ligand density, mesh size, and fibrous morphology[60] and therefore chemical modifications (such

as PEGylation[61]) are typically necessary in order to utilize these native materials as mechanically-tunable systems.

*1.4.2 Hydrogels with Spatially and Temporally Modulated Mechanics*

Although many hydrogel systems afford mechanical tunability in terms of achieving a physiological range of mechanics, few systems exist with the ability to mimic the inherent mechanical complexities found *in vivo* both during development and in fully mature tissue. The importance of spatially controlled mechanics is best exemplified by looking at native tissue organizations such as the osteochondral interface[62] and the aforementioned pathologically distinct mechanics profile present post-myocardial infarction.[43] In these examples there are not only distinct spatial organizations of cell types and matrix composition, but also the mechanical properties of the tissues. Furthermore, tissues also possess dynamic mechanics such as during development[63],injury (i.e., decrease in mechanics associated with MMP activation[64]), and wound repair (i.e., increased mechanics associated with fibrosis[45, 65]).

In order to better understand how stem cells respond to these heterogeneous, dynamic environments present in native and pathological conditions, material systems with both spatial and temporal control of mechanics are desirable. Currently, most systems with the ability to spatially control material properties employ light due to the precise control light affords in terms of exposure time and intensity. By restricting light to specific regions, complex patterns of exposed and non-exposed locations within the same hydrogel system can be achieved in order to locally control cell behaviour.[66-68]

Gradients in mechanics have also been investigated using both microfluidics[69, 70] and photomasks[51, 71] in order to monitor cell responses such as durotaxis and differentiation.

Hydrogels with temporally modulated mechanics have also been developed in order to investigate the dynamic nature of mechanosensing in cells. Again, UV light was employed in one system to locally degrade the matrix (using photodegradable crosslinks) after myofibroblasts were seeded in order to monitor the effect of decreasing mechanics on myofibroblast activation (**Figure 1.7**).[72] The effects of temporally increasing mechanics were investigated in another system in which cardiomyocytes were seeded on thiolated-hyaluronic acid/PEGDA crosslinked hydrogels, which increased in crosslinked density with time in order to mimic native cardiac tissue development.[63]

## 1.5 Summary

While significant advances in our knowledge of stem cell responses to mechanics have been made in the past decade, there is a greater need for understanding stem cell responses to more complex mechanical environments. Mechanically-tunable hydrogel systems exist and have provided initial insight into stem cell responses to heterogeneous and dynamic mechanical signals. However, significant limitations are apparent in many of these hydrogel systems as they lack the ability to both spatially and temporally modulate mechanics, as well as the ability to be translated into a more biologically relevant 3D presentation of controlled mechanics. A system with the ability to spatially and temporally modulate the magnitude and presentation (2D vs. 3D) of mechanics would provide essential insight into fundamental stem cell behaviour, as well as provide a

platform upon which to build future tissue engineering strategies. Thus, the work presented in this dissertation builds on this goal.

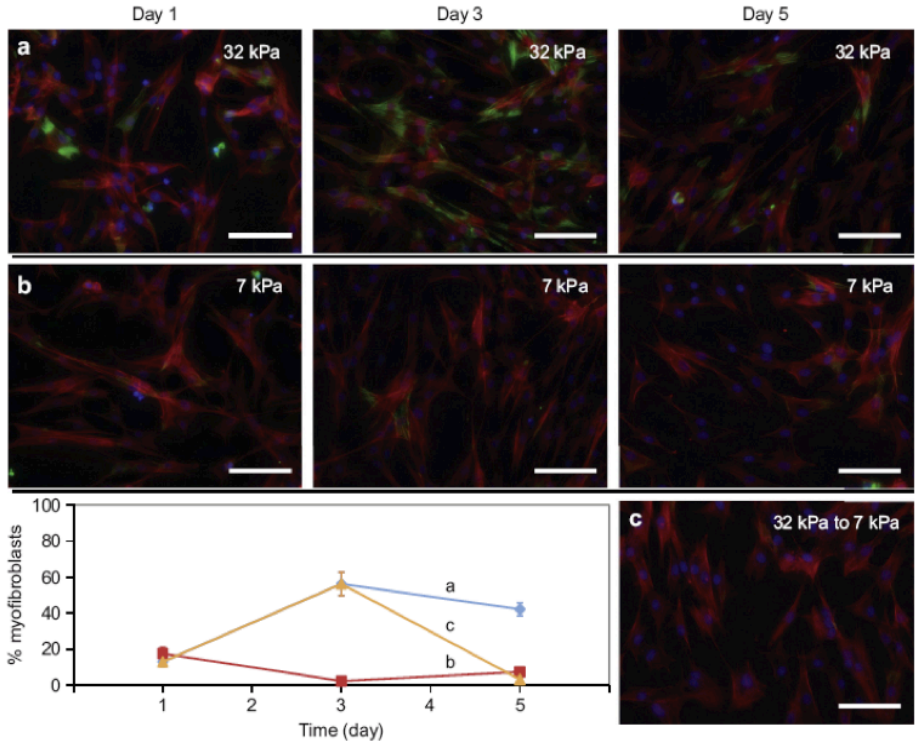


**Figure 1.7** Modulation of substrate elasticity *in situ* directs myofibroblast de-activation. Valvular interstitial cells (VICs) were cultured on myofibroblast promoting or suppressing substrates for 5 days and immunostained to assess activation: (a) 32 kPa and (b) 7 kPa. On Day 3, a portion of the 32 kPa substrates with activated cells were irradiated for 5 min, decreasing the substrate modulus. By Day 5, almost all cells were de-activated by this *in situ* modulus change ((c) 32–7 kPa on Day 3), with a similar number of myofibroblasts present on substrates with a modulus of 7 kPa for the full 5 days. Modulation of substrate elasticity in dynamic cellular processes such as this can lead to a better understanding of its influence on cell function. Scale bars, 100 μm. From Kloxin, et al. [72]

**REFERENCES:**


1. P. R. Baraniak and T. C. McDevitt. Stem cell paracrine actions and tissue regeneration, *Regenerative medicine*, 2010, **5**, 121-143.
2. J. Burdick and G. Vunjak-Novakovic. Review: Engineered Microenvironments for Controlled Stem Cell Differentiation, *Tissue Engineering Part A*, 2008.
3. A. I. Caplan. Why are MSCs therapeutic? New data: new insight, *J Pathol*, 2009, **217**, 318-324.
4. C. M. Metallo, J. C. Mohr, C. J. Detzel, J. J. de Pablo, B. J. Van Wie and S. P. Palecek. Engineering the stem cell microenvironment, *Biotechnol Prog*, 2007, **23**, 18-23.
5. A. I. Caplan and J. E. Dennis. Mesenchymal stem cells as trophic mediators, *J Cell Biochem*, 2006, **98**, 1076-1084.
6. R. J. Pelham and Y. l. Wang. Cell locomotion and focal adhesions are regulated by substrate flexibility, *Proc Natl Acad Sci USA*, 1997, **94**, 13661-13665.
7. A. J. Engler, S. Sen, H. L. Sweeney and D. E. Discher. Matrix elasticity directs stem cell lineage specification, *Cell*, 2006, **126**, 677-689.
8. M. Radmacher. Studying the mechanics of cellular processes by atomic force microscopy, *Methods Cell Biol*, 2007, **83**, 347-372.
9. A. S. Rowlands, P. A. George and J. J. Cooper-White. Directing osteogenic and myogenic differentiation of MSCs: interplay of stiffness and adhesive ligand presentation, *AJP: Cell Physiology*, 2008, **295**, C1037-C1044.

10. F. P. Seib, M. Prewitz, C. Werner and M. Bornhaeuser. Matrix elasticity regulates the secretory profile of human bone marrow-derived multipotent mesenchymal stromal cells (MSCs), *Biochem Biophys Res Commun*, 2009, **389**, 663-667.

11. L.-S. Wang, J. Boulaire, P. P. Y. Chan, J. E. Chung and M. Kurisawa. The role of stiffness of gelatin-hydroxyphenylpropionic acid hydrogels formed by enzyme-mediated crosslinking on the differentiation of human mesenchymal stem cell, *Biomaterials*, 2010.

12. D. E. Discher, D. J. Mooney and P. W. Zandstra. Growth Factors, Matrices, and Forces Combine and Control Stem Cells, *Science*, 2009, **324**, 1673-1677.

13. R. Assoian and E. Klein. Growth control by intracellular tension and extracellular stiffness, *Trends in Cell Biology*, 2008, **18**, 347-352.

14. M. Guvendiren and J. A. Burdick. Stiffening hydrogels to probe short- and long-term cellular responses to dynamic mechanics, *Nat Commun*, 2012, **3**, 792.

15. M. P. Lutolf and J. A. Hubbell. Synthetic biomaterials as instructive extracellular microenvironments for morphogenesis in tissue engineering, *Nat Biotechnol*, 2005, **23**, 47-55.

16. H. Hirata, H. Tatsumi and M. Sokabe. Mechanical forces facilitate actin polymerization at focal adhesions in a zyxin-dependent manner, *J Cell Sci*, 2008, **121**, 2795-2804.

17. H. J. Kong, J. Liu, K. Riddle, T. Matsumoto, K. Leach and D. J. Mooney. Non-viral gene delivery regulated by stiffness of cell adhesion substrates, *Nature materials*, 2005, **4**, 460-464.

18. J. C. Friedland, M. H. Lee and D. Boettiger. Mechanically activated integrin switch controls alpha5beta1 function, *Science*, 2009, **323**, 642-644.

19. M. M. Martino, M. Mochizuki, D. A. Rothenfluh, S. A. Rempel, J. A. Hubbell and T. H. Barker. Controlling integrin specificity and stem cell differentiation in 2D and 3D environments through regulation of fibronectin domain stability, *Biomaterials*, 2009, **30**, 1089-1097.

20. S. Nemir and J. L. West. Synthetic materials in the study of cell response to substrate rigidity, *Annals of biomedical engineering*, 2010, **38**, 2-20.

21. Y.-R. V. Shih, K.-F. Tseng, H.-Y. Lai, C.-H. Lin and O. K. Lee. Matrix stiffness regulation of integrin-mediated mechanotransduction during osteogenic differentiation of human mesenchymal stem cells, *J Bone Miner Res*, 2011, **26**, 730-738.

22. R. McBeath, D. M. Pirone, C. M. Nelson, K. Bhadriraju and C. S. Chen. Cell shape, cytoskeletal tension, and RhoA regulate stem cell lineage commitment, *Dev Cell*, 2004, **6**, 483-495.

23. A. Engler, L. Bacakova, C. Newman, A. Hategan, M. Griffin and D. Discher. Substrate compliance versus ligand density in cell on gel responses, *Biophysical Journal*, 2004, **86**, 617-628.

24. A. J. Engler, C. Carag-Krieger, C. P. Johnson, M. Raab, H.-Y. Tang, D. W. Speicher, J. W. Sanger, J. M. Sanger and D. E. Discher. Embryonic cardiomyocytes beat best on a matrix with heart-like elasticity: scar-like rigidity inhibits beating, *J Cell Sci*, 2008, **121**, 3794-3802.

25. J. Winer, P. Janmey, M. McCormick and M. Funaki. Bone Marrow-Derived Human Mesenchymal Stem Cells Become Quiescent on Soft Substrates but Remain Responsive to Chemical or Mechanical Stimuli, *Tissue Engineering Part A*, 2008.

26. C. S. Chen, M. Mrksich, S. Huang, G. M. Whitesides and D. E. Ingber. Geometric control of cell life and death, *Science*, 1997, **276**, 1425-1428.

27. P. C. Georges. Matrices with Compliance Comparable to that of Brain Tissue Select Neuronal over Glial Growth in Mixed Cortical Cultures, *Biophysical Journal*, 2006, **90**, 3012-3018.

28. C. B. Khatiwala, S. R. Peyton, M. Metzke and A. J. Putnam. The regulation of osteogenesis by ECM rigidity in MC3T3-E1 cells requires MAPK activation, *J. Cell. Physiol.*, 2007, **211**, 661-672.

29. K.-S. Park, Y.-S. Kim, J.-H. Kim, B. Choi, S.-H. Kim, A. H.-K. Tan, M.-S. Lee, M.-K. Lee, C.-H. Kwon, J.-W. Joh, S.-J. Kim and K.-W. Kim. Trophic molecules derived from human mesenchymal stem cells enhance survival, function, and angiogenesis of isolated islets after transplantation, *Transplantation*, 2010, **89**, 509-517.

30. M. F. Pittenger and B. J. Martin. Mesenchymal stem cells and their potential as cardiac therapeutics, *Circ Res*, 2004, **95**, 9-20.

31. D. J. Prockop. Repair of tissues by adult stem/progenitor cells (MSCs): controversies, myths, and changing paradigms, *Mol Ther*, 2009, **17**, 939-946.

32. Y. Wu, L. Chen, P. G. Scott and E. E. Tredget. Mesenchymal stem cells enhance wound healing through differentiation and angiogenesis, *Stem Cells*, 2007, **25**, 2648-2659.

33. R. M. Nerem. Tissue engineering: the hope, the hype, and the future, *Tissue Engineering*, 2006, **12**, 1143-1150.

34. E. M. Chandler, C. M. Berglund, J. S. Lee, W. J. Polacheck, J. P. Gleghorn, B. J. Kirby and C. Fischbach. Stiffness of photocrosslinked RGD-alginate gels regulates adipose progenitor cell behavior, *Biotechnol. Bioeng.*, 2011, **108**, 1683-1692.

35. L. Chen, E. E. Tredget, P. Y. G. Wu and Y. Wu. Paracrine factors of mesenchymal stem cells recruit macrophages and endothelial lineage cells and enhance wound healing, *PLoS ONE*, 2008, **3**, e1886.

36. G. Chen, M. Nayan, M. Duong, J.-F. Asenjo, Y. Ge, R. C.-J. Chiu and D. Shum-Tim. Marrow stromal cells for cell-based therapy: the role of antiinflammatory cytokines in cellular cardiomyoplasty, *Ann Thorac Surg*, 2010, **90**, 190-197.

37. J.-Y. Hahn, H.-J. Cho, H.-J. Kang, T.-S. Kim, M.-H. Kim, J.-H. Chung, J.-W. Bae, B.-H. Oh, Y.-B. Park and H.-S. Kim. Pre-treatment of mesenchymal stem cells with a combination of growth factors enhances gap junction formation, cytoprotective effect on cardiomyocytes, and therapeutic efficacy for myocardial infarction, *J Am Coll Cardiol*, 2008, **51**, 933-943.

38. X. Li, X. Yu, Q. Lin, C. Deng, Z. Shan, M. Yang and S. Lin. Bone marrow mesenchymal stem cells differentiate into functional cardiac phenotypes by cardiac microenvironment, *J Mol Cell Cardiol*, 2007, **42**, 295-303.

39. D. Paul, S. M. Samuel and N. Maulik. Mesenchymal stem cell: present challenges and prospective cellular cardiomyoplasty approaches for myocardial regeneration, *Antioxid Redox Signal*, 2009, **11**, 1841-1855.

40. M. Breitbach, T. Bostani, W. Roell, Y. Xia, O. Dewald, J. M. Nygren, J. W. U. Fries, K. Tiemann, H. Bohlen, J. Hescheler, A. Welz, W. Bloch, S. E. W. Jacobsen and B. K. Fleischmann. Potential risks of bone marrow cell transplantation into infarcted hearts, *Blood*, 2007, **110**, 1362-1369.

41. K. C. Ribeiro, E. C. Mattos, J. P. S. Werneck-de-castro, V. P. Ribeiro, R. H. Costa-e-Sousa, A. Miranda, E. L. Olivares, M. Farina, J. G. Mill, J. R. C. d. S. Goldenberg, M. O. Masuda and A. C. C. de Carvalho. Ectopic ossification in the scar tissue of rats with myocardial infarction, *Cell Transplant*, 2006, **15**, 389-397.

42. B. I. Jugdutt. Limiting fibrosis after myocardial infarction, *N Engl J Med*, 2009, **360**, 1567-1569.

43. M. F. Berry, A. J. Engler, Y. J. Woo, T. J. Pirolli, L. T. Bish, V. Jayasankar, K. J. Morine, T. J. Gardner, D. E. Discher and H. L. Sweeney. Mesenchymal stem cell injection after myocardial infarction improves myocardial compliance, *Am J Physiol Heart Circ Physiol*, 2006, **290**, H2196-2203.

44. A. Uccelli, L. Moretta and V. Pistoia. Mesenchymal stem cells in health and disease, *Nat Rev Immunol*, 2008, **8**, 726-736.

45. W. L. K. Chen and C. A. Simmons. Lessons from (patho)physiological tissue stiffness and their implications for drug screening, drug delivery and regenerative medicine, *Advanced Drug Delivery Reviews*, 2011, **63**, 269-276.

46. E. M. Chandler, M. P. Saunders, C. J. Yoon, D. Gourdon and C. Fischbach. Adipose progenitor cells increase fibronectin matrix strain and unfolding in breast tumors, *Phys Biol*, 2011, **8**, 015008.

47. K. R. Levental, H. Yu, L. Kass, J. N. Lakins, M. Egeblad, J. T. Erler, S. F. T. Fong, K. Csiszar, A. Giaccia, W. Weninger, M. Yamauchi, D. L. Gasser and V. M. Weaver. Matrix crosslinking forces tumor progression by enhancing integrin signaling, *Cell*, 2009, **139**, 891-906.

48. T. A. Ulrich, E. M. d. J. Pardo and S. Kumar. The Mechanical Rigidity of the Extracellular Matrix Regulates the Structure, Motility, and Proliferation of Glioma Cells, *Cancer Res*, 2009, **69**, 4167-4174.

49. E. Hadjipanayi, V. Mudera and R. A. Brown. Guiding cell migration in 3D: a collagen matrix with graded directional stiffness, *Cell Motil. Cytoskeleton*, 2009, **66**, 121-128.

50. S. Nemir, H. N. Hayenga and J. L. West. PEGDA hydrogels with patterned elasticity: Novel tools for the study of cell response to substrate rigidity, *Biotechnol. Bioeng.*, 2010, **105**, 636-644.

51. J. R. Tse and A. J. Engler. Stiffness gradients mimicking in vivo tissue variation regulate mesenchymal stem cell fate, *PLoS ONE*, 2011, **6**, e15978.

52. K. Suzuki, R. Sun, M. Origuchi, M. Kanehira, T. Takahata, J. Itoh, A. Umezawa, H. Kijima, S. Fukuda and Y. Saijo. Mesenchymal stromal cells promote tumor growth through the enhancement of neovascularization, *Mol Med*, 2011, **17**, 579-587.

53. N. K. Satija, V. K. Singh, Y. K. Verma, P. Gupta, S. Sharma, F. Afrin, M. Sharma, P. Sharma, R. P. Tripathi and G. U. Gurudutta. Mesenchymal stem cell-based therapy: a new paradigm in regenerative medicine, *J Cell Mol Med*, 2009, **13**, 4385-4402.

54. F. Rehfeldt, A. Engler, A. Eckhardt, F. Ahmed and D. Discher. Cell responses to the mechanochemical microenvironment—Implications for regenerative medicine and drug delivery☆, *Advanced Drug Delivery Reviews*, 2007, **59**, 1329-1339.

55. S. X. Hsiong, P. Carampin, H.-J. Kong, K.-Y. Lee and D. J. Mooney. Differentiation stage alters matrix control of stem cells, *J. Biomed. Mater. Res.*, 2008, **85**, 145-156.

56. N. Huebsch, P. R. Arany, A. S. Mao, D. Shvartsman, O. A. Ali, S. A. Bencherif, J. Rivera-Feliciano and D. J. Mooney. Harnessing traction-mediated manipulation of the cell/matrix interface to control stem-cell fate, *Nature materials*, 2010, **9**, 1-9.

57. T. Boontheekul, E. E. Hill, H.-J. Kong and D. J. Mooney. Regulating Myoblast Phenotype Through Controlled Gel Stiffness and Degradation, *Tissue Engineering*, 2007, **13**, 1431-1442.

58. F. Byfield, R. Reen, T. Shentu, I. Levitan and K. Gooch. Endothelial actin and cell stiffness is modulated by substrate stiffness in 2D and 3D, *Journal of biomechanics*, 2009.

59. M. P. Linnes, B. D. Ratner and C. M. Giachelli. A fibrinogen-based precision microporous scaffold for tissue engineering, *Biomaterials*, 2007, **28**, 5298-5306.

60. M. A. Kotlarchyk, S. G. Shreim, M. B. Alvarez-Elizondo, L. C. Estrada, R. Singh, L. Valdevit, E. Kniazeva, E. Gratton, A. J. Putnam and E. L. Botvinick. Concentration independent modulation of local micromechanics in a fibrin gel, *PLoS ONE*, 2011, **6**, e20201.

61. O. Sarig-Nadir and D. Seliktar. Compositional Alterations of Fibrin-Based Materials for Regulating In VitroNeural Outgrowth, *Tissue Engineering Part A*, 2008, **14**, 401-411.

62. M. L. Knothe Tate, T. D. Falls, S. H. McBride, R. Atit and U. R. Knothe. Mechanical modulation of osteochondroprogenitor cell fate, *Int J Biochem Cell Biol*, 2008, **40**, 2720-2738.

63. J. L. Young and A. J. Engler. Hydrogels with time-dependent material properties enhance cardiomyocyte differentiation in vitro, *Biomaterials*, 2011, **32**, 1002-1009.

64. R. Mukherjee, J. T. Mingoia, J. A. Bruce, J. S. Austin, R. E. Stroud, G. P. Escobar, D. M. McClister, C. M. Allen, M. A. Alfonso-Jaume, M. E. Fini, D. H. Lovett and F. G. Spinale. Selective spatiotemporal induction of matrix metalloproteinase-2 and matrix metalloproteinase-9 transcription after myocardial infarction, *Am J Physiol Heart Circ Physiol*, 2006, **291**, H2216-2228.

65. R. G. Wells. The role of matrix stiffness in regulating cell behavior, *Hepatology*, 2008, **47**, 1394-1400.

66. S. J. Bryant, J. L. Cuy, K. D. Hauch and B. D. Ratner. Photo-patterning of porous hydrogels for tissue engineering, *Biomaterials*, 2007, **28**, 2978-2986.

67. S. Lee, J. Moon and J. West. Three-dimensional micropatterning of bioactive hydrogels via two-photon laser scanning photolithography for guided 3D cell migration, *Biomaterials*, 2008, **29**, 2962-2968.

68. S. Suri and C. Schmidt. Photopatterned collagen-hyaluronic acid interpenetrating polymer network hydrogels, *Acta Biomaterialia*, 2009.

69. J. A. Burdick, A. Khademhosseini and R. Langer. Fabrication of gradient hydrogels using a microfluidics/photopolymerization process, *Langmuir : the ACS journal of surfaces and colloids*, 2004, **20**, 5153-5156.

70. N. Zaari, P. Rajagopalan, S. K. Kim, A. J. Engler and J. Y. Wong. Photopolymerization in Microfluidic Gradient Generators: Microscale Control of Substrate Compliance to Manipulate Cell Response, *Adv Mater*, 2004, **16**, 2133-2137.

71. A. M. Kloxin, A. M. Kasko, C. N. Salinas and K. S. Anseth. Photodegradable hydrogels for dynamic tuning of physical and chemical properties, *Science*, 2009, **324**, 59-63.

72. A. M. Kloxin, J. A. Benton and K. S. Anseth. In situ elasticity modulation with dynamic substrates to direct cell phenotype, *Biomaterials*, 2010, **31**, 1-8.

# CHAPTER 2

*Research Overview*

## 2.1 Introduction

The ability of stem cells to respond to the mechanics of their microenvironment has received considerable attention in the past decade within the realms of tissue engineering and stem cell biology. Although efforts have been made to investigate the effects of uniform, static mechanics on stem cell behavior, few systems exist with the ability to control mechanics spatially and temporally for the purpose of elucidating stem cell responses to complex mechanical environments. This dissertation outlines the development of a sequentially crosslinked hydrogel system with the unique ability to spatially and temporally control mechanics and subsequently investigate the response of adult stem cells to these heterogeneous, dynamic microenvironments. The implications of this research extend not only to biomaterial design for tissue engineering, but also toward furthering our knowledge of stem cell responses to native and pathological mechanics *in vivo*.

*Hypotheses:* The global hypothesis of this work is that a sequentially crosslinked hydrogel system, based on naturally-derived hyaluronic acid (HA), would afford a means to study the effects of distinct spatially and temporally controlled mechanical microenvironments on stem cell behavior. Specifically, we hypothesized that 1) Hydrogels possess controlled spatial and temporal mechanics in a sequentially

crosslinked system based on the extent of initial crosslinking (Michael Addition), as well as the location and timing of UV exposure (radical polymerization), 2) human mesenchymal stem cell (hMSC) morphology, proliferation, and differentiation behavior is dependent on the local matrix mechanics in both uniform and patterned systems, 3) hMSCs alter their phenotype based on the timing of matrix "stiffening," and 4) hMSC morphology, proliferation, differentiation, and secretion of trophic factors are dependent on the 3D contextual presentation of mechanics in non-porous and porous hydrogels.

In order to test these hypotheses, the following specific aims were proposed:

**Specific Aim 1: Develop sequentially crosslinked hydrogel systems with both spatially and temporally controlled mechanics.** Two approaches will be investigated, where crosslink density is modified through an interpenetrating network (e.g., polyethylene glycol diacrylate in alginate) or where one molecule is crosslinked using two means (e.g., methacrylated hyaluronic acid) In the latter approach, the methacrylated hyaluronic acid will be crosslinked *via* Michael Addition (using a dithiol crosslinker) and radical polymerization (using UV light) in series. Mechanics will be characterized for each of these tunable mechanical systems

**Specific Aim 2: Spatially and temporally control human mesenchymal stem cell (hMSC) behavior on sequentially crosslinked hyaluronic acid hydrogels.** Using the system developed in Specific Aim 1, hydrogels with distinct uniform, patterned, and dynamic mechanics will be investigated in order to spatially and temporally direct stem

cell morphology, proliferation, and differentiation in both non-inductive and inductive (osteogenic-adipogenic) medium.

**Specific Aim 3: Investigate hMSC response to 3D presentation of mechanical signals in hyaluronic acid hydrogels.** hMSCs will be presented with controlled mechanical signals in non-porous and porous 3D contexts. For non-porous studies, hMSCs will be fully encapsulated within photocrosslinked hydrogels, while porous studies will consist of hMSCs seeded within sequentially crosslinked macroporous hydrogels (formed using a degradable microsphere template). Stem cell morphology, proliferation, differentiation, and secretion of angiogenic and cytokine factors will be monitored for each 3D context. The effects of spatial and temporal mechanics will be investigated in the macroporous system due to the sequential crosslinking process.

## 2.2 Research Summary

The motivation for the development of a hydrogel with spatially and temporally modulated mechanics was outlined in Chapter 1. As tissue engineering strategies strive to recapitulate the complex mechanical properties of native tissue, it is important to understand how stem cells respond to these microenvironments and understand how desired stem cell outcomes can be achieved through biomaterial design. Chapter 3 provides a review of literature summarizing the field of biomaterials and how material cues can be controlled in order to elicit a desired stem cell response.

Chapter 4 outlines the mechanically-tunable systems developed to direct stem cell behavior. Within this chapter, several candidate hydrogel systems based on natural and

synthetic polymers are investigated in order to arrive at a system capable of fulfilling the requirements for a system that adequately supports stem cells and presents complex mechanical cues. The effects of spatially controlled mechanics on stem cell morphology and proliferation in 2D are first investigated in Chapter 5 using a non-inductive culture system. In Chapter 6, a well-established bipotential induction system is used to investigate the effects of spatially controlled mechanics on hMSC lineage specification towards either adipogenic or osteogenic fates.

Chapter 7 depicts the translation of the mechanically-tunable 2D system into a non-porous photocrosslinked 3D network with controlled mechanics. hMSCs encapsulated in non-porous hydrogels across a range of physiologic mechanics are investigated in terms of their effects on hMSC morphology, proliferation, differentiation, and secretion of angiogenic and cytokine factors. As this system does not rely upon sequential crosslinking (radically crosslinked only), we are only able to investigate the effect of uniform mechanics on hMSCs in this non-porous context.

Chapter 8 introduces another 3D presentation of mechanics using the same hyaluronic acid material except in a macroporous context. Sequential crosslinking allows for macroporous hydrogels with spatial and temporal mechanics as crosslinking can be controlled by not only the amount of UV exposure, but also the location and timing. hMSC responses to uniform, patterned, and dynamic porous hydrogels are investigated and compared to responses in other 2D and 3D contexts.

Finally, Chapter 9 illustrates the overall conclusions and future directions for this dissertation. Stem cell responses to complex mechanical signals are assessed in the context of this study, as well as in the context of other mechanically-tunable systems and

native biological systems. Limitations of the work are also presented and followed by proposal of future studies that take advantage of the sequential crosslinking process in order to further investigate stem cell mechanosensitivity and provide a platform for tissue engineering applications.

# CHAPTER 3

## *Controlling Stem Cell Fate with Material Design: A Review*

*Adapted from Marklein, RA, Burdick, JA. "Controlling Stem Cell Fate with Material Design," Adv Mater, 2010, 22(2): 175-89.*

### 3.1 Introduction

Stem cells are becoming an important component of approaches for regenerative medicine, especially within the rapidly expanding field of tissue engineering. Tissue engineering aims to develop biologically inspired 3-dimensional (3D) constructs that integrate with native tissue and/or stimulate the body's innate repair mechanisms to regenerate damaged tissue and restore function.[1] Due to an aging population and demand for a higher quality of life, the emergence of tissue engineering as a solution to repair a multitude of tissues is evident. Within the tissue engineering paradigm, the selection of the appropriate cells, materials, and biological molecules will ultimately determine success or failure. With their ability to proliferate, self-renew, and differentiate, stem cells are becoming a promising cell source for these applications. The successful incorporation of stem cells into tissue engineering strategies is contingent upon a thorough knowledge of factors influencing stem cell behavior. Uncommitted stem cells in the developing embryo, for example, are subjected to regional differences in their microenvironments, which result in the formation of every tissue in the human body. Through an understanding of the cues that drive stem cell fate decisions, it may be possible to incorporate these cues into the design of future 3D microenvironments to

optimize and facilitate tissue repair and regeneration. These cues include soluble/immobilized factors, chemical and physical signals from the extracellular matrix (ECM), cell morphology, and external stresses. Furthermore, it is not only the simple presence of these cues that is crucial to a stem cell's response, but also their spatial and temporal context. Due to the complex nature of stem cell fate decisions and the constant "crosstalk" among different signals, it is necessary to design 3D microenvironments that consider the interplay of these diverse cues.

Biomaterials design is expanding with new material syntheses and processing techniques to enhance the complexity of 3D environments in order to direct stem cell lineage commitment.[2, 3] These materials can be utilized as cell delivery vehicles, scaffolds for cell adhesion, surfaces for cell culture, and a source of soluble/immobilized factors, among others. Microenvironments can be designed to feature an intense signal to drive differentiation, or a myriad of signals that address the biologically relevant sequence of events leading to lineage commitment (**Figure 3.1**). An understanding of materials science and chemical syntheses allows for the creation of biomaterials that can manipulate stem cells for specific tissue engineering applications. Much of this work has focused on mesenchymal stem cells (MSCs), possibly due to the ease of culture and widespread applicability in regenerative medicine, yet this technology is widely applicable to numerous stem cell types. This progress report will focus on general concepts of using materials to control stem cells, as well as provide examples of recent advances within this rapidly expanding field.

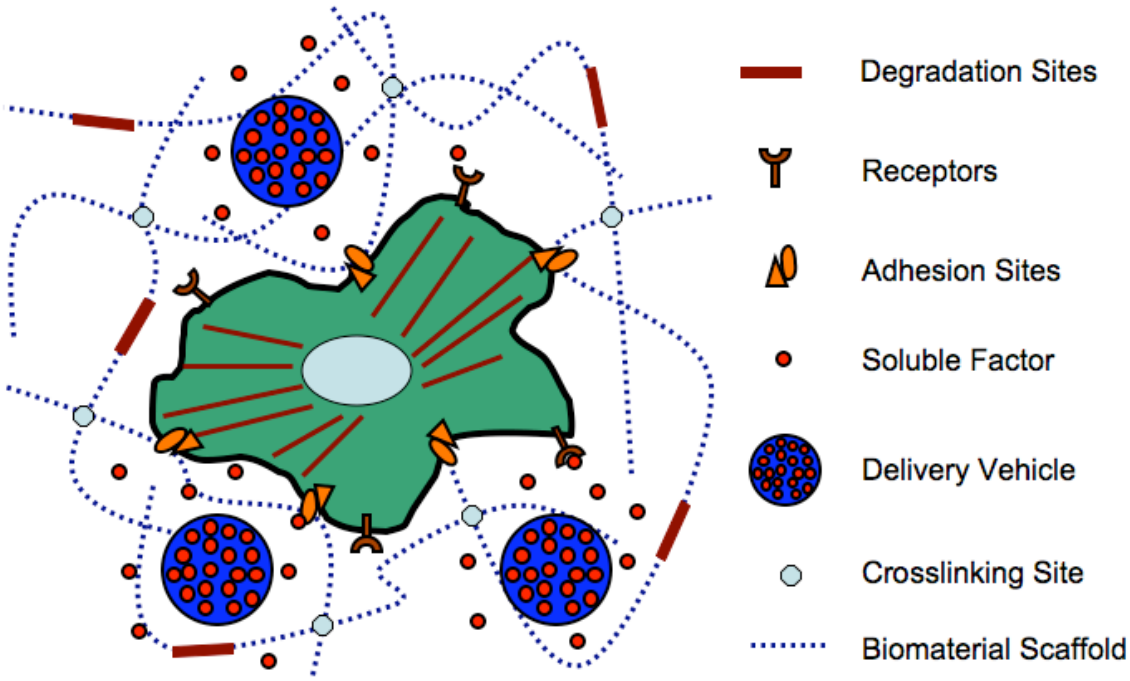


**Figure 3.1 The stem cell microenvironment.** Material control can be exerted at many levels through adhesion, cell factor binding, material degradation and mechanics, and cell morphology to manipulate stem cell interactions and fate.

### 3.2 Biomaterial Structure and Chemistry as Differentiation Cues

The use of biomaterials as scaffolds is a fundamental and important component of tissue engineering since these materials serve as templates for tissue formation and are engineered depending on the tissue of interest. These scaffolds not only provide mechanical and 3D structural support for cells, but can also provide cues to induce tissue repair. The structure and morphology, chemistry and presentation of adhesive cues, and degradation are all important parameters in material design for these applications and may signal the differentiation of stem cells.

*3.2.1 Structures of Biomaterials for 3D Cellular Environments*

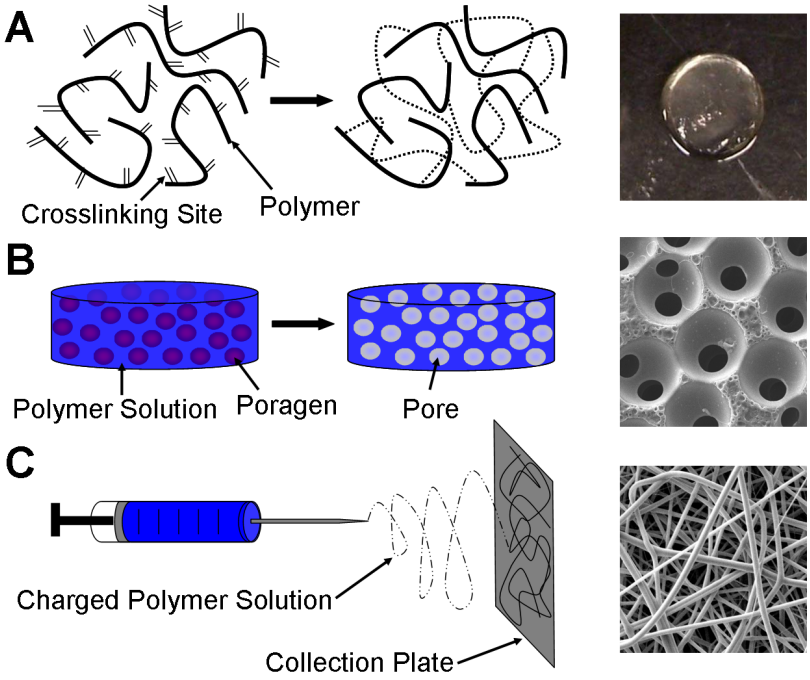


**Figure 3.2 Scaffold fabrication and morphology.** A) Polymers with reactive groups are crosslinked to form a highly swollen hydrogel network. B) Porous network formation through a poragen leaching process. C) Polymer electrospinning where an electric field causes a charged polymer solution to travel from a syringe to a grounded surface leaving distinct nano/micro sized fibers.

Biomaterial scaffolds take on a variety of structures based on their material composition and processing to form 3D environments for cell delivery or invasion. These materials consist of natural polymers such as collagen, hyaluronic acid (HA), fibrin, or alginate, or synthetic polymers such as polyethylene glycol (PEG), dextran, or polyvinyl alcohol and can be formed into hydrogels, fibrous structures, and macroporous

scaffolds.[4, 5] **Figure 3.2** illustrates examples of the formation and structure of each of these scaffold types. The biomaterial structure controls how a cell interacts with the material and is important in stem cell fate decisions since the presentation of cues and cellular morphology are dependent on this structure.

*3.2.1.1 Hydrogels*

Hydrogels are comprised of insoluble networks of crosslinked polymers with high water contents (>90%).[6] Hydrogels with the ability to encapsulate stem cells have been used for applications such as cartilage[7, 8] and cardiac[9, 10] tissue regeneration. In order to achieve tissue formation, stem cells must either be encapsulated within or recruited to the hydrogel. Cells can be encapsulated in hydrogels through various means including self-assembly, ionic crosslinking, and radical polymerizations.[11] For example, the water-soluble photoinitiator I2959 (Irgacure, 2-hydroxy-1-[4-(hydroxyethoxy)phenyl]-2-methyl-1-propanone) can be used to initiate crosslinking upon exposure to UV light with materials containing acrylate or methacrylate groups.[5, 12] It is important to note that potential side effects to UV light should be thoroughly assessed, particularly with stem cells that may be susceptible to damage. Hydrogels are advantageous for cell encapsulation due to the high water content and diversity in chemistry and properties that can be obtained. It is important to consider the viability of stem cells during the encapsulation process and with culture, including the diffusion of nutrients and wastes to and from the cells. Hydrogel properties are dependent on factors such as the charge and chemistry of the polymer and crosslinking density. Additionally, interpenetrating networks (IPNs) can be used to further alter hydrogel properties by combining properties

of each polymer.[13] One class of hydrogels that is gaining interest for stem cell encapsulation is HA based gels. HA is a natural polymer that was initially used as an implantable biomaterial to study wound healing and biocompatibility in order to monitor vascularization, inflammatory responses, and matrix secretion.[14, 15] While HA does not possess any inherent crosslinking ability, chemical modification allows for photocrosslinking.[16, 17]

*3.2.1.2 Fibrous scaffolds*

Although hydrogels provide a highly controlled 3D microenvironment for cells, the nature of this scaffold does not entirely mimic the structure of native ECM. In particular, the crosslinked polymer network does not possess a fibrillar architecture that is prevalent in ECM components such as collagen and fibrin.[18, 19] One common method to create scaffolds with a fibrous morphology is the process of electrospinning. This method involves extruding a charged polymer solution through a blunt needle, which is attracted to a grounded material due to a large potential difference.[18] Electrospinning has been used to produce fibrous scaffolds from a wide range of polymers with diverse properties, both synthetic and natural, for a range of tissue applications.[20] Another attractive feature is that the fibers can be aligned by spinning on a rotating mandrel to produce anisotropy in both the bulk physical properties and in cellular morphology and matrix production.[21, 22] However, one of the limitations of this technique is the potentially poor cell infiltration into the scaffold, either when seeded or when implanted. As demonstrated by Baker et al., it is possible to combine multiple polymer jets and a rotating mandrel to create electrospun scaffolds that have desired anisotropic mechanical

properties, as well as enhanced mesenchymal stem cell (MSC) infiltration (due to removal of "sacrificial fibers").[23] In general, the diversity in materials that can be obtained with fibrous morphologies and the potential advantages of the structure makes these scaffolds useful for controlling stem cells.

*3.2.1.3. Macroporous scaffolds*

Potentially, the most widely used biomaterial structure for tissue engineering involves macroporous scaffolds, which can form interconnected porous networks that allow for cellular infiltration and tissue formation. These scaffolds are often formed with leachable components (such as salt crystals or microspheres) around which the desired polymer forms a scaffold.[24] Upon removal of the leachable components, a 3D structure can be obtained with varying parameters such as pore size, porosity, and interconnectivity. Linnes et al. created a macroporous scaffold based on fibrinogen using sintered PMMA microspheres, which allowed for a highly porous, interconnected 3D microenvironment that upon addition of thrombin or genipin significantly increased in stability and mechanics.[25] In another study, poly(ε-caprolactone) scaffolds (formed using a gas foaming technique) with varied pore size and interconnectivity were created to monitor osteogenesis of dura mater stem cells.[26] In the case of large pore sizes, cells may interpret the environment as 2D; however, the macrostructure of the scaffold allows for the creation of a 3D tissue as cells synthesize and interact with secreted matrix.

*3.2.2 Chemical Signals in Biomaterials*

Stem cells may interact with biomaterials through surface receptors such as

integrins and cell adhesion molecules.[27] The selection of a biomaterial must take into consideration the inherent cell adhesivity of a material (e.g., in the case of natural materials) or the ability to confer additional biofunctionality in order to elicit a particular response from stem cells. Adhesion may be desirable or undesirable depending on the desired differentiation path and native cell environment. There are a wide range of techniques to control adhesion, including altering the hydrophobicity of a material to influence protein adsorption or by tethering proteins or their analogues directly to a material. Beyond adhesion, other chemical cues may be included to manipulate stem cell interactions and differentiation, either directly or indirectly by controlling protein interactions.

*3.2.2.1 Cell adhesion motifs*

A simple and common technique in many tissue engineering strategies is to incorporate analogues of native ECM components into scaffolds in order to control stem cell interactions. The fibronectin binding domain arginine-glycine-aspartic acid (RGD) has been used widely to promote binding sites for $\alpha v\beta 3$ integrins in applications such as osteogenesis and chondrogenesis.[28, 29] The effects of RGD concentration and its spatial organization have been investigated and determined to be regulators of stem cell morphology, proliferation, and differentiation.[30] While RGD is used as a "default" binding site for biomaterials, efforts have been made to investigate the contextual presentation of RGD within fibronectin and its effect on stem cell behavior. Martino et al. demonstrated that the presentation of certain fibronectin domains, including RGD and its synergy sequence PHSRN, can significantly affect MSC spreading and proliferation.[31]

Additionally, other sequences are being investigated for cell specific differentiation such as laminin-derived IKVAV and YIGSR.[32]

*3.2.2.2 Chemistry of biomaterials*

More indirect approaches (e.g., controlling hydrophobicity) towards addressing cell recognition of biomaterials have produced interesting results. For example, by altering the hydrophobicity of a surface, the formation and differentiation potential of embryonic stem cells (ESCs) within embryoid bodies (EBs) could be tuned to promote desirable EB size and composition.[33] In another study, Benoit et al. altered the microenvironment by introducing different small molecules such as phosphates, carboxylic acids, and aliphatic chains (very hydrophobic).[34] The presence of these molecules led to increased MSC expression of bone, cartilage, and fat associated markers of differentiation, respectively.

It is often difficult to predict how a stem cell will respond to its environmental cues and thus methods have been developed to rapidly screen biomaterials and stem cell interactions.[35-37] The use of a combinatorial library of biomaterials formed from different acrylate and methacrylate monomers proved to be useful for identifying environments suitable for uniform ESC differentiation into epithelial cells.[38] **Figure 3.3** shows one example of a screening of the influence of material chemistry on ESC differentiation.

Further combinatorial studies were performed on MSCs, neural stem cells, and primary articular chondrocytes using monomers with varied degradation, hydrophobicity, molecular weight, and crosslinking.[39] This method allows for determination of ideal microenvironments for stem cell differentiation and can also be coupled with other

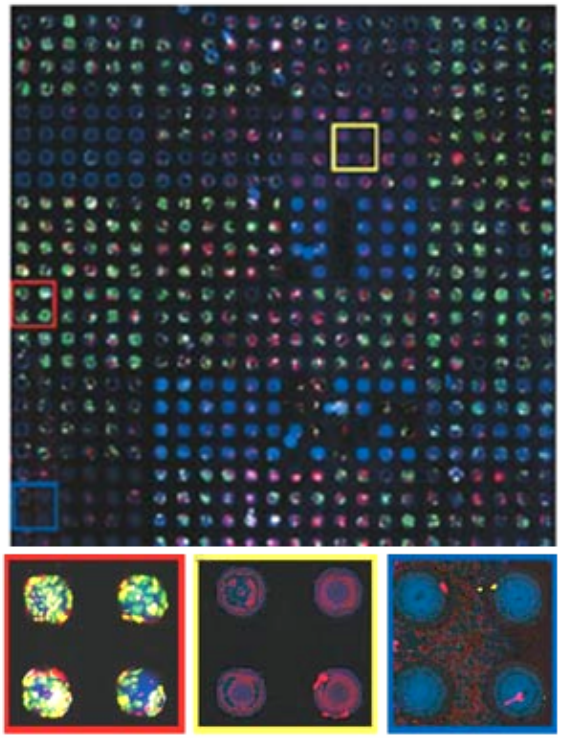

**Figure 3.3 Investigating stem cell and material interactions with polymer arrays.** Top: Human ESCs cultured on a polymer in the presence of retinoic acid for 6 days and then stained for cytokeratin 7 (green), vimentin (red), and nuclei (blue). Bottom: 3 examples of polymers highlighted from above array. Reproduced with permission from [36].

induction factors (as discussed later) to screen thousands of possible scenarios for controlling stem cell behavior.[40] Rapid screening techniques are useful in that they can identify unique environments that can not be predicted based on material structure and chemistry. The materials in these studies are also inexpensive and much easier to synthesize than scaffolds possessing complex chemistries and cell recognition sites.[41-43] These studies indicate that biomaterial design does not need to exactly mimic native tissue, but rather possess the fundamental characteristics that promote desired stem cell

behavior.

*3.2.2.3 Natural and synthetic biomaterials*

A major advantage of using naturally derived materials is that they possess desired cell recognition sites to control cellular behavior such as adhesion and degradation. For example, fibrin hydrogels consist of polymerized fibrinogen, which possesses multiple direct binding sites, as well as sites that bind growth factors, fibronectin, HA, and von Willebrand factor.[19] The addition of thrombin to fibrinogen allows for the formation of fibrin hydrogels consisting of nanometer scaled fibers that can be recognized by cells. Early studies using dorsal root ganglia demonstrated the effects of varied fibrin network formation on neurite extension by adding biorecognition molecules and factor XIII, which participates in covalent crosslinking.[44] PEGylated fibrinogen has been used by several groups in order to utilize the stem cell recognition of fibrinogen while also allowing for more control and variation of network degradation and mechanics.[25, 45, 46] Another route for creating desirable 3D microenvironments for stem cells is to harness the potential regenerative properties of stem cell-derived biomaterials. Nair et al. developed a biomaterial from acellularized EBs using Triton-X/DNAse treatments to remove cellular components while maintaining the ECM components such as collagen IV, laminin, and fibronectin.[47, 48] EBs induced towards a specific lineage and subsequently acellularized could create a stem cell-derived biomaterial with desired morphogenic cues for a given tissue engineering application.

HA is another naturally occurring material (i.e., polysaccharide) consisting of repeating disaccharide units and has been implicated in many stem cell fate decisions.49

Extensive work by Shu et al. has involved chemically modifying HA to confer additional cell recognition, degradability, and crosslinking ability.[14, 50] The presence of hydroxyl and carboxyl groups allows for chemical modification of the HA backbone with methods such as carbodiimide chemistry. Another useful modification of HA (and other hydroxyl containing polymers) is the addition of methacrylates or acrylates, which allows for radical polymerization.[16] Significant work has been performed using photocrosslinkable HA hydrogels for stem cell encapsulation, specifically involving cartilage tissue engineering.[7, 51]

While natural materials provide inherent instructive cues for stem cells, limitations of these materials include a possible immune response, potential loss of biological activity during processing, and insufficient mechanical properties. In many cases, synthetic materials are used as "blank slates" that can be modified to confer biofunctionality and promote stem cell differentiation. One of the most common synthetic materials used as a backbone for hydrogel systems is PEG. Due to its hydrophilicity and ease of modification, highly swollen hydrogels can be formed that also contain cell recognition sites.[52] For example, PEG coupled to poly(L-Lysine) promotes greater neural progenitor survival and differentiation to mature neural phenotypes than unmodified PEG hydrogels.[53] This is potentially due to the charged amino side chains present in lysine, which allow for cell adhesion and survival and can also provide sites for further chemical modification. A recent study demonstrated the temporally controlled presentation of cell binding using PEG hydrogels coupled with a matrix metalloproteinase (MMP)-cleavable RGD peptide.[54] The motivation behind this study

was that initiation of chondrogenesis is dependent on fibronectin, but persistence of this binding inhibits long-term chondrogenesis.[55, 56] The incorporation of an MMP-13 cleavable linker resulted in increased glycosaminoglycan production, as well as a greater percentage of collagen II positive cells compared to undifferentiated MSCs.

*3.2.3 Scaffold Degradation*

While biomaterials may consist of either natural or synthetic materials, it is generally accepted that they serve as a temporary scaffold and, as new tissue is formed, they should degrade. Therefore, it is necessary to design materials that degrade over a timescale that corresponds with a given application (i.e., formation of mature, functional tissue). Structurally, scaffold degradation allows for cellular infiltration, as well as ECM synthesis and distribution. The ideal degradation profile, in terms of tissue mechanical properties, may be a decrease in scaffold mechanical properties over time, with the concurrent synthesis of ECM by cells.[1] While this may be oversimplified, it is important to address biodegradability of biomaterials when designing a scaffold. Beyond structural importance, scaffold degradation also controls temporal properties, including the presentation of chemical and mechanical cues at different times in development and regeneration.

Cell-mediated degradation is best evidenced by naturally occurring MMP degradation of ECM components such as collagen. In more synthetic materials, MMP-sensitive sequences can be incorporated as crosslinkers, which degrade once the encapsulated or migrating cells begin to secrete MMPs.[57-59] These sequences are typically used to promote degradation of the biomaterial as the cells begin to secrete matrix

components and remodel their surroundings. Stem cells secrete specific MMPs that correlate with their lineage commitment (e.g., MMP-3 for ESC cardiogenesis, MMP-9 for neural stem cell commitment, and MMP-13 for chondrogenesis).[54, 60, 61] Scaffolds possessing MMP-1 sensitive sites promoted greater cell infiltration and matrix deposition than scaffolds without these sites when implanted in a cranial defect.[58] Therefore, biomaterials have been designed to incorporate these sequences in order to allow for cell spreading/infiltration and matrix remodeling.[54, 58, 62] Importantly, the ability to remodel and spread in matrices may be a signal in controlling differentiation and lineage commitment in stem cells, both through cell-cell interactions and spreading cues.

Hydrolysis represents another major route for scaffold degradation that can be utilized to facilitate tissue formation or alter scaffold properties with time. By incorporating hydrolytically degradable units into a scaffold or by altering the amount of a given degradable unit, a desired degradation profile can be achieved. For example, although cells can secrete hyaluronidases, which have the ability to degrade HA, this degradation does not occur on a time scale that promotes adequate matrix deposition in covalently crosslinked HA gels. Hydrolytically degradable lactic acid units can be incorporated into the HA backbone in order to allow for a controlled degradation rate and increased matrix production.[63] Additionally, lactic acid groups have also been incorporated into non-degradable PEG hydrogels in order to facilitate scaffold degradation and promote neural precursor differentiation into neurons and glial cells.[64] In another PEG system, the step growth polymerization of dithiothreitol (DTT) and PEG diacrylate (PEGDA) formed acrylate terminated PEG-DTT with a range of molecular

weights. Varying the extent of polymerization allowed for different molecular weights, which resulted in varied degradation and swelling properties. MSC morphology and viability were found to be dependent on network degradability as cells encapsulated in more degradable gels were more viable and spread.[65]

## 3.3 Controlled Presentation and Delivery of Differentiation Factors

In standard stem cell cultures, growth factors are simply added to culture media to induce a differentiation program. Significant advances have been made in understanding how these factors can control stem cell fates in controlled in vitro cultures.[66] While this method of simply adding a cocktail of factors to cells can be quite powerful, it is typically not possible for implantable materials and does not account for desirable spatial presentation. Thus, efforts are being made to control the spatial and temporal presentation of these factors in order to mimic the native tissue development. From a materials perspective, differentiation factors can be added directly to the medium for in vitro cultures (including with bioreactors), physically entrapped or sequestered within a scaffold, or encapsulated in micro/nanoparticles for controlled release.

### *3.3.1 Soluble Factor Delivery*

The ability to easily manipulate and control the addition of soluble factors to culture medium makes this approach the most well characterized effector of stem cell

differentiation. In combination with the morphology of clusters of cells (e.g., 2D surface for osteogenesis, 3D pellets for chondrogenesis), much is known about stem cell differentiation using standard tissue culture approaches. These factors not only participate in the commitment of cells, but also the decision of cells to remain quiescent or undifferentiated. For example, Leukemia Inhibitory Factor (LIF) is commonly employed to prevent ESCs from differentiating and is added to ESC cultures in order to allow them to proliferate without spontaneously differentiating.[67] Typically, the goal with biomaterials is to aid in stem cell differentiation; however there is also interest in materials that prevent differentiation for use as substrates in cell culture.

The addition of growth factors to cultures (either added to culture media or via material delivery) can act in synergy with other tissue engineering strategies to optimize stem cell differentiation and tissue formation. For example, bone morphogenic protein-2 (BMP-2) has been incorporated into HA hydrogels along with MSCs to promote osteogenesis, as noted by increased osteocalcin and CD31 expression compared to controls without BMP-2.[17] The TGF-β family of proteins are well documented chondrogenic factors and are typically added to scaffolds in combination with encapsulated stem cells.[7, 68] However, it is not only the addition of this growth factor that is crucial to chondrogenesis, but also the temporal presentation. Long term exposure to TGF-β2 resulted in greater GAG and collagen II production and an upregulation in Sox-9 when compared to MSCs with shorter exposure time.[69] As mentioned previously, high throughput screening can also be a useful tool for determining which factors are regulators of stem cell fate so that they can be incorporated into tissue engineering

applications.[40, 70]

*3.3.2 Immobilized Factors*

Similar to coupling cell adhesion motifs to scaffolds, differentiation factors can be specifically immobilized on a biomaterial surface to elicit a desired response. This is a common theme in nature as stem cell niches contain covalently and noncovalently bound factors that maintain the cell's undifferentiated state. Stem cell factor (SCF) and LIF are membrane-bound cytokines found in niches that support undifferentiated stem cells.[32] LIF can be added to inhibit ESC differentiation, but the immobilization of LIF can also affect ESC commitment.[71] LIF immobilized to a nonwoven polyester fabric (NWPF) using carbodiimide chemistry was shown to support a greater percentage of undifferentiated ESC colonies when compared to the NWPF only groups. The immobilized LIF was shown to be bound in its active form and had a similar effect (in terms of pluripotency maintenance) to adding soluble LIF to the culture medium. Another study immobilized both LIF and SCF in order to observe the threshold behavior of certain factors on stem cell maintenance.[72] Additionally, growth factors such as TGF-β1 have been immobilized on surfaces to promote chondrogenesis of MSCs rather than simply adding it to the culture.[73, 74]

While the ability to covalently tether factors to biomaterials has shown great promise, another technique involves a more biomimetic approach by which growth factors are sequestered using noncovalent means. Heparin is a sulfated proteoglycan that has the ability to bind and sequester growth factors and thus slow their release while maintaining their biological activity. Specifically, heparin can bind TGF- β proteins and

influence stem cell differentiation into chondrocytes, which has been demonstrated using poly(N-isopropylacrylamide-co-acrylic acid) thermoresponsive hydrogels[75] In this system, MSCs in gels containing heparin-bound TGF-β3 had significantly greater upregulation of chondrogenic markers of differentiation, specifically collagen II, Sox-9, and aggrecan. However, the applicability of this system depends specifically on the binding affinity of the protein to heparin. A similar strategy was used with a porous PLGA scaffold in which both dexamethasone and heparin-bound TGF-β1 were incorporated and its chondrogenic potential evaluated using MSCs.[76] Heparin-binding has also been utilized in electrospinning applications so that cells not only experience the desired fibrous morphology and adhesive properties of the electrospun material, but also the added effect of immobilized factors. Casper et al. covalently linked both heparin and perlecan (another sulfated proteoglycan associated with mesenchymal tissues) to collagen and gelatin electrospun scaffolds using EDC/NHS carbodiimide chemistry.[77] Using fibroblast growth factor-2 (FGF-2) as their model growth factor, they demonstrated that both heparin and perlecan effectively bound FGF-2, but perlecan displayed better binding at lower concentrations. FGF-2 is secreted by osteoblastic cells and is present in the early stages of bone repair and its biological activity is significantly enhanced by heparan sulfate binding. This method could prove useful in bone regeneration applications along with the inclusion of other heparan sulfate binding proteins such as BMP-2 and platelet-derived growth factor (PDGF).

### *3.3.3 Encapsulated Delivery Vehicles*

Another means to control the presentation of differentiation factors to the stem

cell microenvironment is through the use of biodegradable delivery vehicles. These vehicles can take the form of polymeric microparticles as well as the scaffold itself, which can be tailored to release encapsulated factors. Release is controlled through both diffusion and degradation, and thus material design is essential for released molecule presentation to stem cells.

*3.3.3.1 Controlled release from scaffolds*

A direct method to release differentiation factors to the stem cell microenvironment is through encapsulation within the 3D scaffold. As biodegradability is a desired property of biomaterials, many researchers have utilized this degradation to not only allow for remodeling of the microenvironment and ECM synthesis, but to also allow for local delivery of factors to aid in stem cell commitment and tissue repair.

Due to their highly swollen state, hydrogels are able to rapidly deliver factors to surrounding tissue or to encapsulated cells within the hydrogel. Cardiogenesis can be affected by controlled release of basic fibroblast growth factor (bFGF) from gelatin hydrogels with or without cardiosphere derived cells (CDCs) or MSCs.[78] bFGF release significantly enhanced vascularization, as well as myocardial perfusion and contractility. While coupling the delivery of bFGF with CDCs resulted in greater myocardiocyte differentiation and engraftment than bFGF treatment alone, MSCs did not exhibit the same additive effects of combined growth factor and cell transplantation on recovery of myocardial function. In order to promote greater chondrogenesis of MSCs encapsulated in hydrogels, TGF-β3 has been encapsulated during the hydrogel formation process in order to locally deliver the factor for in vivo and in vitro tissue formation.[7, 79] In one

example, MSCs were encapsulated in methacrylated HA (to allow for photocrosslinking) and either polymerized in situ with TGF-β3 or pre-cultured for 2 weeks in growth medium containing TGF-β3 and subsequently implanted subcutaneously.[7] Pre-cultured constructs exhibited higher collagen II, aggrecan, and chondroitin sulfate expression compared to constructs encapsulated with TGF-β3 and negative controls without growth factor. These results emphasize the importance of sustained release of a factor to stem cells in order to elicit the desired differentiation and tissue formation response. One approach to control release from hydrogels is by modifying the degradation rate of the network structure. Using a PEG dimethacrylate system incorporating hydrolytically degradable lactide units into the PEG backbone, Benoit et al. demonstrated a highly regulated delivery of fluvastatin, which stimulates BMP-2 production and osteogenic differentiation.[80] The release rate and dose were controlled by adjusting the lactide repeat unit length and initial fluvastatin concentration, respectively. The incorporation of controlled release into this network resulted in increased ALP, collagen I, and BMP-2 production by encapsulated human MSCs.

Both microparticles and nanoparticles have received considerable attention in applications such as cancer therapeutics and biomedical imaging modalities, but are also useful for the delivery of molecules to stem cells.[81, 82] Since stem cells undergoing lineage commitment require a specific spatio-temporal presentation of factors, efforts have been made to incorporate these particles into biomaterials for controlled release rates. It is also important to consider the activity of the encapsulated factor upon release, which is dependent upon the process for encapsulation.

*3.3.3.2 Controlled Delivery Using Particles*

Microparticles can also be utilized without a biomaterial scaffold in order to control the stem cell microenvironment. Micro- and nanoparticles have been injected with and without stem cells into injury sites to promote both neurogenesis and chondrogenesis.[83, 84] Using a water-in-oil-in-water (W/O/W) emulsion technique, ciliary neurotrophic factor and brain-derived neurotrophic factor were encapsulated in PLGA microspheres to allow for sustained release and aid in regeneration of central nervous tissue and retinal tissue, respectively. By coating larger oil-in-water (O/W) PLGA microspheres encapsulating one factor (dexamethasone, DEXA) with smaller W/O/W emulsion microspheres encapsulating another factor (dehydroepiandrosterone, DHEA), the release of multiple factors is possible.[85] The negative charges of the carboxyl on PLGA microspheres containing DHEA are electrostatically attracted to the positive charge of poly(ethyleneimine) incorporated into the DEXA-loaded microspheres. This minimally invasive injection of microspheres and stem cells could prove to be advantageous as the cells form cartilage tissue around the microspheres and then fill in the voids once they degrade.

Microspheres can also be utilized in ESC differentiation to allow for more control over the 3D microenvironment within EBs. EBs consist of an aggregate of pluripotent stem cells that possess the ability to differentiate into all the germ layers (endoderm, mesoderm, ectoderm). However, within this aggregate, the microenvironment varies by location due initially to cell-cell contact and diffusional constraints and later by local matrix and paracrine factor secretion.[86] Efforts have been made to influence the

aggregation of ESCs into EBs in order to create more uniform EB populations, but significant improvements are needed in order to exercise more control over differentiation within these aggregates.[87, 88] Encapsulation of differentiation factors into microspheres and incorporating them into differentiating EBs could allow for more control over the ESC microenvironment. Carpenedo et al. demonstrated a highly controlled method of incorporating retinoic-acid (RA) loaded PLGA microspheres into embryoid bodies.[89] Rotary suspension culture was used to allow for uniform EB formation and to facilitate the microsphere incorporation. Compared to normal EBs and EBs incorporating unloaded microspheres, EBs containing RA-loaded microspheres exhibited a very homogeneous and organized structure. Furthermore, EBs incorporating RA-loaded microspheres exhibited a completely different structure than EBs exposed to soluble RA. **Figure 3.4** illustrates these morphological differences in EBs exposed to different microenvironments as microsphere-mediated delivery of RA led to an increase in endoderm/epiblast organization as compared to the non-cystic unorganized EBs exposed to soluble RA. The desired cellular morphology, whether it is uniform or heterogeneous, of the EBs is dependent on the application. This method of locally delivering factors within a differentiating EB bypasses the limitations associated with soluble delivery as it has been shown that a dense shell containing collagen I, tight cell-cell junctions, and basement membrane hinder diffusive transport.[90]

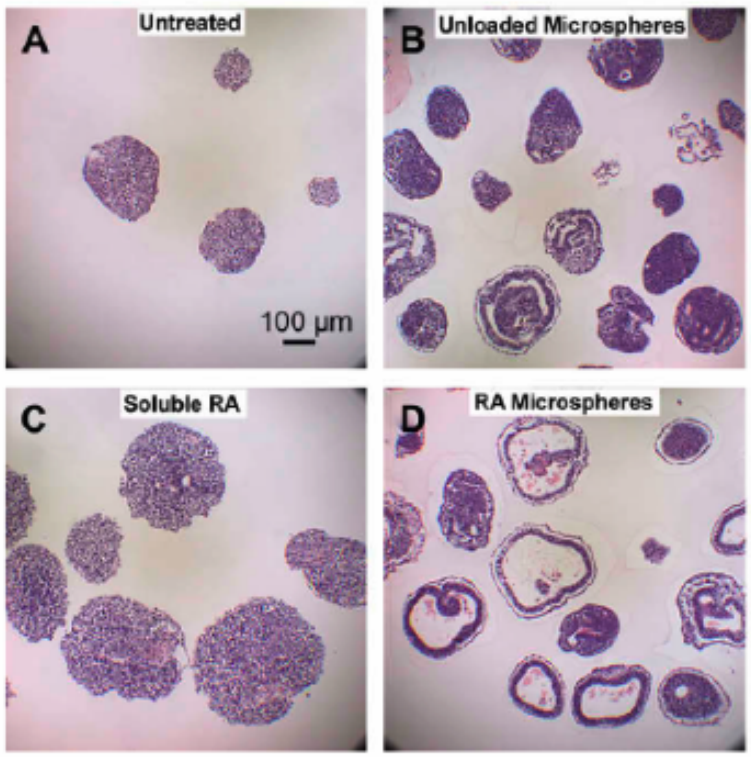


**Figure 3.4 Microsphere molecule delivery.** Hematoxylin-Eosin staining of embryoid bodies (EBs) in untreated (A), soluble retinoic acid delivery (B), unloaded incorporated microspheres (C), retinoic acid loaded incorporated microspheres (D) groups, indicating that controlled and local RA delivery controls the morphology of EBs. Reproduced with permission from [89].

Angiogenesis is a critical process with the formation of many tissue types because it allows for adequate nutrient supply and integration with native tissue. In tissue engineering applications, it is necessary to not only stimulate the differentiation of stem cells into the specialized tissue cell of interest, but to also allow for formation of vasculature in the tissue.[91] Two growth factors intimately involved in the process of vascularization are vascular endothelial growth factor (VEGF) and PDGF. However, it is

not only the presence of these two factors that influences angiogenesis, but also their temporal presentation. VEGF is responsible for the initiation of angiogenesis and involves endothelial cell activation and proliferation while PDGF is required after VEGF activation in order to allow for blood vessel maturation through recruitment of smooth muscle cells.[92] Richardson et al. developed a dual growth factor release system in which VEGF is encapsulated in the porous poly(lactide-co-glycolide) (PLG) scaffold and PDGF is encapsulated in PLG microspheres dispersed throughout the scaffold. Based on release kinetics, they demonstrated an initial rapid release of VEGF and a delayed release of PDGF, which contributed to greater maturation of vessels as evidenced by α-smooth muscle actin compared to VEGF or PDGF factor addition only. In a similar system, BMP-2 and BMP-7 loaded into PLG microspheres at different concentrations (and thus different release rates) was investigated as a system for bone tissue regeneration.93 The sequential delivery of BMP-2 and BMP-7 in porous PLG scaffolds resulted in enhanced osteogenic differentiation of MSCs as evidenced by cell proliferation and alkaline phosphatase (ALP) activity.

While PLGA microparticles have received the most attention as delivery vehicles for stem cell applications other notable microencapsulating carriers exist. Naturally-derived materials such as alginate, chitosan, and gelatin have been used to encapsulate factors based on their biocompatibility and ability to crosslink by ionic and chemical means.[94-96] Based on a given application, the release kinetics can be tailored by altering the polymer composition, method of formation and encapsulation, and post-formation processing (such as coating or complexing with other materials).

## 3.4 Material Control of Cell Morphology

Fully differentiated cells take on a variety of well-recognized shapes both in vivo and during in vitro culture ranging from striated, contractile myoblasts to spherical chondrocytes, to highly branched neurons. While there has been considerable research concerning the adoption of specific cell morphologies as a result of differentiation, the concept of cell morphology as an effector of differentiation, and not simply a consequence, has only recently received significant attention.

### *3.4.1 Cell Adhesion Regulates Morphology*

The importance of cell adhesion to materials not only involves the general support of cells and signal transduction (as mentioned in previous sections), but can also dictate cellular morphology. For instance, the effects of integrin binding and cytoskeletal organization on cell morphology and chondrogenesis were investigated using RGD-coupled agarose and alginate gels.[29, 56] Increased RGD concentrations in alginate gels resulted in a diminished expression of chondrogenic genes and deposition of collagen II and proteoglycans by encapsulated MSCs. Furthermore, soluble RGD peptide addition helped recover the chondrogenic potential since it competed with bound ligands in the gel.[56] In a follow up study, RGD coupled agarose gels were used to investigate the effect of morphology and cytoskeletal organization on MSC chondrogenesis.[29] Increased cell spreading and differences in cytoskeleton arrangement were observed in gels with higher RGD concentrations. The addition of a potent inhibitor of actin polymerization

(cytochalasin D) prevented the inhibitory effects of RGD on chondrogenesis, which reinforces the concept that integrin binding and coupling with the cytoskeleton can play a pivotal role in MSC differentiation.

The distribution of cell binding molecules also influences stem cell morphology and lineage commitment. Specifically, the formation of focal adhesion complexes has been well documented to involve integrin clustering and inside-out coupling with the actin cytoskeleton.[97, 98] Comisar et al. studied the effects of different ligand presentations on pre-osteoblast morphology and osteogenic differentiation.[30] RGD was covalently coupled to alginate gels using carbodiimide chemistry and the degree of substitution was varied to create alginate chains with a range of peptide modifications. By changing the ratio of modified to unmodified alginate for different degrees of substitution, they were able to control the total bulk RGD density, as well as the spacing of adhesive "islands." Cell morphology and osteogenic differentiation were found to be dependent on ligand spacing, while proliferation was found to be dependent on bulk RGD density. Lower ligand spacing favored focal adhesion formation and cell spreading, while higher spacing resulted in greater osteocalcin expression. The effects of bulk RGD on proliferation were shown to be biphasic, as an increase in RGD led to a maximal proliferation rate beyond which any increase in RGD density resulted in diminished proliferation.

The organization of a stem cell's cytoskeleton as a result of its microenvironment can also have a pronounced effect on lineage specification. Non-muscle myosins (NMM) have been implicated in the regulation of cell morphology and NMMIIs are particularly implicated in stem cell morphological processes.[99-101] Myoblast alignment and striation,

which are crucial to its contractility, are a result of the cell's adhesion and surrounding microenvironment. Specifically, the roles of NMMIIA and NMMIIB include involvement in the formation of myoblast bipolar morphology and prevention of over-elongating differentiating myotubes, respectively.[102] The importance of polarization is also evident as neurons exhibit a preferential directionality that is required for their functionality. Aligned fibrous scaffolds and micropatterned surfaces have been used to direct neural progenitor cells to adopt the appropriate cell morphologies due to either fiber morphology or the presence of desired adhesion molecules.[103] The addition of gelatin to PCL electrospun fibers resulted in enhanced neurite outgrowth and alignment of neural stem cells (C17.2 cells) in the direction of the electrospun fibers. The presence of alignment in collagen and collagen/carbon nanotube structures also resulted in preferential ectoderm differentiation of ESCs compared to nonaligned gelatin scaffolds, which showed differentiation into all three germ layers.[104] The synergy between adhesion and neural progenitor alignment was also demonstrated using a co-culture of hippocampal progenitor cells (HPCs) and astrocytes in the presence of patterned laminin substrates.[105] The neural stem cell niche involves specific cell-cell and cell-matrix contact and this study demonstrated that the presence of both factors (i.e., alignment and cellular interactions) influenced progenitor morphology and resulted in greater expression of a neural marker of differentiation (β3-tubulin). Similar results were found in a study involving MSCs differentiating into cardiac muscle cells.[106] Co-culture of these predifferentiated cells on aligned substrates with cardiomyocytes resulted in greater electrical conduction and upregulation of cardiogenic markers of differentiation compared to co-cultures on isotropic substrates. While adhesion to specific molecules can

initiate a differentiation program, the presentation of these adhesion sites allows for proper coupling of cell morphological and signal transduction pathways.

### *3.4.2 Control of Cell Shape Directs Differentiation*

The physical control of stem cell binding and morphology results in profound effects on stem cell behavior, including differentiation. Controlling materials through crosslinking, feature sizes, and topography represent various means to influence cell morphology, and thus differentiation.

#### *3.4.2.1 Extent and type of crosslinking controls cell morphology*

Within a 3D scaffold such as a hydrogel, the ability of a cell to spread and adopt a specific morphology can be influenced by the crosslinking density, which is either static or dynamic using nondegradable or degradable components, respectively. PEG hydrogels have been modified by several groups with varied crosslinking (e.g., length of crosslinker or incorporation of interpenetrating networks) and to incorporate hydrolytic and cell-sensitive degradation to modulate stem cell spreading.[107-109] As stated above, the mesh size can be used to control features such as ECM distribution by encapsulated stem cells. As an additional example, MSCs encapsulated in degradable PEG-co-cyclic acetal gels exhibited different morphologies based on the crosslinking density. For example, gels that were more swollen promoted a more spindled morphology than highly crosslinked gels.[110] Cell viability was high in all formulations and cell morphology was directly correlated to crosslinking density as cells were more spread in less crosslinked

networks.

Network degradation plays a temporal role in both the restriction of cell morphology and ECM synthesis of stem cells. Biomaterials provide initial adhesion and mechanical cues that influence cell morphology and signal transduction and the subsequent commitment and formation of tissue is contingent upon proper material degradation. HA hydrogels have been developed that not only influence stem cell fate decisions, but have controlled degradation to enhance ECM distribution.[63] For instance, a comparison of two nondegradable hydrogel networks (methacrylated HA and PEG diacrylate) indicated that where MSCs are maintained in a spherical shape, other factors such as cell recognition sites (such as CD44 binding to HA) and growth factors (such as TGF-β3) can control differentiation.[7] Further modifications to HA to control cell morphology have included incorporating MMP-sensitive cleavage sites, which allow for MSC spreading compared to the rounded morphology found in nondegradable crosslinked gels.[111] In a system involving vinyl-terminated 4-arm PEG, the inclusion of MMP-degradable sites allowed for spreading and the adoption of a smooth muscle cell phenotype for MSCs.[112] In this gel, both MSCs and SMCs acquired a spindled, elongated shape that influenced cytoskeletal organization and adoption of the desired smooth muscle cell phenotype. It is expected that these same trends of crosslinking and degradation are important for all types of stem cells, yet this area has focused primarily on MSCs.

*3.4.2.2 Differentiation effects of feature sizes*

Cell morphology can also be controlled by the size of features on a 2D substrate

or the size of individual components of a scaffold. The growth and differentiation of EBs in microwells of defined size has provided definitive evidence of how feature size influences stem cell fate decisions.[113] Compared to traditional suspension culture, EBs cultured in PEG-coated wells of different diameters showed remarkably lower levels of variability in terms of SSEA-1 and alpha-fetoprotein expression. EB size homogeneity is crucial for applications in which other material effects on stem cell differentiation are being studied, in order to eliminate unaccountable variability.[33, 86, 87, 89, 114] The restriction of cell spreading on functionalized surfaces has also produced interesting results concerning stem cell differentiation. MSCs cultured on fibronectin-coated islands of various sizes resulted in commitment of cells to adipocytes on smaller islands and osteoblasts on larger islands.[115] Surfaces with varying degrees of hydrophobicity and terminal end groups were also studied to determine how EB size and morphology affect ESC differentiation (similar to the microwell study).[33] After separating EB populations based on size, it was discovered that intermediate sized EBs (100-300 μm) showed the highest viability, lowest apoptotic rate, and highest differentiation potential.

Stem cells grown on fibrous scaffolds have also shown differentiation dependent behavior in terms of the fiber chemistry, size, and alignment. For example, MSCs grown on electrospun aligned PCL scaffolds showed preferential differentiation to a chondrogenic lineage on nanoscale versus microscale fibers.[116] While cells aligned in the direction of the fibers for both nano- and microscale scaffolds, the nanofibers (~500 nm diameter) promoted higher GAG and mRNA expression of collagen II and aggrecan. Similar results were observed in the case of neural stem cells (NSCs) grown on poly(L-

lactic acid) (PLLA) electrospun fibers.[117] Again, while fiber diameter did not influence the extent of alignment, NSCs were found to have a higher level of differentiation on nanofibers compared to microfibers based on neurofilament expression and neurite outgrowth. Since native ECM components possess features on the order of nanometers, these findings emphasize the importance of biomimicry when developing scaffolds for stem cell differentiation. Electrospinning allows for a great degree of control over fiber chemistry through choice of polymer, fiber size through changes in polymer concentration, and fiber alignment through design of the electrospinning apparatus.[20]

*3.4.2.3 Topography influences differentiation*

Electrospun fibers represent one means by which scaffold features can be designed in order to influence stem cell spreading and adhesion. In the same study that found that nanoscale fibers promoted chondrogenic differentiation of MSCs, it was also found that chondrogenic differentiation was enhanced on nanofibers over porous PCL scaffolds.[116] Similar to fibers of controlled diameter, several studies have been performed to investigate the influence of micropatterned ridges or grooves on stem cells. For example, patterned grooves 300 nm deep were formed with varying widths (10, 25, and 100 μm) and the osteogenic effects on MSCs were compared.[118] Based on gene microarray analysis, MSCs grown on 100 μm grooves showed a significant upregulation in genes associated with skeletal development compared to other groove sizes. In another study, the effects of topography were found to have a greater influence on MSC neurogenesis than a potent neurogenic soluble factor (retinoic acid).[119] Nanoscale grooves showed greater enhancement in MSC neural differentiation compared to smooth

or microscale groove substrates. This also provides interesting insight into the concept of transdifferentiation of stem cells, particularly MSCs transdifferentiating into neuronal cells as evidenced by increased β3-tubulin, MAP2, and glial fibrillary acidic protein expression. It should be noted that the concept of transdifferentiation of MSCs into neurons is controversial and work still needs to be performed in this area.

Beyond fibers and grooves, surface roughness has also been shown to regulate stem cell behavior. MSCs on PLGA scaffolds treated with an alkalizing agent to incorporate surface roughness resulted in upregulation of ALP, bone sialoprotein, osteocalcin, and VEGF during the initial stages of MC3T3 pre-osteoblast culture compared to non-treated PLGA scaffolds.[120] In another study, MSCs grown on He-irradiated PCL showed an increase in ALP activity and collagen production compared to non-irradiated and tissue culture polystyrene (TCPS) controls.[121] The irradiation resulted in a "smoothening" of the PCL material and, most importantly, no change in surface energy that could affect protein adsorption, thus confirming the effect surface topography has on stem cell differentiation. While these studies show conflicting results, they demonstrate a clear dependence of stem cell differentiation on surface topography.

*3.4.3 Patterned Stem Cell Morphology*

The ability to spatially control stem cell spreading and subsequent fate decisions is of great importance in tissue engineering applications due to the heterogeneous nature of tissues. Specialized zonal architecture in cartilage, cardiac muscle fiber arrangement, and the varied degrees of vascularity represent critical hierarchical organizations within tissues that provide their unique functions.[122-124] Patterning of biomaterials can be

achieved by spatially controlling the physical restraints surrounding a cell or by patterning adhesion molecules in order to control stem cell spreading.

One of the most prevalent methods of patterning 3D microenvironments is through the use of photopolymerization. The ability to spatially control the location, intensity, and duration of light allows for high pattern fidelity and extensive processing capabilities.[5] Complex hydrogel features can be produced by an additive-polymerization process in which a crosslinked PEG network is immersed in a solution of non-crosslinked PEGDA and subsequently exposed to UV light.[125] The use of a photomask restricts light (and consequently, crosslinking) to certain regions. In another additive polymerization process, PEGDA combined with amino-functionalized PEG allowed for multilayered assemblies of gels that resembled microvascular networks through multiple photopolymerization steps.[126] Another means to spatially control cell morphology is through the combination of sequential crosslinking steps that occur by distinct methods. This has been demonstrated by groups using HA as the base network, which is first crosslinked with chemical crosslinks (e.g., Michael addition) and then exposed to UV light in order to crosslink remaining methacrylate or acrylate functional groups.[127, 128] Khetan et al. demonstrated with acrylated HA hydrogels that MSC spreading can be patterned based on the type of crosslinking in specific regions. Using an MMP-degradable and thiol-terminated crosslinker, a fraction of available acrylates were consumed during the initial Michael addition crosslinking step. Exposing one half of the gel to UV light effectively restricted cell spreading in these dual crosslinked regions and allowed MSCs in non-exposed regions to thoroughly spread (**Figure 3.5**). In vasculature

and nervous tissue, the maintenance of organized cell spreading is of critical importance and the ability to photopattern and control cell morphology in distinct regions could prove useful for these applications.

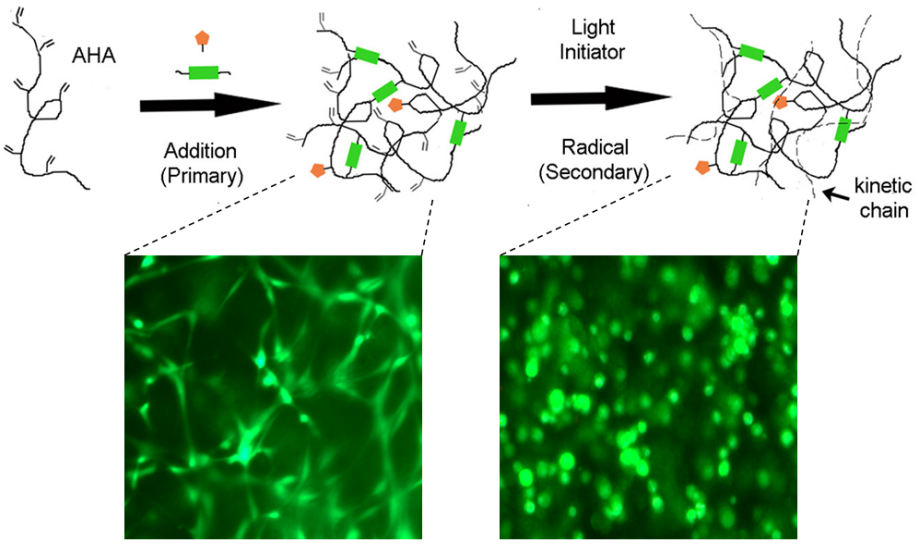


**Figure 3.5** Controlling stem cell spreading. Sequential crosslinking of hyaluronic acid hydrogels containing adhesive (orange symbols) and MMP-degradable (green rectangles) sites. Encapsulated MSCs are able to remodel the matrix after the addition crosslinking (left), but not after the radical polymerization (right). This technique allows for spatial patterning of cellular spreading when light is used for the secondary radical polymerization step.

Patterning of cell adhesion sites can also serve to control cell morphology and stem cell differentiation within a 3D scaffold. The ability of multi-photon confocal microscopy to focus light in a specific plane (and certain regions within this plane) provides the technology to photopattern adhesive molecules within a hydrogel network.[129] Similar to the additive polymerization methods, a solution of acrylated PEG-

coupled RGD peptide was allowed to equilibrate within a PEGDA network. By programming the region of interest and depth of the feature, channels of RGD adhesion sites were conferred within the PEG hydrogel. Cell spreading was restricted in regions not exposed to UV light and the coupling of RGD to exposed regions (in the form of channels) allowed for spreading and migration of cells from a fibrin cluster encapsulated within the gel. This method could be used to spatially control cell spreading and promote infiltration of recruited stem cells and vasculature.

## 3.5 Matrix Mechanics Direct Stem Cell Differentiation

Considerable evidence exists for cell mechanosensitivity, primarily in systems where cells experience external stresses, such as shear and tension, which results in changes in protein expression and, in some cases, differentiation.[130, 131] Recently, the inherent mechanical properties of a material have received considerable attention with regards to controlling stem cell behavior. The stiffness of a material is governed by the structure and composition of the network components, extent of crosslinking (both physical and covalent), and the organization of the network (whether it is anisotropic or part of an IPN).

### *3.5.1 Cell Mechanosensitivity*

Native tissues range widely in composition (ECM components) and mechanics

(0.1-1 kPa in neural tissue to on the order of GPa for fully mineralized bone tissue).[100, 132] When adhesion-dependent cells are grown on materials of varying mechanics, depending on the cell type, there are noticeable differences in terms of cell morphology and gene expression. Initial insight into the possibility of mechanics influencing stem cell fate decisions can be gained by observing the native tissue mechanics. Muscle tissue exhibits a stiffness of ~10 kPa and myoblasts cultured on polyacrylamide gels of varying mechanics showed optimal alignment and striation on substrates that mimicked this mechanical environment.[133] Furthermore, when myoblasts were cultured in multiple layers, cells exposed to the soft environment (on top of other myoblasts) differentiated into multi-nucleated, aligned myotubes more readily than those in contact with the rigid glass substrate in the bottom layer. Hepatocytes and neural cells exhibit similar stiffness-dependent behavior as the hepatocytes aggregate and neurons extend neurites (both indicative of their associated phenotypes) on more compliant (less stiff) matrices.[134] The consequences of aberrant tissue mechanics are apparent in situations such as myocardial infarction and liver disease, in which the stiffening of tissues results in changes in cell morphology and loss of tissue function.[100] Therefore, the mechanics of the tissue of interest should be accounted for when designing a material for tissue regeneration.

### *3.5.2 Controlling Stem Cells with Material Mechanics*

The ability of stem cells to sense their 3D microenvironmental mechanics is not fully understood, although there are several well-documented factors involved in mechanosensing and mechanotransduction. Specifically, the coupling of cell adhesion

molecules (such as integrins) to the cytoskeleton and the formation of focal adhesion complexes is highly dependent on matrix stiffness in both differentiated and undifferentiated cells.[135, 136] The interplay of adhesion ligands and stiffness was investigated in one study to determine possible synergistic effects of the two factors on MSC differentiation.[135] MSCs grown on substrates containing collagen I, collagen IV, fibronectin, or laminin with varying stiffness were investigated for their myogenic and osteogenic potential. Osteogenesis was regulated by both stiffness and ligand type, as MSCs showed the highest upregulation in Runx2 (a transcription factor in osteoblasts) in the stiffest polyacrylamide gels containing collagen I (a major component of native bone tissue). Myogenesis, while not as stiffness dependent as osteogenesis, required a threshold stiffness (>9 kPa) before sufficient cell spreading and upregulation in MyoD1 occurred. Non-muscle myosin (NMM) has also been implicated as part of the mechanosensing machinery. Adhesion to the matrix is governed by integrins, and coupling with the actin cytoskeleton allows the cell to form a direct link with its microenvironment, which can then be sensed through intracellular tension governed by myosin II motors. The addition of blebbistatin, a potent inhibitor of NMMII, resulted in a significant reduction in elasticity of developing zebrafish embryos and disruption of stem cell differentiation.[137] Different isoforms of NMMII also showed varied expression at different stiffnesses, but one isoform (NMMIIA) showed little variation among different stiffnesses, possibly suggesting its ubiquitous role in mechanosensing.

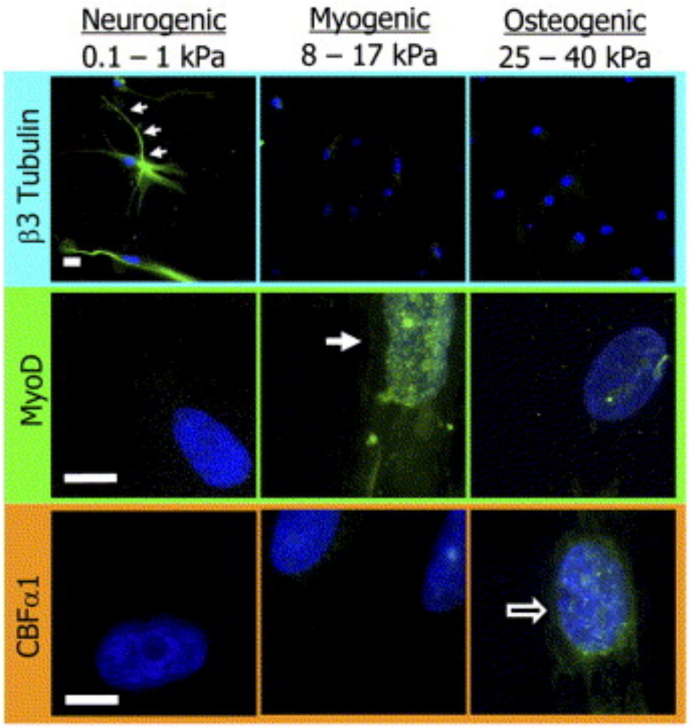


**Figure 3.6** Matrix mechanics dictates MSC differentiation. MSCs grown on polacrylamide gels of 3 stiffnesses (0.1-1 kPa, 8-17 kPa, and 25-40 kPa) expressed differentiation markers characteristic of cells found in tissues exhibiting similar stiffnesses. b3-tubulin indicates presence of neurogenic cytoskeletal filaments, myogenic differentiation factor 1 (MyoD1) a myogenic transcription factor, and core binding factor alpha 1 (CBFA1) an osteogenic transcription factor. Reproduced with permission from [138].

The effect of stiffness on stem cell differentiation is best exemplified by Engler et al. in which polyacrylamide gels of varying stiffness and constant collagen I concentration were used to examine MSC behavior.[138] **Figure 3.6** illustrates the striking expression profiles for cells grown on gels with elasticity matching the native tissue elasticity. Cells grown on soft (0.1-1 kPa), intermediate (11 kPa), and stiff (34 kPa,

similar to non-mineralized bone) gels differentiated to neurogenic, myogenic, and osteogenic lineages, respectively. Addition of blebbistatin to cultures effectively inhibited this mechanosensing by disrupting the actin cytoskeleton and intracellular tension. This lineage commitment was found to depend solely on the elasticity of the substrate since the cells were exposed to a constant collagen density and cultured in growth medium without differentiation factors.

The effects of mechanics on NSCs were examined using a semi-IPN network of polyacrylamide and PEG.[139] The addition of PEG to the network allows for modulation of mechanics (due to PEG hydrophilicity) without contributing to the biofunctionality of the material, as the RGD concentration was kept constant. NSCs cultured on these semi-IPNs showed differentiation profiles that correlated well with native tissue (i.e., neurons formed on softer substrates and astrocytes formed on stiffer substrates). This observed differentiation behavior is consistent with other studies in which primary neurons and astrocytes were cultured on gels of various moduli.[140, 141]

Local mechanical control of stem cell microenvironments can also be accomplished by patterning colonies of cells. In MSC aggregates grown on patterned cell adhesive surfaces, patterns of differentiation were observed that corresponded with local strains experienced by cells.[142] In rounded aggregates, a radial pattern of differentiation was observed where cells in the center were committed to an adipogenic lineage and cells in the periphery were driven to an osteogenic lineage (**Figure 3.7**). Furthermore, in more complex geometries, field strains experienced by cells resulted in patterned differentiation behavior, where cells in softer regions were driven to adipogenesis versus

stiffer regions where cells were driven to osteogenesis. In this same study, MSCs exhibited a differentiation pattern similar to that of long bones (i.e., osteogenic zones on the outside and an inner adipogenic zone) when cultured in 3D tubular collagen hydrogels. The use of a constitutively active Rho-kinase gene (involved in cytoskeletal tension) resulted in a thicker osteogenic outer zone due to an increase in tractional forces and local mechanics.

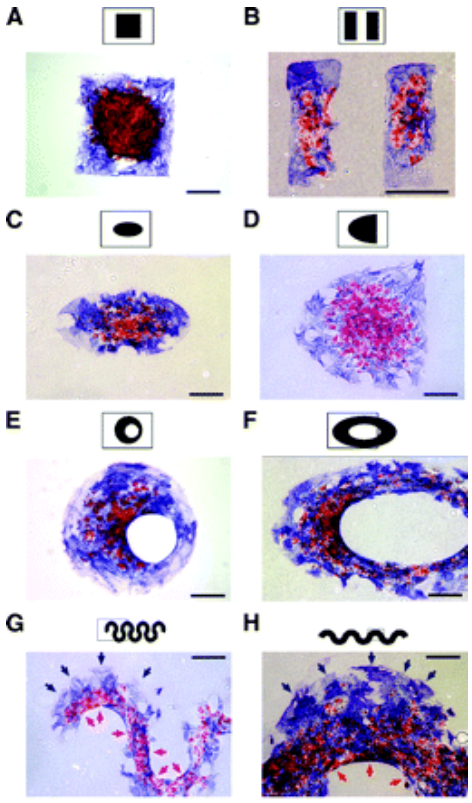


**Figure 3.7** Patterned organization of differentiating MSC aggregates. Fat droplets (red) and alkaline phosphatase (blue) activity were localized to specific regions corresponding to traction forces and geometry: square (A), rectangle (B), ellipse (C), half-ellipse (D), offset annulus (E), elliptical annulus (F), and sinusoidal bands (G, H) after 14 days. Red arrows indicate adipogenesis at concave edges, and blue arrows indicate osteogenesis at convex edges. Scale bars = 250 μm. Reproduced with permission from [142].

Pre-osteoblasts exposed to soft and stiff RGD-functionalized PEG gels expressed higher levels of MAPK activation and osteocalcin secretion on stiffer gels.[143] Activation of MAPK (through phosphorylation) has been associated with focal adhesions and further downstream activation of Runx2, which regulates osteocalcin and ALP expression. RhoA is another molecule involved in the generation of intracellular tension, and is influenced by matrix mechanics in both differentiated and undifferentiated cells. RhoA expression can be controlled by altering the cell morphology, as well as the stiffness of the substrate.[115, 144] Changes in RhoA expression in MSCs seeded on soft and stiff polyacrylamide gels resulted in different Ca2+ oscillations.[145] MSC Ca2+ oscillations are controlled by ROCK, a downstream effector molecule of RhoA, and therefore can be modulated by the mechanics of the substrate. Cells such as pancreatic acinar cells and cardiomyocytes demonstrate spontaneous Ca2+ oscillations, and applications involving these tissues would likely benefit from the use of materials with tunable mechanics to direct stem cell differentiation.

Hydrogels with controlled mechanics have also been used to investigate the differences in mechanosensitivity of various cell types. Cells can possess varied degrees of mechanosensitivity, from highly sensitive cells (fibroblasts) to highly insensitive cells (neutrophils).[146] Interestingly, stem cells alter their mechanosensitivity based on their level of commitment or "differentiation stage." A clonally derived bone marrow stem cell line (D1), able to differentiate to adipo-, chondro-, and osteogenic lineages, and a more committed pre-osteoblast cell line were cultured in the presence of RGD-coupled alginate gels with varied mechanics (20, 60, 110 kPa) by changing the amount of

Ca2+.[147] The pre-osteoblasts showed higher mechanosensitivity (as evidenced by cell proliferation) than the undifferentiated D1 cell line. However, when the D1 cells were pre-differentiated to a pre-osteoblast-like state, their mechanosensitivity increased dramatically and was nearly identical to the MC3T3 cells. This change in mechanosensitivity may be attributed to different integrin expression patterns of the uncommitted and more committed pre-osteoblast cells. This could also explain the observed difference in mechanosensitivity for MSCs undergoing myogenesis and osteogenesis differentiation.[135]

### 3.6 Conclusions

In order to effectively control stem cell differentiation, many aspects of the microenvironment must be considered including soluble factor presentation, matrix mechanics and chemistry, and topography. Because cells in the body are exposed to highly evolved, complex environments, biomaterials that provide these cues can not be passive or static, but should be instructive and dynamic. If a material is to be used to direct stem cell lineage commitment, it is important to consider the desired spatial and temporal context of specific cues. While many of the methods to control stem cell differentiation can be utilized individually, it is the incorporation of material control over many aspects of the 3D microenvironment that will be necessary to create fully functional tissue equivalents, particularly with complex multi-cellular tissues.

**REFERENCES:**


1. R. M. Nerem. Tissue engineering: the hope, the hype, and the future, *Tissue Engineering*, 2006, **12**, 1143-1150.
2. E. Dawson, G. Mapili, K. Erickson, S. Taqvi and K. Roy. Biomaterials for stem cell differentiation, *Advanced Drug Delivery Reviews*, 2008, **60**, 215-228.
3. J. Elisseeff, A. Ferran, S. Hwang, S. Varghese and Z. Zhang. The role of biomaterials in stem cell differentiation: applications in the musculoskeletal system, *Stem Cells Dev*, 2006, **15**, 295-303.
4. J. A. Burdick and G. Vunjak-Novakovic. Review: Engineered Microenvironments for Controlled Stem Cell Differentiation, *Tissue Engineering Part A*, 2008.
5. J. Ifkovits and J. Burdick. Review: Photopolymerizable and Degradable Biomaterials for Tissue Engineering Applications, *Tissue Engineering*, 2007, **13**, 2369-2385.
6. M. Lutolf and J. Hubbell. Synthetic biomaterials as instructive extracellular microenvironments for morphogenesis in tissue engineering, *Nat Biotechnol*, 2005, **23**, 47-55.
7. C. Chung and J. Burdick. Influence of three-dimensional hyaluronic Acid microenvironments on mesenchymal stem cell chondrogenesis, *Tissue Engineering Part A*, 2009, **15**, 243-254.
8. J. Xu, W. Wang, M. Ludeman, K. Cheng, T. Hayami, J. Lotz and S. Kapila. Chondrogenic Differentiation of Human Mesenchymal Stem Cells in Three-Dimensional Alginate Gels, *Tissue Engineering Part A*, 2008, **14**, 667-680.

9. T. P. Kraehenbuehl, P. Zammaretti, A. J. Van der Vlies, R. G. Schoenmakers, M. P. Lutolf, M. E. Jaconi and J. A. Hubbell. Three-dimensional extracellular matrix-directed cardioprogenitor differentiation: systematic modulation of a synthetic cell-responsive PEG-hydrogel, *Biomaterials*, 2008, **29**, 2757-2766.

10. Y. Yeo, W. Geng, T. Ito, D. Kohane, J. Burdick and M. Radisic. Photocrosslinkable hydrogel for myocyte cell culture and injection, *J. Biomed. Mater. Res.*, 2007, **81B**, 312-322.

11. J. J. Schmidt, J. Rowley and H. Kong. Hydrogels used for cell-based drug delivery, *J. Biomed. Mater. Res.*, 2008, **87**, 1113-1122.

12. N. S. Hwang, S. Varghese, P. Theprungsirikul, A. Canver and J. Elisseeff. Enhanced chondrogenic differentiation of murine embryonic stem cells in hydrogels with glucosamine, *Biomaterials*, 2006, **27**, 6015-6023.

13. K. Saha, E. F. Irwin, J. Kozhukh, D. V. Schaffer and K. E. Healy. Biomimetic interfacial interpenetrating polymer networks control neural stem cell behavior, *J. Biomed. Mater. Res.*, 2007, **81**, 240-249.

14. X. Zheng Shu, Y. Liu, F. S. Palumbo, Y. Luo and G. D. Prestwich. In situ crosslinkable hyaluronan hydrogels for tissue engineering, *Biomaterials*, 2004, **25**, 1339-1348.

15. J. Baier Leach, K. A. Bivens, C. W. Patrick and C. E. Schmidt. Photocrosslinked hyaluronic acid hydrogels: natural, biodegradable tissue engineering scaffolds, *Biotechnol. Bioeng.*, 2003, **82**, 578-589.

16. K. A. Smeds, A. Pfister-Serres, D. Miki, K. Dastgheib, M. Inoue, D. L. Hatchell and M. W. Grinstaff. Photocrosslinkable polysaccharides for in situ hydrogel formation, *J. Biomed. Mater. Res.*, 2001, **54**, 115-121.

17. J. Kim, I. S. Kim, T. H. Cho, K. B. Lee, S. J. Hwang, G. Tae, I. Noh, S. H. Lee, Y. Park and K. Sun. Bone regeneration using hyaluronic acid-based hydrogel with bone morphogenic protein-2 and human mesenchymal stem cells, *Biomaterials*, 2007, **28**, 1830-1837.

18. C. Barnes, S. Sell, E. Boland, D. Simpson and G. Bowlin. Nanofiber technology: Designing the next generation of tissue engineering scaffolds☆, *Advanced Drug Delivery Reviews*, 2007, **59**, 1413-1433.

19. P. Janmey, J. P. Winer and J. W. Weisel. Fibrin gels and their clinical and bioengineering applications, *Journal of the Royal Society, Interface / the Royal Society*, 2009, **6**, 1-10.

20. T. J. Sill and H. A. von Recum. Electrospinning: applications in drug delivery and tissue engineering, *Biomaterials*, 2008, **29**, 1989-2006.

21. A. R. Tan, J. Ifkovits, B. M. Baker, D. M. Brey, R. L. Mauck and J. Burdick. Electrospinning of photocrosslinked and degradable fibrous scaffolds, *J. Biomed. Mater. Res.*, 2008, **87**, 1034-1043.

22. B. M. Baker and R. L. Mauck. The effect of nanofiber alignment on the maturation of engineered meniscus constructs, *Biomaterials*, 2007, **28**, 1967-1977.

23. B. M. Baker, A. O. Gee, R. B. Metter, A. S. Nathan, R. A. Marklein, J. A. Burdick and R. L. Mauck. The potential to improve cell infiltration in composite

fiber-aligned electrospun scaffolds by the selective removal of sacrificial fibers, *Biomaterials*, 2008, **29**, 2348-2358.

24. X. Liu and P. Ma. Polymeric scaffolds for bone tissue engineering, *Annals of biomedical engineering*, 2004, **32**, 477-486.

25. M. P. Linnes, B. D. Ratner and C. M. Giachelli. A fibrinogen-based precision microporous scaffold for tissue engineering, *Biomaterials*, 2007, **28**, 5298-5306.

26. C. E. Petrie Aronin, J. A. Cooper, L. S. Sefcik, S. S. Tholpady, R. C. Ogle and E. A. Botchwey. Osteogenic differentiation of dura mater stem cells cultured in vitro on three-dimensional porous scaffolds of poly(epsilon-caprolactone) fabricated via co-extrusion and gas foaming, *Acta biomaterialia*, 2008, **4**, 1187-1197.

27. M. R. Alison and S. Islam. Attributes of adult stem cells, *J Pathol*, 2009, **217**, 144-160.

28. F. Yang, C. G. Williams, D. A. Wang, H. Lee, P. N. Manson and J. Elisseeff. The effect of incorporating RGD adhesive peptide in polyethylene glycol diacrylate hydrogel on osteogenesis of bone marrow stromal cells, *Biomaterials*, 2005, **26**, 5991-5998.

29. J. T. Connelly, A. J. García and M. E. Levenston. Interactions between integrin ligand density and cytoskeletal integrity regulate BMSC chondrogenesis, *J. Cell. Physiol.*, 2008, **217**, 145-154.

30. W. A. Comisar, N. H. Kazmers, D. Mooney and J. J. Linderman. Engineering RGD nanopatterned hydrogels to control preosteoblast behavior: a combined computational and experimental approach, *Biomaterials*, 2007, **28**, 4409-4417.

31. M. M. Martino, M. Mochizuki, D. A. Rothenfluh, S. A. Rempel, J. A. Hubbell and T. H. Barker. Controlling integrin specificity and stem cell differentiation in 2D and 3D environments through regulation of fibronectin domain stability, *Biomaterials*, 2009, **30**, 1089-1097.

32. S. M. Dellatore, A. S. Garcia and W. M. Miller. Mimicking stem cell niches to increase stem cell expansion, *Current Opinion in Biotechnology*, 2008, **19**, 534-540.

33. B. Valamehr, S. J. Jonas, J. Polleux, R. Qiao, S. Guo, E. H. Gschweng, B. Stiles, K. Kam, T. J. Luo, O. N. Witte, X. Liu, B. Dunn and H. Wu. Hydrophobic surfaces for enhanced differentiation of embryonic stem cell-derived embryoid bodies, *Proc Natl Acad Sci USA*, 2008, **105**, 14459-14464.

34. D. S. Benoit, M. P. Schwartz, A. R. Durney and K. S. Anseth. Small functional groups for controlled differentiation of hydrogel-encapsulated human mesenchymal stem cells, *Nature materials*, 2008, **7**, 816-823.

35. L. Jongpaiboonkit, W. J. King and W. L. Murphy. Screening for 3D Environments That Support Human Mesenchymal Stem Cell Viability Using Hydrogel Arrays, *Tissue Engineering Part A*, 2008.

36. C. J. Flaim, S. Chien and S. N. Bhatia. An extracellular matrix microarray for probing cellular differentiation, *Nat Methods*, 2005, **2**, 119-125.

37. G. H. Underhill and S. N. Bhatia. High-throughput analysis of signals regulating stem cell fate and function, *Current opinion in chemical biology*, 2007, **11**, 357-366.

38. D. G. Anderson, S. Levenberg and R. Langer, in *Nat Biotechnol*, 2004, vol. 22, pp. 863-866.

39. D. G. Anderson, D. Putnam, E. B. Lavik, T. A. Mahmood and R. Langer. Biomaterial microarrays: rapid, microscale screening of polymer-cell interaction, *Biomaterials*, 2005, **26**, 4892-4897.

40. A. Peters, D. M. Brey and J. A. Burdick. High-throughput and Combinatorial Technologies for Tissue Engineering Applications, *Tissue engineering Part B, Reviews*, 2009.

41. D. M. Brey, I. Erickson and J. Burdick. Influence of macromer molecular weight and chemistry on poly(beta-amino ester) network properties and initial cell interactions, *J. Biomed. Mater. Res.*, 2008, **85**, 731-741.

42. D. M. Brey, J. Ifkovits, R. I. Mozia, J. S. Katz and J. Burdick. Controlling poly(beta-amino ester) network properties through macromer branching, *Acta biomaterialia*, 2008, **4**, 207-217.

43. D. G. Anderson, C. A. Tweedie, N. Hossain, S. M. Navarro, D. M. Brey, K. J. Van Vliet, R. Langer and J. Burdick, in *Adv Mater*, 2006, vol. 18, pp. 2614-+.

44. J. C. Schense and J. Hubbell. Cross-linking exogenous bifunctional peptides into fibrin gels with factor XIIIa, *Bioconjug Chem*, 1999, **10**, 75-81.

45. H. Liu, S. F. Collins and L. J. Suggs. Three-dimensional culture for expansion and differentiation of mouse embryonic stem cells, *Biomaterials*, 2006, **27**, 6004-6014.

46. G. Zhang, X. Wang, Z. Wang, J. Zhang and L. Suggs. A PEGylated fibrin patch for mesenchymal stem cell delivery, *Tissue Engineering*, 2006, **12**, 9-19.

47. R. Nair, S. Shukla and T. C. McDevitt. Acellular matrices derived from differentiating embryonic stem cells, *J. Biomed. Mater. Res.*, 2008, **87**, 1075-1085.

48. R. Nair, A. V. Ngangan and T. C. McDevitt. Efficacy of solvent extraction methods for acellularization of embryoid bodies, *Journal of biomaterials science Polymer edition*, 2008, **19**, 801-819.

49. M. A. Serban and G. D. Prestwich. Modular extracellular matrices: solutions for the puzzle, *Methods*, 2008, **45**, 93-98.

50. X. Shu, Y. Liu, Y. Luo, M. Roberts and G. D. Prestwich. Disulfide Cross-Linked Hyaluronan Hydrogels, *Biomacromolecules*, 2002, **3**, 1304-1311.

51. I. E. Erickson, A. H. Huang, C. Chung, R. T. Li, J. A. Burdick and R. L. Mauck. Differential Maturation and Structure-Function Relationships in MSC- and Chondrocyte-Seeded Hydrogels, *Tissue Engineering Part A*, 2009.

52. D. L. Hern and J. A. Hubbell. Incorporation of adhesion peptides into nonadhesive hydrogels useful for tissue resurfacing, *J. Biomed. Mater. Res.*, 1998, **39**, 266-276.

53. S. Royce Hynes, L. M. McGregor, M. Ford Rauch and E. B. Lavik. Photopolymerized poly(ethylene glycol)/poly(L-lysine) hydrogels for the delivery of neural progenitor cells, *Journal of biomaterials science Polymer edition*, 2007, **18**, 1017-1030.

54. C. N. Salinas and K. S. Anseth. The enhancement of chondrogenic differentiation of human mesenchymal stem cells by enzymatically regulated RGD functionalities, *Biomaterials*, 2008, **29**, 2370-2377.

55. A. M. DeLise, L. Fischer and R. S. Tuan. Cellular interactions and signaling in cartilage development, *Osteoarthr Cartil*, 2000, **8**, 309-334.

56. J. T. Connelly, A. J. García and M. E. Levenston. Inhibition of in vitro chondrogenesis in RGD-modified three-dimensional alginate gels, *Biomaterials*, 2007, **28**, 1071-1083.

57. Y. J. Li, E. H. Chung, R. T. Rodriguez, M. T. Firpo and K. E. Healy. Hydrogels as artificial matrices for human embryonic stem cell self-renewal, *J. Biomed. Mater. Res.*, 2006, **79**, 1-5.

58. M. Lutolf, J. L. Lauer-Fields, H. G. Schmoekel, A. T. Metters, F. E. Weber, G. B. Fields and J. Hubbell. Synthetic matrix metalloproteinase-sensitive hydrogels for the conduction of tissue regeneration: engineering cell-invasion characteristics, *Proc Natl Acad Sci USA*, 2003, **100**, 5413-5418.

59. L. Urech, A. G. Bittermann, J. A. Hubbell and H. Hall. Mechanical properties, proteolytic degradability and biological modifications affect angiogenic process extension into native and modified fibrin matrices in vitro, *Biomaterials*, 2005, **26**, 1369-1379.

60. S. Hong, J. K. Kang, J. J. Park, E. S. Ryu, S. S. Choi, S. H. Lee, J. H. Lee and J. S. Seo. Association of Matrix metalloproteinase-3 with cardiogenic activity during Noggin-induced differentiation of mouse embryonic stem cells, *Int J Cardiol*, 2009.

61. B. Z. Barkho, A. E. Munoz, X. Li, L. Li, L. A. Cunningham and X. Zhao. Endogenous matrix metalloproteinase (MMP)-3 and MMP-9 promote the

differentiation and migration of adult neural progenitor cells in response to chemokines, *Stem Cells*, 2008, **26**, 3139-3149.

62. S. Khetan, J. S. Katz and J. Burdick. Sequential crosslinking to control cellular spreading in 3-dimensional hydrogels *Soft Matter*, 2009.

63. S. Sahoo, C. Chung, S. Khetan and J. Burdick. Hydrolytically degradable hyaluronic acid hydrogels with controlled temporal structures, *Biomacromolecules*, 2008, **9**, 1088-1092.

64. M. Mahoney and K. Anseth. Three-dimensional growth and function of neural tissue in degradable polyethylene glycol hydrogels, *Biomaterials*, 2006, **27**, 2265-2274.

65. G. A. Hudalla, T. S. Eng and W. L. Murphy. An approach to modulate degradation and mesenchymal stem cell behavior in poly(ethylene glycol) networks, *Biomacromolecules*, 2008, **9**, 842-849.

66. A. Khademhosseini, R. Langer, J. Borenstein and J. P. Vacanti. Microscale technologies for tissue engineering and biology, *Proc Natl Acad Sci USA*, 2006, **103**, 2480-2487.

67. C. M. Metallo, J. C. Mohr, C. J. Detzel, J. J. de Pablo, B. J. Van Wie and S. P. Palecek. Engineering the stem cell microenvironment, *Biotechnol Prog*, 2007, **23**, 18-23.

68. B. Shen, A. Wei, H. Tao, A. D. Diwan and D. D. Ma. BMP-2 Enhances TGF-beta3-Mediated Chondrogenic Differentiation of Human Bone Marrow Multipotent Mesenchymal Stromal Cells in Alginate Bead Culture, *Tissue Engineering Part A*, 2008.

69. H. J. Kim, Y. J. Kim and G. I. Im. Is Continuous Treatment with Transforming Growth Factor-Beta Necessary to Induce Chondrogenic Differentiation in Mesenchymal Stem Cells?, *Cells Tissues Organs (Print)*, 2008.

70. A. H. Huang, N. A. Motlekar, A. Stein, S. L. Diamond, E. M. Shore and R. L. Mauck. High-throughput screening for modulators of mesenchymal stem cell chondrogenesis, *Annals of biomedical engineering*, 2008, **36**, 1909-1921.

71. G. Cetinkaya, H. Türkoğlu, S. Arat, H. Odaman, M. A. Onur, M. Gümüşderelioğlu and A. Tümer. LIF-immobilized nonwoven polyester fabrics for cultivation of murine embryonic stem cells, *J. Biomed. Mater. Res.*, 2007, **81**, 911-919.

72. K. Alberti, R. E. Davey, K. Onishi, S. George, K. Salchert, F. P. Seib, M. Bornhäuser, T. Pompe, A. Nagy, C. Werner and P. W. Zandstra. Functional immobilization of signaling proteins enables control of stem cell fate, *Nat Methods*, 2008, **5**, 645-650.

73. C. H. Chou, W. T. Cheng, C. C. Lin, C. H. Chang, C. C. Tsai and F. H. Lin. TGF-beta1 immobilized tri-co-polymer for articular cartilage tissue engineering, *J Biomed Mater Res Part B Appl Biomater*, 2006, **77**, 338-348.

74. M. C. Degat, L. Dahri-Correia, F. Lavigne, A. Meunier, L. Sedel, J. Correia, H. Petite and D. Logeart-Avramoglou. Benzylaminated dextran-modified hydrogels: A long-term bioactive TGF-beta1 carrier, *J. Biomed. Mater. Res.*, 2009.

75. J. S. Park, D. G. Woo, H. N. Yang, H. J. Lim, H. M. Chung and K. H. Park. Heparin-bound transforming growth factor-beta3 enhances neocartilage formation by rabbit mesenchymal stem cells, *Transplantation*, 2008, **85**, 589-596.

76. K. Park, K. J. Cho, J. J. Kim, I. H. Kim and D. K. Han. Functional PLGA Scaffolds for Chondrogenesis of Bone-Marrow-Derived Mesenchymal Stem Cells, *Macromol. Biosci.*, 2008, **9**, 221-229.

77. C. L. Casper, W. Yang, M. C. Farach-Carson and J. F. Rabolt. Coating electrospun collagen and gelatin fibers with perlecan domain I for increased growth factor binding, *Biomacromolecules*, 2007, **8**, 1116-1123.

78. N. Takehara, Y. Tsutsumi, K. Tateishi, T. Ogata, H. Tanaka, T. Ueyama, T. Takahashi, T. Takamatsu, M. Fukushima, M. Komeda, M. Yamagishi, H. Yaku, Y. Tabata, H. Matsubara and H. Oh. Controlled delivery of basic fibroblast growth factor promotes human cardiosphere-derived cell engraftment to enhance cardiac repair for chronic myocardial infarction, *J Am Coll Cardiol*, 2008, **52**, 1858-1865.

79. K. H. Park and K. Na. Effect of growth factors on chondrogenic differentiation of rabbit mesenchymal cells embedded in injectable hydrogels, *J Biosci Bioeng*, 2008, **106**, 74-79.

80. D. S. Benoit, C. R. Nuttelman, S. D. Collins and K. S. Anseth. Synthesis and characterization of a fluvastatin-releasing hydrogel delivery system to modulate hMSC differentiation and function for bone regeneration, *Biomaterials*, 2006, **27**, 6102-6110.

81. J. Kettenbach, A. Stadler, I. V. Katzler, R. Schernthaner, M. Blum, J. Lammer and T. Rand. Drug-loaded microspheres for the treatment of liver cancer: review of current results, *Cardiovascular and interventional radiology*, 2008, **31**, 468-476.

82. A. L. Doiron, K. A. Homan, S. Emelianov and L. Brannon-Peppas. Poly(Lactic-co-Glycolic) Acid as a Carrier for Imaging Contrast Agents, *Pharm Res*, 2009, **26**, 674-682.

83. M. K. Nkansah, S. Y. Tzeng, A. M. Holdt and E. B. Lavik. Poly(lactic-co-glycolic acid) nanospheres and microspheres for short- and long-term delivery of bioactive ciliary neurotrophic factor, *Biotechnol. Bioeng.*, 2008, **100**, 1010-1019.

84. M. J. Seiler, B. B. Thomas, Z. Chen, S. Arai, S. Chadalavada, M. J. Mahoney, S. R. Sadda and R. B. Aramant. BDNF-treated retinal progenitor sheets transplanted to degenerate rats: improved restoration of visual function, *Exp Eye Res*, 2008, **86**, 92-104.

85. K. Park, J. S. Park, D. G. Woo, H. N. Yang, H. M. Chung and K. H. Park. The use of chondrogenic differentiation drugs to induce stem cell differentiation using double bead microsphere structure, *Biomaterials*, 2008, **29**, 2490-2500.

86. A. M. Bratt-Leal, R. L. Carpenedo and T. C. McDevitt. Engineering the embryoid body microenvironment to direct embryonic stem cell differentiation, *Biotechnol Prog*, 2009, **25**, 43-51.

87. R. L. Carpenedo, C. Y. Sargent and T. C. McDevitt. Rotary suspension culture enhances the efficiency, yield, and homogeneity of embryoid body differentiation, *Stem Cells*, 2007, **25**, 2224-2234.

88. A. Mogi, H. Ichikawa, C. Matsumoto, T. Hieda, D. Tomotsune, S. Sakaki, S. Yamada and K. Sasaki. The method of mouse embryoid body establishment affects structure and developmental gene expression, *Tissue & cell*, 2009, **41**, 79-84.

89. R. L. Carpenedo, A. M. Bratt-Leal, R. A. Marklein, S. A. Seaman, N. J. Bowen, J. F. McDonald and T. C. McDevitt. Homogeneous and organized differentiation within embryoid bodies induced by microsphere-mediated delivery of small molecules, *Biomaterials*, 2009.

90. E. Sachlos and D. T. Auguste. Embryoid body morphology influences diffusive transport of inductive biochemicals: a strategy for stem cell differentiation, *Biomaterials*, 2008, **29**, 4471-4480.

91. M. W. Laschke, Y. Harder, M. Amon, I. Martin, J. Farhadi, A. Ring, N. Torio-Padron, R. Schramm, M. Rücker, D. Junker, J. M. Häufel, C. Carvalho, M. Heberer, G. Germann, B. Vollmar and M. D. Menger. Angiogenesis in tissue engineering: breathing life into constructed tissue substitutes, *Tissue Engineering*, 2006, **12**, 2093-2104.

92. T. P. Richardson, M. C. Peters, A. B. Ennett and D. J. Mooney. Polymeric system for dual growth factor delivery, *Nat Biotechnol*, 2001, **19**, 1029-1034.

93. F. B. Basmanav, G. T. Kose and V. Hasirci. Sequential growth factor delivery from complexed microspheres for bone tissue engineering, *Biomaterials*, 2008, **29**, 4195-4204.

94. Y. Qin, G. X. Pei, D. M. Xie, D. Jin and K. H. Wei. [Effect of bone morphogenetic protein microspheres on biological behavior of rabbit bone marrow stem cells], *Di Yi Jun Yi Da Xue Xue Bao*, 2003, **23**, 1021-1024.

95. X. Niu, Q. Feng, M. Wang, X. Guo and Q. Zheng. Preparation and characterization of chitosan microspheres for controlled release of synthetic oligopeptide derived from BMP-2, *Journal of Microencapsulation*, 2008, 1-9.

96. H. Fan, C. Zhang, J. Li, L. Bi, L. Qin, H. Wu and Y. Hu. Gelatin microspheres containing TGF-beta3 enhance the chondrogenesis of mesenchymal stem cells in modified pellet culture, *Biomacromolecules*, 2008, **9**, 927-934.

97. E. Cukierman, R. Pankov, D. R. Stevens and K. M. Yamada. Taking cell-matrix adhesions to the third dimension, *Science*, 2001, **294**, 1708-1712.

98. M. Kato and M. Mrksich. Using model substrates to study the dependence of focal adhesion formation on the affinity of integrin-ligand complexes, *Biochemistry*, 2004, **43**, 2699-2707.

99. A. L. Zajac and D. E. Discher. Cell differentiation through tissue elasticity-coupled, myosin-driven remodeling, *Curr Opin Cell Biol*, 2008, **20**, 609-615.

100. F. Rehfeldt, A. Engler, A. Eckhardt, F. Ahmed and D. Discher. Cell responses to the mechanochemical microenvironment—Implications for regenerative medicine and drug delivery☆, *Advanced Drug Delivery Reviews*, 2007, **59**, 1329-1339.

101. P. Patwari and R. T. Lee. Mechanical control of tissue morphogenesis, *Circ Res*, 2008, **103**, 234-243.

102. N. T. Swailes, M. Colegrave, P. J. Knight and M. Peckham. Non-muscle myosins 2A and 2B drive changes in cell morphology that occur as myoblasts align and fuse, *J Cell Sci*, 2006, **119**, 3561-3570.

103. L. Ghasemi-Mobarakeh, M. P. Prabhakaran, M. Morshed, M. H. Nasr-Esfahani and S. Ramakrishna. Electrospun poly(epsilon-caprolactone)/gelatin nanofibrous scaffolds for nerve tissue engineering, *Biomaterials*, 2008, **29**, 4532-4539.

104. I. Sridharan, T. Kim and R. Wang. Adapting collagen/CNT matrix in directing hESC differentiation, *Biochem Biophys Res Commun*, 2009.

105. J. B. Recknor, D. S. Sakaguchi and S. K. Mallapragada. Directed growth and selective differentiation of neural progenitor cells on micropatterned polymer substrates, *Biomaterials*, 2006, **27**, 4098-4108.

106. D. A. Pijnappels, M. J. Schalij, A. A. Ramkisoensing, J. van Tuyn, A. A. de Vries, A. van der Laarse, D. L. Ypey and D. E. Atsma. Forced alignment of mesenchymal stem cells undergoing cardiomyogenic differentiation affects functional integration with cardiomyocyte cultures, *Circ Res*, 2008, **103**, 167-176.

107. A. Buxton, J. Zhu, R. Marchant, J. West, J. Yoo and B. Johnstone. Design and characterization of poly(ethylene glycol) photopolymerizable semi-interpenetrating networks for chondrogenesis of human mesenchymal stem cells, *Tissue Engineering*, 2007, **13**, 2549-2560.

108. H. Park, X. Guo, J. S. Temenoff, Y. Tabata, A. I. Caplan, F. K. Kasper and A. G. Mikos. Effect of Swelling Ratio of Injectable Hydrogel Composites on Chondrogenic Differentiation of Encapsulated Rabbit Marrow Mesenchymal Stem Cells In Vitro, *Biomacromolecules*, 2009.

109. S. Varghese, N. S. Hwang, A. C. Canver, P. Theprungsirikul, D. W. Lin and J. Elisseeff. Chondroitin sulfate based niches for chondrogenic differentiation of mesenchymal stem cells, *Matrix Biol*, 2008, **27**, 12-21.

110. S. Kaihara, S. Matsumura and J. P. Fisher. Cellular responses to degradable cyclic acetal modified PEG hydrogels, *J. Biomed. Mater. Res.*, 2008.

111. J. Kim, Y. Park, G. Tae, K. B. Lee, S. J. Hwang, I. S. Kim, I. Noh and K. Sun. Synthesis and characterization of matrix metalloprotease sensitive-low molecular

weight hyaluronic acid based hydrogels, *Journal of materials science Materials in medicine*, 2008, **19**, 3311-3318.

112. C. Adelöw, T. Segura, J. A. Hubbell and P. Frey. The effect of enzymatically degradable poly(ethylene glycol) hydrogels on smooth muscle cell phenotype, *Biomaterials*, 2008, **29**, 314-326.

113. J. M. Karp, J. Yeh, G. Eng, J. Fukuda, J. Blumling, K. Y. Suh, J. Cheng, A. Mahdavi, J. Borenstein, R. Langer and A. Khademhosseini. Controlling size, shape and homogeneity of embryoid bodies using poly(ethylene glycol) microwells, *Lab on a chip*, 2007, **7**, 786-794.

114. S. Battista, D. Guarnieri, C. Borselli, S. Zeppetelli, A. Borzacchiello, L. Mayol, D. Gerbasio, D. R. Keene, L. Ambrosio and P. A. Netti. The effect of matrix composition of 3D constructs on embryonic stem cell differentiation, *Biomaterials*, 2005, **26**, 6194-6207.

115. R. McBeath, D. M. Pirone, C. M. Nelson, K. Bhadriraju and C. S. Chen. Cell shape, cytoskeletal tension, and RhoA regulate stem cell lineage commitment, *Dev Cell*, 2004, **6**, 483-495.

116. J. K. Wise, A. L. Yarin, C. M. Megaridis and M. Cho. Chondrogenic Differentiation of Human Mesenchymal Stem Cells on Oriented Nanofibrous Scaffolds: Engineering the Superficial Zone of Articular Cartilage, *Tissue Engineering Part A*, 2008.

117. F. Yang, R. Murugan, S. Wang and S. Ramakrishna. Electrospinning of nano/micro scale poly(L-lactic acid) aligned fibers and their potential in neural tissue engineering, *Biomaterials*, 2005, **26**, 2603-2610.

118. M. J. Biggs, R. G. Richards, S. McFarlane, C. D. Wilkinson, R. O. Oreffo and M. J. Dalby. Adhesion formation of primary human osteoblasts and the functional response of mesenchymal stem cells to 330nm deep microgrooves, *Journal of the Royal Society, Interface / the Royal Society*, 2008, **5**, 1231-1242.

119. E. K. Yim, S. W. Pang and K. W. Leong. Synthetic nanostructures inducing differentiation of human mesenchymal stem cells into neuronal lineage, *Exp Cell Res*, 2007, **313**, 1820-1829.

120. K. H. Carpizo, M. J. Saran, W. Huang, K. Ishida, J. Roostaeian, D. Bischoff, C. K. Huang, G. H. Rudkin, D. T. Yamaguchi and T. A. Miller. Pretreatment of poly(l-lactide-co-glycolide) scaffolds with sodium hydroxide enhances osteoblastic differentiation and slows proliferation of mouse preosteoblast cells, *Plast Reconstr Surg*, 2008, **121**, 424-434.

121. G. Marletta, G. Ciapetti, C. Satriano, F. Perut, M. Salerno and N. Baldini. Improved osteogenic differentiation of human marrow stromal cells cultured on ion-induced chemically structured poly-epsilon-caprolactone, *Biomaterials*, 2007, **28**, 1132-1140.

122. Y. Liu and M. B. Chan-Park. Hydrogel based on interpenetrating polymer networks of dextran and gelatin for vascular tissue engineering, *Biomaterials*, 2009, **30**, 196-207.

123. G. Forte, F. Carotenuto, F. Pagliari, S. Pagliari, P. Cossa, R. Fiaccavento, A. Ahluwalia, G. Vozzi, B. Vinci, A. Serafino, A. Rinaldi, E. Traversa, L. Carosella, M. Minieri and P. Di Nardo. Criticality of the Biological and Physical Stimuli Array Inducing Resident Cardiac Stem Cell Determination, *Stem Cells*, 2008.

124. D. L. Cohen, E. Malone, H. Lipson and L. J. Bonassar. Direct freeform fabrication of seeded hydrogels in arbitrary geometries, *Tissue Engineering*, 2006, **12**, 1325-1335.

125. V. Tsang, A. Chen, L. Cho, K. Jadin, R. Sah, S. Delong, J. West and S. Bhatia. Fabrication of 3D hepatic tissues by additive photopatterning of cellular hydrogels, *The FASEB Journal*, 2007, **21**, 790-801.

126. G. Papavasiliou, P. Songprawat, V. Pérez-Luna, E. Hammes, M. Morris, Y. Chiu and E. Brey. Three-Dimensional Patterning of Poly(Ethylene Glycol) Hydrogels Through Surface-Initiated Photopolymerization, *Tissue Engineering Part C: Methods*, 2008, **14**, 129-140.

127. S. Khetan, J. S. Katz and J. Burdick. Sequential crosslinking to control cellular spreading in 3-dimensional hydrogels, *Soft Matter*, 2009, **E-published**.

128. S. A. Zawko, S. Suri, Q. Truong and C. E. Schmidt. Photopatterned anisotropic swelling of dual-crosslinked hyaluronic acid hydrogels, *Acta Biomaterialia*, 2009, **5**, 14-22.

129. S. Lee, J. Moon and J. West. Three-dimensional micropatterning of bioactive hydrogels via two-photon laser scanning photolithography for guided 3D cell migration, *Biomaterials*, 2008, **29**, 2962-2968.

130. S. Obi, K. Yamamoto, N. Shimizu, S. Kumagaya, T. Masumura, T. Sokabe, T. Asahara and J. Ando. Fluid shear stress induces arterial differentiation of endothelial progenitor cells, *J Appl Physiol*, 2009, **106**, 203-211.

131. D. F. Ward, R. M. Salasznyk, R. F. Klees, J. Backiel, P. Agius, K. Bennett, A. Boskey and G. E. Plopper. Mechanical strain enhances extracellular matrix-

induced gene focusing and promotes osteogenic differentiation of human mesenchymal stem cells through an extracellular-related kinase-dependent pathway, *Stem Cells Dev*, 2007, **16**, 467-480.

132. G. H. van Lenthe, J. P. van den Bergh, A. R. Hermus and R. Huiskes. The prospects of estimating trabecular bone tissue properties from the combination of ultrasound, dual-energy X-ray absorptiometry, microcomputed tomography, and microfinite element analysis, *J Bone Miner Res*, 2001, **16**, 550-555.

133. A. J. Engler, M. A. Griffin, S. Sen, C. G. Bönnemann, H. L. Sweeney and D. E. Discher. Myotubes differentiate optimally on substrates with tissue-like stiffness: pathological implications for soft or stiff microenvironments, *J Cell Biol*, 2004, **166**, 877-887.

134. P. Georges. Cell type-specific response to growth on soft materials, *Journal of Applied Physiology*, 2005, **98**, 1547-1553.

135. A. S. Rowlands, P. A. George and J. J. Cooper-White. Directing osteogenic & myogenic differentiation of MSCs: interplay of stiffness & adhesive ligand presentation, *Am J Physiol, Cell Physiol*, 2008.

136. R. J. Pelham and Y. Wang. Cell locomotion and focal adhesions are regulated by substrate flexibility, *Proc Natl Acad Sci USA*, 1997, **94**, 13661-13665.

137. D. Discher. Tissue Cells Feel and Respond to the Stiffness of Their Substrate, *Science*, 2005, **310**, 1139-1143.

138. A. Engler, S. Sen, H. Sweeney and D. Discher. Matrix Elasticity Directs Stem Cell Lineage Specification, *Cell*, 2006, **126**, 677-689.

139. K. Saha, A. J. Keung, E. F. Irwin, Y. Li, L. Little, D. V. Schaffer and K. E. Healy. Substrate modulus directs neural stem cell behavior, *Biophys J*, 2008, **95**, 4426-4438.

140. P. Georges, W. J. Miller, D. F. Meaney, E. S. Sawyer and P. Janmey. Matrices with compliance comparable to that of brain tissue select neuronal over glial growth in mixed cortical cultures, *Biophys J*, 2006, **90**, 3012-3018.

141. J. Leach, X. Brown, J. Jacot, P. Dimilla and J. Wong. Neurite outgrowth and branching of PC12 cells on very soft substrates sharply decreases below a threshold of substrate rigidity, *J. Neural Eng.*, 2007, **4**, 26-34.

142. S. A. Ruiz and C. S. Chen. Emergence of patterned stem cell differentiation within multicellular structures, *Stem Cells*, 2008, **26**, 2921-2927.

143. C. Khatiwala, S. Peyton, M. Metzke and A. Putnam. The regulation of osteogenesis by ECM rigidity in MC3T3-E1 cells requires MAPK activation, *J. Cell. Physiol.*, 2007, **211**, 661-672.

144. S. Peyton, P. Kim, C. Ghajar, D. Seliktar and A. Putnam. The effects of matrix stiffness and RhoA on the phenotypic plasticity of smooth muscle cells in a 3-D biosynthetic hydrogel system, *Biomaterials*, 2008, **29**, 2597-2607.

145. T. J. Kim, J. Seong, M. Ouyang, J. Sun, S. Lu, J. P. Hong, N. Wang and Y. Wang. Substrate rigidity regulates Ca2+ oscillation via RhoA pathway in stem cells, *J. Cell. Physiol.*, 2009, **218**, 285-293.

146. R. Wells. The role of matrix stiffness in regulating cell behavior, *Hepatology*, 2008, **47**, 1394-1400.

147. S. X. Hsiong, P. Carampin, H. J. Kong, K. Y. Lee and D. J. Mooney. Differentiation stage alters matrix control of stem cells, *J. Biomed. Mater. Res.*, 2008, **85**, 145-156.

# CHAPTER 4

*Development and Characterization of Hydrogel Systems with Spatially and Temporally Controlled Mechanics*

## 4.1 Introduction

As outlined in Chapter 3, there are many factors within the stem cell microenvironment that contribute to its fate. While significant work has been completed to investigate the effects of uniform and static presentation of various cues on stem cell behavior, investigations of the effects of non-uniform and dynamic environments on stem cells are limited. Specifically, matrix mechanics have a profound effect on stem cell morphology, proliferation, and differentiation,[1-3] yet few systems exist with the ability to spatially and temporally control mechanics. While some systems have demonstrated spatially controlled cell responses based on mechanics,[4-6] these systems lack the potential for 3D encapsulation (due to inherent material toxicity and/or scaffold fabrication), as well as the ability to effectively modulate mechanics in a temporal manner. Other systems with the ability to temporally control mechanics possess either a limited range of mechanics (2-8 kPa[7]) or result in a decrease in mechanics (due to photodegradation of hydrogel network[8]), which is not as biologically relevant as temporally-increasing mechanics (hallmarks of many pathologies and tissue development[7, 9, 10]).

In order to thoroughly investigate the effects of complex mechanical microenvironments on stem cell behavior, several hydrogel systems (both synthetic and naturally-derived) were developed and characterized and reported in this chapter. Human mesenchymal stem cells (hMSCs) were chosen for these studies due to their ease of

isolation, multi-lineage differentiation capacity, and their well-established therapeutic potential.[11, 12] In order to first confirm hMSC response to uniform mechanics, a synthetic hydrogel system based on biocompatible poly(ethylene glycol) (PEG) was used. Once hMSC response to uniform mechanics was confirmed, more complex systems involving sequential crosslinking were developed in order to create hydrogels with spatially and temporally modulated mechanics.

Two systems were investigated and both involved the use of two types of crosslinking, where the first step was used to fabricate a uniform hydrogel and the second step was a radical polymerization using light. Specifically, the first system used both alginate and PEG-diacrylate (PEGDA) precursors, where ionic crosslinking of alginate occurs in the presence of $Ca^{2+}$ and radical polymerization (in the presence of light and photoinitiator) crosslinks the PEGDA within the alginate network in order to create an interpenetrating network (IPN). A second system was developed and termed sequential crosslinking, where naturally-derived hyaluronic acid (HA) was chemically modified with a methacrylate functionality to allow for crosslinking *via* both Michael Addition (using a dithiol crosslinker) and radical polymerization. HA is present in native tissue and is involved in processes such as wound repair, cell motility, tissue morphogenesis, and inflammation.[13, 14] Due to its susceptibility to chemical modification (carboxyl and hydroxyl groups on the HA backbone) and biological significance, HA represents an attractive target for development of a mechanically-tunable system for studying hMSC responses.

The crosslinking density of these hydrogel systems directly correlates with modulus, and therefore local and time-dependent control of crosslinking density using

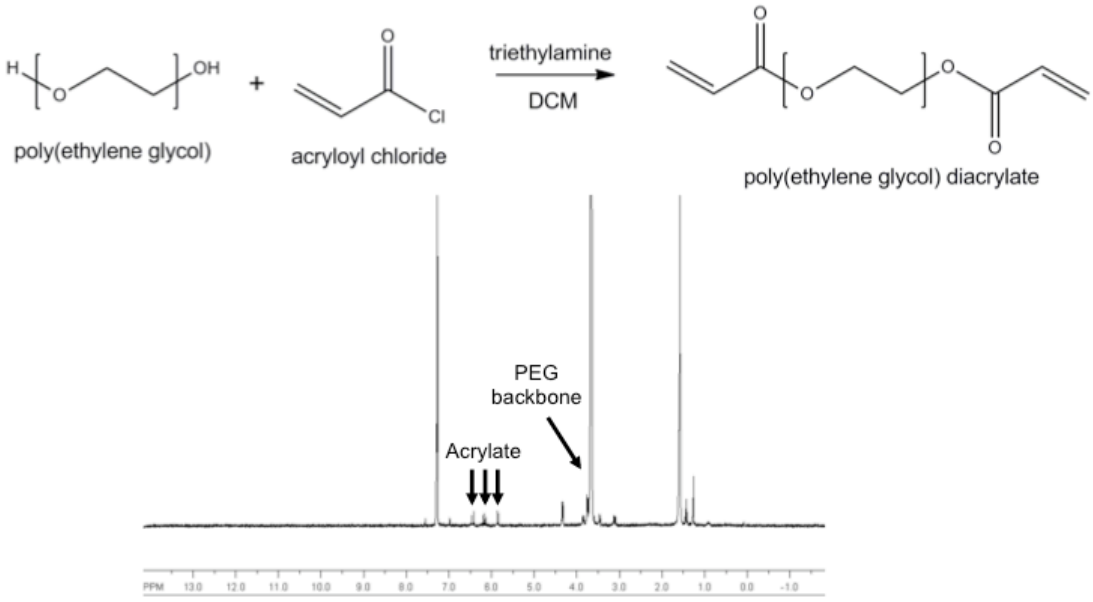


**Figure 4.1** Synthetic scheme and $^{1}$H NMR spectrum for poly(ethylene glycol) diacrylate (PEGDA) denoting acrylate peaks (arrows) and PEG backbone.

sequential crosslinking permits the formation of hydrogels with complex mechanical environments to study the effects of heterogeneous, dynamic microenvironments on hMSCs. A mechanically-tunable hydrogel system would be very beneficial not only for understanding stem cell responses to complex mechanical microenvironments, but to also provide a new biomaterial platform suitable for tissue engineering applications.

## 4.2 Materials & Methodology

### *4.2.1 PEGDA Synthesis, Characterization, and Initial Cell Response*

PEGDA was synthesized as described previously[15] and illustrated in **Figure 4.1**. Briefly, 10 g PEG-4000 (Sigma) was dissolved in 300 mL methylene chloride and 3X

excess triethylamine was added while stirring @ 4°C. 3X excess acryloyl chloride was then added dropwise and reacted under nitrogen overnight. The solution was then precipitated in ethyl acetate, filtered, and redissolved in $dIH_2O$. Following dialysis for 72 hours, the PEGDA solution was frozen overnight at -80°C and lyophilized. Modification of PEG was quantified using $^1H$ NMR with corresponding spectrum shown in **Figure 4.1** and found to be ~100% acrylated. PEGDA hydrogels were formed by dissolving PEGDA at 4, 6, 8, 10, and 12 wt% in PBS containing 0.05 % I2959 (Irgacure), as well as 1 mM mono-acrylated PEG3400 coupled to a cell adhesive peptide (Y***RGD***S). 1 mm thick PEGDA hydrogel slabs were radically polymerized by exposing to 10 $mW/cm^2$ UV light (Blak-Ray) for 4 min for both mechanical testing and cell studies.

Mechanical characterization of PEGDA hydrogels was performed using atomic force microscopy (AFM, Veeco Bioscope I). A silicon bead AFM tip with spring constant 0.06 N/m was used to obtain force curves for each hydrogel condition (n=15 measurements per condition) from which a local elastic modulus was calculated using a Hertz model.

For cell studies, human mesenchymal stem cells (hMSCs, Lonza) were cultured in α-MEM medium supplemented with 20% fetal bovine serum (FBS), 1% L-glutamine and penicillin-streptomycin and seeded at a density of 5000 $cells/cm^2$ for each hydrogel condition. Prior to cell seeding, hydrogels were sterilized by exposing to germicidal UV for 2 hours in sterile PBS. 24 hours after cell seeding, samples were fixed with 10% formalin, permeabilized with 0.25% Triton-X, and stained for actin and nuclei using phalloidin and DAPI (Invitrogen), respectively. Cell morphology was quantified for several conditions using ImageJ (NIH) after 24 hours (n=50 cells/condition).

*4.2.2 Alginate-PEGDA IPN Synthesis, Characterization, and Initial Cell Response*

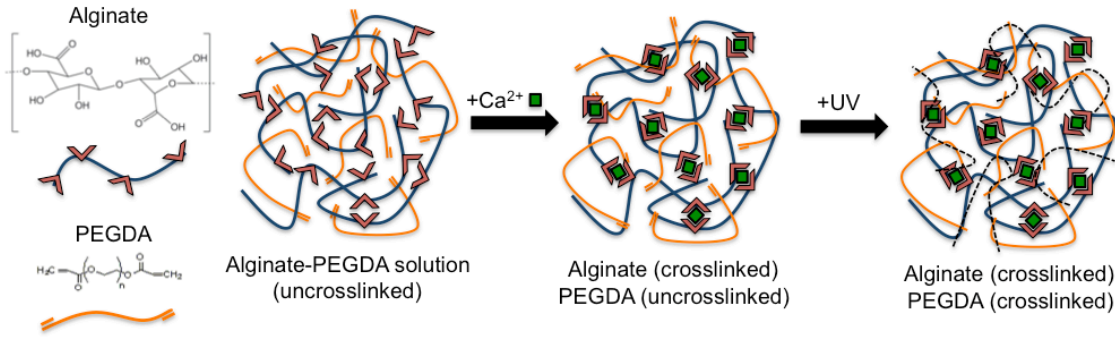


**Figure 4.2** Alginate and PEGDA are suspended in solution (PBS containing 0.05% I2959) and upon addition of $Ca^{2+}$, ionic crosslinking of alginate occurs with uncrosslinked PEGDA dispersed throughout (semi-IPN). Exposure to UV light radically crosslinks the PEGDA within the alginate network (kinetic chains shown with dotted lines) to create an IPN where mechanical heterogeneity is defined by where and when the light exposure occurs.

PEGDA was synthesized as described in Section 4.2.1. The alginate-PEGDA crosslinking scheme is outlined in **Figure 4.2**. In this system, mechanics are varied by maintaining a constant ionically-crosslinked alginate network and varying the amount of PEGDA initially dissolved within the precursor solution. Because PEG is a relatively inert polymer,[13] this would allow for a change in crosslinking density (and thus mechanics), without altering the cell reactivity of the hydrogel. The "base" alginate network consisted of 2 wt% alginate (Sigma) crosslinked with 25 mg/mL $CaSO_4$ (Sigma) mixed at a ratio of 3:1 in PBS containing 0.05% I2959, as well as a range of PEGDA (0-12 wt%). In order to allow for cell attachment to the hydrogel, RGD-containing peptides were covalently attached to alginate using EDC-NHS chemistry as illustrated in **Figure**

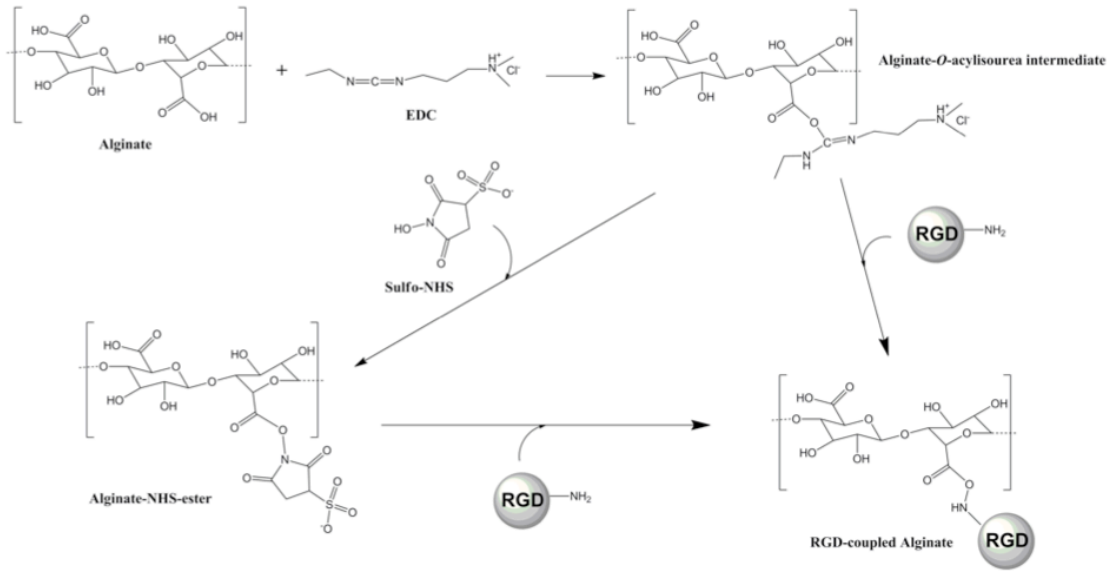


**Figure 4.3** EDC-NHS coupling of RGD peptides to alginate backbone forms amide bond between carboxyl group on alginate and amine terminus of peptide.

**4.3**. To investigate the accessibility of the RGD peptide, two different RGD peptides were used to determine if the length of the tether attaching the RGD affected cell adhesion to the hydrogel. The RGD sequences used for these studies were G**RGD**S and GCGYG**RGD**SPG and were designated RGD(short) and RGD(long), respectively. Conditions for EDC-NHS coupling were chosen based on optimization performed in a previous study.[16] Briefly, 1 g of alginate was dissolved in 100 mL buffer solution containing 0.3 M NaCl, 0.1 M MES at pH 6.5. Approximately 5% of uronic acid repeat units were activated using a 1:2 molar ratio of Sulfo-NHS:EDC and 1 mmol of each RGD peptide was added in order to create two batches of RGD-coupled alginate. The solutions were reacted for 20 hours, followed by dialysis for 72 hours, frozen at -80°C and then lyophilized.

For all formulations, the $CaSO_4$ solution was added to the alginate solution to ionically crosslink the alginate for 10 minutes at 20°C between glass slides with 1 mm spacers. A constant ratio of alginate-RGD:alginate (50:50) was used in order to maintain a constant RGD ligand density for all formulations. Following ionic crosslinking, the hydrogels were exposed to 10 mW/cm$^2$ UV light for 4 min and 8-mm cylindrical samples were cored from the hydrogel slabs for mechanical testing and cell studies. Mechanical testing was performed as outlined in Section 4.2.1 with a range of PEGDA (0-12 wt%) within the same base alginate network. 24 hour cell attachment studies were performed with assessment of cell viability and morphology using Calcein AM (Invitrogen). To confirm the presence of secondary crosslinking, methacryloxyethyl thiocarbonyl Rhodamine B (MeRho, Polysciences, Inc.) was dissolved in the precursor solution and incorporated into the radically crosslinked network due to the presence of the methacrylate on the fluorescent dye.

*4.2.3 Methacrylated-HA Synthesis, Characterization, and Initial Cell Response*

Methacrylated hyaluronic acid (MeHA) was synthesized as described previously.[17, 18] Briefly, sodium hyaluronate (Lifecore, 59 kDa) was dissolved at 1 wt% in $dIH_2O$ and methacrylic anhydride (MA) was added dropwise (2.4 mL MA per g HA) while stirring at 4°C. The pH was maintained above 8 during the reaction by adding 5 N NaOH intermittently for 8 hours, followed by overnight reaction and further addition of MA (1.2 mL per g HA) and pH maintenance for 4 hours the following day. The macromer solution was dialyzed against $dIH_2O$ (SpectraPor, *MW* cutoff 6000-8000 Da) for 4 days, frozen at -80 °C, lyophilized and stored in powder form. The MeHA synthetic

scheme is shown in **Figure 4.4A** with resulting $^{1}$H NMR spectrum revealing approximately 100% modification of the hydroxyl groups on the HA backbone (**Figure 4.4B**).

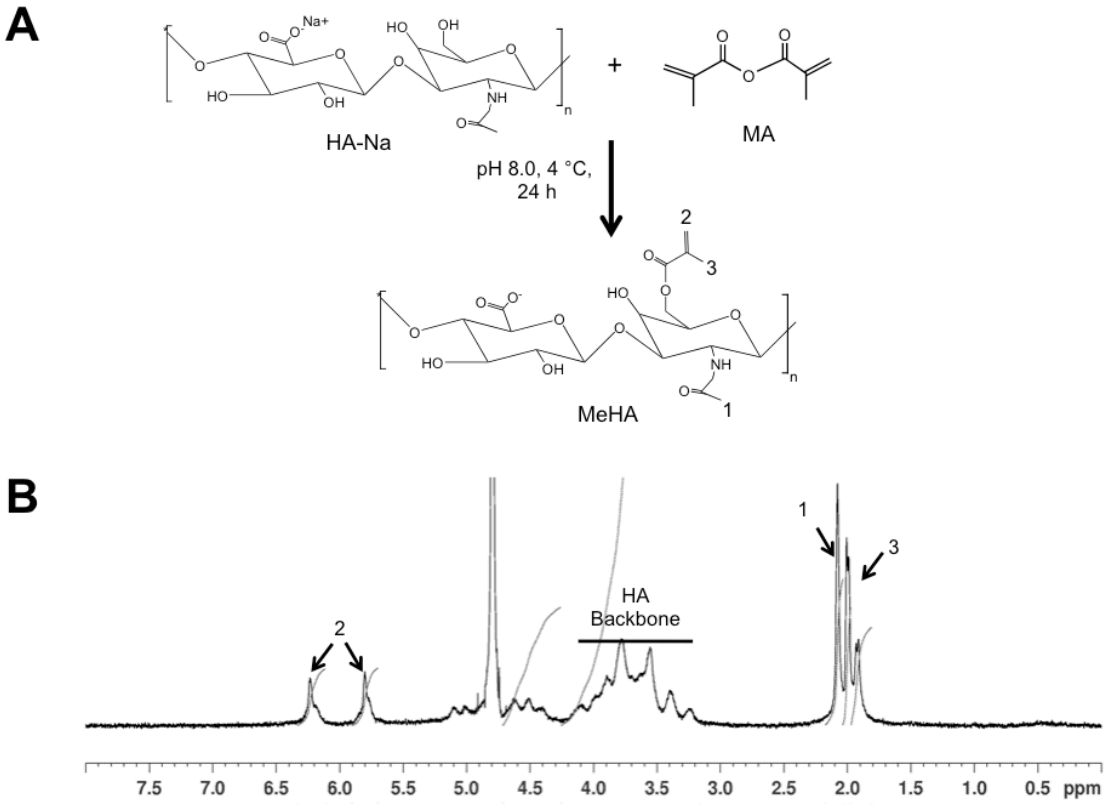


**Figure 4.4** A) Synthesis of MeHA through the reaction of sodium hyaluronate (HA-Na) with methacrylic anhydride (MA). B) $^{1}$H NMR spectrum shows peaks corresponding to HA backbone and protons associated with the methacrylate group in order to determine the degree of methacrylation.

For the MeHA hydrogel system, methacrylated glass coverslips were used to covalently attach thin hydrogel films to facilitate mechanical characterization and cell studies. 22 mm x 22 mm coverslips were first plasma coated for 3 min to activate the surface for methacrylation. Next, 100 µL of 3-(trimethoxysilyl)propyl methacrylate

(Sigma) was placed on each activated slide and reacted at 100 °C for 1 hour followed by 10 min at 110 °C. Finally, slides were rinsed with $dIH_2O$ and ethanol and allowed to dry.

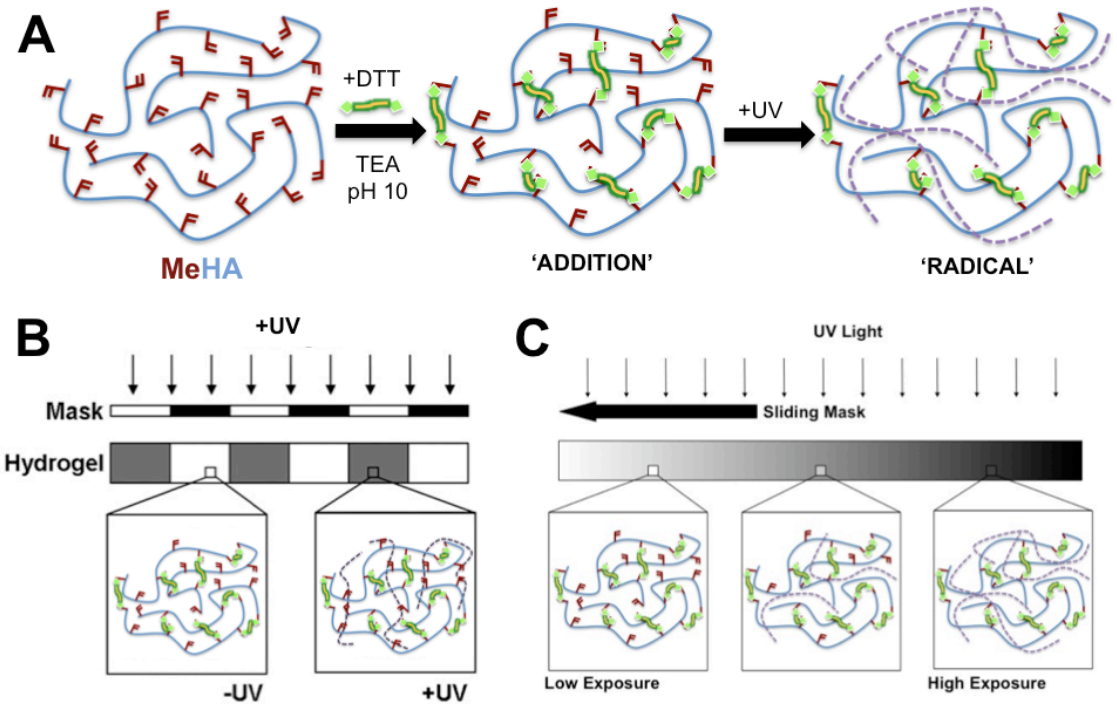


**Figure 4.5** MeHA sequential crosslinking schematic. A) Step 1: dithiothreitol (DTT) solution was added to MeHA macromer resulting in Michael addition crosslinking in presence of TEA at pH 10. Step 2: unconsumed methacrylates remaining after 'Addition' crosslinking can underwent further crosslinking ('Radical') upon exposure to UV light in the presence of photoinitiator. Spatial variations in hydrogel mechanics can be introduced by restricting UV light to certain regions of the addition crosslinked hydrogel using a photomask (B) or varying the time of UV exposure (*via* a sliding mask) to create gradients (C).

MeHA hydrogels were formed using one- or two-step crosslinking processes (**Figure 4.5A**). In the first step, Michael-type 'Addition' crosslinking occurred *via* introduction of dithiothreitol (DTT, Sigma) to a 3 wt% solution of MeHA in PBS

containing 0.2 M triethanolamine (TEA, Sigma) containing 0.05 wt% I2959. Various amounts of DTT were added to vary the theoretical molar consumption of methacrylates present on the HA backbone (12, 15, 30, 50, and 100%) to achieve a range of initial mechanics in this first crosslinking step. The oligopeptide GCGYG*RGDS*PG was added prior to DTT crosslinking to allow for coupling of the well-established RGD adhesion moiety to the network. Hydrogel thin films were formed between slides with 150 μm spacers and a methacrylated slide was used on one side to allow for covalent gel attachment. After mixing, solutions were reacted for 1 hour at 37 °C to complete the 'Addition' crosslinking step ("-UV gels").

When desired, hydrogels were further exposed to UV light in order to initiate 'Radical' crosslinking of the remaining unconsumed methacrylates. Collimated 10 $mW/cm^2$ 365 nm UV light (Omnicure S1000 UV Spot Cure System, Exfo) was used to uniformly expose the hydrogels for 4 min ("+UV gels"). This step could be performed to create uniform hydrogels or to create hydrogels with spatially or temporally controlled mechanics. Patterned hydrogels were created using photomasks (**Figure 4.5B**) to restrict the presentation of UV light. Photomasks consisted of printed transparencies containing striped patterns ranging from 100-1000 μm in width that were created using Adobe Photoshop and printed at a resolution of 20,000 DPI. Mechanics were also spatially modulated in a graded manner by passing a photomask across the surface of the gel at a linear velocity (10 mm/min using a syringe pump, **Figure 4.5C**) to create a range of exposure times and crosslinking across a 15 mm distance.

Mechanical characterization was performed with AFM as outlined above using a range of DTT consumptions with and without UV exposure for uniform hydrogels. For

patterned and gradient hydrogels, local moduli were measured at discrete points (n=10 measurements at each point) across the hydrogel surfaces. Initial 24 hour cell attachment studies were performed for both -UV and +UV hydrogels and cell morphology was assessed using rhodamine-phalloidin to observe the actin cytoskeleton.

### *4.2.4 Statistical Analysis*

Values are reported as means and standard deviation for mechanics and means and standard error for cell spreading. Statistical differences ($p<0.05$) were determined using a Student's t-test (JMP software) to compare mechanics and cell spreading area for a specific formulation and with or without light exposure.

## 4.3 Results and Discussion

Two systems were successfully developed and characterized that use two modes of crosslinking to first form a uniform hydrogel and then to introduce mechanical complexity with a second spatially controlled and light-initiated radical polymerization.

### *4.3.1 PEGDA System Characterization and Initial Cell Response*

By varying the wt% of PEGDA from 4-12%, a range of moduli were obtained from ~3-59 kPa (**Figure 4.6**). This range corresponds well with the physiologic range of tissue moduli as adipose tissue is typified by a modulus of approximately 2-3 kPa[19, 20] while stiffer, pre-mineralized bone tissue is typified by a modulus >30 kPa.[1] In order to determine if hMSCs are sensitive to differences in PEGDA hydrogel mechanics, three hydrogel formulations were tested that spanned this broad mechanics range. As shown in

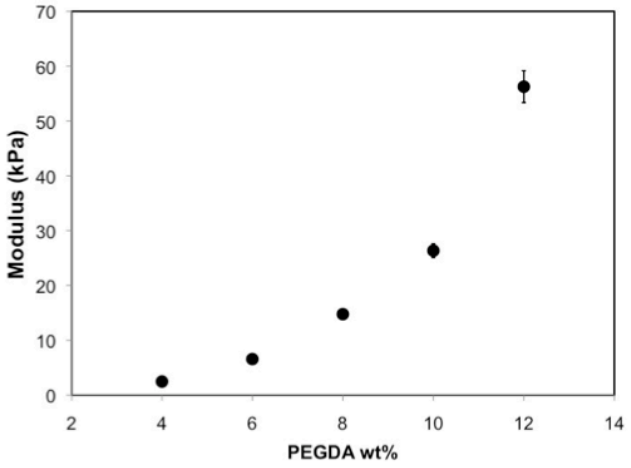


**Figure 4.6** AFM mechanical characterization of PEGDA hydrogels fabricated with a range of concentrations

**Figure 4.7**, cells on the softest ~3 kPa hydrogels remained rounded and possessed a diffuse, unorganized cytoskeleton. On the stiffer ~11 kPa and ~59 kPa hydrogels, cells were more spread and possessed highly organized cytoskeletons with pronounced stress fibers. These results are in good agreement with other findings that stem cells become more spread with more distinct stress fibers on stiffer substrates (e.g. polyacrylamide substrates).[2, 3] While these results further demonstrate the effect of mechanics on stem cells, this PEGDA hydrogel system is limited to uniform, static mechanics and thus a different system is necessary to probe more complex stem cell responses to non-uniform and dynamic mechanics.

*4.3.2 Alginate-PEGDA IPN Synthesis, Characterization, and Initial Cell Response*

A system consisting of alginate and PEGDA was investigated to determine if spatially controlled mechanics in hydrogels was possible through a combination of ionic

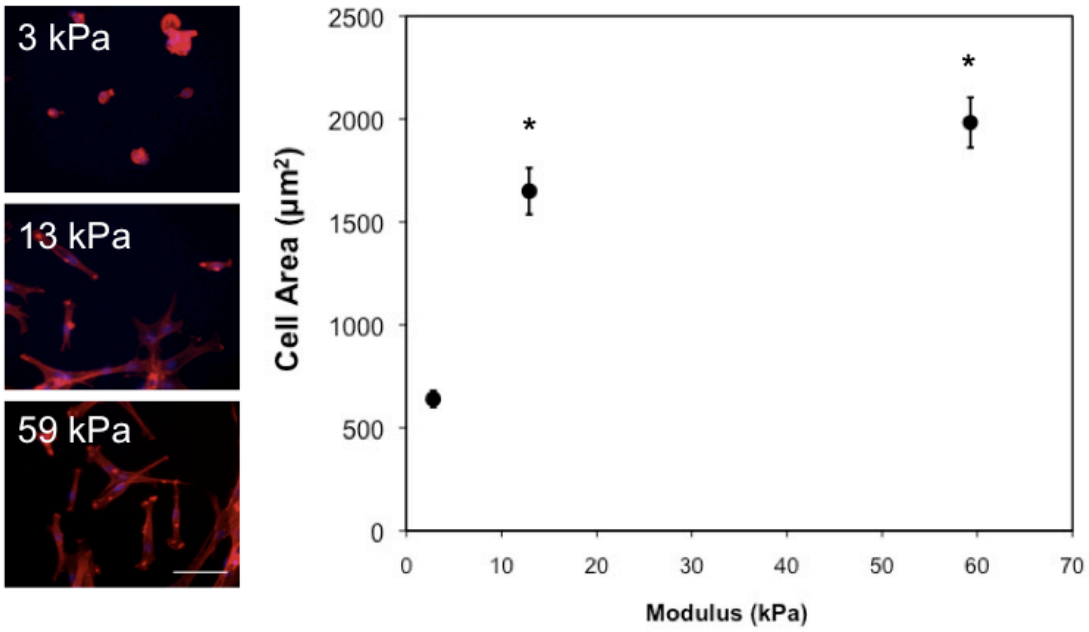


**Figure 4.7** hMSC response to PEGDA hydrogels with uniform mechanics. Left: representative images of hMSCs 1 day after seeding showing cytoskeleton (actin, red) and nuclei (blue) on uniform PEGDA hydrogels over a range of moduli. Scale bar=200 μm. Right: quantification of day 1 cell spread area (mean±SE) for 3, 13, and 59 kPa PEGDA hydrogels. 13 and 59 kPa cell spread area significantly different than 3 kPa (*$p<0.01$)

and radical crosslinking. Two-component networks have been developed previously,[5, 21] and this system was developed to determine if two orthogonally crosslinked networks (ionic and radical) would allow for a range of physiological mechanics that could also be spatially modulated. **Figure 4.8A** shows the mechanics range achievable using ionically-crosslinked alginate in conjunction with an interpenetrating PEGDA network that has been radically crosslinked. By combining these two polymer networks, there was a significant increase in mechanics between 6 and 12 wt% PEGDA between the alginate-PEGDA IPN and PEGDA only hydrogels. Of note, alginate only hydrogels of the same

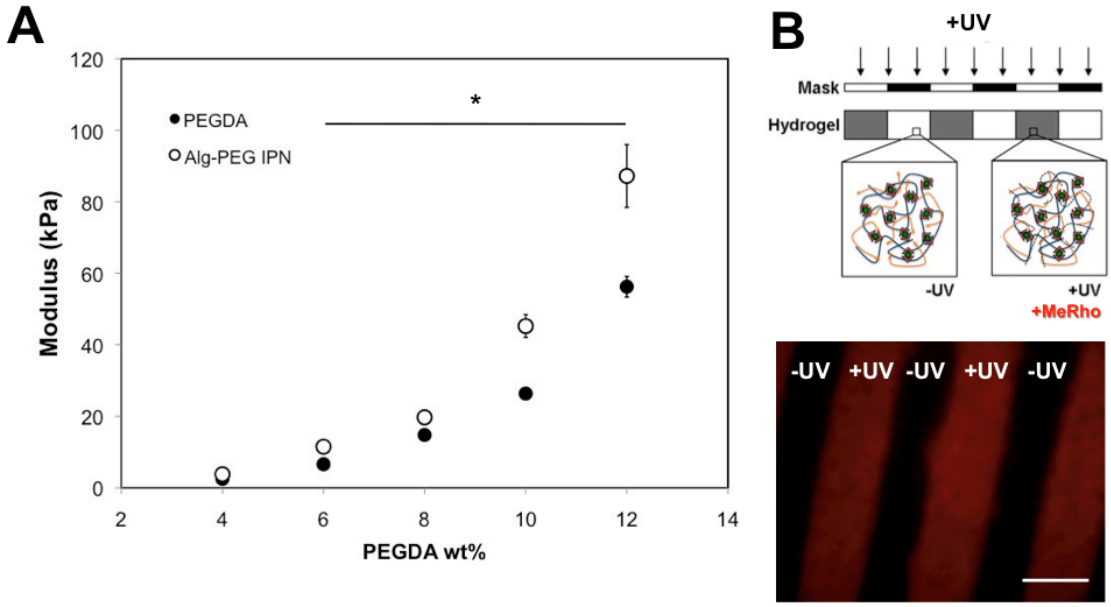


**Figure 4.8** A) AFM mechanical characterization of alginate-PEG IPN hydrogels (open circles) with a range of PEGDA wt % (alginate composition held constant). Moduli for PEG-only hydrogels (black circles) shown for comparison. Significant differences between Alg-PEG IPN and PEG *p<0.01 B) Photopatterning schematic showing how spatially restricting UV light using a photomask can result in local control of PEGDA crosslinking. Incorporation of a photoreactive dye (MeRho, red) allows for confirmation of patterning. Scale bar= 200 μm

formulation used for all IPN conditions had moduli of ~1.6 kPa and thus the combination of this soft ionically crosslinked network with the PEGDA network results in a dramatic increase in moduli over both single-component hydrogels. Other dual component systems exist in which the combination of two polymers produce an interpenetrating network with mechanical properties significantly higher than each individual component,[22] or in another instance the second component acts to interfere with crosslinking of the first component (and thus resulted in decreased mechanics).[23]

By spatially restricting UV light exposure (**Figure 4.8B** schematic) alginate-PEGDA hydrogels with spatially controlled crosslinking were investigated. **Figure 4.8B** shows the successful photopatterning capability of this system as the incorporation of MeRho indicates that radical crosslinking occurred only in these regions designated "+UV". The pattern resolution indicates that feature sizes as small as hundreds of μm are achievable using this IPN system, which would be beneficial for studying stem cell responses to mechanically-distinct regions of size similar to that of the cells themselves.

Although the alginate-PEG IPN system exhibited a desirable mechanics range (2-85 kPa) and the ability to photopattern, cell adhesion to these hydrogels was severely compromised. As shown in **Figure 4.9**, the alginate only hydrogels had minimal cell adhesion and spreading in the absence of cell-adhesive RGD, but the incorporation of RGD (through EDC-NHS coupling directly to alginate) resulted in greater cell attachment in these single component hydrogels. However, with the addition of the PEGDA network cell attachment was significantly abrogated. Since the RGD peptide used in the PEGDA only hydrogels (Section 4.3.1) was covalently attached to a monoacrylated PEG tether (3400 Da) and allowed for sufficient cell attachment and spreading, there was a possibility that the short RGD peptide did not allow for adequate presentation and binding recognition by the hMSCs. Therefore, two more methods of RGD presentation were used (longer sequence and the same PEG-RGD tether used in previous section) to see if greater cell accessibility was possible. **Figure 4.9** illustrates that neither of these RGD presentations allowed for cell interaction even though the PEG tether provided adequate cell binding in the PEGDA-only hydrogels. Cell adhesion requires not only the presence of cell adhesion sites, but also the ability to organize and

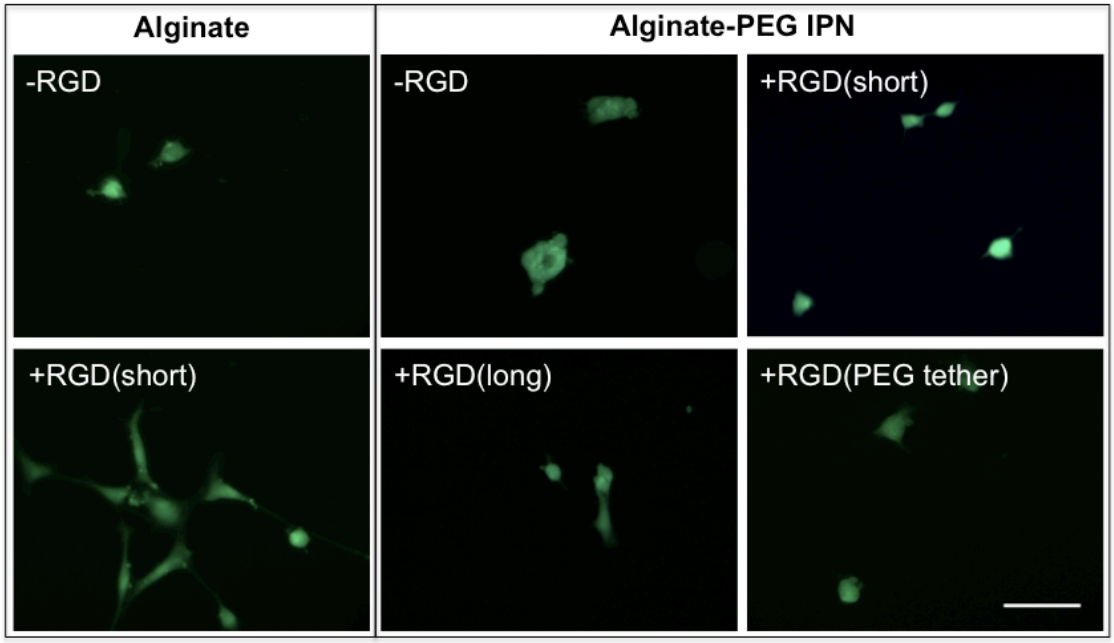


**Figure 4.9** Day 1 hMSC response (Calcein AM, green) to alginate only (Alg) and alginate-PEG (Alg-PEG) IPN with and without various presentations of cell adhesive RGD peptide. Scale bar = 200 μm

cluster these adhesions,[24] and it is possible that the presence of the IPN results in reduced flexibility of the RGD sites or complete blocking (e.g., through film of PEG at surface) and the observed poor cell adhesion. There is also a possibility that the positively-charged guanidinium group (located on the arginine of the RGD peptide) non-covalently interacted with the alginate (negatively charged carboxyl groups),[25] and the presence of the rigid IPN may have enhanced this interaction compared to softer alginate only hydrogels with more flexible polymer chains.

### *4.3.3 MeHA Synthesis, Characterization, and Initial Cell Response*

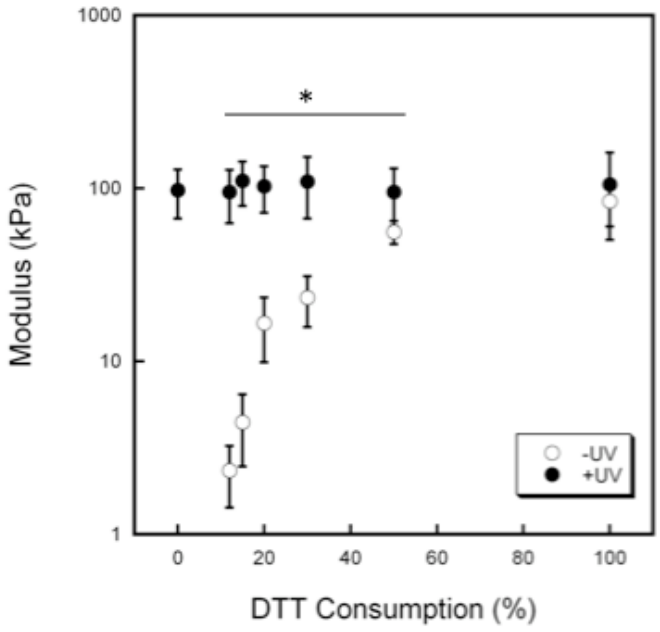


**Figure 4.10** AFM characterization of MeHA hydrogel moduli for various DTT consumptions (theoretical value plotted on x-axis based on molar ratio of DTT thiols to methacrylates on MeHA) before (-UV, white circles) and after (+UV, black circles) UV exposure.

While the alginate-PEGDA IPN system afforded a hydrogel system with tunable mechanics and the ability to pattern, the poor observed cell interaction required development of a new system that possessed similar mechanical properties and the ability to spatially control crosslinking while maintaining adhesion. A sequentially crosslinked MeHA hydrogel system was developed and found to possess a similar wide range in mechanical properties (from ~2-100 kPa) as shown in **Figure 4.10**. By varying the initial methacrylate consumption *via* molar ratio of DTT added, the hydrogel modulus ranged from 2.3 kPa (12% DTT -UV) to 84 kPa (100% DTT -UV). Furthermore, the exposure of these hydrogels to UV light resulted in an increase in modulus to ~100 kPa in all

sequentially crosslinked hydrogels, which agreed well with the hydrogel polymerized using only the radical crosslinking step (**Figure 4.10** 0% DTT +UV). Excluding the 100% -/+ UV DTT hydrogels, there were significant differences (**p<0.001) in the mechanics between -/+ UV hydrogels in all cases.

The ability to sequentially crosslink hydrogels has been used in a similar addition-radical sequential crosslinking system[26] and in other systems containing multi-component interpenetrating networks in which the two networks crosslink by different means.[21, 27-29] However, none of these systems exhibited the wide range of mechanics achievable with this dual crosslinkable MeHA system. While multi-component hydrogel systems allow for incorporation of multiple cell recognition sites and spatio-temporal control over mechanics and degradation, the complexity of these microenvironments makes determination of factors influencing stem cell behavior more difficult. In our system we use a constant polymer and ligand concentration while only altering the crosslinking of the same macromer, and thus mechanics. Therefore, any observed differences in hMSC behavior should be attributed to mechanics and not regional differences in ligand density and matrix components.

Initial hMSC response to MeHA hydrogels was assessed using -/+ UV hydrogels with and without RGD. Cells on -/+ UV hydrogels without RGD did not attach or spread as expected after 24 hours (**Figure 4.11**). The addition of RGD to the MeHA backbone resulted in increased cell attachment in both -UV and +UV hydrogels with similar spreading behavior to the uniform PEGDA hydrogels (**Figure 4.7**) as cells were rounded on the softer -UV hydrogels (2.3 kPa) and highly spread on the stiffer +UV hydrogels (100 kPa). These results indicate that MeHA can serve as a mechanically-tunable single

component system that cells interact with and exhibit responses similar to other 2D systems.[1, 3, 30] Unlike the alginate IPN system, the use of one macromer that contains both the adhesion and reactive sites for secondarily crosslinking appears to lead to both tunable mechanics and the ability to facilitate adhesion.

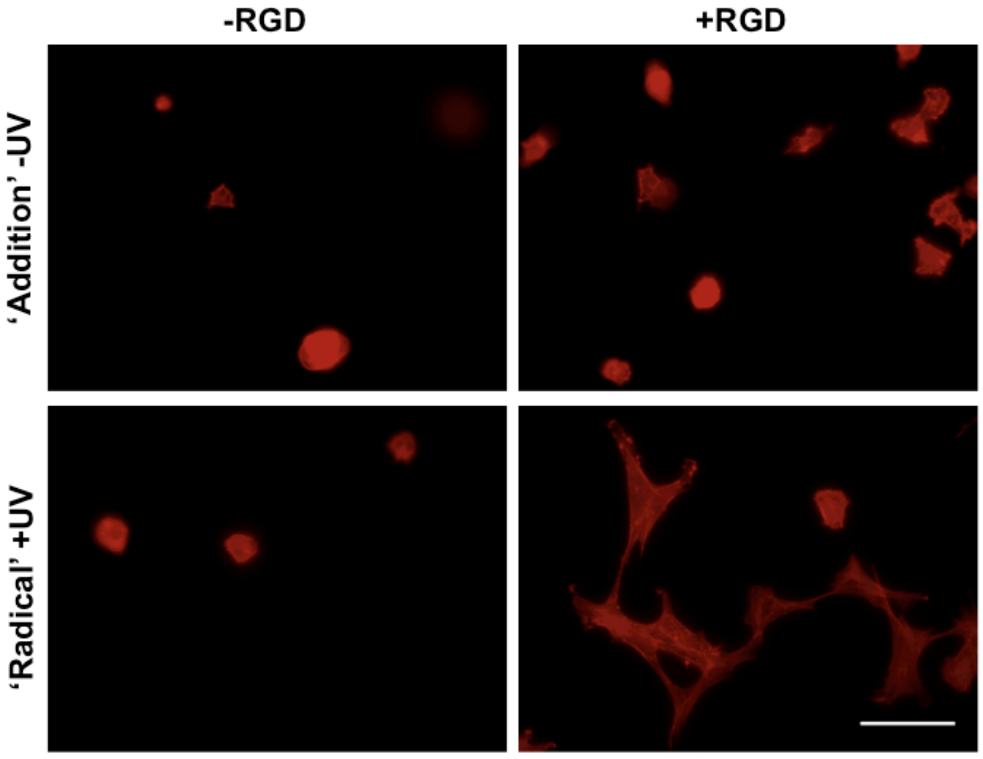


**Figure 4.11** Day 1 hMSC response (actin, red) to MeHA sequentially crosslinked hydrogels. Softer –UV hydrogels (12% DTT -UV, top row) and stiffer +UV hydrogels (12% DTT +UV, bottom row) seeded with hMSCs with (right column) and without (left column) RGD cell-adhesive peptide.

The ability to control mechanics spatially and temporally was also investigated for the sequentially crosslinked MeHA hydrogel system. Understanding and directing stem cell spatial and temporal behavior is necessary due to the heterogeneous nature of

tissues (both native and pathological). Spatially controlling stem cells based on mechanics would be useful for advanced tissue engineering approaches, as well as in understanding multi-phenotype differentiation from a single cell population. Photopatterning was similarly employed as in the alginate-PEGDA IPN system using a photomask to restrict UV light (and subsequent radical crosslinking) to desired locations within the hydrogel. Confirmation of photopatterning is shown in **Figure 4.12A** as the incorporation of MeRho denotes regions where radical crosslinking (+UV) has occurred. AFM mechanical testing allowed for local quantification of the hydrogel modulus across the length of the photopattern (**Figure 4.12B**). For 500 μm photopatterned stripes, the local moduli varied from ~6 kPa (-UV, non-exposed) to ~31 kPa (+UV, exposed).

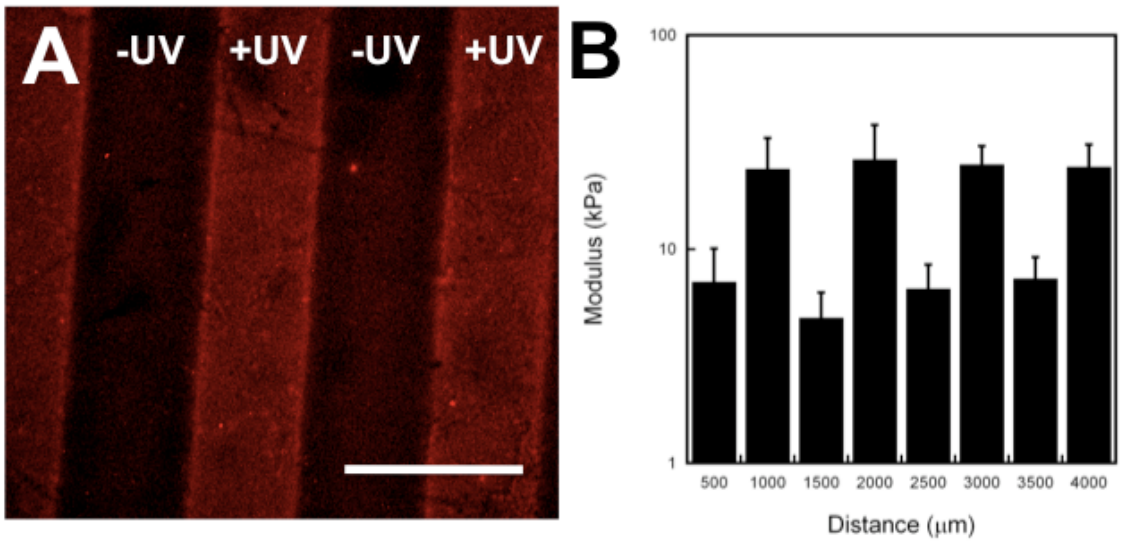


**Figure 4.12** A) Confocal cross-section of photopatterned gel illustrating exposed (+UV, red) and unexposed (-UV, black) regions. Scale bar = 400 μm B) Local moduli measured using AFM for a photopatterned hydrogel with 500 μm stripes.

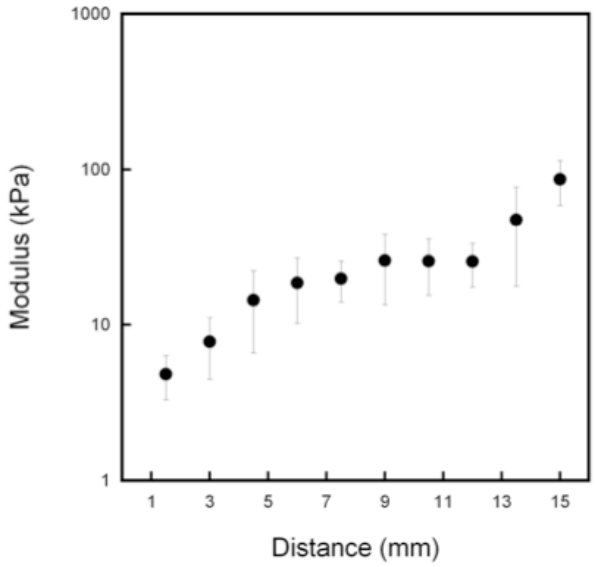


**Figure 4.13** Sequentially crosslinked hydrogels with gradient in moduli measured across the length of the gradient using AFM.

In a different photopatterning strategy, UV light exposure was linearly varied across the surface of the hydrogel in order to create a gradient in mechanics as shown in **Figure 4.13A**. Locally probing the modulus at regular intervals along the length of the gradient allowed for correlation of matrix mechanics with distance (i.e., time of light exposure). As shown in **Figure 4.13B**, the modulus gradually increases from a minimum of ~6 kPa to ~25 kPa over regions with up to a minute of exposure followed by a sharp increase in mechanics for regions with an additional 30 s of exposure up to a maximum elasticity comparable to the 12% DTT +UV uniform gel (~90 kPa). Other sequentially crosslinked systems saw similar rapid secondary crosslinking upon exposure of UV to radically polymerize remaining photoreactive groups.[26, 29]

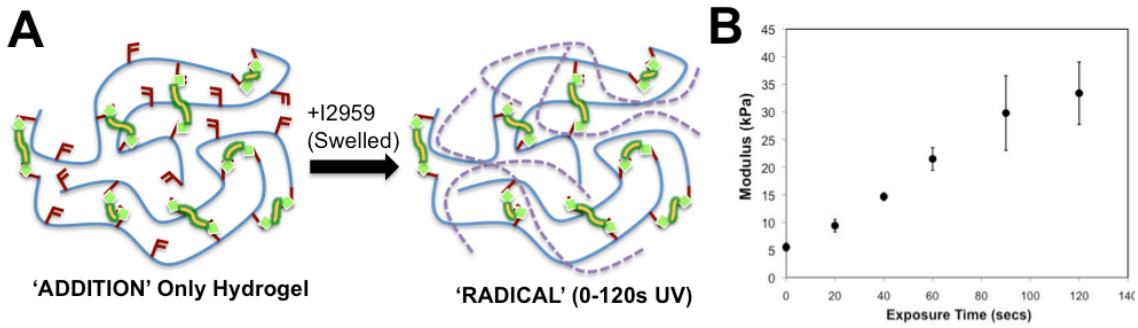


**Figure 4.14** A) Temporally-modulated mechanics achieved by swelling photoinitiator into 'Addition'-only hydrogels after reaching swelling equilibrium and exposing to UV light for a range of exposure times. B) Varying exposure time results in a physiological range of moduli (5-35 kPa).

Temporally modulated mechanics were developed using the strategy outlined in **Figure 4.14A**. 'Addition' only hydrogels were formed and allowed to equilibrate overnight followed by incubation in a 0.05% I2959 initiator solution. By reintroducing initiator into the hydrogel, further radical polymerization could occur at later time points during cell culture in order to investigate the effects of temporally increased mechanics on hMSCs. A range of UV exposure (0-120 s) was used on a given 'Addition' only hydrogel formulation (15% DTT) to vary the hydrogel mechanics from ~6 kPa (0 s UV) up to ~34 kPa (120 s UV). A hydrogel system with the ability to temporally modulate mechanics would prove useful for investigating the effects of dynamic mechanics on hMSC fate decisions and to further understand the mechanism by which cells dynamically sense and interact with their surrounding microenvironment. Understanding stem cell plasticity and fate decisions in response to changing mechanics would provide further insight into basic stem cell biology, as well as a greater understanding of

pathologies where aberrant mechanics have been implicated as both a cause and effect of the disease.[9, 31-33]

## 4.4 Conclusions

Overall, this chapter summarizes the progressive material development that led towards the selection of sequentially crosslinked MeHA hydrogels as a tunable mechanical system with the ability to spatially and temporally control mechanics. While the alginate-PEGDA IPN system showed promise in terms of a wide range of mechanics and the ability to photopattern, the poor cell interactions observed using several cell adhesive peptide presentations necessitated the development of another hydrogel system with tunable mechanics that promoted adequate cell adhesion. The presence of the methacrylate functionality of MeHA allowed for initial crosslinking *via* Michael-type Addition and secondary radical crosslinking through UV exposure in the presence of a photoinitiator. Photopolymerization allowed for both spatial and temporal control of MeHA secondary crosslinking since UV light could be presented either non-uniformly (in a pattern or gradient) or at a later time point to effectively "stiffen" the substrate. This system provides the foundation for the remainder of this thesis as sequentially crosslinked MeHA hydrogels are used to investigate the effects of uniform, as well as spatial and temporal mechanics on hMSC behavior.

**REFERENCES:**


1. A. J. Engler, S. Sen, H. L. Sweeney and D. E. Discher. Matrix elasticity directs stem cell lineage specification, *Cell*, 2006, **126**, 677-689.
2. A. S. Rowlands, P. A. George and J. J. Cooper-White. Directing osteogenic and myogenic differentiation of MSCs: interplay of stiffness and adhesive ligand presentation, *AJP: Cell Physiology*, 2008, **295**, C1037-C1044.
3. J. Winer, P. Janmey, M. McCormick and M. Funaki. Bone Marrow-Derived Human Mesenchymal Stem Cells Become Quiescent on Soft Substrates but Remain Responsive to Chemical or Mechanical Stimuli, *Tissue Engineering Part A*, 2008.
4. J. A. Burdick, A. Khademhosseini and R. Langer. Fabrication of gradient hydrogels using a microfluidics/photopolymerization process, *Langmuir : the ACS journal of surfaces and colloids*, 2004, **20**, 5153-5156.
5. S. Nemir, H. N. Hayenga and J. L. West. PEGDA hydrogels with patterned elasticity: Novel tools for the study of cell response to substrate rigidity, *Biotechnol. Bioeng.*, 2010, **105**, 636-644.
6. J. R. Tse and A. J. Engler. Stiffness gradients mimicking in vivo tissue variation regulate mesenchymal stem cell fate, *PLoS ONE*, 2011, **6**, e15978.
7. J. L. Young and A. J. Engler. Hydrogels with time-dependent material properties enhance cardiomyocyte differentiation in vitro, *Biomaterials*, 2011, **32**, 1002-1009.

8. A. M. Kloxin, A. M. Kasko, C. N. Salinas and K. S. Anseth. Photodegradable hydrogels for dynamic tuning of physical and chemical properties, *Science*, 2009, **324**, 59-63.

9. M. F. Berry, A. J. Engler, Y. J. Woo, T. J. Pirolli, L. T. Bish, V. Jayasankar, K. J. Morine, T. J. Gardner, D. E. Discher and H. L. Sweeney. Mesenchymal stem cell injection after myocardial infarction improves myocardial compliance, *Am J Physiol Heart Circ Physiol*, 2006, **290**, H2196-2203.

10. K. R. Levental, H. Yu, L. Kass, J. N. Lakins, M. Egeblad, J. T. Erler, S. F. T. Fong, K. Csiszar, A. Giaccia, W. Weninger, M. Yamauchi, D. L. Gasser and V. M. Weaver. Matrix crosslinking forces tumor progression by enhancing integrin signaling, *Cell*, 2009, **139**, 891-906.

11. A. I. Caplan. Why are MSCs therapeutic? New data: new insight, *J Pathol*, 2009, **217**, 318-324.

12. M. F. Pittenger and B. J. Martin. Mesenchymal stem cells and their potential as cardiac therapeutics, *Circ Res*, 2004, **95**, 9-20.

13. C. Chung and J. A. Burdick. Influence of three-dimensional hyaluronic Acid microenvironments on mesenchymal stem cell chondrogenesis, *Tissue Engineering Part A*, 2009, **15**, 243-254.

14. M. A. Serban and G. D. Prestwich. Modular extracellular matrices: solutions for the puzzle, *Methods*, 2008, **45**, 93-98.

15. J. A. Burdick and K. S. Anseth. Photoencapsulation of osteoblasts in injectable RGD-modified PEG hydrogels for bone tissue engineering, *Biomaterials*, 2002, **23**, 4315-4323.

16. J. A. Rowley, G. Madlambayan and D. J. Mooney. Alginate hydrogels as synthetic extracellular matrix materials, *Biomaterials*, 1999, **20**, 45-53.

17. C. Chung, J. Mesa, M. A. Randolph, M. Yaremchuk and J. A. Burdick. Influence of gel properties on neocartilage formation by auricular chondrocytes photoencapsulated in hyaluronic acid networks, *J. Biomed. Mater. Res.*, 2006, **77**, 518-525.

18. I. Erickson, A. Huang, C. Chung, R. Li, J. Burdick and R. Mauck. Differential Maturation and Structure-Function Relationships in MSC- and Chondrocyte-Seeded Hydrogels, *Tissue Engineering Part A*, 2009.

19. E. M. Chandler, C. M. Berglund, J. S. Lee, W. J. Polacheck, J. P. Gleghorn, B. J. Kirby and C. Fischbach. Stiffness of photocrosslinked RGD-alginate gels regulates adipose progenitor cell behavior, *Biotechnol. Bioeng.*, 2011, **108**, 1683-1692.

20. A. Samani, J. Bishop, C. Luginbuhl and D. B. Plewes. Measuring the elastic modulus of ex vivo small tissue samples, *Phys Med Biol*, 2003, **48**, 2183-2198.

21. S. Suri and C. Schmidt. Photopatterned collagen-hyaluronic acid interpenetrating polymer network hydrogels, *Acta Biomaterialia*, 2009.

22. L. Weng, A. Gouldstone, Y. Wu and W. Chen. Mechanically strong double network photocrosslinked hydrogels from N,N-dimethylacrylamide and glycidyl methacrylated hyaluronan, *Biomaterials*, 2008, **29**, 2153-2163.

23. A. N. Buxton, J. Zhu, R. Marchant, J. L. West, J. U. Yoo and B. Johnstone. Design and Characterization of Poly(Ethylene Glycol) Photopolymerizable Semi-

Interpenetrating Networks for Chondrogenesis of Human Mesenchymal Stem Cells, *Tissue Engineering*, 2007, **13**, 2549-2560.

24. U. Hersel, C. Dahmen and H. Kessler. RGD modified polymers: biomaterials for stimulated cell adhesion and beyond, *Biomaterials*, 2003, **24**, 4385-4415.

25. G. Orive, R. M. Hernández, A. R. Gascón, M. Igartua and J. L. Pedraz. Development and optimisation of alginate-PMCG-alginate microcapsules for cell immobilisation, *International Journal of Pharmaceutics*, 2003, **259**, 57-68.

26. S. Khetan, J. S. Katz and J. A. Burdick. Sequential crosslinking to control cellular spreading in 3-dimensional hydrogels, *Soft Matter*, 2009, **5**, 1601-1606.

27. Y. Liu and M. Chanpark. Hydrogel based on interpenetrating polymer networks of dextran and gelatin for vascular tissue engineering, *Biomaterials*, 2009, **30**, 196-207.

28. A. M. Rokstad, I. Donati, M. Borgogna, J. Oberholzer, B. L. Strand, T. Espevik and G. Skjåk-Braek. Cell-compatible covalently reinforced beads obtained from a chemoenzymatically engineered alginate, *Biomaterials*, 2006, **27**, 4726-4737.

29. S. A. Zawko, S. Suri, Q. Truong and C. E. Schmidt. Photopatterned anisotropic swelling of dual-crosslinked hyaluronic acid hydrogels, *Acta Biomaterialia*, 2009, **5**, 14-22.

30. R. A. Marklein and J. A. Burdick. Controlling Stem Cell Fate with Material Design, *Adv Mater*, 2010, **22**, 175-189.

31. M. Breitbach, T. Bostani, W. Roell, Y. Xia, O. Dewald, J. M. Nygren, J. W. U. Fries, K. Tiemann, H. Bohlen, J. Hescheler, A. Welz, W. Bloch, S. E. W.

Jacobsen and B. K. Fleischmann. Potential risks of bone marrow cell transplantation into infarcted hearts, *Blood*, 2007, **110**, 1362-1369.

32. K. C. Ribeiro, E. C. Mattos, J. P. S. Werneck-de-castro, V. P. Ribeiro, R. H. Costa-e-Sousa, A. Miranda, E. L. Olivares, M. Farina, J. G. Mill, J. R. C. d. S. Goldenberg, M. O. Masuda and A. C. C. de Carvalho. Ectopic ossification in the scar tissue of rats with myocardial infarction, *Cell Transplant*, 2006, **15**, 389-397.

33. C. Y. Y. Yip and C. A. Simmons. The aortic valve microenvironment and its role in calcific aortic valve disease, *Cardiovascular pathology : the official journal of the Society for Cardiovascular Pathology*, 2011, **20**, 177-182.

# CHAPTER 5

## *Spatially and Temporally Controlled Hydrogel Mechanics to Modulate Stem Cell Interactions*

*Adapted from: Marklein, RA. and Burdick, JA. "Spatially controlled hydrogel mechanics to modulate stem cell interactions." Soft Matter, 2010, 6, 136-143.*

### 5.1 Introduction

The ability of stem cells to interact with and respond to their environment is being increasingly investigated both in native tissues and in synthetic systems.[1] For example, it is now clear that cells respond to the mechanical properties of their surroundings, which was originally investigated in somatic cells such as fibroblasts and endothelial cells[2, 3] and more recently in stem cells, including the effects of mechanics on specifying lineage commitment.[4] Native tissues can vary in stiffness (*e.g.* 0.1-1 kPa in brain tissue, ~10 kPa in relaxed muscle, and >30 kPa for pre-mineralized bone[5]) and stem cells differentiate down tissue specific lineages based on these properties. Thus, a clear understanding of this behaviour may be useful in the design of materials for applications in tissue engineering or for better understanding of cellular behaviour in disease states. For instance, stem cells in fibrotic myocardium after injury, where mechanics are greater than in healthy tissue, may differentiate and mineralize their surrounding matrix.[6]

Tissue engineering strategies have begun to incorporate matrix mechanics as a means to control stem cell behaviour, including morphology, proliferation, and extracellular matrix (ECM) secretion.[7] Coupled with other differentiation cues such as growth factors or adhesive ligands, an engineered biomimetic approach to tissue repair and regeneration may be possible by controlling the inherent mechanical properties of the

engineered scaffold. However, one limitation of current biomaterial systems used in these investigations is the inability to spatially and temporally control the network properties of the scaffold. Due to the heterogeneous and dynamic nature of tissues, it is necessary to design scaffolds that reflect these complex presentations of spatial and temporal matrix properties in order to facilitate proper cell behavior and tissue integration. Spatial and temporal differences in local mechanics are also relevant in certain pathologies[8, 9] and wound healing processes,[12, 13] and therefore the characterization and understanding of cell responses to these complex micorenvironments are critical for better understanding of fundamental stem cell behaviour and developing an effective tissue engineering strategy.

Only a few examples exist where hydrogel properties are controlled both spatially and temporally. Much of this is dependent on the use of light, due to the precise control that light affords. Photopolymerization with UV light is a commonly employed technique that involves radical polymerization using methacrylate or acrylate functionalized polymers.[10] By restricting UV light to certain regions, complex patterns of exposed and non-exposed regions can be imparted in hydrogels to spatially control cell behaviour.[11-13] Beyond patterning, gradients are useful in many applications and are found in many tissues and can direct cell migration.[14] Hydrogel gradients can be formed using specific mixing devices[15] or microfluidic chambers,[16, 17] but these techniques rely on the use of complex systems or only permit gradients of a certain magnitude. Furthermore, current system with the ability to temporally control hydrogel mechanics either involve a limited range in mechanics[18] or don't allow for matrix stiffening,[19] which is a widely observed response both in development and in certain pathologies.[20, 21] Thus,

a need exists for a hydrogel system that can be manipulated in space and time with respect to mechanical properties.

Hyaluronic acid (HA) is a polysaccharide that is present in native tissue and is also intimately involved in processes such as wound healing, cell motility, embryogenesis, and inflammation.[22, 23] HA possesses properties desirable for tunable scaffolds as a wide range of molecular weights can be obtained, as well as the presnce of chemically modifiable groups (hydroxyl and carboxyl groups) on the backbone. Functionalize HA with reactive groups such as methacrylates and acrylates has been utilized to form HA-based hydrogels for controlling stem cell differentiation.[22-27] These systems allow for uniform hydrogel properties and effective cell encapsulation, but do not allow for local control of the spatial and temporal properties of the network.

In this chapter, the sequential crosslinking process developed in Chapter 4 was utilized to explore the effects of mechanics on 2D hMSC behaviour, namely spreading and proliferation. Additionally, spatial and temporal modulation of mechanics was realized by regionally restricting light exposure and also the temporal presentation of UV light in the presence of cells. Although this is only a preliminary step towards the utility of these systems for actual tissue engineering constructs, this novel system allows for spatial and temporal control of mechanics for the purpose of driving stem cell behaviour.

## 5.2 Materials and Methodology

### *5.2.1 Methacrylated hyaluronic acid (MeHA) synthesis*

Methacrylated hyaluronic acid (MeHA) was synthesized as described in Chapter 4 in order to obtain a macromer with 100% modification (% methacrylation).[28]

Modification efficiency was defined as percentage of HA repeat units containing methacrylates based on $^{1}$H-NMR. Briefly, sodium hyaluronate (Lifecore, 59 kDa) was dissolved at 1 wt% in $dIH_2O$ and methacrylic anhydride (MA) was added dropwise (2.4 mL MA per g HA) while stirring at 4°C. The pH was maintained above 8 during the reaction by adding 5 N NaOH for 8 hours, followed by overnight reaction and further addition of MA (1.2 mL per g HA) and pH maintenance for 4 hours the following day. The macromer solution was dialyzed against $dIH_2O$ (SpectraPor, *MW* cutoff 6000-8000 Da) for 4 days, frozen at -80 °C, lyophilized and stored in powder form.

*5.2.2 Methacrylated Slide Preparation*

In order to easily handle and process thin hydrogels, slides were methacrylated to allow for covalent attachment of the hydrogels to the glass. 22 mm x 22 mm coverslips were first plasma coated for 3 min in order to activate the surface for methacrylation. Next, 100 μL of 3-(trimethoxysilyl)propyl methacrylate (Sigma) were placed on each activated slide and reacted at 100 °C for 1 h followed by 110 °C for 10 min. Finally, the slides were rinsed with deionized water and ethanol and allowed to dry.

*5.2.3 MeHA Hydrogel Crosslinking*

MeHA hydrogels were formed using one- or two-step crosslinking processes (**Figure 5.1A**). In the first step, Michael-type 'addition' crosslinking occurs *via* introduction of dithiothreitol (DTT, Sigma) to a 3 wt% solution of MeHA in PBS buffer containing 0.2 M triethanolamine (TEA, Sigma) and 0.05% I2959 (Irgacure). Various amounts of DTT were added to vary the theoretical molar consumption of methacrylates

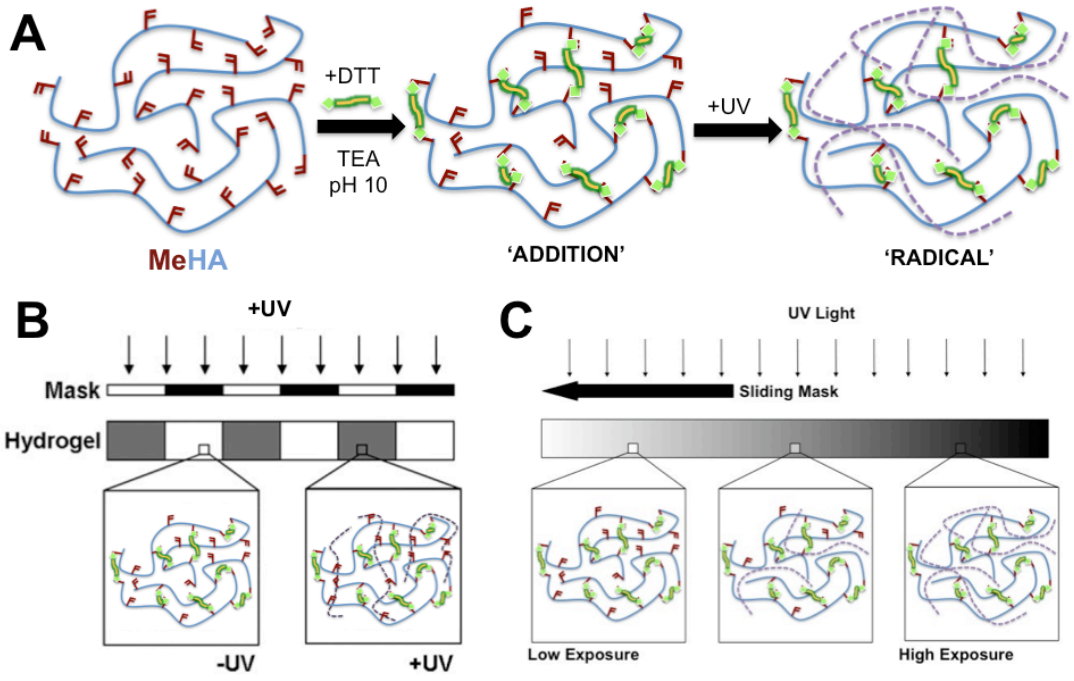


**Figure 5.1** (A) Michael addition of methacrylates with DTT (dithiol crosslinker) induces partial crosslinking of a solution of MeHA in TEA buffer at pH 10. Remaining methacrylates undergo radical polymerization when exposed to UV light in the presence of a photoinitiator (dotted lines represent kinetic chains) to increase crosslinking density (*i.e.* mechanics). Spatial variations in hydrogel mechanics can be introduced by restricting UV light to certain regions of the addition crosslinked gel using a photomask to create patterns (B) or varying the time of UV exposure (*via* a sliding mask) to create gradients (C).

(12, 15, 20, 30, 50, 100%) to achieve a range of initial mechanics during the first step. The oligopeptide GCGYG*RGDS*PG was added prior to DTT crosslinking to allow for coupling of the well-established RGD adhesion moiety to the network. Hydrogels were formed between slides with 150 μm spacing and methacrylated slides were used on one

side to allow for covalent hydrogel attachment. After mixing, the solutions were reacted for 1 h at 37 °C to complete the 'addition' crosslinking step ("-UV" gels).

Hydrogels could be further exposed to UV light in order to initiate 'Radical' crosslinking of the remaining unconsumed methacrylates. Collimated 10 mW/cm$^2$ 365 nm UV light (Omnicure S1000 UV Spot Cure System, Exfo Life Sciences Division) was used to uniformly expose the entire hydrogels for 4 min ("+UV" gels). This step could be performed to create uniform hydrogels or to create hydrogels with spatially or temporally controlled mechanics. Spatially controlled mechanics were achieved by restricting UV light to create patterns using a photomask (**Figure 5.1B**) or by varying the UV exposure time using a sliding photomask in order to create gradients (**Figure 5.1C**). For patterns, photomasks consisted of printed transparencies containing 500 μm stripe patterns that were created using Adobe Photoshop and printed at a resolution of 20,000 DPI. Gradient hydrogels were formed by passing a photomask over the surface of the hydrogel at a constant linear velocity (10 mm/min using a calibrated syringe pump) to create a range of varied exposure times and crosslinking (0-90 s) across a 15 mm distance. In order to temporally modulate mechanics, 'Addition'-only hydrogels were allowed to equilibrate overnight after which a 0.05% I2959 solution in PBS was swelled into the hydrogel (**Figure 5.2**) either in the presence or absence of cells. A range of UV exposures was used (0-120 s) and following exposure, the hydrogels were rinsed 3X with PBS (for mechanical testing) or cell culture medium (for cell culture studies).

### *5.2.4 Characterization of Hydrogel Mechanics*

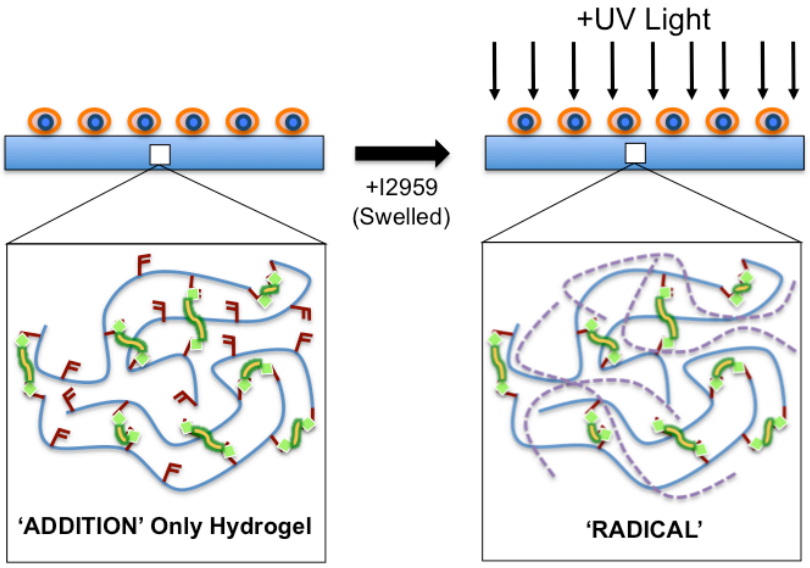


**Figure 5.2** Temporal modulation of MeHA hydrogel mechanics. hMSCs seeded initially on 'Addition'-only hydrogels and 0.05% I2959 solution is swelled into the hydrogel and then UV light exposure results in radical crosslinking ('stiffening') of hydrogel in the presence of cells.

Hydrogel surface mechanics were quantified using atomic force microscopy (AFM, Veeco Bioscope I). A silicon bead AFM tip with a spring constant of 0.06 N/m was used to obtain force curves for individual points on the hydrogels (15 points chosen for each condition) from which a local elastic modulus was calculated. For patterned and gradient hydrogels, points were chosen at regular intervals along the distance of the hydrogel (500 μm for stripe patterns or every 1.5 mm for gradient patterns). Dynamic hydrogel mechanics were measured as the uniform, static hydrogels (n=15 per condition).

### *5.2.5 Cell Seeding on MeHA Hydrogels*

hMSCs were obtained from Lonza and used at low passage for all studies (passages 2-5). Prior to cell seeding, hydrogels were sterilized using germicidal UV for 2 h in a cell culture hood. Cells were expanded and cultured in standard growth medium (α-MEM, 10% fetal bovine serum (FBS), 1% L-glutamine, and 1% penicillin-streptomycin) and seeded at a density of 5,000 cells per $cm^2$ on hydrogel surfaces. For most studies, an RGD concentration of 1 mM was used to promote hMSC adhesion and spreading. In order to determine whether the swelling of the softest hydrogels resulted in effective diluting of the RGD ligand, we tested several ligand densities (1, 2, and 5 mM) to elucidate the influence of ligand density on cellular spreading. For dynamic culture studies, cells were seeded on initially 'soft' 15% DTT crosslinked hydrogels and cultured for 24 h. A 0.05% I2959 solution was introduced into the samples and incubated for 30 min and finally exposed to 10 $mW/cm^2$ UV light (Spot Cure) for 2 min. Following exposure, samples were rinsed 3X with growth medium and analyzed for morphology 24 h after UV exposure.

*5.2.6 Cell Imaging and Quantification*

Cell spread area was calculated after 24 h for uniform and patterned hydrogels using an inverted microscope (Axiovert 200, Carl Zeiss Inc.). ImageJ (NIH) was used to calculate average cell spread area (>50 cells/condition) for each uniform hydrogel condition (-/+ UV), as well as regions of both striped and gradient hydrogels. Cells were stained with calcein AM (Invitrogen) for imaging on photopatterned hydrogels. Further staining was performed by fixing cells with 4% formalin followed by permeabilization with 0.25% Triton-X (Sigma) and cell nuclei staining using 2 μg/mL DAPI (Invitrogen).

Cel proliferation was quantified by counting cell nuclei on 5 images at 10X magnification on days 1, 4, and 7 for uniform hydrogels.

### *5.2.7 Statistical Analysis*

Values are reported as means and standard deviations (mechanics, proliferation) or standard errors of the mean (cell spreading). Statistical differences ($p<0.05$) were determined using a Student's *t*-test (JMP Software) to compare either mechanics, cell spreading, or cell proliferation on -/+ UV hydrogels.

## 5.3 Results and Discussion

### *5.3.1 MeHA Hydrogel Characterization and Cellular Response*

Hydrogels with uniform mechanics were formed by a multi-step crosslinking procedure, where addition crosslinking (*via* DTT) is performed initially (-UV) to consume all or a fraction of reactive groups and then followed by radical crosslinking (+UV) to further consume reactive groups. In this case, the reactivity was due to the methacrylates on HA that can react with thiols (on DTT) *via* an addition reaction or with each other during a radical polymerization to form kinetic chains in the presence of light and a photoinitiator. A highly functionalized HA (~100% modified) was used to allow for large changes in mechanics at a uniform macromer concentration (3 wt%); however, these parameters can be varied to alter overall hydrogel properties. Notably, the second step uses light that can be controlled spatially and temporally to obtain hydrogels with heterogenous and dynamic properties.

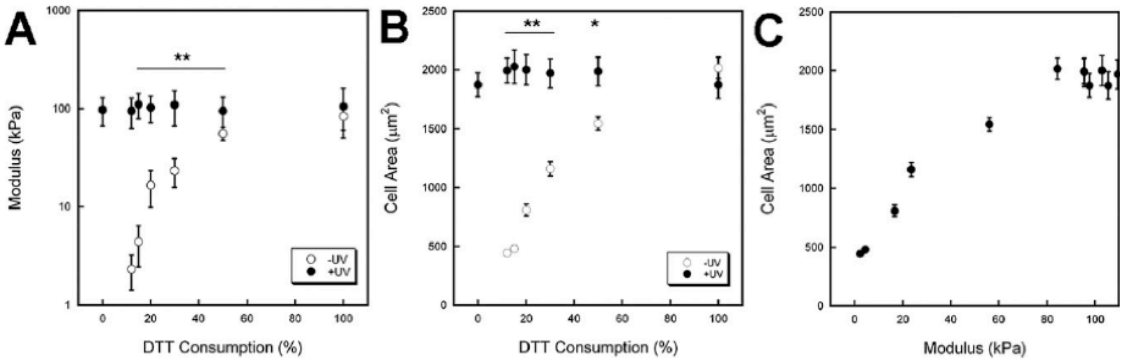


**Figure 5.3** Characterization of mechanics and hMSC response to hydrogels with uniform properties. (A) Hydrogel modulus for variable DTT consumption (theoretical values shown, based on molar ratio of thiols in DTT to methacrylates on MeHA) before (-UV, white) and after (+UV, black) light exposure. The mechanics can be tailored over two orders of magnitude with this system and result in a peak modulus of ~100 kPa. (B) hMSC spread area 24 h after seeding for the same hydrogel systems. (C) hMSC spread area 24 h after seeding *versus* mechanics shows increased cell area with increasing mechanics. Significant differences (**$p<0.001$, *$p<0.01$) were found between –UV and +UV gels.

AFM mechanical testing allowed for local probing of the surface hydrogel mechanical properties, which is representative of what a cell would sense when interacting with the material. **Figure 5.3A** illustrates the wide range of mechanics (nearly three orders of magnitude) achieved using this sequential crosslinking system. By varying the initial methacrylate consumption *via* molar ratio of DTT added, the hydrogel modulus ranged from 2.3 kPa (12% DTT -UV) to 84 kPa (100% DTT -UV). Furthermore, the exposure of these hydrogels to UV light resulted in an increase in modulus to ~100 kPa in all sequentially crosslinked hydrogels, which agreed well with the hydrogel polymerized using only the radical crosslinking step (**Figure 5.3A**, 0% DTT

+UV). Excluding the 100% DTT hydrogels, there were significant differences between the mechanics for all other -/+ hydrogel conditions.

The ability to sequentially crosslink hydrogels has been used in a similar addition-radical crosslinking system[29] and in other systems containing multi-component interpenetrating networks in which the two networks crosslink by different means.[17, 34-36] However, none of these systems exhibit the wide range of mechanics achievable using this sequentially crosslinkable MeHA system. While multi-component hydrogel systems allow for incorporation of multiple cell recognition sites and spatiotemporal control over mechanics and degradation, the complexity of these microenvironments makes determination of factors influencing stem cell behaviour more difficult. In our system we use a constant polymer and ligand concentration while only altering the crosslinking of the same macromer, and thus mechanics. Therefore, any observed differences in hMSC behaviour should be attributed to mechanics and not regional differences in ligand density and matrix components.

**Figure 5.3B** shows the spread area of hMSCs on hydrogels with a range of DTT consumptions -/+ UV after 24 h. Again, significant differences were found between the cell responses on -/+ hydrogels for all cases except the 100% DTT -/+ UV (where there was not a significant change in mechanics). The spread area is also plotted as a function of hydrogel mechanics in **Figure 5.3C**. This demonstrates a clear dependence of hMSC spreading on the mechanics of the substrate as spreading increases until it plateaus. Increases in cell area with increasing moduli have also been shown in studies using other substrates[4, 30] and other cell types.[3, 31, 32] The ability of stem cells to mechanosense has been linked to integrin binding and coupling of the cytoskeleton to these adhesion sites,

which is responsible for development of cellular tension and is stiffness dependent for many adherent cell types.[3, 33, 34] The presence of the RGD motif allows for binding with α5β1 integrins, which have been implicated in stem cell morphology and fate decisions.[35-37] The importance of RGD is further exemplified in negative controls consisting of HA hydrogels without coupled RGD, which showed no cell spreading on both soft and stiff substrates (see **Figure 4.11**).

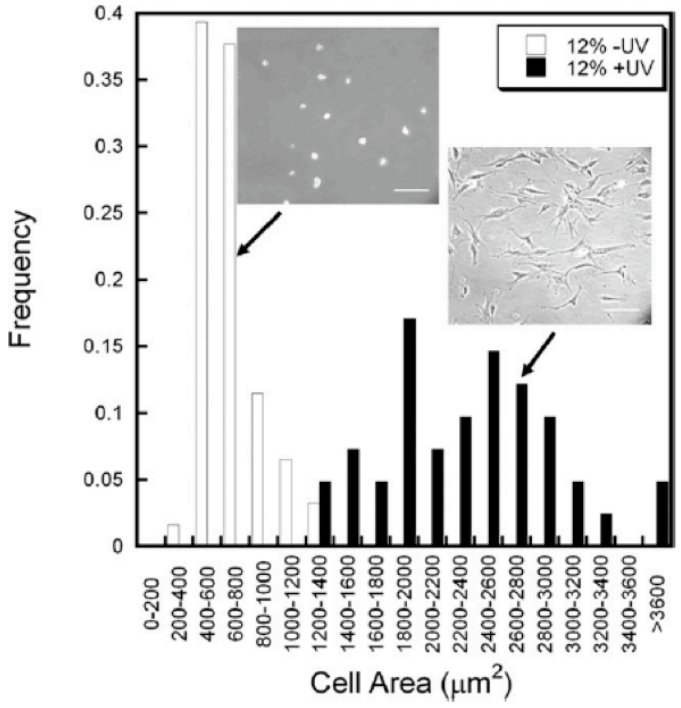


**Figure 5.4** Distribution of hMSC spreading on 'soft' (12% DTT –UV, white) and 'stiff' (12% DTT, +UV, black) hydrogels 24 h after seeding. Representative images are shown for each population. Scale bar = 200 μm

Histogram analysis of 12% DTT -/+ UV hydrogels showed two distinct populations of hMSCs in terms of spread area (**Figure 5.4**). Cells on the 'soft' 12% -UV

hydrogels exhibited a rounded morphology with few extensions, while cells on the 'stiff' +UV hydrogels showed a much more spread morphology with a wide distribution in cell area. Inset images are representative of cells for each condition after 24 h. These differences in morphology (due to mechanics) could specify further lineage commitment as stem cells have shown differentiation responses to imposed cell morphologies where less spread cells undergo adipogenesis and more spread cells undergo osteogenesis at a constant ligand density.[38] However, this study was performed on a relatively 'stiff' substrate (PDMS) and lacks the ability to create continuous patterns of cell behaviours, as well as temporally modulate the interactions.

*5.3.2 RGD Concentration Dependence*

While we were able to show orders of magnitude difference in mechanics for -/+ UV hydrogels, it was necessary to demonstrate that the lack of spreading observed on 12% DTT -UV hydrogels was a result of mechanics and not an effective diluting of the RGD due to swelling. Large changes in surface area due to swelling were not observed, potentially due to the hydrogel binding to the glass substrate, yet it is important to investigate how minor changes may influence outcomes. This potential decrease in surface ligand density could result in hMSCs not forming sufficient integrin binding sites to allow for spreading on soft substrates. To investigate this, cells were seeded on 'soft' hydrogels (12% DTT -UV) containing 1, 2, and 5 mM RGD to see if the increase in ligand density would result in spreading. Due to the high modification of HA used in this system, the percentages of methacrylates consumed by the RGD coupling were ~1.5, 3, and 7.5% for 1, 2, and 5 mM RGD, respectively. This low percentage of methacrylates

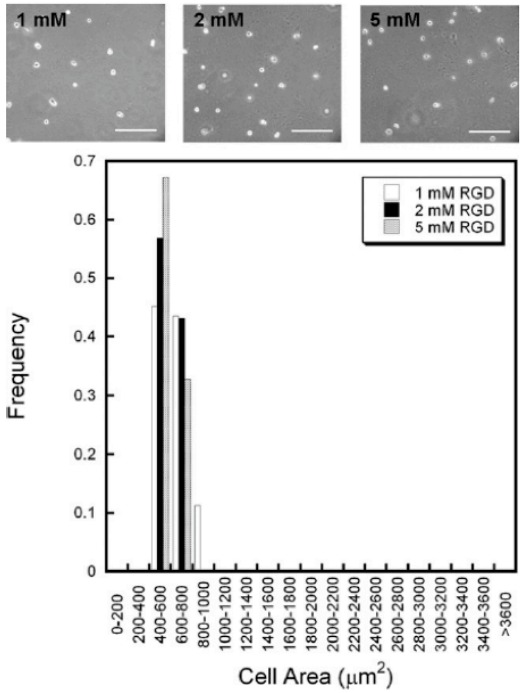


**Figure 5.5** Representative images (top) and histogram (bottom) of the relationship between hMSC spreading and adhesive ligand density for 'soft' (12% DTT –UV) hydrogels 24 h after seeding. No significant differences in cell area or morphology were observed with increasing ligand density of 1, 2, and 5 mM RGD. Scale bar = 200 μm

consumed by RGD coupling would therefore not result in competition with the DTT crosslinking step for available methacrylates. As shown in **Figure 5.5**, cells at all ligand concentrations exhibit the same rounded morphology, indicating that the lack of cell spreading is not a result of potential ligand density issues arising from hydrogel swelling. The strength of α5β1 integrin binding to fibronectin (specifically RGD and its synergy sequences) is tension dependent and while the amount of available integrin binding sites on each mechanics is constant, the adhesive strength of these binding complexes is stiffness dependent.[39] Although the cell may be forming more or less adhesive bonds to

the MeHA hydrogels at different RGD concentrations, these 'relaxed bonds' do not allow the cell to develop sufficient tension to spread on these soft substrates. Based on these findings, 1 mM RGD was used for the remaining studies.

*5.3.3 Stiffness Effects on Long Term Cell Behaviour*

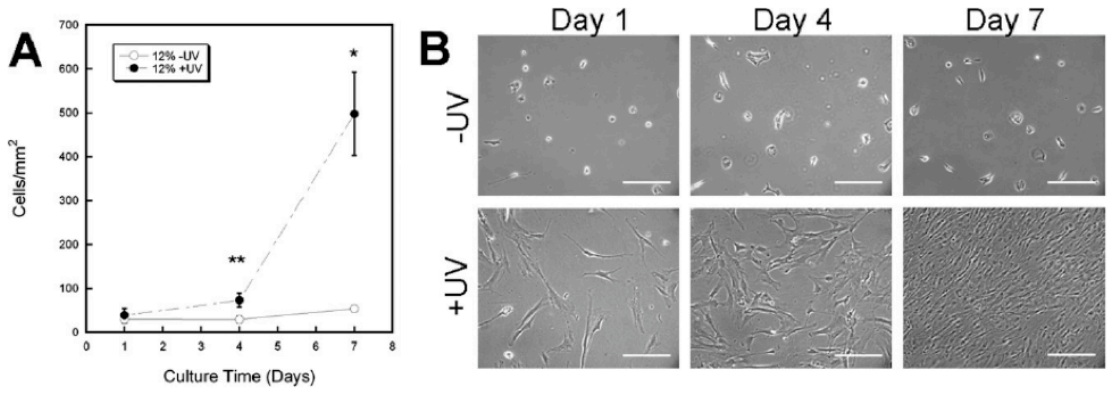


**Figure 5.6** (A) hMSC proliferation for up to 7 days on 'soft' (12% DTT –UV, white) and 'stiff' (12% DTT +UV, black) hydrogels. (B) Representative images with culture time for both hydrogels reveal the qualitative differences in hMSC number and morphology over 7 days. Scale bar = 200 μm. Significant differences (**p<0.001, *p<0.01) found between –UV and +UV hydrogels.

After determining the effects of matrix mechanics on short-term cell morphology, we investigated the long-term cell response to 12% DTT -/+ UV hydrogels by monitoring cell morphology and proliferation at several time points. **Figure 5.6A** shows the dramatic differences in cell proliferation over 7 days for the -/+ UV hydrogels. Cells on the +UV hydrogels proliferated much more than their -UV counterparts over the course of 7 days. Representative images indicate that the cells on the softer hydrogels

maintained their rounded morphologies while the cells on the stiffer hydrogels remained highly spread and became fully confluent after 7 days.

Cell proliferation has been shown to be dependent on matrix mechanics in several notable studies.[36, 40, 41] Highly spread cells possess a greater proportion of phosphorylated focal adhesion kinase (FAK), which has been shown to increase intracellular tension through Rho signaling. The maintenance of intracellular tension has significant consequences on whether a cell proliferates, differentiates, remains quiescent, or undergoes apoptosis.[42-44] The effects of spreading and mechanics have also been shown to result in changes in nuclear volume and chromatin condensation. In one study, increases in endothelial cell spreading led to an increase in nuclear volume and a greater proportion of cells in the S phase of cell division.[45] Our findings show a similar behaviour in hMSCs as proliferation was significantly higher on the stiffer substrates.

*5.3.4 Spatially Controlled Mechanics and Stem Cell Response*

The ability to control stem cell spreading and proliferation has been demonstrated on substrates wit uniform mechanics; however, spatial control of these behaviours is necessary due to the heterogeneous nature of many tissues. This is useful for intial steps towards advanced tissue engineering approaches, as well as to understand multi-phenotype differentiation from a single cell population. **Figure 5.7A** shows the differences in moduli on photopatterned regions of non-exposed (~6 kPa) and exposed (~31 kPa) stripes of 500 μm width. After 24 h, cells acquire morphologies reminiscent of the uniform hydrogels on the corresponding mechanical environments (*i.e.* rounded on 'soft' regions and highly spread on 'stiff' regions, **Figure 5.7B**). This is observed in

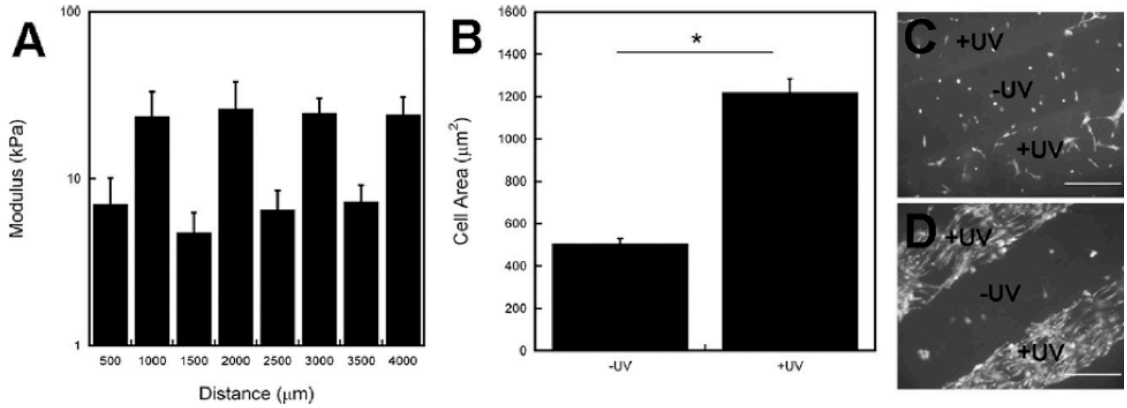


**Figure 5.7** Spatially controlled mechanics (A) and hMSC spreading (B) on photopatterned stripes (500 μm width) on 12% DTT hydrogels. The mechanics vary across the hydrogel based on exposure to UV light and is correlated with hMSC morphology response. Cellular morphology on patterns after 1 day (C) and 7 days (D) illustrates local hMSC response to mechanics. Statistically significant difference in hydrogel modulus and cell area ($p<0.001$),

representative images of photopatterned stripes with cells showing the spatial control of cell morphology based on local mechanics. It is clear that cells maintain a rounded morphology on the softer -UV regions and are highly spread on the stiffer +UV regions (**Figure 5.7C**). Of note, many cells aligned along the soft/stiff interface just as NIH3T3 fibroblasts do on similar mechanical interfaces.[46, 47] Cell migration due to durotaxis can also take place in these interfacial regions as cell adhesion sites on the stiffer regions result in greater traction generation, and subsequent greater adhesion strength, which allows the cells to migrate from soft to stiff regions. After 7 days, cells became confluent on the 'stiff' regions, but not in the 'soft' regions (**Figure 5.7D**). These large differences in confluence could be due to cells proliferatin, as well as cells migrating from the softer to stiffer regions.

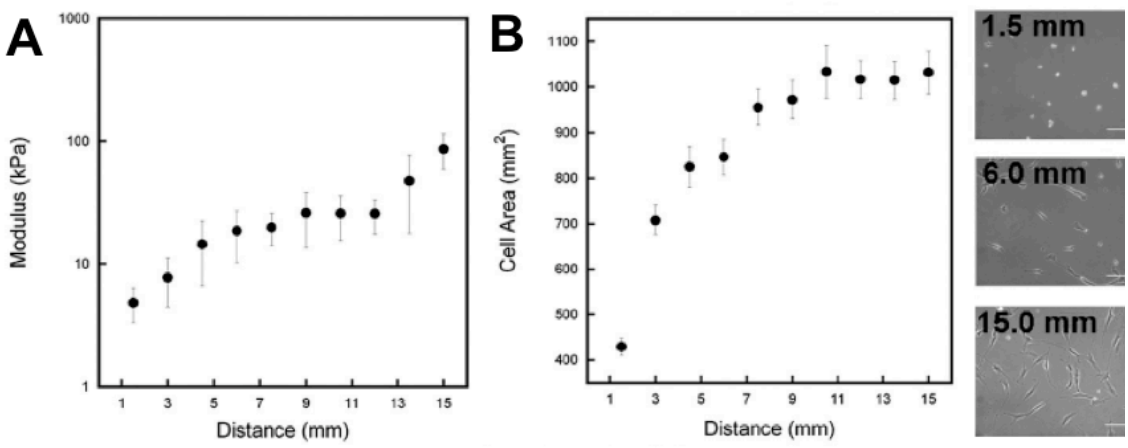


**Figure 5.8** Mechanical gradients were achieved using a sliding photomask to locally vary the light exposure time and thus mechanics nearly two orders of magnitude across a single hydrogel (A). hMSC response to the mechanical gradient (B) with representative images shown at different distance (exposure) along the gradient hydrogel (right). Scale bar = 200 μm

In another photopattern strategy, the extent of exposure was linearly varied by passing a photomask across the surface of the preliminarily crosslinked hydrogel (see schematic in **Figure 5.1C**). Locally probing the modulus at regular intervals along the length of the gradient allowed for correlation of matrix mechanics with distance (*i.e.* time of light exposure). As shown in **Figure 5.8A**, the modulus gradually increases form a minimum of ~6 kPa to ~25 kPa over regions with up to a minute of exposure followed by a sharp increase in mechanics for regions with an additional 30 s of exposure up to a maximum modulus comparable to the 12% DTT +UV uniform hydrogel (~90 kPa). Other sequentially crosslinked systems saw similar rapid secondary crosslinking upon exposure of UV to radically polymerize remaining photoreactive groups.[29, 48] As expected, the hMSC spreading increased locally along the length of the gradient, reacing a spreading plateau in regions of the hydrogel that had been exposed for greater than 60 s.

These photopatterning studies not only indicate that we can control matrix mechanics in a binary manner (-/+ UV), but also in a gradient manner with the capability to create a wide range of mechanics using the same base HA network composition.

*5.3.5 Dynamic Control of Hydrogel Mechanics and Stem Cell Morphology*

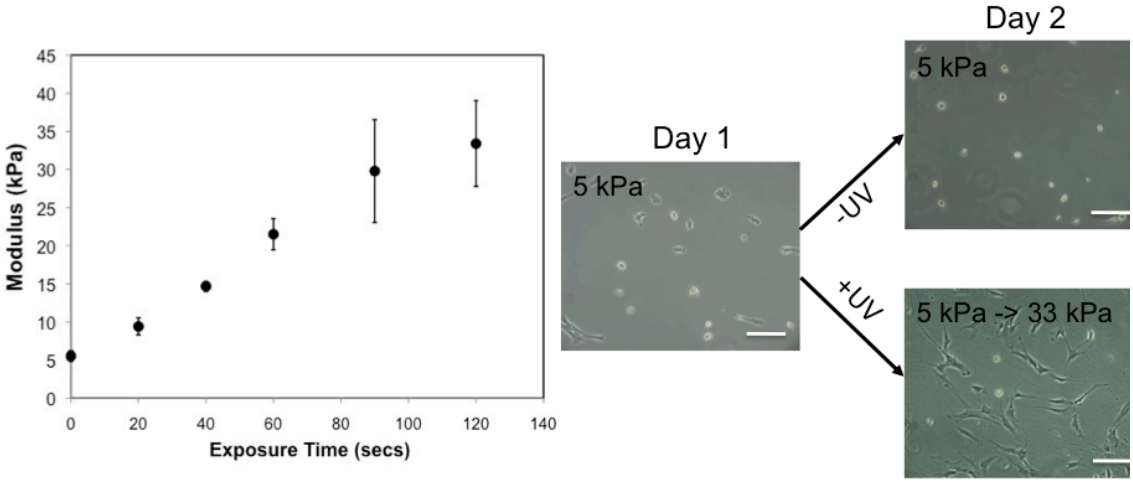


**Figure 5.9** Temporal modulation of hMSC morphology. (A) hMSC hydrogel mechanics controlled by varying UV exposure time on 'Addition'-only hydrogels (15% DTT) after swelling in I2959 solution. (B) Representative images of hMSC morphology on initially 'soft' 5 kPa hydrogels (Day 1), swelled with I2959 solution and either unexposed (-UV) or exposed (+UV) and morphology assessed after 24 h (Day 2). Scale bar = 200 μm

In order to investigate the dynamic nature of hMSC responses to mechanics, the sequentially crosslinked system was adapted to allow for secondary crosslinking to occur in the presence of cells. To accomplish this, an 'Addition'-only hydrogel (15% DTT consumption) was formed and exposed to a range of UV exposure times after re-introducing photoinitiator into the network (I2959 solution swelled into hydrogel). As shown in **Figure 5.9**, a wide range in mechanics (from 5-33 kPa) was achieved using this

modified sequential crosslinking approach with a more gradual increase in mechanics with increasing exposure time compared to the modulation in mechanics observed in the gradient hydrogel system (**Figure 5.8A**). hMSCs seeded on initially 'soft' 5 kPa hydrogels were rounded after 1 day of culture (similar to uniform hydrogels). However, after introducing photoinitiator and exposing to 2 min of UV (thus increasing the modulus to 33 kPa), hMSCs became spread much like cells that were initially cultured on 'stiff' static substrates. On samples that were not exposed to UV, the cells remained rounded as expected for cells initially seeded on uniform, static 'soft' hydrogels. This provides evidence for dynamic sensing of the mechanical environment and could prove to be a useful tool for investigating stem cell fate decisions in response to dynamic environments as well as investigating aberrant cell responses associated with 'stiffening' of the tissue (*i.e.* fibrosis[9, 21]).

## 5.4 Conclusions

Chapter 5 demonstrates how hMSC responses (morphology and proliferation) can be impacted by mechanics of the MeHA hydrogel. By changing the initial crosslinker concentration, elastic moduli over several orders of magnitude were obtained that could be significantly increased through the incorporation of sequential radical crosslinking. Furthermore, the ability to spatially and temporally control mechanics was possible by controlling the location and timing of UV light exposure. This allowed for patterned cell responses, as hMSCs exhibited morphologies corresponding well with the local substrate mechanics. Stem cell behaviour was also temporally modulated as stiffening of the hydrogel resulted in a dramatic switch from a rounded morphology to a more spread

morphology. While these outputs are not necessarily indicative of stem cell differentiation, morphology and proliferation can be determinants and effectors of differentiation in both 2D and 3D microenvironments.[30, 36, 40, 49, 50] As mechanical differences are also relevant in certain pathologies and development, the characterization and understanding of cell responses to mechanics in a controlled manner are critical for developing effective tissue engineering strategies.

**REFERENCES:**


1. R. A. Marklein and J. A. Burdick. Controlling stem cell fate with material design, *Advanced materials*, 2010, **22**, 175-189.
2. R. J. Pelham and Y. l. Wang. Cell locomotion and focal adhesions are regulated by substrate flexibility, *Proc Natl Acad Sci USA*, 1997, **94**, 13661-13665.
3. T. Yeung, P. C. Georges, L. A. Flanagan, B. Marg, M. Ortiz, M. Funaki, N. Zahir, W. Ming, V. Weaver and P. A. Janmey. Effects of substrate stiffness on cell morphology, cytoskeletal structure, and adhesion, *Cell Motil. Cytoskeleton*, 2004, **60**, 24-34.
4. A. J. Engler, S. Sen, H. L. Sweeney and D. E. Discher. Matrix elasticity directs stem cell lineage specification, *Cell*, 2006, **126**, 677-689.
5. F. Rehfeldt, A. Engler, A. Eckhardt, F. Ahmed and D. Discher. Cell responses to the mechanochemical microenvironment—Implications for regenerative medicine and drug delivery, *Advanced Drug Delivery Reviews*, 2007, **59**, 1329-1339.
6. M. Breitbach, T. Bostani, W. Roell, Y. Xia, O. Dewald, J. M. Nygren, J. W. U. Fries, K. Tiemann, H. Bohlen, J. Hescheler, A. Welz, W. Bloch, S. E. W. Jacobsen and B. K. Fleischmann. Potential risks of bone marrow cell transplantation into infarcted hearts, *Blood*, 2007, **110**, 1362-1369.
7. J. Burdick and G. Vunjak-Novakovic. Review: Engineered Microenvironments for Controlled Stem Cell Differentiation, *Tissue Engineering Part A*, 2008.

8. K. R. Johnson, J. L. Leight and V. M. Weaver. Demystifying the effects of a three-dimensional microenvironment in tissue morphogenesis, *Methods Cell Biol*, 2007, **83**, 547-583.

9. R. G. Wells. The role of matrix stiffness in regulating cell behavior, *Hepatology*, 2008, **47**, 1394-1400.

10. J. L. Ifkovits and J. A. Burdick. Review: Photopolymerizable and Degradable Biomaterials for Tissue Engineering Applications, *Tissue Engineering*, 2007, **13**, 2369-2385.

11. S. J. Bryant, J. L. Cuy, K. D. Hauch and B. D. Ratner. Photo-patterning of porous hydrogels for tissue engineering, *Biomaterials*, 2007, **28**, 2978-2986.

12. S. Lee, J. Moon and J. West. Three-dimensional micropatterning of bioactive hydrogels via two-photon laser scanning photolithography for guided 3D cell migration, *Biomaterials*, 2008, **29**, 2962-2968.

13. S. Suri and C. Schmidt. Photopatterned collagen-hyaluronic acid interpenetrating polymer network hydrogels, *Acta Biomaterialia*, 2009.

14. M. Singh, C. Berkland and M. S. Detamore. Strategies and applications for incorporating physical and chemical signal gradients in tissue engineering, *Tissue engineering Part B, Reviews*, 2008, **14**, 341-366.

15. S. A. DeLong, A. S. Gobin and J. L. West. Covalent immobilization of RGDS on hydrogel surfaces to direct cell alignment and migration, *Journal of controlled release : official journal of the Controlled Release Society*, 2005, **109**, 139-148.

16. J. A. Burdick, A. Khademhosseini and R. Langer. Fabrication of gradient hydrogels using a microfluidics/photopolymerization process, *Langmuir : the ACS journal of surfaces and colloids*, 2004, **20**, 5153-5156.

17. N. Zaari, P. Rajagopalan, S. K. Kim, A. J. Engler and J. Y. Wong. Photopolymerization in Microfluidic Gradient Generators: Microscale Control of Substrate Compliance to Manipulate Cell Response, *Adv Mater*, 2004, **16**, 2133-2137.

18. J. L. Young and A. J. Engler. Hydrogels with time-dependent material properties enhance cardiomyocyte differentiation in vitro, *Biomaterials*, 2011, **32**, 1002-1009.

19. A. M. Kloxin, A. M. Kasko, C. N. Salinas and K. S. Anseth. Photodegradable hydrogels for dynamic tuning of physical and chemical properties, *Science*, 2009, **324**, 59-63.

20. M. F. Berry, A. J. Engler, Y. J. Woo, T. J. Pirolli, L. T. Bish, V. Jayasankar, K. J. Morine, T. J. Gardner, D. E. Discher and H. L. Sweeney. Mesenchymal stem cell injection after myocardial infarction improves myocardial compliance, *Am J Physiol Heart Circ Physiol*, 2006, **290**, H2196-2203.

21. K. R. Levental, H. Yu, L. Kass, J. N. Lakins, M. Egeblad, J. T. Erler, S. F. T. Fong, K. Csiszar, A. Giaccia, W. Weninger, M. Yamauchi, D. L. Gasser and V. M. Weaver. Matrix crosslinking forces tumor progression by enhancing integrin signaling, *Cell*, 2009, **139**, 891-906.

22. C. Chung and J. A. Burdick. Influence of three-dimensional hyaluronic Acid microenvironments on mesenchymal stem cell chondrogenesis, *Tissue Engineering Part A*, 2009, **15**, 243-254.

23. M. A. Serban and G. D. Prestwich. Modular extracellular matrices: solutions for the puzzle, *Methods*, 2008, **45**, 93-98.

24. I. Erickson, A. Huang, C. Chung, R. Li, J. Burdick and R. Mauck. Differential Maturation and Structure-Function Relationships in MSC- and Chondrocyte-Seeded Hydrogels, *Tissue Engineering Part A*, 2009.

25. N. E. Fedorovich, M. H. Oudshoorn, D. van Geemen, W. E. Hennink, J. Alblas and W. J. A. Dhert. The effect of photopolymerization on stem cells embedded in hydrogels, *Biomaterials*, 2009, **30**, 344-353.

26. N. S. Hwang, S. Varghese, P. Theprungsirikul, A. Canver and J. Elisseeff. Enhanced chondrogenic differentiation of murine embryonic stem cells in hydrogels with glucosamine, *Biomaterials*, 2006, **27**, 6015-6023.

27. J. Kutty, E. Cho, J. Soolee, N. Vyavahare and K. Webb. The effect of hyaluronic acid incorporation on fibroblast spreading and proliferation within PEG-diacrylate based semi-interpenetrating networks, *Biomaterials*, 2007, **28**, 4928-4938.

28. R. A. Marklein and J. A. Burdick. Spatially controlled hydrogel mechanics to modulate stem cell interactions, *Soft Matter*, 2010, **6**, 136-143.

29. S. Khetan, J. S. Katz and J. A. Burdick. Sequential crosslinking to control cellular spreading in 3-dimensional hydrogels, *Soft Matter*, 2009, **5**, 1601-1606.

30. A. S. Rowlands, P. A. George and J. J. Cooper-White. Directing osteogenic and myogenic differentiation of MSCs: interplay of stiffness and adhesive ligand presentation, *AJP: Cell Physiology*, 2008, **295**, C1037-C1044.

31. X. Q. Brown, K. Ookawa and J. Y. Wong. Evaluation of polydimethylsiloxane scaffolds with physiologically-relevant elastic moduli: interplay of substrate mechanics and surface chemistry effects on vascular smooth muscle cell response, *Biomaterials*, 2005, **26**, 3123-3129.

32. A. Engler, L. Bacakova, C. Newman, A. Hategan, M. Griffin and D. Discher. Substrate compliance versus ligand density in cell on gel responses, *Biophysical Journal*, 2004, **86**, 617-628.

33. F. Byfield, R. Reen, T. Shentu, I. Levitan and K. Gooch. Endothelial actin and cell stiffness is modulated by substrate stiffness in 2D and 3D, *Journal of biomechanics*, 2009.

34. J. Solon, I. Levental, K. Sengupta, P. C. Georges and P. A. Janmey. Fibroblast Adaptation and Stiffness Matching to Soft Elastic Substrates, *Biophysical Journal*, 2007, **93**, 4453-4461.

35. D. S. W. Benoit, A. R. Durney and K. S. Anseth. The effect of heparin-functionalized PEG hydrogels on three-dimensional human mesenchymal stem cell osteogenic differentiation, *Biomaterials*, 2007, **28**, 66-77.

36. W. A. Comisar, N. H. Kazmers, D. J. Mooney and J. J. Linderman. Engineering RGD nanopatterned hydrogels to control preosteoblast behavior: a combined computational and experimental approach, *Biomaterials*, 2007, **28**, 4409-4417.

37. M. M. Martino, M. Mochizuki, D. A. Rothenfluh, S. A. Rempel, J. A. Hubbell and T. H. Barker. Controlling integrin specificity and stem cell differentiation in 2D and 3D environments through regulation of fibronectin domain stability, *Biomaterials*, 2009, **30**, 1089-1097.

38. R. McBeath, D. M. Pirone, C. M. Nelson, K. Bhadriraju and C. S. Chen. Cell shape, cytoskeletal tension, and RhoA regulate stem cell lineage commitment, *Dev Cell*, 2004, **6**, 483-495.

39. J. C. Friedland, M. H. Lee and D. Boettiger. Mechanically activated integrin switch controls alpha5beta1 function, *Science*, 2009, **323**, 642-644.

40. S. X. Hsiong, P. Carampin, H.-J. Kong, K.-Y. Lee and D. J. Mooney. Differentiation stage alters matrix control of stem cells, *J. Biomed. Mater. Res.*, 2008, **85**, 145-156.

41. J. Winer, P. Janmey, M. McCormick and M. Funaki. Bone Marrow-Derived Human Mesenchymal Stem Cells Become Quiescent on Soft Substrates but Remain Responsive to Chemical or Mechanical Stimuli, *Tissue Engineering Part A*, 2008.

42. R. Assoian and E. Klein. Growth control by intracellular tension and extracellular stiffness, *Trends in Cell Biology*, 2008, **18**, 347-352.

43. C. S. Chen, M. Mrksich, S. Huang, G. M. Whitesides and D. E. Ingber. Geometric control of cell life and death, *Science*, 1997, **276**, 1425-1428.

44. A. L. Zajac and D. E. Discher. Cell differentiation through tissue elasticity-coupled, myosin-driven remodeling, *Curr Opin Cell Biol*, 2008, **20**, 609-615.

45. P. Roca-Cusachs, J. Alcaraz, R. Sunyer, J. Samitier, R. Farré and D. Navajas. Micropatterning of single endothelial cell shape reveals a tight coupling between nuclear volume in G1 and proliferation, *Biophys J*, 2008, **94**, 4984-4995.

46. S.-Y. Chou, C.-M. Cheng and P. R. Leduc. Composite polymer systems with control of local substrate elasticity and their effect on cytoskeletal and morphological characteristics of adherent cells, *Biomaterials*, 2009, **30**, 3136-3142.

47. C. M. Lo, H. B. Wang, M. Dembo and Y. l. Wang. Cell movement is guided by the rigidity of the substrate, *Biophys J*, 2000, **79**, 144-152.

48. S. A. Zawko, S. Suri, Q. Truong and C. E. Schmidt. Photopatterned anisotropic swelling of dual-crosslinked hyaluronic acid hydrogels, *Acta Biomaterialia*, 2009, **5**, 14-22.

49. D. Dikovsky, H. Bianco-Peled and D. Seliktar. Defining the Role of Matrix Compliance and Proteolysis in Three-Dimensional Cell Spreading and Remodeling, *Biophysical Journal*, 2007, **94**, 2914-2925.

50. S. Khetan and J. A. Burdick. Patterning network structure to spatially control cellular remodeling and stem cell fate within 3-dimensional hydrogels, *Biomaterials*, 2010, **31**, 8228-8234.

# CHAPTER 6

*Spatially Controlled Stem Cell Differentiation on Sequentially Crosslinked Hydrogels with Patterned and Gradient Mechanics*

## 6.1 Introduction

Chapter 5 demonstrated the effect of spatially controlled mechanics on stem cell behaviors, such as morphology and proliferation, in a system that is absent of known soluble inductive factors in the culture media. While distinct morphologies can be representative of commitment to a specific lineage,[1-3] a well-established adipogenic-osteogenic bipotential induction system[1-5] was investigated here in order to monitor the effects of spatially modulated mechanics on hMSC fate decisions. Adipogenesis and osteogenesis are two widely studied lineage commitments for hMSCs and the interplay between these two differentiation programs is implicated in regular bone maintenance and disease states such as osteoporosis.[6-8] Due to the spatial heterogeneity inherent in both the matrix composition and properties of bone and adipose tissue,[9, 10] development of a system to investigate hMSC commitment to osteogenic and adipogenic lineages in controlled mechanical microenvironments would be useful for not only fundamental stem cell biological questions, but also towards the development of scaffolds for bone and adipose tissue regeneration.

Using the sequentially crosslinked hydrogel system developed in Chapter 5, hMSC differentiation into adipogenic and osteogenic lineages was monitored on both uniform and spatially modulated hydrogels with distinct mechanics. The effect of mechanics on hMSC differentiation in bipotential inductive media has been investigated

previously using adipogenic-osteogenic[5] and myogenic-chondrogenic[11] systems on hydrogels with spatially uniform mechanics. Distinct differentiation behaviors were observed where the favored lineage specification correlated well with the mechanics associated with the given tissue (i.e., adipogenesis and chondrogenesis on softer substrates and osteogenesis and myogenesis on stiffer substrates). In order to further investigate the multi-lineage differentiation potential of hMSCs, sequentially crosslinked hydrogels with distinct spatial presentation of mechanics (i.e., stripes and gradients) were developed and evaluated for their ability to spatially control stem cell differentiation.

## 6.2 Materials and Methodology

### *6.2.1 Methacrylated Hyaluronic Acid (MeHA) Synthesis*

Methacrylated hyaluronic acid (MeHA) was synthesized as described in Chapter 4 in order to obtain a macromer with 100% modification (% methacrylation). Modification efficiency was defined as the percentage of HA repeat units containing methacrylates based on $^{1}$H NMR. Briefly, sodium hyaluronate (Lifecore, 59 kDa) was dissolved at 1 wt% in $dIH_2O$ and methacrylic anhydride (MA) was added dropwise (2.4 mL MA per g HA) while stirring at 4°C. The pH was maintained above 8 during the reaction by adding 5 N NaOH for 8 hours, followed by overnight reaction and further addition of MA (1.2 mL per g HA) and pH maintenance for 4 hours the following day. The macromer solution was dialyzed against $dIH_2O$ (SpectraPor, *MW* cutoff 6000-8000 Da) for 4 days, frozen at -80 °C, lyophilized and stored in powder form.

### *6.2.2 Methacrylated Slide Preparation*

In order to easily handle and process thin hydrogels, slides were methacrylated to allow for covalent attachment of the hydrogels to the glass. 22 mm x 22 mm coverslips were first plasma coated for 3 min in order to activate the surface for methacrylation. Next, 100 μL of 3-(trimethoxysilyl)propyl methacrylate (Sigma) was placed on each activated slide and reacted at 100 °C for 1 h followed by 110 °C for 10 min. Finally, the slides were rinsed with deionized water and ethanol and allowed to dry.

*6.2.3 MeHA Hydrogel Crosslinking*

MeHA hydrogels were formed using one- or two-step crosslinking processes as outlined in Chapter 5 (see **Figure 5.2**). In the first step, Michael-type 'addition' crosslinking occured *via* introduction of dithiothreitol (DTT, Sigma) to a 3 wt% solution of MeHA in PBS buffer containing 0.2 M triethanolamine (TEA, Sigma) and 0.05% I2959 (Irgacure). The base hydrogel (-UV) consisted of a 17% DTT-crosslinked MeHA hydrogel. The oligopeptide GCGYG*RGDS*PG was added prior to DTT crosslinking to allow for coupling of the well-established RGD adhesion moiety to the network. Hydrogels were formed using square PDMS molds with 150 μm spacing and methacrylated slides were used on one side to allow for covalent hydrogel attachment. After mixing, the solutions were reacted for 1 h at 37 °C to complete the 'addition' crosslinking step. In order to vary mechanics, the -UV hydrogels were equilibrated overnight and a 0.05% I2959 solution was introduced for 1 hour. Uniform +UV hydrogels were formed by exposing to 10 mW/cm$^2$ UV light (Omnicure S1000 Spotcure) for 2 min and rinsing 3X with PBS. Photopatterned hydrogels were formed by placing a photomask consisting of 750 μm stripes over the hydrogel and exposing to UV light for 2

min followed by 3X PBS washes. Hydrogels with mechanical gradients were formed by passing a sliding mask across the surface of the hydrogel at a linear velocity of 12.5 mm/min for 2 min in order to create a gradient with a length of 25 mm. Distinct unexposed and exposed regions were present at each end of the gradient to represent regions similar to the uniform -/+ UV conditions.

*6.2.4 Characterization of Hydrogel Mechanics*

Hydrogel surface mechanics were quantified using atomic force microscopy (AFM, Veeco Bioscope I). A silicon bead AFM tip with a spring constant of 0.06 N/m was used to obtain force curves for individual points on the hydrogels (15 points chosen for each condition) from which a local elastic modulus was calculated. For patterned and gradient hydrogels, points were chosen at regular intervals along the distance of the hydrogel (750 μm for stripe patterns and every 5 mm for gradient patterns).

*6.2.5 Cell Seeding on MeHA Hydrogels*

hMSCs were obtained from Lonza and used at low passage for all studies (passage 3). Prior to cell seeding, hydrogels were sterilized using germicidal UV for 2 h in a cell culture hood. In order to prevent observed differences in cell behavior based on proliferation, cells were subjected to Mitomycin C treatment (10 μg/mL in serum-free medium) for 2 hours prior to seeding and then washed 3X in growth medium. Cells were expanded and cultured in standard growth medium (α-MEM, 20% fetal bovine serum (FBS), 1% L-glutamine, and 1% penicillin-streptomycin) and seeded at a density of 5,000 cells per $cm^2$ on hydrogel surfaces. After 24 hours of initial cell attachment to hydrogel

surfaces, the growth medium was replaced with 1:1 adipogenic-osteogenic mixed inductive medium (R&D Systems) and maintained for 14 days in order to induce hMSC differentiation.

*6.2.6 Cell Imaging and Quantification*

For early time points, cells were fixed using 10% formalin and stained for nuclei and actin using DAPI and phalloidin (Invitrogen), respectively. On uniform hydrogels, the expression of the focal adhesion protein vinculin was assessed using immunostaining. Samples were fixed in formalin for 10 min, permeabilized in 0.25% Triton-X for 5 min, and blocked for 1 hour (10% goat serum, 1% BSA, 0.1% Triton-X). Primary mouse anti-vinculin antibody (Sigma, 1:200 dilution) was reacted overnight at 4°C and washed 3X using PBS containing 1% BSA. Secondary anti-mouse FITC-labeled antibody (Sigma, 1:200 dilution) was reacted at room temperature for 1 hour and washed 3X with PBS. For the late time point (day 14), hMSC adipogenic and osteogenic differentiation were assessed using Oil Red O and alkaline phosphatase stains, respectively. Alkaline phosphatase staining was performed using FastBlue/napthol solution (Sigma) for 1 hour at room temperature. Oil Red O staining was performed by washing samples with graded isopropanol solutions (20%, 40%, 60% isopropanol) followed by incubation with 3 mg/mL Oil Red O (Sigma) in 60% isopropanol for 30 min at room temperature. Cell areas were quantified on day 1 for gradient hydrogels using ImageJ at discrete locations along the length of the gradient (every 5 mm) with >30 cells per location and n=4 samples. For later time points, cell differentiation was evaluated by counting the total number of differentiated cells (osteogenic and adipogenic) and calculating the percentage

of cells from this differentiating population that underwent either lineage specification. For uniform, patterned, and gradient hydrogels, >30 cells were evaluated for each condition (or location on a patterned/gradient hydrogel) for n=4 hydrogels. The cell density for gradient hydrogels was assessed at early (day 1) and late (day 14) time points by calculating the cell density at each gradient position (every 5 mm) for n=4 hydrogels.

### *6.2.7 Statistical Analysis*

Values are reported as means and standard deviations. Statistical analyses were performed with Student's t-test and One-way ANOVA using R Statistical Software.

## 6.3 Results and Discussion

### *6.3.1 Uniform Hydrogel Mechanics and hMSC Response*

Uniform soft (-UV) and stiff (+UV) hydrogels were formed in order to recapitulate mechanics of adipose and bone tissue. As shown in **Figure 6.1A**, significant differences were observed between the -UV and +UV hydrogels as they possessed moduli of ~2 and ~31 kPa, respectively. These values agree well with reported values for adipose tissue (2-4 kPa) and pre-mineralized osteoid (20-50 kPa).[12-14] Similar to the results in Chapter 5, cells possessed distinct rounded and spread morphologies on the soft and stiff substrates, respectively (**Figure 6.1B**, phase). The focal adhesion complex protein vinculin was involved in cell mechanosensing and osteogenic differentiation and the increased expression (and presence of punctate structures) on stiffer +UV hydrogels coupled with a more organized cytoskeleton possessing stress fibers (**Figure 6.1B**) agrees with previous findings.[5, 15]

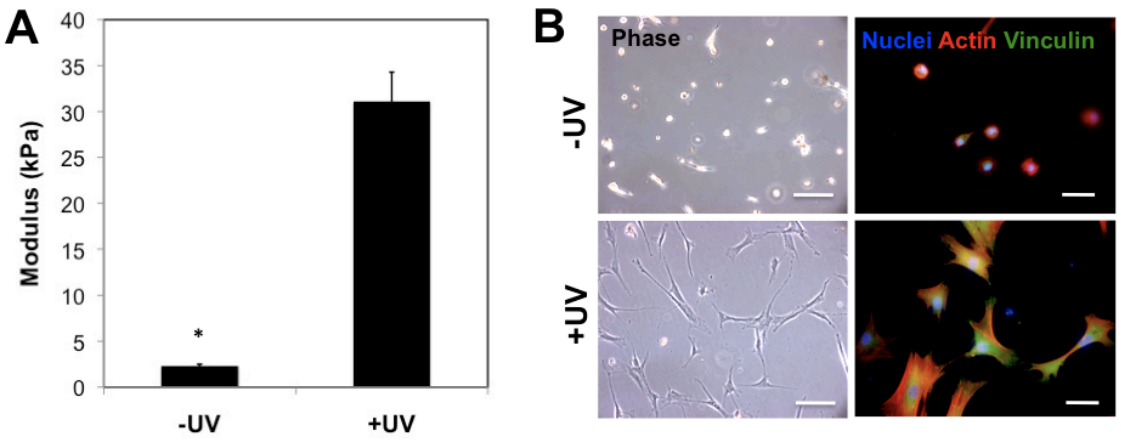


**Figure 6.1** (A) Mechanical characterization for uniform MeHA hydrogels assessed using AFM. Significant differences between –UV and +UV hydrogels (*p<0.001) (B) Day 1 morphology assessment of hMSCs cultured on soft (-UV) and stiff (+UV) hydrogels. Cytoskeletal and focal adhesion proteins (actin and vinculin, respectively) fluorescently evaluated for each uniform condition. Scale bars = 200 μm (for Phase) and 50 μm (for Fluorescence)

Following 14 days in mixed adipogenic-osteogenic media, hMSCs stained positively for Oil Red O (red lipid droplets) on softer substrates and alkaline phosphatase (blue) on stiffer substrates (**Figure 6.2A**). Similar differences in cytoskeletal assembly were noted at day 14 as cells on softer substrates had a more diffuse actin cytoskeleton (disrupted by presence of lipid droplets) while cells on stiffer substrates were highly spread with more organized actin cytoskeleton. Quantification of differentiation revealed stark differences in lineage specification, with significant differences observed between lineages on a given substrate and for a given lineage between each substrate (**Figure 6.2B**).

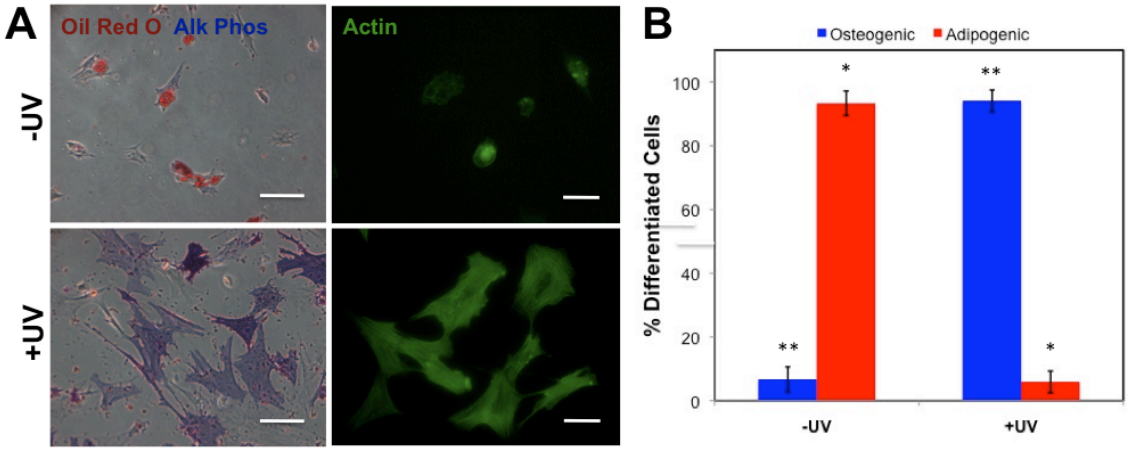


**Figure 6.2** (A) Day 14 images of hMSCs cultured in adipogenic-osteogenic inductive medium on soft (-UV, ~2 kPa) and stiff (+UV, ~30 kPa) uniform hydrogels. Phase images show staining for markers of adipogenesis (Oil Red O, red) and osteogenesis (Alkaline Phosphatase, blue) while fluoresecent images reveal cytoskeletal organization after 14 days in the mixed induction medium (actin, green). Scale bar = 200 μm (for phase) and 50 μm (for fluorescence) (B) Quantification of differentiation into each lineage shown on right with significant differences between –UV and +UV conditions observed for both osteogenesis (**p<0.001) and adipogenesis (*p<0.001)

*6.3.2 hMSC Differentiation Response to Photopatterned Mechanics*

MeHA hydrogels with spatially modulated mechanics were first investigated using 750 μm stripe patterns of unexposed (soft, -UV) and exposed (stiff, +UV) regions. A spatial mechanical profile of a given photopatterned hydrogel is shown in **Figure 6.3A,** and the -UV regions possessed a modulus ~1.6 kPa, while +UV regions possessed a modulus of ~30 kPa. At early time points, cells exhibited local morphological and

cytoskeletal behaviors similar to their responses on uniform hydrogels as cells on the softer -UV regions were rounded while cells on the stiffer +UV regions were highly spread (**Figure 6.3B and C**). After mixed induction, cells preferentially differentiated into the lineage as a result of their local mechanics with adipogenesis on -UV regions and osteogenesis on +UV regions, as indicated by Oil Red O and alkaline phosphatase staining, respectively (**Figure 6.4A-C**). Differences in differentiation marker expression on each mechanically-distinct region were also quantitatively assessed and reported in **Figure 6.4D** with statistically significant differences in differentiation observed between -UV and +UV stripe regions. Hydrogels with distinct spatially-defined regions of mechanics have been used previously to investigate cell-material interactions[16]; however, evidence of patterned differentiation from a single cell population based on local mechanics has not yet been demonstrated.

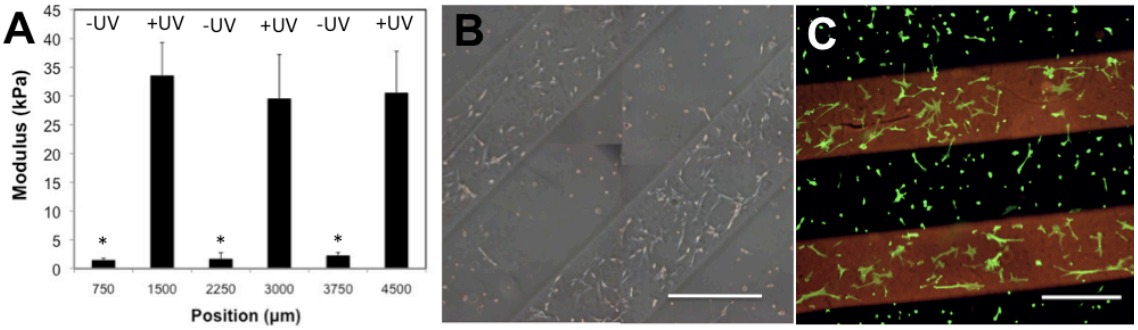


**Figure 6.3** (A) Mechanics profile for photopatterned MeHA hydrogels using 750 μm stripes. Significant differences observed between –UV stripes and +UV stripes (*$p<0.001$) Day 1 phase (B) and fluorescent (C) images showing distinct spatial organization of cells on stripe patterns. Fluorescent images indicate regions of UV exposure due to incorporation of methacrylated-rhodamine dye (red) and cytoskeletal organization (actin, green). Scale bars = 750 μm

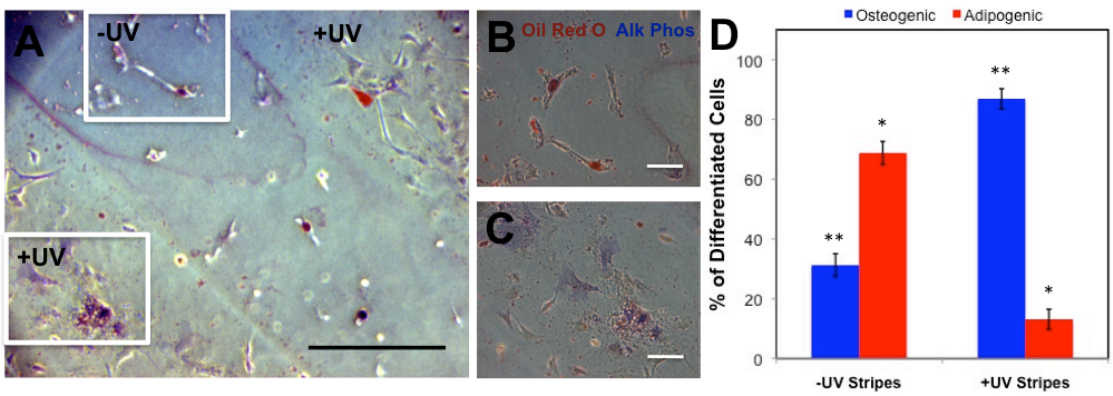


**Figure 6.4** (A) Low magnification phase image showing distinct soft (-UV) and stiff (+UV) regions in the same MeHA hydrogel with staining for adipogenic (Oil Red O, red) and osteogenic (Alkaline Phosphatase, blue) markers of differentiation. Scale bar = 500 μm. (B) Higher magnification of –UV (B) and +UV (C) regions highlighted by white boxes in (A). Scale bar = 100 μm (D) Quantification of differentiation into each lineage on each distinct region with significant differences between –UV and +UV stripes observed for both osteogenesis (**$p<0.001$) and adipogenesis (*$p<0.001$)

*6.3.3 Gradient Hydrogel Characterization and hMSC Differentiation Response*

A hydrogel with a gradient in mechanics across a length of 25 mm was developed in order to investigate the effects of a wide range in mechanics on stem cell lineage specification to adipogenic or osteogenic fates. As shown in **Figure 6.5A**, distinct soft and stiff regions existed at both ends of the gradient hydrogels with moduli of ~1.8 and 32 kPa, respectively. The gradient between these two regions was formed by linearly varying the exposure time using a sliding photomask and responded in a linear manner across the length of the gradient with approximate gradient magnitude of ~1 kPa/mm. Initial cell spreading was found to vary in a gradient manner as cells were rounded in the

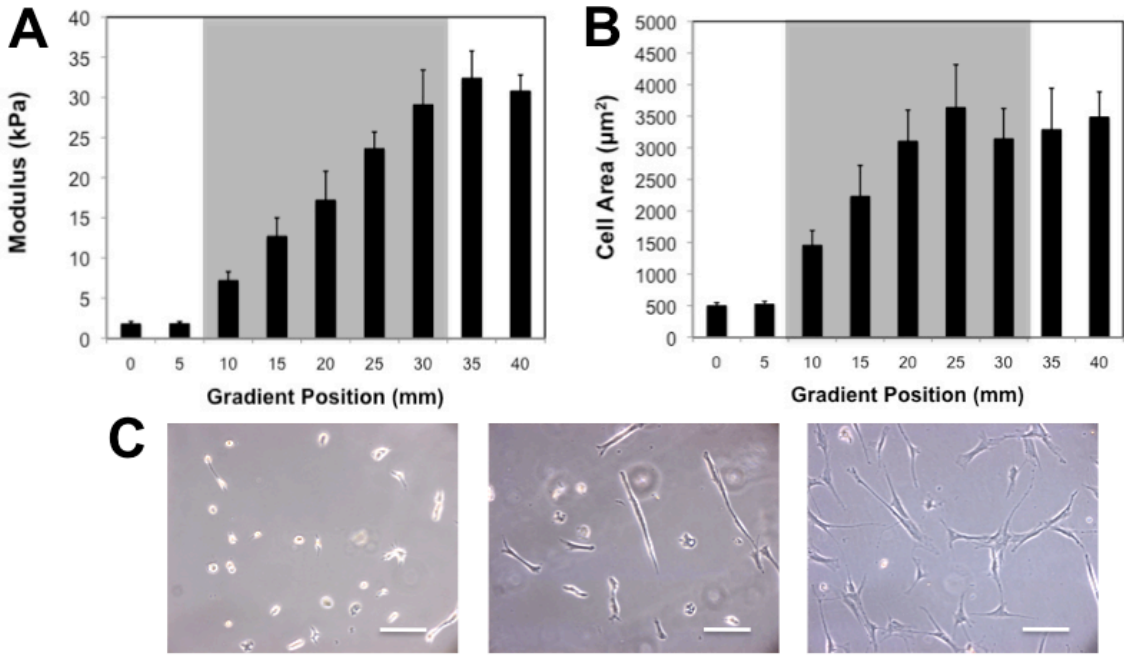


**Figure 6.5** (A) Mechanical characterization of gradient hydrogels at discrete points. (B) hMSC day 1 cell spreading response (mean±SEM) at points along gradient. Region of gradient highlighted in gray (C) Representative day 1 images of hMSCs with distinct morphological responses along length of gradient. Scale bar = 200 μm.

softer regions and exhibited increasing cell spread area with the increase in local moduli observed across the gradients (**Figure 6.5B**). Representative images of regions with distinct cell morphologies are shown in **Figure 6.5C** with characteristic rounded cells on the soft regions, mixed populations of rounded and spread cells on intermediate gradient positions, and fully spread cells on the stiffest region of the gradient hydrogel.

Following 14 days in mixed inductive media, hMSCs demonstrated a gradient response in differentiation (**Figure 6.6A**) as adipogenesis was favored on the softer regions, osteogenesis favored on the stiffer regions, and a dramatic shift in the ratio of

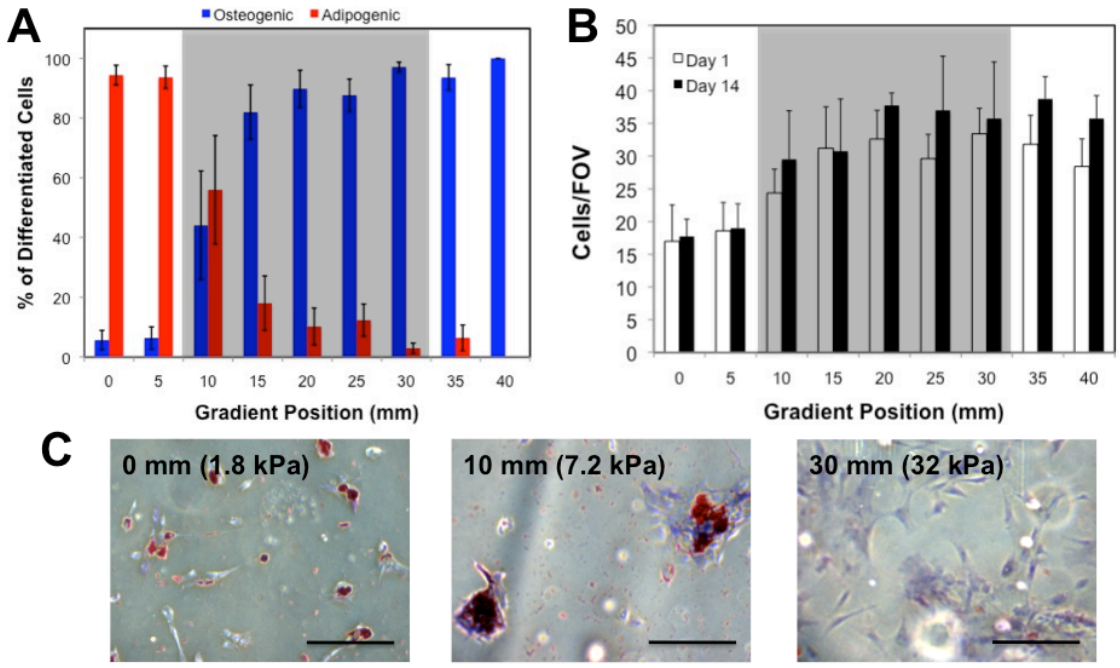


**Figure 6.6** (A) Quantification of hMSC differentiation at discrete points along length of gradient (B) Cell density per field of view (FOV) measured along length of gradient at day 1 (white) and day 14 (black). Region of gradient highlighted in gray (C) Representative images of hMSCs stained for markers of adipogenic (Oil Red O, red) and osteogenic (Alkaline Phosphatase, blue) differentiation at positions along gradient with distinct morphological behaviors. Scale bar = 500 μm

osteogenesis:adipogenesis occurred at the beginning of the gradient (10 mm, 7.2 kPa). Increased cell spreading has been shown to induce osteogenesis in mixed induction systems[1, 3, 5], and it follows in our gradient system that increases in cell spreading due to increasing mechanics across the length of the gradient results in a greater proportion of hMSCs expressing markers for osteogenesis (**Figure 6.6C**). In order to eliminate the possibility of cell proliferation influencing local cell density effects on differentiation, hMSCs were treated with Mitomycin C prior to cell seeding in order to inhibit

proliferation. **Figure 6.6B** shows that the cell density remained constant at each location from day 1 to day 14, indicating that cells did not proliferate or preferentially migrate from one region of the gradient hydrogel to another. Migration across gradients in mechanics have been observed for hMSCs in growth medium in a different system with moduli ranging from 1-14 kPa and a gradient magnitude of ~1 kPa/mm.[17] While our system did show similar mechanical gradients, the differences in culture conditions (adipogenic/osteogenic vs. growth medium) likely influenced the motility and fate decisions of cells cultured on hydrogels with heterogeneous mechanics.

Furthermore, the location that resulted in a nearly 50:50 mixed differentiation response showed distinct multicellular aggregates (**Figure 6.6C**, 'intermediate') with the center of the aggregates showing intense red staining (indicative of adipogenesis) and the surrounding of these aggregates with more intense blue staining (indicative of osteogenesis). This behavior was also observed in a different 2D system[18] that employed spatially restricted adhesive islands that allowed for distinct organizations of hMSCs. Similarly, cells located in the center of the aggregates stained more positively for adipogenic markers, while cells located on the outer regions of the aggregates typically stained more positively for osteogenesis. These findings were determined to be a result of differences in local cell traction force generation as cells within the aggregates exert less traction (and undergo adipogenesis), while periphery cells are able to develop traction, spread, and undergo osteogenesis.

## 6.4 Conclusions

As shown in Chapter 5, the spatial control of hydrogel mechanics resulted in distinct patterns of stem cell behavior according to the local mechanics. In this chapter, a mixed adipogenic-osteogenic induction medium was used to determine if local mechanics could dictate long term hMSC responses such as differentiation. Stem cell differentiation on hydrogels with uniform mechanics favored adipogenesis on softer substrates, while osteogenesis was favored on stiffer substrates. This trend was also evident on patterned hydrogels, as hMSCs preferentially differentiated into a given lineage based on the local mechanics (i.e., adipogenesis on softer stripes and osteogenesis on stiffer stripes). Finally, a gradient differentiation response was observed on hydrogels with a gradient in mechanics ranging from ~2-32 kPa with the ratio of osteogenesis:adipogenesis increasing as mechanics locally increased along the gradient. These findings further emphasize the importance of the spatial presentation of microenvironmental factors on stem cell fate decisions and illustrate the utility of this hydrogel system for investigating cell interactions with heterogeneous mechanical signals.

**REFERENCES:**


1. S. Khetan and J. A. Burdick. Patterning network structure to spatially control cellular remodeling and stem cell fate within 3-dimensional hydrogels, *Biomaterials*, 2010, **31**, 8228-8234.
2. K. A. Kilian, B. Bugarija, B. T. Lahn and M. Mrksich. Geometric cues for directing the differentiation of mesenchymal stem cells, *Proc Natl Acad Sci USA*, 2010, **107**, 4872-4877.
3. R. McBeath, D. M. Pirone, C. M. Nelson, K. Bhadriraju and C. S. Chen. Cell shape, cytoskeletal tension, and RhoA regulate stem cell lineage commitment, *Dev Cell*, 2004, **6**, 483-495.
4. M. Guvendiren and J. A. Burdick. The control of stem cell morphology and differentiation by hydrogel surface wrinkles, *Biomaterials*, 2010, **31**, 6511-6518.
5. M. Guvendiren and J. A. Burdick. Stiffening hydrogels to probe short- and long-term cellular responses to dynamic mechanics, *Nat Commun*, 2012, **3**, 792.
6. P. Augat, U. Simon, A. Liedert and L. Claes. Mechanics and mechano-biology of fracture healing in normal and osteoporotic bone, *Osteoporos Int*, 2005, **16 Suppl 2**, S36-43.
7. T. Hoshiba, N. Kawazoe and G. Chen. The balance of osteogenic and adipogenic differentiation in human mesenchymal stem cells by matrices that mimic stepwise tissue development, *Biomaterials*, 2012, **33**, 2025-2031.

8. H. Koshiyama, Y. Ogawa, K. Tanaka and I. Tanaka. The unified hypothesis of interactions among the bone, adipose and vascular systems: 'osteo-lipo-vascular interactions', *Med Hypotheses*, 2006, **66**, 960-963.

9. J.-H. Chen, C. Liu, L. You and C. A. Simmons. Boning up on Wolff's Law: mechanical regulation of the cells that make and maintain bone, *Journal of biomechanics*, 2010, **43**, 108-118.

10. U. A. Gurkan and O. Akkus. The mechanical environment of bone marrow: a review, *Annals of biomedical engineering*, 2008, **36**, 1978-1991.

11. J. S. Park, J. S. Chu, A. D. Tsou, R. Diop, Z. Tang, A. Wang and S. Li. The effect of matrix stiffness on the differentiation of mesenchymal stem cells in response to TGF-β, *Biomaterials*, 2011, **32**, 3921-3930.

12. E. M. Chandler, C. M. Berglund, J. S. Lee, W. J. Polacheck, J. P. Gleghorn, B. J. Kirby and C. Fischbach. Stiffness of photocrosslinked RGD-alginate gels regulates adipose progenitor cell behavior, *Biotechnol. Bioeng.*, 2011, **108**, 1683-1692.

13. D. E. Discher, D. J. Mooney and P. W. Zandstra. Growth Factors, Matrices, and Forces Combine and Control Stem Cells, *Science*, 2009, **324**, 1673-1677.

14. A. J. Engler, S. Sen, H. L. Sweeney and D. E. Discher. Matrix elasticity directs stem cell lineage specification, *Cell*, 2006, **126**, 677-689.

15. R. A. Marklein and J. A. Burdick. Spatially controlled hydrogel mechanics to modulate stem cell interactions, *Soft Matter*, 2010, **6**, 136-143.

16. S.-Y. Chou, C.-M. Cheng and P. R. Leduc. Composite polymer systems with control of local substrate elasticity and their effect on cytoskeletal and

morphological characteristics of adherent cells, *Biomaterials*, 2009, **30**, 3136-3142.

17. J. R. Tse and A. J. Engler. Stiffness gradients mimicking in vivo tissue variation regulate mesenchymal stem cell fate, *PLoS ONE*, 2011, **6**, e15978.

18. S. A. Ruiz and C. S. Chen. Emergence of Patterned Stem Cell Differentiation Within Multicellular Structures, *Stem Cells*, 2008, **26**, 2921-2927.

# CHAPTER 7

*3D Encapsulation of Adult Stem Cells in Hyaluronic Acid Hydrogels with Varied Mechanics*

## 7.1 Introduction

As demonstrated in Chapters 5 and 6, the controlled presentation of mechanics in 2D (where a cell sits atop a hydrogel film) can result in profound effects on stem cell behavior, including morphology, proliferation, and differentiation. Cells interacting with a 2D substrate possess an inherently polarized morphology[1] due to only engaging cell adhesion on the basal side of the cell; however, most systems investigating stem cell responses to mechanics have relied upon primarily 2D presentations of mechanics.[2-6] In order to more accurately mimic the cellular microenvironment in many tissues, systems that present mechanical signals in a 3D context are necessary and have become the focus of many recent studies.[7, 8] Development of a mechanically-tunable 3D system would not only advance our understanding of stem cell responses in a more biologically relevant context, but provide a platform for future tissue engineering applications.

Several studies have demonstrated that stem cells encapsulated in hydrogels of varying moduli do indeed behave in a mechanodependent manner. Murine mesenchymal stem cells (mMSCs) encapsulated in RGD-functionalized alginate hydrogels expressed differentiation markers for osteogenesis in stiffer 20 kPa hydrogels and markers for adipogenesis in softer 2.5 kPa hydrogels.[8] Also, adipocyte progenitor cells (APCs) encapsulated in photopolymerized alginate hydrogels also exhibited mechanosensitive responses as APCs in softer hydrogels (3.3 kPa) showed greater expression of adipogenic markers of differentiation while APCs in stiffer hydrogels (12.4 kPa) had markedly

reduced adipogenesis and a concurrent increase in VEGF secretion.[7] In these studies cells possessed a restricted, rounded morphology, which did not allow for matrix remodeling and proliferation as exists in other 3D hydrogel systems;[9, 10] yet, cells still were able to exhibit mecho-dependent responses. This chapter focuses on the translation of the MeHA material system outlined in previous chapters into a 3D hydrogel system with controlled mechanics where cells are directly encapsulated.

Photopolymerized MeHA hydrogels have been investigated for their potential to facilitate cartilage repair[11, 12] and this chapter investigates the effects of modulating MeHA hydrogel mechanics in 3D on hMSC morphology, proliferation, differentiation, and secretion of angiogenic and cytokine factors. A physiologic range of mechanics (4.2-25.5 kPa) was achieved by tailoring the ratio of low modified (~30% methacrylated) MeHA to high modified (~100% methacrylated) MeHA. While this system did not allow for spatial and temporal modulation of mechanics (due to the lack of sequential crosslinking), it allows for investigation into how mechanical signals from the same base material (in this case, hyaluronic acid) can affect hMSC behavior based on its contextual presentation (2D vs. 3D).

## 7.2 Materials and Methodology

### *7.2.1 MeHA Synthesis and Characterization*

Methacrylated hyaluronic acid (MeHA) was synthesized as described in Chapter 4 in order to obtain macromers with ~30% and 100% modification (% methacrylation). Modification efficiency was defined as the percentage of HA repeat units containing

methacrylates based on $^{1}H$ NMR. Briefly, sodium hyaluronate (Lifecore, 59 kDa) was dissolved at 1 wt% in $dIH_2O$ and methacrylic anhydride (MA) was added dropwise (0.72 and 2.4 mL MA per g HA for 30% and 100%, respectively) while stirring at 4°C. The pH was maintained above 8 during the reaction by adding 5 N NaOH for 8 hours, followed by overnight reaction and further addition of MA (0.36 and 1.2 mL per g HA for 30% and 100%, respectively) and pH maintenance for 4 hours the following day. The macromer solution was dialyzed against $dIH_2O$ (SpectraPor, *MW* cutoff 6000-8000 Da) for 4 days, frozen at -80 °C, lyophilized, and stored in powder form.

*7.2.2 MeHA Hydrogel Formation and Mechanical Characterization*

Low modification (low mod) MeHA and high modification (high mod) MeHA were individually dissolved at 3 wt% in 0.2 M triethanolamine (TEA) buffer at pH 8 containing 0.05% of the photoinitiator I2959. In order to vary mechanics, the ratio of low mod: high mod was varied and the mechanical groups chosen were 100:0, 60:40, 30:70, and 0:100. 50 μL of MeHA precursor solution was pipetted into syringe tip molds and exposed to 10 $mW/cm^2$ UV light (Omnicure S1000 UV Spot Cure Systems) for 2 minutes and then allowed to equilibrate overnight in PBS. The compressive moduli of the hydrogels were determined using a Dynamic Mechanical Analyzer (DMA, TA Instruments). A mechanical testing regimen of 10% strain/min was used and the compressive modulus for each hydrogel was determined by evaluating the stress-strain slope between 5% and 20% strain (n=4 hydrogels/group).

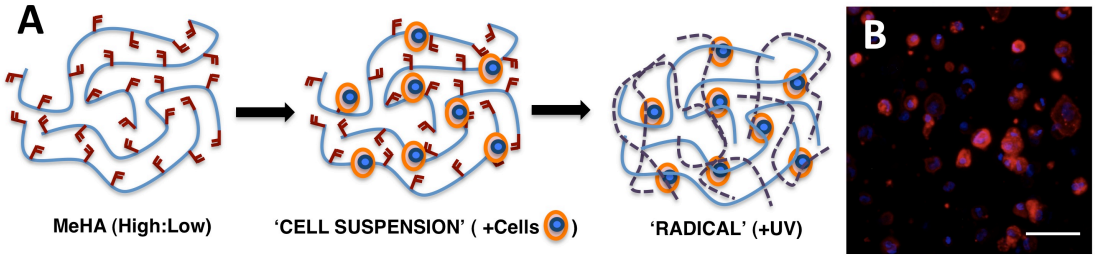


**Figure 7.1** Encapsulation of hMSCs in photocrosslinked MeHA hydrogels. (A) MeHA precursor solution containing MeHA at ratio of high:low modification dissolved in buffer was used to resuspend cells. Upon exposure to UV light (in presence of photoinitiator), MeHA crosslinks *via* 'Radical' polymerization and entraps cells within the hydrogel. (B) Representative confocal stack showing cells (actin and nuclei stained red and blue, respectively) encapsulated within MeHA hydrogel at day 1. Scale bar = 50 μm

### *7.2.3 Encapsulation and Culture of hMSCs in MeHA Hydrogels*

Prior to encapsulation, the cell adhesive oligopeptide GCGYG*RGD*SPG was coupled to the MeHA backbone (through Michael Addition) by incubating overnight at 37°C in a sterile 3 wt% MeHA solution containing 0.2 M TEA and 0.05% I2959 at pH 8. Although the RGD peptide effectively "consumes" methacrylates available for radical crosslinking, the concentration of RGD used in this study (1 mM) consumed less than 1% of available methacrylates on the MeHA backbone. 250,000 hMSCs (Lonza, passage 3) were encapsulated in each 50 μL hydrogel (**Figure 7.1**) and crosslinked under identical conditions as hydrogels that underwent mechanical testing (10 mW/cm$^2$ for 2 min). Hydrogels were cultured in 1 mL growth medium consisting of base medium α-MEM, 20% FBS, 1% L-glutamine, and 1% Pen-Strep (Gibco for all components).

*7.2.4 Cell Morphology Assessment and Proliferation/Metabolic Activity Quantification*

hMSC morphology was assessed using rhodamine-phalloidin staining on days 2, 7, and 14 for each condition. Cells were fixed in 10% formalin for 10 min, permeabilized with 0.25% Triton-X for 10 min, and stained with rhodamine-phalloidin for 40 min with 3X PBS washes after each step. Cells were imaged using a Zeiss LSM510 confocal microscope. Cell proliferation was quantified using the PICOGREEN dsDNA assay on days 2, 7, and 14 for all uniform conditions. Samples (n=4) were placed in CellLytic (Sigma) solution for 1 hour and vortexed gently at 37° C. Samples were measured on a TECAN InfiniteM200 plate reader and compared with a dsDNA standard curve in order to determine the total DNA content.

*7.2.5 Gene Expression and Secretory Profile Characterization*

In order to assess cell differentiation, RNA was extracted from each sample (n=4) using Trizol reagent (Invitrogen) and a manual tissue grinder. RNA was reverse-transcribed into cDNA and PCR was performed on the following genes: Collagen II (COL2) and SOX9 (chondrogenic), α-Smooth Muscle Actin (aSMA) and Calponin (CALP) (myogenic), Osteocalcin (OC) and Alkaline Phosphatase (ALP) (osteogenic), Fatty-Acid Binding Protein (FABP) and Peroxisome Proliferator-Activated Receptor γ (PPARG) (adipogenic). Using GAPDH as a housekeeping gene, relative gene expression was determined using the $\Delta\Delta C_T$ method and all experimental values are plotted relative to the day 0 undifferentiated hMSCs seeded into each hydrogel. Note that $C_T$ for GAPDH were consistent between all groups and controls (data not shown).

hMSC secretory profiles were characterized for both angiogenesis and cytokine

factors (R&D Systems, kits ARY005 and ARY007) by collecting culture media on days 2, 7, and 14 and pooling for each condition (n=3). The protein arrays were threshold adjusted and analyzed using a protein array analyzer (ImageJ, NIH) to quantify pixel intensity. Each value was then normalized to the max expression of that protein and plotted in descending order with the protein most highly expressed plotted at the top and proteins minimally expressed plotted at the bottom.

### 7.2.6 Statistical Analysis

Statistics were performed using One-Way and Two-Way ANOVA and Tukey's post-hoc test (R, Free Software Foundation) for hydrogel mechanics, cell proliferation and gene expression studies.

## 7.3 Results and Discussion

### 7.3.1 Mechanical Characterization of MeHA Hydrogels

MeHA hydrogel mechanics were effectively modulated by varying the ratio of low mod MeHA:high mod MeHA and the compressive moduli was quantified using DMA. As shown in **Figure 7.2**, increasing the amount of high mod MeHA resulted in increased moduli as the mechanics groups obtained were '4.2 kPa' (0% high mod MeHA, 100% low mod MeHA), '9.7 kPa' (40% high mod MeHA, 60% low mod MeHA), '18.5 kPa' (70% high mod MeHA, 30% low mod MeHA), and '25.5 kPa' (100% high mod MeHA, 0% low mod MeHA). A similar trend was observed in another mechanically-tunable system in which the ratio of two modifications of glycidylmethacrylate-

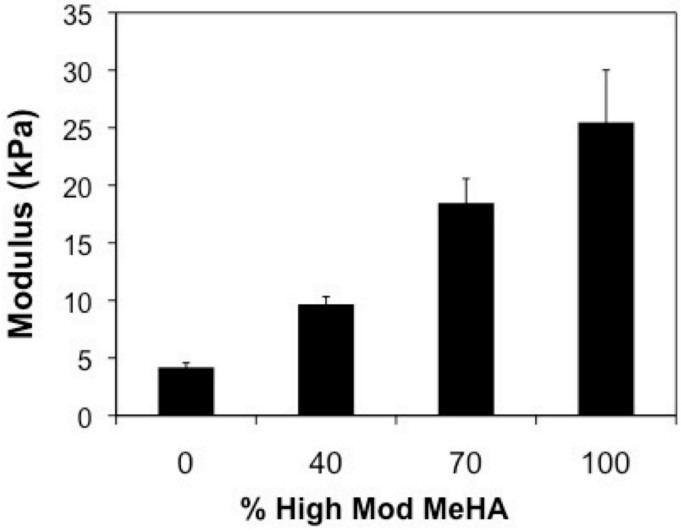


**Figure 7.2** Hydrogel compressive moduli for bulk non-porous radically polymerized MeHA hydrogels. Statistically significant differences ($p<0.05$) were observed between all groups except 70% and 100% High Mod MeHA.

functionalized dextran was varied in order to achieve a range of mechanics.[13] This process allows for the maintenance of the same base network material (hyaluronic acid) and simply varying the crosslinking density in order to create hydrogels with mechanics encompassing a wide range of tissues.[14]

*7.3.2 hMSC Morphology and Proliferation Response to Mechanics*

In the non-porous hydrogel system, the extent of crosslinking had a significant effect on initial stem cell morphology as hMSCs as cells were found to only spread in the softest '4.2 kPa' hydrogels and above this threshold mechanics cells were rounded and unspread at day 2 (**Figure 7.3A**). These trends in morphology were maintained

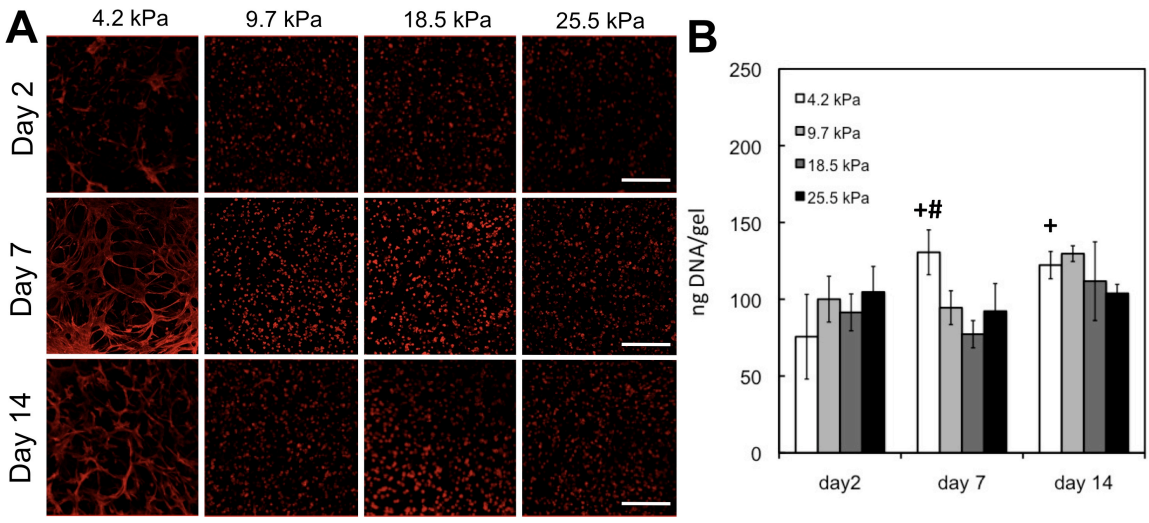


**Figure 7.3** (A) hMSC morphology/cytoskeletal organization (actin, red) in non-porous hydrogels at day 2, 7, and 14. (B) Cell numbers (represented with DNA content) with culture time in the various non-porous hydrogels. Statistically significant differences were observed between '4.2 kPa' and '18.5 kPa' at day 7 (# $p<0.01$) and '4.2 kPa' at day 7 and 14 compared to '4.2 kPa' at day 2 (+ $p<0.05$). Scale bar = 400 μm.

throughout the experiment as cells only remained spread in the '4.2 kPa' group even after 7 and 14 days in culture. By day 7, cells in the '4.2 kPa' also began to significantly contract the hydrogel, resulting in enhanced cell-cell contact and a reduction in scaffold volume due to compaction. While there was a significant increase in cell number in the '4.2 kPa' gels from day 2 to day 7 and day 14, there were very few statistically significant differences across mechanics at any given time point (**Figure 7.3B**). Due to the non-degradable nature of the non-porous hydrogel network, the cells are unable to remodel, develop adequate tension, and proliferate as compared to the other 3D hydrogel systems that incorporate degradability and cell remodeling capabilities.[15-17]

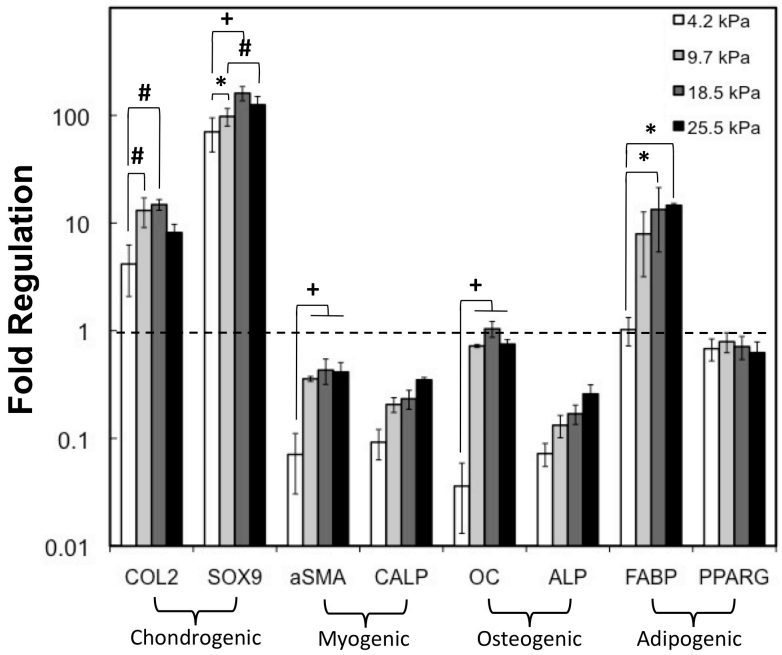


**Figure 7.4** Day 14 expression of various genes for hMSCs cultured in non-porous hydrogels. Values above dotted line indicate upregulation relative to d0 hMSCs. Statistically significant differences: *$p < 0.05$, #$p < 0.01$, +$p < 0.001$.

*7.3.3 hMSC Lineage Marker Expression in Response to 3D Mechanics*

hMSC differentiation was evaluated after 14 days in growth medium for four lineage programs: chondrogenesis, myogenesis, osteogenesis, and adipogenesis. The most notable upregulation in genes (relative to day 0 hMSCs) occurred for the chondrogenic and adipogenic markers: Col2 and Sox9 for chondrogenesis, and FABP for adipogenesis. In non-porous hydrogels, there was a general trend of '4.2 kPa' hydrogels exhibiting significantly reduced upregulation (from two- to ten-fold) in Col 2, Sox9, and

FABP compared to other groups (**Figure 7.4**). Cell morphology can be a determinant of cell fate[9, 18] and these results reinforce this concept as cells that maintain a rounded morphology showed significantly greater upregulation in genes associated with rounded phenotypes (i.e., chondrocytes and adipocytes). Photocrosslinked hydrogels have been shown to cultivate hMSC chondrogenesis and adipogenesis,[7, 19, 20] and the results of this study further validate the utility of hyaluronic acid hydrogels for tissue engineering applications as these experiments were performed in the absence of any inductive factors. Lack of proliferation is often associated with differentiation in cells,[21] and the upregulation in adipogenic and chondrogenic markers in non-porous hydrogels correlated well with relatively stable DNA content (**Figure 7.3B**). Although there was no observed upregulation in lineage marker expression for genes associated with a 'spread' morphology (myogenesis and osteogenesis), significantly decreased expression in both α-smooth muscle actin (four-fold) and osteocalcin (twenty-fold) were associated with the softest '4.2 kPa' hydrogel group, which correlated well with the dramatic increases in chondrogenic and adipogenic marker expression.

### *7.3.4 hMSC Secretory Profile Response to Mechanics*

Conditioned medium was analyzed for 55 angiogenesis and 36 cytokine factors using proteome profile arrays and results are plotted in **Figure 7.5**. The conserved trend of cell responses differing above the '4.2 kPa' threshold was maintained in terms of secretory responses as well. hMSCs in '4.2 kPa' non-porous hydrogels were the only group that supported cell spreading (**Figure 7.3A**) and had the lowest degree of chondrogenesis/adipogenesis (**Figure 7.4**) and it also followed that they demonstrated the

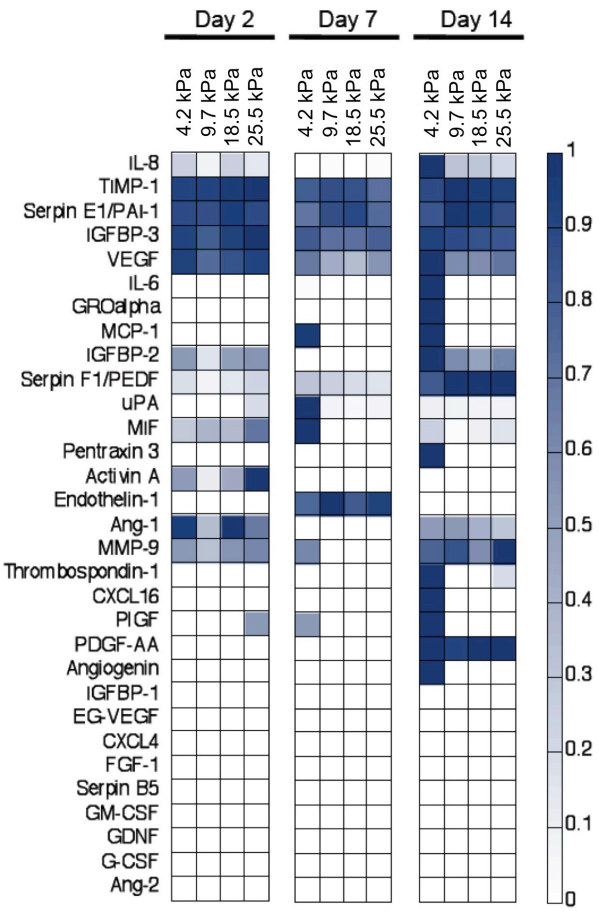


**Figure 7.5** Secretory profiles for angiogenic and cytokine factors by hMSCs interacting with non-porous hydrogels at days 2, 7, and 14. Molecule expression is normalized to the maximum detected expression. Molecules are then plotted with those having the highest maximal expression at the top and those with minimal detection at the bottom. Normalized colorimetric scale bar displayed on the right.

greatest expression of factor secretion. Initially, there were no marked differences in secretion between the 4 mechanics groups (with the exception of slightly increased Activin A and PlGF in ’25.5 kPa’ hydrogels) at day 2. However, by day 7, the ‘4.2 kPa’ group exhibited maximal expression of 5 proteins (MCP-1, uPA, MIF, MMP-9, and PlGF). Endothelin-1 showed transient maximal expression for all mechanics groups at

day 7 with no detection of this protein at either day 2 or 14 for any group. By day 14, the '4.2 kPa' hydrogel group emerged as the most favorable environment for secretion as there was maximal expression of 11 factors (IL-8, VEGF, GROalpha, MCP-1, IGFBP-2, Pentraxin 3, Thrombospondin-1, CXCL16, PlGF, and Angiogenin). Increased pro-angiogenic behavior was associated with a decrease in adipogenesis in a study involving adipose progenitor cells, and our system showed similar behavior with the '4.2 kPa' non-porous hydrogels.[7]

Greater factor secretion present in the softest '4.2 kPa' hydrogel condition agrees well with the observation that stem cells implanted into stiffer, pathological tissues behave in a non-trophic manner.[22] This emphasizes the importance of injection time and scaffold mechanics for cell therapies in diseases that involve a fibrotic response, such as myocardial infarction, chronic kidney disease, and muscular dystrophy in which the pathological environments are stiffer than normal tissue.[23-25]

### 7.5 Conclusions

In summary, Chapter 7 demonstrates how translation of the 2D hyaluronic acid system developed in Chapter 4 into a 3D non-porous hydrogel can also impact hMSC behaviour based on the mechanical microenvironment. However, in this 3D context the observed results appeared more dependent on the adoption of a specific morphology as threshold responses were observed primarily above the '4.2 kPa' condition, which was the only condition that promoted cell spreading. There were no substantial differences in cell morphology, proliferation, differentiation, and secretion above this threshold mechanics, which suggests that hMSCs in this non-degradable, non-porous hydrogel

cannot effectively interpret these differences in mechanics and display mechanosensitive responses similar to those observed in 2D. Therefore, the 3D presentation of controlled mechanics to hMSCs using MeHA must be reimagined in order to allow hMSCs to more effectively sense the differences in mechanics and respond accordingly.

**REFERENCES:**


1. E. Cukierman, R. Pankov, D. R. Stevens and K. M. Yamada. Taking cell-matrix adhesions to the third dimension, *Science*, 2001, **294**, 1708-1712.
2. A. J. Engler, S. Sen, H. L. Sweeney and D. E. Discher. Matrix elasticity directs stem cell lineage specification, *Cell*, 2006, **126**, 677-689.
3. T.-J. Kim, J. Seong, M. Ouyang, J. Sun, S. Lu, J. P. Hong, N. Wang and Y. Wang. Substrate rigidity regulates Ca2+ oscillation via RhoA pathway in stem cells, *J. Cell. Physiol.*, 2009, **218**, 285-293.
4. R. A. Marklein and J. A. Burdick. Spatially controlled hydrogel mechanics to modulate stem cell interactions, *Soft Matter*, 2010, **6**, 136-143.
5. A. S. Rowlands, P. A. George and J. J. Cooper-White. Directing osteogenic and myogenic differentiation of MSCs: interplay of stiffness and adhesive ligand presentation, *AJP: Cell Physiology*, 2008, **295**, C1037-C1044.
6. J. R. Tse and A. J. Engler. Stiffness gradients mimicking in vivo tissue variation regulate mesenchymal stem cell fate, *PLoS ONE*, 2011, **6**, e15978.
7. E. M. Chandler, C. M. Berglund, J. S. Lee, W. J. Polacheck, J. P. Gleghorn, B. J. Kirby and C. Fischbach. Stiffness of photocrosslinked RGD-alginate gels regulates adipose progenitor cell behavior, *Biotechnol. Bioeng.*, 2011, **108**, 1683-1692.
8. N. Huebsch, P. R. Arany, A. S. Mao, D. Shvartsman, O. A. Ali, S. A. Bencherif, J. Rivera-Feliciano and D. J. Mooney. Harnessing traction-mediated manipulation

of the cell/matrix interface to control stem-cell fate, *Nature materials*, 2010, **9**, 1-9.

9. S. Khetan and J. A. Burdick. Patterning network structure to spatially control cellular remodeling and stem cell fate within 3-dimensional hydrogels, *Biomaterials*, 2010, **31**, 8228-8234.

10. M. P. Lutolf, J. L. Lauer-Fields, H. G. Schmoekel, A. T. Metters, F. E. Weber, G. B. Fields and J. A. Hubbell. Synthetic matrix metalloproteinase-sensitive hydrogels for the conduction of tissue regeneration: engineering cell-invasion characteristics, *Proc Natl Acad Sci USA*, 2003, **100**, 5413-5418.

11. C. Chung and J. A. Burdick. Influence of three-dimensional hyaluronic Acid microenvironments on mesenchymal stem cell chondrogenesis, *Tissue Engineering Part A*, 2009, **15**, 243-254.

12. I. Erickson, A. Huang, C. Chung, R. Li, J. Burdick and R. Mauck. Differential Maturation and Structure-Function Relationships in MSC- and Chondrocyte-Seeded Hydrogels, *Tissue Engineering Part A*, 2009.

13. M. H. Lee, D. Boettiger and R. J. Composto. Biomimetic carbohydrate substrates of tunable properties using immobilized dextran hydrogels, *Biomacromolecules*, 2008, **9**, 2315-2321.

14. D. E. Discher, D. J. Mooney and P. W. Zandstra. Growth Factors, Matrices, and Forces Combine and Control Stem Cells, *Science*, 2009, **324**, 1673-1677.

15. C. M. Ghajar, S. Kachgal, E. Kniazeva, H. Mori, S. V. Costes, S. C. George and A. J. Putnam. Mesenchymal cells stimulate capillary morphogenesis via distinct proteolytic mechanisms, *Exp Cell Res*, 2010, **316**, 813-825.

16. J. Kim, Y. Park, G. Tae, K. B. Lee, S. J. Hwang, I. S. Kim, I. Noh and K. Sun. Synthesis and characterization of matrix metalloprotease sensitive-low molecular weight hyaluronic acid based hydrogels, *Journal of materials science Materials in medicine*, 2008, **19**, 3311-3318.

17. J. S. Miller, C. J. Shen, W. R. Legant, J. D. Baranski, B. L. Blakely and C. S. Chen. Bioactive hydrogels made from step-growth derived PEG-peptide macromers, *Biomaterials*, 2010, **31**, 3736-3743.

18. R. McBeath, D. M. Pirone, C. M. Nelson, K. Bhadriraju and C. S. Chen. Cell shape, cytoskeletal tension, and RhoA regulate stem cell lineage commitment, *Dev Cell*, 2004, **6**, 483-495.

19. C. Chung, J. Mesa, M. A. Randolph, M. Yaremchuk and J. A. Burdick. Influence of gel properties on neocartilage formation by auricular chondrocytes photoencapsulated in hyaluronic acid networks, *J. Biomed. Mater. Res.*, 2006, **77**, 518-525.

20. I. L. Kim, R. L. Mauck and J. A. Burdick. Hydrogel design for cartilage tissue engineering: a case study with hyaluronic acid, *Biomaterials*, 2011, **32**, 8771-8782.

21. K. H. von Wangenheim and H. P. Peterson. Control of cell proliferation by progress in differentiation: clues to mechanisms of aging, cancer causation and therapy, *J Theor Biol*, 1998, **193**, 663-678.

22. M. Breitbach, T. Bostani, W. Roell, Y. Xia, O. Dewald, J. M. Nygren, J. W. U. Fries, K. Tiemann, H. Bohlen, J. Hescheler, A. Welz, W. Bloch, S. E. W.

Jacobsen and B. K. Fleischmann. Potential risks of bone marrow cell transplantation into infarcted hearts, *Blood*, 2007, **110**, 1362-1369.

23. V. Persy and P. D'Haese. Vascular calcification and bone disease: the calcification paradox, *Trends Mol Med*, 2009, **15**, 405-416.

24. M. F. Pittenger and B. J. Martin. Mesenchymal stem cells and their potential as cardiac therapeutics, *Circ Res*, 2004, **95**, 9-20.

25. L. Zhou and H. Lu. Targeting fibrosis in Duchenne muscular dystrophy, *J Neuropathol Exp Neurol*, 2010, **69**, 771-776.

# CHAPTER 8

## *Spatially and Temporally Dependent Human Mesenchymal Stem Cell Responses to 3D Mechanical Signals In Sequentially Crosslinked Macroporous Hydrogels*

*Adapted from: Marklein, RA, Soranno, DE, Burdick, JA. "Magnitude and Presentation of Mechanical Signals Influence Adult Stem Cell Behavior in 3Dimensional Macroporous Hydrogels." Soft Matter, 2012 doi: 10.1039/c2sm25501d*

### 8.1 Introduction

As demonstrated in Chapter 5 and 6, the mechanics of the stem cell environment have a profound effect on morphology, proliferation, and differentiation in 2D. Furthermore, stem cells were shown to be sensitive to the local mechanics of their substrate, as well as dynamic changes in substrate mechanics. Chapter 7 demonstrated the importance of contextual presentation of uniform non-porous 3D mechanics on hMSCs as morphology, differentiation, and secretion of factors were shown to be highly dependent on the extent of crosslinking. However, in order to effectively incorporate stem cells into therapeutic applications, a more thorough understanding of how stem cells respond to more complex 3D mechanical signals is necessary.[1, 2]

A wealth of natural and synthetic hydrogels have been used to investigate the effect of mechanics on stem cells.[2] However, few systems possess the ability to spatially and temporally control mechanics[3-6] despite the distinct mechanical heterogeneity that exists in many pathologies (*e.g.* post-myocardial infarction, calcification and fibrosis in heart valves)[7, 8] as well as during tissue development.[9] Additionally, few studies present mechanically-tunable hydrogels in a 3D context, rather using hydrogels as simple 2D substrates. The limited studies on 3D stem cell mechanosensitivity include systems such as static alginate gels of varied crosslinking density[1] and photodegradable gels with

tunable mechanics.[10] Thus, there still exists the need for advanced material systems to further investigate complex mechanical environments in more biologically relevant 3D contexts.

Chapter 7 illustrated one approach to modulate mechanics in 3D, but the photocrosslinking method employed in that system did not allow for the spatial and temporal control of mechanics as sequential crosslinking provided in 2D. In this chapter, the sequentially crosslinked hydrogel system outlined in previous chapters was translated to a 3D mechanically-tunable system, where gelation occurs around a degradable microsphere template, leading to macroporous structures where cells can be seeded through the pores with a range of mechanical signal presentations. This chapter further emphasizes the utility of MeHA as this polymer not only provides controlled 2D mechanical environments, but also distinct 3D contextual presentations of mechanics i.e non-porous and porous. This porous hydrogel system allows for further insight into hMSC behavior over a physiological range of mechanics (1.5-12.4 kPa) in a 3D macroporous context, as well as a unique method for studying hMSC response to dynamic mechanics (matrix stiffening). There have been initial studies investigating the effects of pore morphology, mechanics, and adhesivity on hMSC motility,[11] however further investigation into other complex stem cell responses, such as differentiation and secretion, are necessary. This macroporous hydrogel system provides advantages over other mechanically-tunable systems as it can serve as a desirable tissue engineering platform due to its high degree of tenability, as well as the benefits imposed by a porous architecture (high water content and potential for cell infiltration).

## 8.2 Materials & Methodology

### *8.2.1 MeHA Synthesis and Characterization*

Methacrylated hyaluronic acid (MeHA) was synthesized as described in Chapter 4 in order to obtain a macromer with 100% modification (% methacrylation).[6] Modification efficiency was defined as percentage of HA repeat units containing methacrylates based on $^{1}$H-NMR. Briefly, sodium hyaluronate (Lifecore, 59 kDa) was dissolved at 1 wt% in $dIH_2O$ and methacrylic anhydride (MA) was added dropwise (2.4 mL MA per g HA) while stirring at 4°C. The pH was maintained above 8 during the reaction by adding 5 N NaOH for 8 hours, followed by overnight reaction and further addition of MA (1.2 mL per g HA) and pH maintenance for 4 hours the following day. The macromer solution was dialyzed against $dIH_2O$ (SpectraPor, *MW* cutoff 6000-8000 Da) for 4 days, frozen at -80 °C, lyophilized and stored in powder form.

### *8.2.2 Macroporous Hydrogel Fabrication and Characterization*

For the sequentially crosslinked hydrogel system, a 3 wt% MeHA solution dissolved in 0.2 M triethanolamine (TEA) at pH 9 was reacted with dithiothreitol (5 mM) in order to ‘‘consume’’ 15% of the methacrylates (**Figure 8.1A** ‘Addition’) for 2h at 37 °C. In order to vary the crosslink density, a solution of 0.05% I2959 (Irgacure) was then incubated with the hydrogels for 1 h, followed by a range of UV exposure times (up to 2 min) using 10 mW/cm$^2$ collimated UV light (Omnicure S1000 UV Spot Cure Systems), where the time of light exposure controlled the extent of secondary crosslinking. The compressive moduli of non-porous hydrogels were determined using a Dynamic

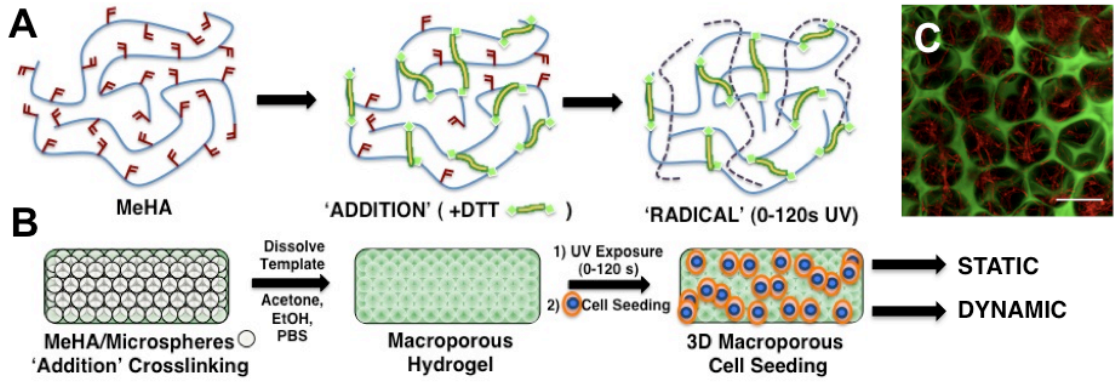


**Figure 8.1** (A) Schematic of sequential crosslinking process used for the fabrication of hydrogels with varying crosslinking. Methacrylates are first consumed using a dithiol crosslinker (DTT) via a Michael Addition ('Addition') reaction. Remaining methacrylates can be further crosslinked using UV light in the presence of photoinitiator (kinetic chains shown with dotted lines, 'Radical'). (B) Addition crosslinking of MeHA around a PMMA microsphere template results in a porous hydrogel architecture following microsphere leaching by solvent exchanges (acetone, ethanol, PBS). Following template removal, the mechanics are tuned by introducing photoinitiator (I2959) and varying UV exposure time (0–120 s). Cells are then seeded on both sides of the porous hydrogel and cultured with static or dynamic mechanics (by performing further radical crosslinking once the cells are seeded). (C) Representative image of hMSCs (actin, red) within porous hydrogels (FITC-coupled, green). Scale bar = 400 μm.

Mechanical Analyzer (DMA, TA Instruments). A mechanical testing regimen of 10% strain/min was used and the compressive modulus for each hydrogel was determined by evaluating the stress-strain slope between 5% and 20% strain (n=4 hydrogels/ group).

Porous hydrogels were fabricated using a similar approach, but the addition crosslinking solution was pipetted onto a cylindrical PMMA microsphere template (Polysciences, Inc. average diameter of beads ~250 μm) with diameter 7.5 mm and

thickness 2.3 mm that had been sonicated to introduce hexagonal close packed order (**Figure 8.1B**). Following incubation for 2h at 37 °C, the hydrogel/template constructs were serially washed to dissolve the beads (3X Acetone, 3X EtOH, 3X PBS). After the final PBS wash, a solution of 0.05% I2959 solution was introduced in order to perform the secondary 'radical crosslinking'. Following UV exposure (0–120 s), the porous hydrogels were again washed in PBS (to remove excess I2959). The compressive modulus of porous samples was determined as above.

In order to characterize the porous morphology of the hydrogels, a 10 mM solution of thiolated-FITC (Toronto Research Chemicals, Inc.) was diffused into the hydrogels for 1h and then rinsed 3X with PBS. Porous hydrogels were imaged using a two-photon confocal microscope (Zeiss LSM510) and pore diameter calculated for each mechanics group using ImageJ (n=20 pores/hydrogel, n=3 hydrogels/group). The same confocal stacks were also threshold adjusted in order to determine the porosity of the hydrogels for each condition (n=5 slices/hydrogel, n=3 hydrogels/group) using ImageJ. The porosity was then used to evaluate compressive moduli of both non-porous and porous hydrogels using the Gibson-Ashby model for open cell foam structures shown in **Equation 8.1**.[12]

$$E^* = (\rho^*/\rho_s)^n E_s \quad (1)$$

$E^*$ represents the modulus of the porous material, $E_s$ the modulus of the material when non-porous, n an arbitrary constant (taken as 2 in this porous context), and $(\rho^*/\rho_s)$ the ratio of the porous and non-porous densities (calculated as stated above using ImageJ).

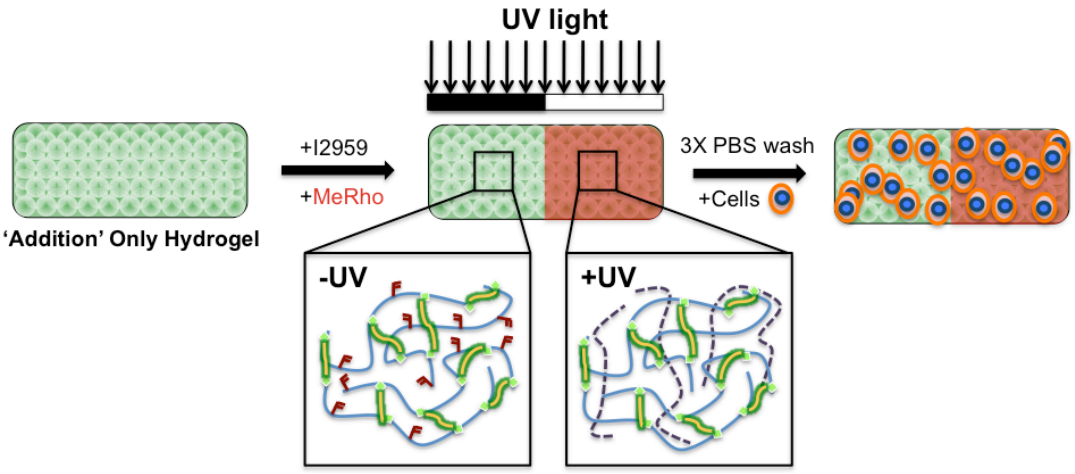


**Figure 8.2** Photopatterning schematic for macroporous hydrogels. Photoinitiator (I2959) and photoreactive dye (MeRho) are swelled into 'Addition' Only Hydrogel and photomask applied to spatially restrict UV light and create soft (-UV, unexposed) and stiff (+UV, exposed) regions within the same hydrogel. hMSCs are then seeded on the patterned hydrogels after removing I2959 and unreacted MeRho with 3X PBS washes.

### *8.2.3 Porous Hydrogel Preparation for Cell Culture*

As above, porous hydrogels were fabricated using microsphere templates and targeting ~15% methacrylate consumption with DTT with secondary UV exposure to alter the crosslink density. Prior to addition crosslinking, the adhesive oligopeptide GCGYG*RGD*SPG was coupled to the MeHA backbone (1 mM RGD) using the same 'addition reaction' method. While the RGD peptide binds to methacrylates that would otherwise be consumed by Michael Addition or radical crosslinking, the percentage of methacrylates consumed (assuming 100% coupling efficiency) was only ~1% for this coupling process and RGD concentration used. Prior to cell-seeding, samples were

sterilized using germicidal UV for 1 h, and pre-incubated with growth medium. Growth medium consisted of the base medium α-MEM, 20% FBS, 1% L-glutamine, and 1% Pen-Strep (Gibco for all components). 125,000 hMSCs (Lonza, passage 3) were pipetted onto each side of the porous hydrogels (**Figure 8.1B**, 250,000 hMSCs total) and cultured for 14 days in growth medium. In order to investigate hMSC response to dynamic (step-wise increase) mechanics, 0.05% I2959 solution was added to 2.6 kPa hydrogel groups on day 2 and day 7 of cell culture for 1 hour and then exposed to UV for 80 s. Following UV exposure, hydrogels were washed 3X with growth medium (30 s per wash) to remove excess initiator. For spatially-controlled porous hydrogels, a PBS solution containing 0.05% I2959 and 10 μM of the photoreactive dye Methacryloxyethyl Thiocarbamoyl Rhodamine B (MeRho, Polysciences, Inc.) was swelled into Addition-Only porous hydrogels (**Figure 8.2**). Using a photomask, UV light exposure (120 s) was restricted to half the porous hydrogel and following exposure, patterned hydrogels were washed 3X with PBS in order to remove excess I2959 and MeRho.

*8.2.4 Cell Morphology Assessment and Proliferation/Metabolic Activity Quantification*

hMSC morphology was assessed using rhodamine-phalloidin staining on days 2, 7, and 14 for uniform static and dynamic conditions. For patterned hydrogels, cell morphology and density were assessed at day 2 only. Cells were fixed in 10% formalin for 10 min, permeabilized with 0.25% Triton-X for 10 min, and stained with rhodamine-phalloidin for 40 min with 3X PBS washes after each step. Cells were imaged using a Zeiss LSM510 confocal microscope. Cell proliferation was quantified using the PICOGREEN dsDNA assay on days 2, 7, and 14 for all uniform conditions. Samples

(n=4) were placed in CellLytic (Sigma) solution for 1 hour and vortexed gently at 37° C. Samples were measured on a TECAN InfiniteM200 plate reader and compared with a dsDNA standard curve in order to determine the total DNA content. For patterned hydrogels, samples were stained with DAPI for 5 min and imaged using confocal microscopy in order to quantify local cell density in exposed and unexposed regions of the hydrogel in order to determine the homogeneity of cell seeding.

In order to assess the effect of UV and free radical exposure on cell metabolic activity, Alamar Blue assay (Invitrogen) was performed on all dynamic conditions at each time point to ensure there were no detrimental effects from the stiffening process. Cells were washed with PBS and 2 mL of Alamar Blue solution (50X dilution) was added to each sample. Following incubation for 3 h, fluorescence of the solution was measured using a TECAN InfiniteM200 plate reader (560 nm excitation, 590 nm emission).

*8.2.5 Gene Expression and Secretory Profile Characterization*

In order to assess cell differentiation, RNA was extracted from each sample (n=4) using Trizol reagent (Invitrogen) and a manual tissue grinder. RNA was reverse-transcribed into cDNA and PCR was performed on the following genes: Collagen II (COL2) and SOX9 (chondrogenic), α-Smooth Muscle Actin (aSMA) and Calponin (CALP) (myogenic), Osteocalcin (OC) and Alkaline Phosphatase (ALP) (osteogenic), Fatty-Acid Binding Protein (FABP) and Peroxisome Proliferator-Activated Receptor γ (PPARG) (adipogenic). Using GAPDH as a housekeeping gene, relative gene expression was determined using the $\Delta\Delta C_T$ method and all experimental values are plotted relative to

the day 0 undifferentiated hMSCs seeded into each hydrogel. Note that $C_T$ for GAPDH were consistent between all groups and controls (data not shown).

hMSC secretory profiles were characterized for both angiogenesis and cytokine factors (R&D Systems, kits ARY005 and ARY007) by collecting culture media on days 2, 7, and 14 and pooling for each condition (n=3). The protein arrays were threshold adjusted and analyzed using a protein array analyzer (ImageJ, NIH) to quantify pixel intensity. Each value was then normalized to the max expression of that protein and plotted in descending order with the protein most highly expressed plotted at the top and proteins minimally expressed plotted at the bottom.

### *8.2.6 Statistical Analysis*

Statistics were performed using One-Way and Two-Way ANOVA and Tukey's post-hoc test (R, Free Software Foundation) for hydrogel mechanics, hydrogel pore sizes, cell proliferation and gene expression studies.

## 8.3 Results and Discussion

### *8.3.1 MeHA Hydrogel Mechanical Characterization*

We used a sequential crosslinking process to obtain a wide range of crosslinking densities from the same starting material, by altering the extent of methacrylate polymerization in already formed networks using UV light exposure. Compressive moduli were obtained for bulk non-porous hydrogels (containing RGD peptide) formed with this sequential crosslinking system (**Figure 8.1A**) using DMA and are reported in **Figure 8.3**. A range of moduli from 1.5 kPa (no UV exposure) to 7.4 kPa (120 s UV

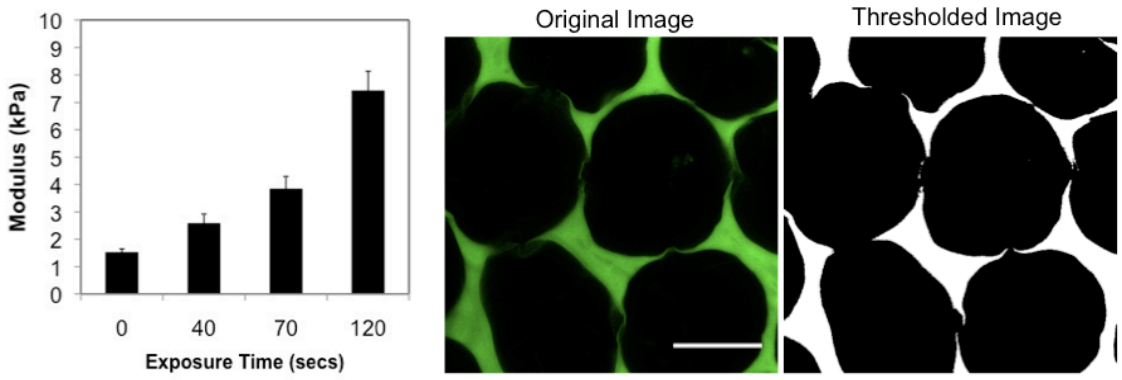


**Figure 8.3** Hydrogel compressive moduli for bulk sequentially crosslinked hydrogels (0-120s UV exposure range). Statistically significant differences ($p<0.05$) were observed between all groups. Example of original confocal slice showing porous morphology (FITC dye used for visualization), as well as thresholded image to determine hydrogel porosity used to validate non-porous vs. porous bulk mechanics using Gibson-Ashby equation. Scale bar = 200 μm.

exposure) was obtained by varying the UV exposure time during the secondary radical crosslinking step. This represents a simple process to alter hydrogel mechanics to form materials with mechanics that encompass a wide range of tissues.[13]

Due to the porosity and low degree of crosslinking, the bulk mechanics of the porous hydrogels were difficult to measure using the DMA for groups below the stiffest condition (7.4 kPa, 120 s UV exposure). The bulk compressive modulus of this formulation in a porous architecture measured ~0.2 kPa, which agrees well with the Gibson-Ashby model give our measured porosity of ~85% (as determined using threshold adjusted confocal images, example shown in **Figure 8.3**). Given that the moduli of both porous (0.2 kPa) and non-porous (7.4 kPa) hydrogels fit the model for open cell foam mechanics, we are confident that the moduli of the reported non-porous

hydrogels were representative of the microscale moduli experienced by the hMSCs at each hydrogel formulation. This local modulus is most relevant as this is what the cell experiences during adhesion, spreading, and traction-mediated behavior.

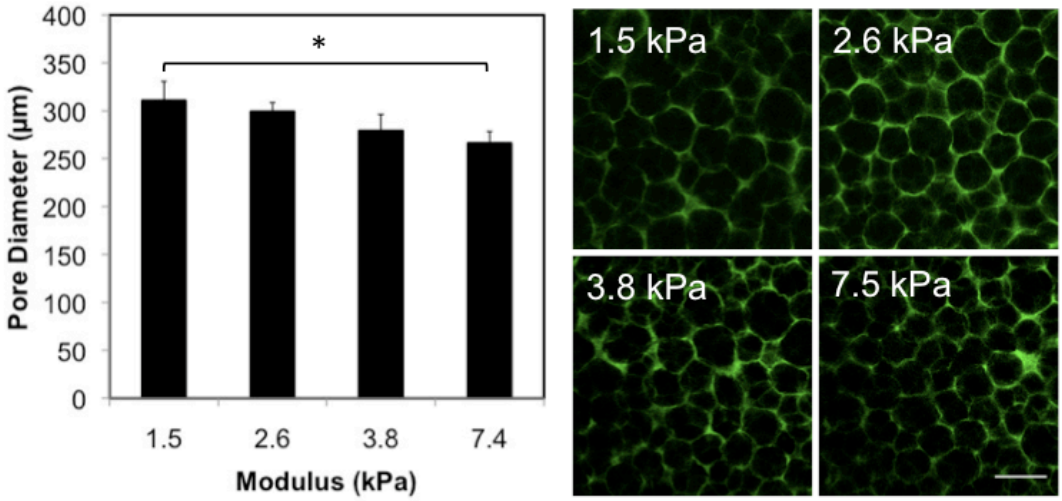


**Figure 8.4** Average pore size and representative images for macroporous hydrogels with varied crosslinking. Scale bar = 400 μm. Significant differences *p<0.05.

Due to the highly swollen nature of porous hydrogels, the average pore size was calculated for each mechanics group as shown in **Figure 8.4** with representative images of the porous architecture for varied UV light exposure. While there was a significant difference in pore size between the softest (1.5 kPa) and stiffest (7.4 kPa) conditions, this difference in pore sizes (310 μm *vs.* 270 μm, respectively) likely has a minimal effect on cell behavior because the pore size scale (hundreds of μm) is much larger than that of cells (tens of μm). However, these differences between the softest and stiffest groups must be considered in the context of the results of this study. In one particular study investigating the effects of porous hydrogel mechanics, pore sizes on the order of cell

diameters (7-20 μm) were used to demonstrate the influence of porous architecture on MSC motility.[11] Our study similarly utilized a mechanically-tunable porous system, however we further investigated the effects of 3D porous mechanics on other stem cell responses (morphology, prolieration, differentiation, and secretion), as well as the effects of spatial and temporally modulated mechanics.

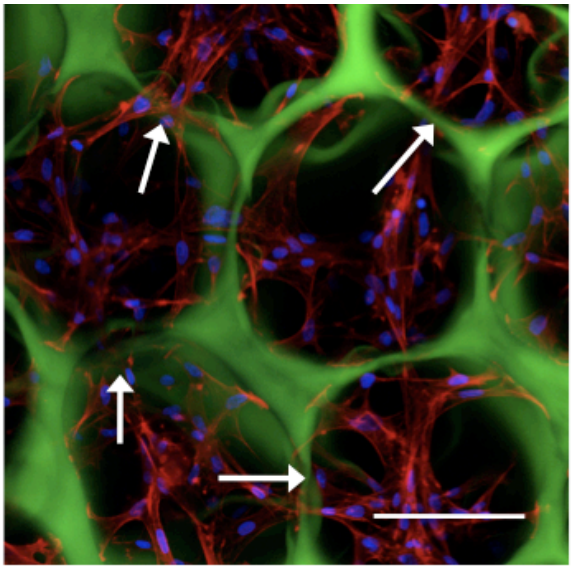

**Figure 8.5** Initial cell seeding within macroporous hydrogels. Cells stained for actin cytoskeleton (rhodamine-phalloidin, red) and nuclei (DAPI, blue) within FITC-labeled hydrogel (green). Arrows indicate interconnected pores allowing for cell infiltration throughout the scaffold. Scale bar = 200 μm

*8.3.2 hMSC Morphology and Proliferation Response to Mechanics*

Uniform distribution of hMSCs within the pores was evident after 24 h (**Figure 8.5**), likely facilitated by the highly-swollen nature of the porous hydrogels, as well as the presence of interconnected pores. Stem cell morphology and proliferation exhibited

mechanodependence in porous hydrogels as shown in **Figure 8.6**. Cells exhibited

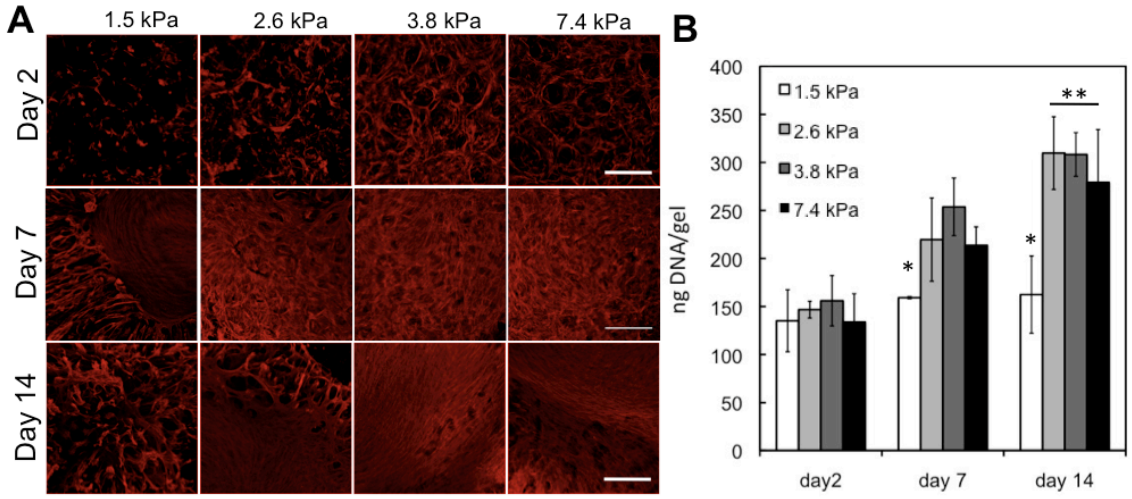


**Figure 8.6** (A) hMSC morphology/cytoskeletal organization (actin, red) in porous hydrogels at day 2, 7, and 14. (B) Cell numbers (represented with DNA content) with culture time in the various macroporous hydrogels. Statistically significant differences were observed between '1.5 kPa' and all other groups at days 7 and 14 (*$p < 0.01$) and with hydrogels at a given mechanics between day 2 and day 14 (**$p < 0.001$). Scale bar = 400 μm.

increased spreading and a more organized actin cytoskeleton with increasing mechanics on day 2 (**Figure 8.6A**), which agrees well with previous findings in 2D systems.[6, 14] Due to the macroporous scaffold morphology, this system represents a quasi-2D presentation of mechanics that directs the formation of a complex 3D environment for the cells seeded within the hydrogel. By day 7, cells in the 2.6, 3.8, and 7.4 kPa groups had similar confluent morphologies with cells filling the scaffold pores as opposed to the 1.5 kPa group, which had begun to contract the scaffold resulting in a distinct cell mass.

Although there was an increase in DNA with time above a threshold mechanics of 2.6 kPa, there was no significant difference in DNA content at any of the time points

among the 2.6, 3.8, and 7.4 kPa groups, potentially due to the high seeding density and cell-cell interactions. Contact inhibition of proliferation is apparent in stem cell culture once confluency is reached[15] and this could contribute to the lack of differences observed in cell number between the groups above 1.5 kPa as the cells completely fill the pores by day 7. Furthermore, there was no significant increase in DNA over time in the 1.5 kPa condition, which was significantly lower at the 7 and 14 day time points than all other conditions (**Figure 8.6B**). Although the observed contraction in the 1.5 kPa hydrogels and the proliferation/confluency of the other groups resulted in differences in cell-scaffold and cell-cell interactions with time (as well as an accompanied decrease in porosity), the initial mechanical cue provided by the porous hydrogels played a role in the resulting stem cell behavior. It was not possible to directly measure the hydrogel mechanics in the presence of cells during the experiment and any cell produced matrix could also influence local interactions within the hydrogel.

*8.3.3 hMSC Lineage Marker Expression in Response to Mechanics*

hMSC expression of lineage markers was evaluated after 14 days in growth medium for four common hMSC fates: chondrogenesis, myogenesis, osteogenesis, and adipogenesis. The growth medium does not include inductive components to direct cells to a specific lineage. The only notable upregulation in genes (relative to d0 hMSCs) occurred for the chondrogenic and adipogenic markers: Col2 (two- to three-fold) and Sox9 (four- to eight-fold) for chondrogenesis and FABP (two-fold) for adipogenesis (**Figure 8.7**). Because the cells were cultured in growth medium, changes in gene expression are likely due to morphology, proliferation, and cell-cell contacts imposed by

differential mechanics and the porous architecture.

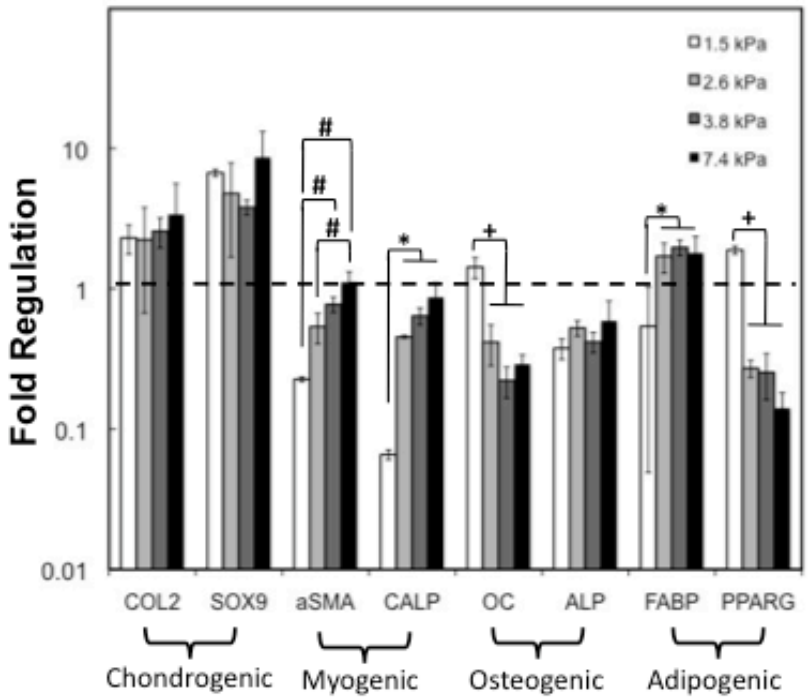


**Figure 8.7** Day 14 expression of various genes for hMSCs cultured in porous hydrogels. Values above dotted line indicate upregulation relative to d0 hMSCs. Statistically significant differences: *$p < 0.05$, #$p < 0.01$, +$p < 0.001$.

There were no significant differences between groups for the chondrogenic genes; however, FABP and PPARG expression significantly differed between 1.5 kPa and all other mechanics. Although osteocalcin expression was highest in the softest hydrogels (contrary to 2D findings),[16] studies have demonstrated increased upregulation of osteocalcin in softer 3D hydrogels that allow for scaffold contraction and reduced proliferation.[17, 18] The increased cell-scaffold compaction also resulted in enhanced cell-cell contact, which has been correlated with chondrogenesis in pellet cultures.[19] There

were also observed differences in myogenic marker aSMA and CALP expression, with the 1.5 kPa condition exhibiting greater downregulation (five-fold and twenty-fold for aSMA and CALP, respectively) while the other mechanics did not exhibit as drastic of a downregulation of these myogenic markers relative to d0 hMSCs. Softer hydrogels (~1 kPa) have demonstrated reduced myogenic potential for hMSCs cultured in growth medium (in the presence and absence of TGFβ) coupled with enhanced chondrogenesis,[20] which correlates well with the differentiation profile observed for stem cells cultured in 1.5 kPa hydrogels. Thus, there is evidence that the outlier in spreading and proliferation (*i.e.* 1.5 kPa) exhibits differences in differentiation marker expression influenced by the initial porous hydrogel mechanics.

*8.3.4 hMSC Secretory Profile Response to Mechanics*

Collected medium was analyzed for 55 angiogenesis and 36 cytokine factors using proteome profile arrays and results for each mechanics group are plotted in **Figure 8.8**. There was a general increase in angiogenic/cytokine factor expression for the softer hydrogels (1.5 and 2.6 kPa) with time. There was maximal expression in the softer hydrogels at day 14 for 9 factors (IL-8, IL-6, GROalpha, MIF, CXCL16, Thrombospondin-1, GDNF, GM-CSF, and G-CSF). With the stiffer hydrogels (3.8 kPa and 7.4 kPa), there was initially a greater overall secretion at day 2 for several factors followed by a noticeable decrease by day 14, such as MMP-9, Ang-1, Ang-2, Endothelin-1, Activin A, Serpin B5, and EG-VEGF. There were also only 2 maximally secreted proteins at day 14 (MCP-1 and IGFBP-1) on the stiffer hydrogels at day 14. Temporal changes in trophic factor secretion have also been demonstrated on 2D substrates,[21]

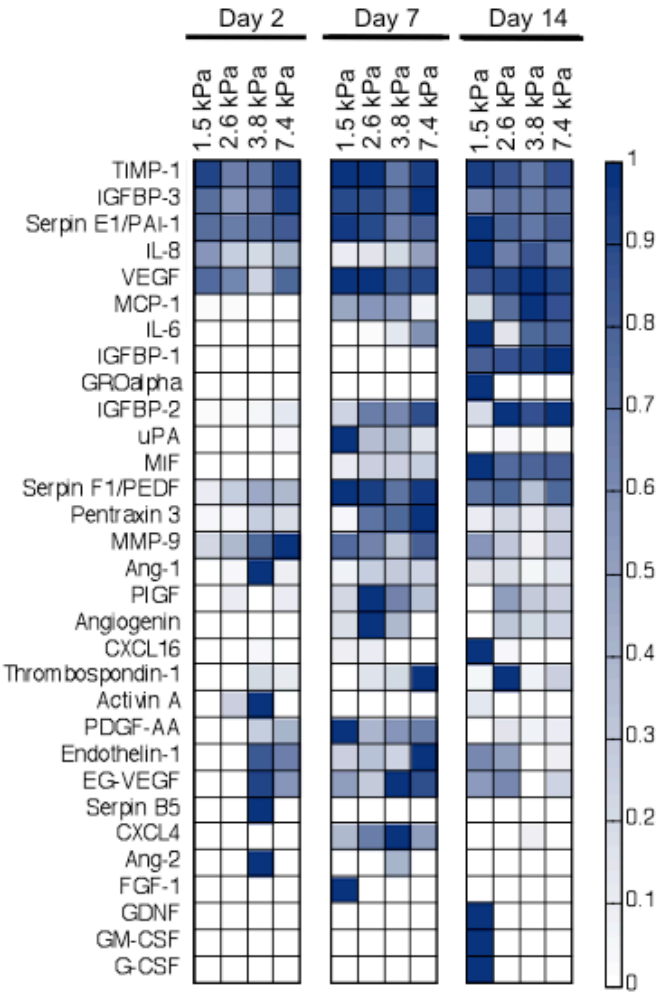


**Figure 8.8** Secretory profiles for angiogenic and cytokine factors by hMSCs interacting with porous hydrogels at days 2, 7, and 14. Molecule expression is normalized to the maximum detected expression. Molecules are then plotted with those having the highest maximal expression at the top and those with minimal detection at the bottom. Normalized colorimetric scale bar displayed on the right.

where stiffer substrates (~20 kPa) have been shown to initially support greater factor secretion while after 2 weeks the secretion profiles shift to greater secretion on softer hydrogels (~2 kPa). Also of note, the angiogenic factors PlGF and Angiogenin exhibited

profiles with both temporal and mechanical dependence as they were transiently secreted from 2.6 kPa hydrogels at day 7, but minimally detected on other days and from other mechanics. With respect to changes in secretory molecules on a per cell basis, the only group that had significantly different cell numbers was the softest 1.5 kPa hydrogel compared to all other groups at day 7 and 14. This further amplifies the findings, as the softest group had the highest total secretion values for several molecules at these later time points.

While the porous hydrogel system did not afford a group with uniformly high factor secretion, the secretome profiles showed distinct temporal behavior based on the initial scaffold mechanics. In tissue engineering applications, the timing of stem cell incorporation is of critical importance[22, 23] and further investigation into the effects of mechanics on not only the factors secreted, but also their temporal expression is necessary. These results reinforce the importance of the mechanics magnitude and presentation on cell behavior with respect to the production and release of trophic factors from cell-hydrogel constructs.

*8.3.5 hMSC Response to Heterogeneous Mechanics*

The sequential crosslinking scheme not only allows for tunable mechanics in uniform hydrogels, but also spatially-controlled mechanics due to the use of UV light in the secondary crosslinking step. Using a photomask, UV light exposure was restricted to half the porous hydrogel in order to create soft (‘1.5 kPa’, -UV) and stiff (‘7.4 kPa’, +UV) regions within the same hydrogel. **Figure 8.9A** shows the distinct mechanics regions within the same hydrogel as regions of UV exposure are indicated through the

incorporation of the photoreactive MeRho (red, +UV). Cells within the +UV region were highly spread and possessed highly organized cytoskeleton (**+UV inset**) compared to cells within the -UV region, which were less spread and possessed diffuse, unorganized cytoskeleton (**-UV inset**). These local responses agreed well with the uniform porous hydrogel responses observed in **Figure 8.6**, and further emphasize the importance of the stem cell microenvironment mechanics on stem cell behavior. In order to determine if differences in cell density contributed to stem cell morphology within the patterned hydrogels, cell nuclei were counted within the soft and stiff regions of the hydrogels. **Figure 8.9B** illustrates the similar cell densities observed in both mechanically-distinct regions thus reducing the possibility of differences in morphology influenced by cell-cell contact and paracrine effects.

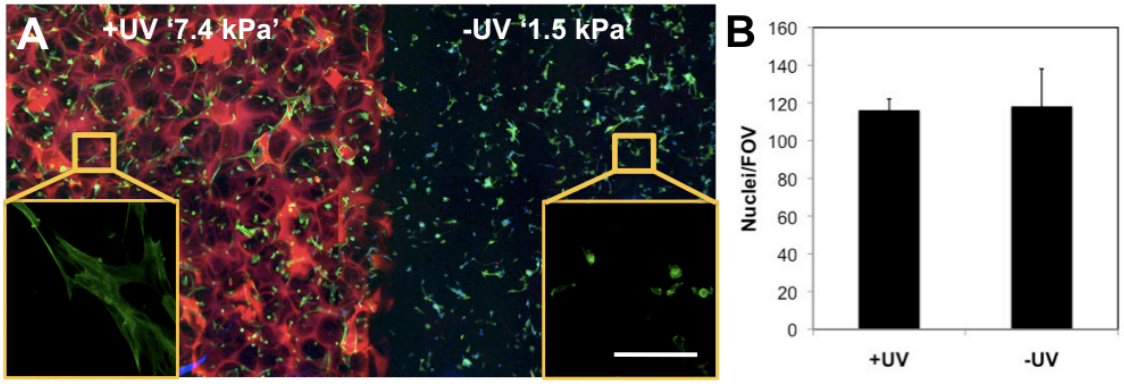


**Figure 8.9** Short term hMSC response to patterned mechanics in macroporous hydrogels. Compiled confocal stacks showing distinct soft (-UV '1.5 kPa') and stiff (+UV '7.4 kPa') regions within the same hydrogel. MeRho (red) indicates region of UV exposure. Insets show representative cytoskeletal organization of cells (actin, green) in each mechanically distinct region. Scale bars = 500 μm (low magnification) and 200 μm (high magnification) Local cell density quantified by staining for cell nuclei (DAPI, blue) in each region (n=4).

*8.3.6 hMSC Responses to Dynamic Mechanics*

In addition to providing a means to alter static mechanical properties in constructs, the sequential crosslinking technique can also temporally alter mechanical properties when the UV light exposure occurs at a later time point once cells are seeded. In this example, this leads to a step-wise increase in mechanical properties. **Figure 8.10A** demonstrates the ability of this hydrogel system to "stiffen" by exposing an initially soft 2.6 kPa hydrogel ('static') to an additional 80 s of UV (120 s total UV exposure, 'dynamic') in order to significantly increase the modulus to 12.4 kPa. The

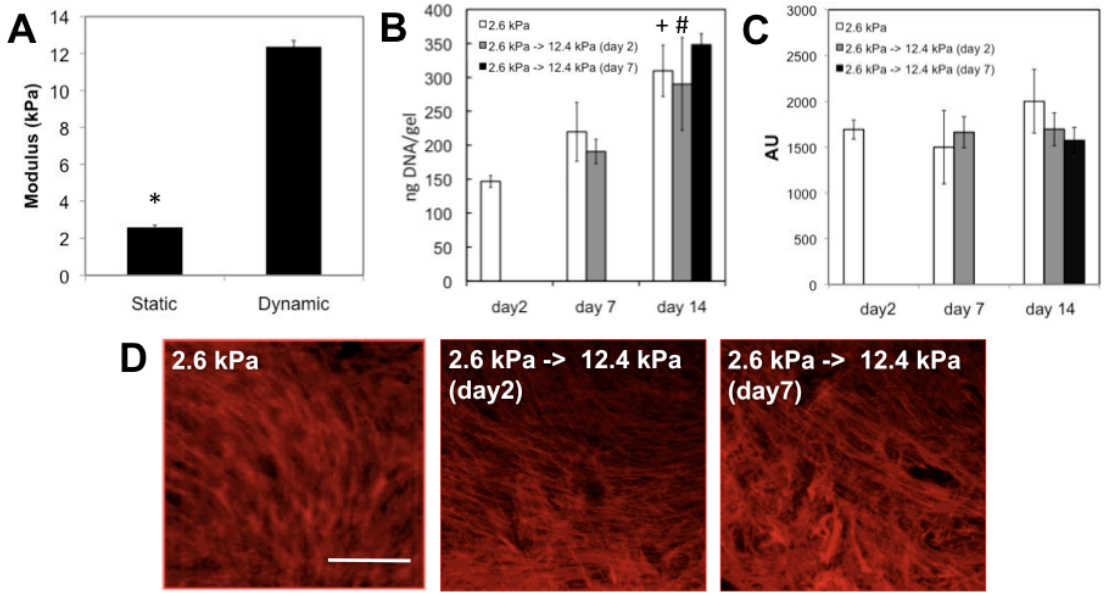


**Figure 8.10** (A) Dynamic mechanics as measured by DMA. Significant differences between stiffened (12.4 kPa) and unstiffened (2.6 kPa) conditions * $p < 0.001$ (B) Cellular DNA content over time in dynamic hydrogels. Significant differences in 2.6 kPa hydrogels from day 2 to day 14 (+$p < 0.01$) and in 12.4 kPa-day 2 stiffened hydrogels from day 7 to day 14 (#$p < 0.05$). (C) Alamar Blue assay shows no difference in cell metabolic activity after stiffening at either time point (D) Cell morphology in dynamic hydrogels (actin, red) at day 14. Scale bar = 400 μm.

intermediate modulus group of 2.6 kPa was chosen as the group to be stiffened as it represented the threshold mechanics above which cell morphology and proliferation did not show significant differences (see **Figure 8.6**). While the stiffened condition of 12.4 kPa did not match the static condition with the highest modulus (7.4 kPa), the ability to dramatically increases the hydrogel mechanics still allowed for insight into the effects of dynamic mechanics on stem cell behavior in 3D. hMSC photoencapsulation under similar crosslinking conditions has been well established and shown not to diminish cell viability,[19, 24, 25] and recent work performed in a similar 2D stiffened system has demonstrated minimal effect of delayed UV exposure on cell viability.[26]

There were no significant differences in cell proliferation and morphology (**Figure 8.10B, D)**, which agreed well with previous results for static hydrogels (**Figure 8.6**) above the 2.6 kPa threshold. Like the static conditions, cell DNA content increased roughly twofold by day 14 for unstiffened and stiffened conditions and cells spread and became confluent throughout the porous hydrogels. There also were no observed differences in metabolic activity as shown in **Figure 8.10C** indicating that hydrogel stiffening and delayed exposure to UV did not significantly impact cell viability at either stiffening time points. Our previous work indicates that the exposure of the cells to this intensity and duration of UV light and the photoinitiator does not have detrimental effects on cell viability.[26] Furthermore, there were no significant differences in cell differentiation for either of the stiffening conditions (day 2 or day 7) compared to unstiffened 2.6 kPa condition (**Figure 8.11**), which also agreed with the static mechanics results above this threshold mechanics (**Figure 8.7**).

While the morphology, proliferation, and differentiation responses to dynamic

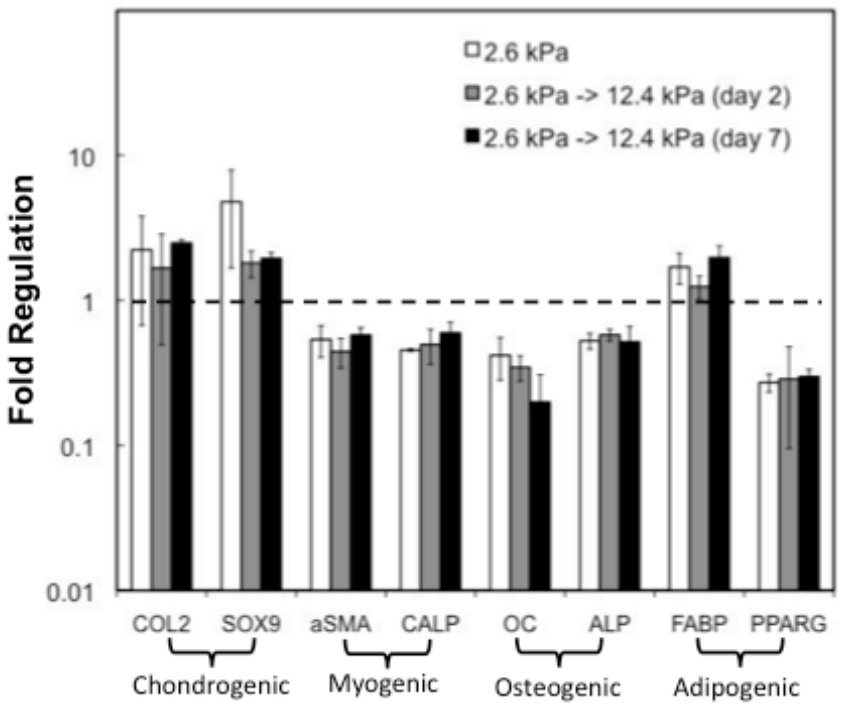


**Figure 8.11** Day 14 hMSC gene expression with values above dotted line indicative of upregulation relative to d0 hMSCs

mechanics do not reveal a significant stem cell response to dynamic mechanics (due to the range selected), the secretory profiles demonstrate otherwise. As shown in **Figure 8.12**, there were overall decreases in stem cell angiogenic and cytokine factor expresson for all stiffening conditions on both day 7 and day 14. On day 7, the hydrogels stiffened on day 2 had recuded expression of 12 proteins: Angiogenin, CXCL16, EG-VEGF, IGFBP-1 and -2, MCP-1, Pentraxin 3, CXCL4, PlGF, IL-8, MIF, and uPA. On day 14, there was an even greater difference in factor secretion between unstiffened 2.6 kPa hydrogels and day 2 stiffened 12.4 kPa hydrogels. Nearly every protein with diminished expression on day 7 (with the exception of uPA and CXCL4) also exhibited lower expression at day 14 along with Ang-1, Endothelin-1, MMP-9, Serpin F1, and

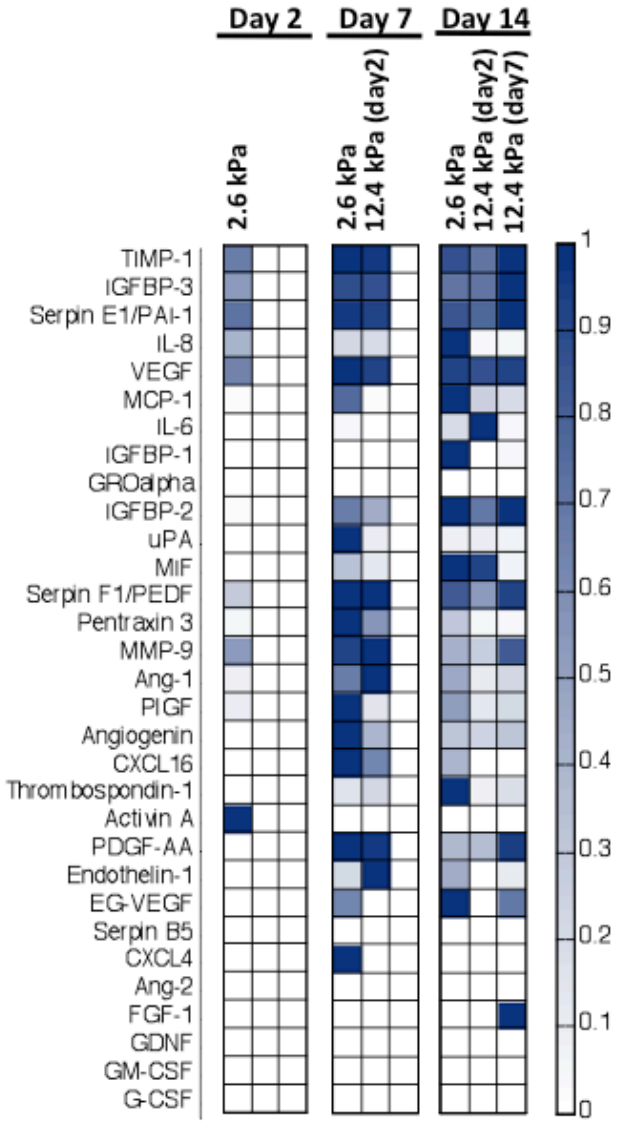


**Figure 8.12** Secretory profiles of static and dynamic cultures plotted with maximally expressed proteins at the top and minimally expressed proteins at the bottom. Values are normalized to maximum expression of unstiffened 2.6 kPa hydrogels and stiffened hydrogels (day 2 and day 7) only. Normalized colorimetric scale bar displayed on the right.

Thrombospondin-1. The secretory profile for hMSCs in day 7 stiffened 12.4 kPa hydrogels also showed diminished expression at day 14, but not quite as different as in

the day 2 stiffened 12.4 kPa condition. At day 14, only 10 factors showed decereased expression for the day 7 stiffened groups when compared to day 2 stiffened hydrogels, which had 15 factors with reduced expression. This provides evidence for dynamic stem cell responses as cells that were exposed to the stiffer 12.4 kPa microenvironment for longer times showed a greater reduction in angiogenic and cytokine factor expression.

The results of this dynamic culture implicate mechanics as a profound effector of stem cell angiogenic and cytokine factor secretion. Although there were no significant differences in stem cell morphology, proliferation, and differentiation that resulted from hydrogel stiffening, the differences in secretor profiles can be attributed to dynamic mechanics. This also provides evidence that hMSCs were responsive to hydrogel mechanics after day 7 even though there is a possibility of ECM during the culture period, which could contribute to a change in local mechanics and stem cell behavior. Further studies are necessary to determine how hMSCs dynamically sense changes in mechanics and how this mechanosensing signal results in changes in secretion of specific factors *in vitro* and *in vivo*.

## 8.4 Conclusions

A range of hydrogel mechanics (1.5-12.4 kPa), as well as heterogeneous and dynamic mechanics, were investigated in this chapter and shown to influence hMSC behavior in 3D macroporous hydrogels. Cell proliferation and morphology in porous hydrogels were mechanosensitive, as cells cultured in hydrogels with modulus >1.5 kPa exhibited greater initial spreading and proliferation over two weeks. Differentiation was also shown to be mechanically-dependent as the expression of several genes differed

between the 1.5 kPa hydrogels and all other mechanics groups. Evidence for hMSC secretory profile dependence on mechanics was apparent, as distinct temporal secretion profiles were evident for softer (1.5 and 2.6 kPa) and stiffer (3.8 and 7.4 kPa) hydrogels. hMSC secretion was also temporally modulated by stiffening 2.6 kPa hydrogels at two different time points and found to decrease more drastically when stiffened at an earlier time poit (day 2). The results of this chapter futher emphasize the importance of the initial mechanics (magnitude, context, timing) on stem cell behavior *in vitro* and how mechanics should be incorporated as a design variable for biomaterials and considered when elucidating stem cell responses *in vivo*.

**REFERENCES:**


1. N. Huebsch, P. R. Arany, A. S. Mao, D. Shvartsman, O. A. Ali, S. A. Bencherif, J. Rivera-Feliciano and D. J. Mooney. Harnessing traction-mediated manipulation of the cell/matrix interface to control stem-cell fate, *Nature materials*, 2010, **9**, 1-9.
2. R. A. Marklein and J. A. Burdick. Controlling Stem Cell Fate with Material Design, *Adv Mater*, 2010, **22**, 175-189.
3. B. M. Gillette, J. A. Jensen, M. Wang, J. Tchao and S. K. Sia. Dynamic hydrogels: switching of 3D microenvironments using two-component naturally derived extracellular matrices, *Advanced materials (Deerfield Beach, Fla)*, 2010, **22**, 686-691.
4. F. X. Jiang, B. Yurke, R. S. Schloss, B. L. Firestein and N. A. Langrana. The relationship between fibroblast growth and the dynamic stiffnesses of a DNA crosslinked hydrogel, *Biomaterials*, 2010, **31**, 1199-1212.
5. A. M. Kloxin, J. A. Benton and K. S. Anseth. In situ elasticity modulation with dynamic substrates to direct cell phenotype, *Biomaterials*, 2010, **31**, 1-8.
6. R. A. Marklein and J. A. Burdick. Spatially controlled hydrogel mechanics to modulate stem cell interactions, *Soft Matter*, 2010, **6**, 136-143.
7. M. F. Berry, A. J. Engler, Y. J. Woo, T. J. Pirolli, L. T. Bish, V. Jayasankar, K. J. Morine, T. J. Gardner, D. E. Discher and H. L. Sweeney. Mesenchymal stem cell injection after myocardial infarction improves myocardial compliance, *Am J Physiol Heart Circ Physiol*, 2006, **290**, H2196-2203.

8. C. Y. Y. Yip and C. A. Simmons. The aortic valve microenvironment and its role in calcific aortic valve disease, *Cardiovascular pathology : the official journal of the Society for Cardiovascular Pathology*, 2011, **20**, 177-182.

9. P. Patwari and R. T. Lee. Mechanical control of tissue morphogenesis, *Circ Res*, 2008, **103**, 234-243.

10. A. M. Kloxin, A. M. Kasko, C. N. Salinas and K. S. Anseth. Photodegradable hydrogels for dynamic tuning of physical and chemical properties, *Science*, 2009, **324**, 59-63.

11. S. R. Peyton, Z. I. Kalcioglu, J. C. Cohen, A. P. Runkle, K. J. Van Vliet, D. A. Lauffenburger and L. G. Griffith. Marrow-derived stem cell motility in 3D synthetic scaffold is governed by geometry along with adhesivity and stiffness, *Biotechnol. Bioeng.*, 2011, **108**, 1181-1193.

12. L. J. Gibson and M. F. Ashby, *Cellular Solids: Structure and Properties*, Cambridge University Press, 1999.

13. D. E. Discher, D. J. Mooney and P. W. Zandstra. Growth Factors, Matrices, and Forces Combine and Control Stem Cells, *Science*, 2009, **324**, 1673-1677.

14. A. S. Rowlands, P. A. George and J. J. Cooper-White. Directing osteogenic and myogenic differentiation of MSCs: interplay of stiffness and adhesive ligand presentation, *AJP: Cell Physiology*, 2008, **295**, C1037-C1044.

15. H. Majd, P.-J. Wipff, L. Buscemi, M. Bueno, D. Vonwil, T. M. Quinn and B. Hinz. A novel method of dynamic culture surface expansion improves mesenchymal stem cell proliferation and phenotype, *Stem Cells*, 2009, **27**, 200-209.

16. A. J. Engler, S. Sen, H. L. Sweeney and D. E. Discher. Matrix elasticity directs stem cell lineage specification, *Cell*, 2006, **126**, 677-689.

17. D.-C. Chen, Y.-L. Lai, S.-Y. Lee, S.-L. Hung and H.-L. Chen. Osteoblastic response to collagen scaffolds varied in freezing temperature and glutaraldehyde crosslinking, *J. Biomed. Mater. Res.*, 2006, **80A**, 399-409.

18. M. B. Keogh, F. J. O'brien and J. S. Daly. Substrate stiffness and contractile behaviour modulate the functional maturation of osteoblasts on a collagenâ€"GAG scaffold, *Acta Biomaterialia*, 2010, **6**, 4305-4313.

19. C. Chung and J. A. Burdick. Influence of three-dimensional hyaluronic Acid microenvironments on mesenchymal stem cell chondrogenesis, *Tissue Engineering Part A*, 2009, **15**, 243-254.

20. J. S. Park, J. S. Chu, A. D. Tsou, R. Diop, Z. Tang, A. Wang and S. Li. The effect of matrix stiffness on the differentiation of mesenchymal stem cells in response to TGF-β, *Biomaterials*, 2011, **32**, 3921-3930.

21. F. P. Seib, M. Prewitz, C. Werner and M. Bornhaeuser. Matrix elasticity regulates the secretory profile of human bone marrow-derived multipotent mesenchymal stromal cells (MSCs), *Biochem Biophys Res Commun*, 2009, **389**, 663-667.

22. J. C. George. Stem cell therapy in acute myocardial infarction: a review of clinical trials, *Transl Res*, 2010, **155**, 10-19.

23. N. K. Satija, V. K. Singh, Y. K. Verma, P. Gupta, S. Sharma, F. Afrin, M. Sharma, P. Sharma, R. P. Tripathi and G. U. Gurudutta. Mesenchymal stem cell-based therapy: a new paradigm in regenerative medicine, *J Cell Mol Med*, 2009, **13**, 4385-4402.

24. J. A. Burdick and K. S. Anseth. Photoencapsulation of osteoblasts in injectable RGD-modified PEG hydrogels for bone tissue engineering, *Biomaterials*, 2002, **23**, 4315-4323.

25. S. Khetan and J. A. Burdick. Patterning network structure to spatially control cellular remodeling and stem cell fate within 3-dimensional hydrogels, *Biomaterials*, 2010, **31**, 8228-8234.

26. M. Guvendiren and J. A. Burdick. Stiffening hydrogels to probe short- and long-term cellular responses to dynamic mechanics, *Nat Commun*, 2012, **3**, 792.

# CHAPTER 9

*Summary, Limitations, and Future Directions*

## 9.1 Summary

As the field of tissue engineering continues to make progress towards the development of sophisticated regenerative medicine therapies, further insight into how stem cells interact with and respond to complex biomaterial signals is essential. The ability of biomaterials to elicit stem cell responses has been the focus of significant research and, more recently, the inherent mechanical properties of biomaterials have been highlighted as a major effector of numerous stem cell behaviors such as morphology, proliferation, differentiation, and secretion of factors. With this in mind, the goal of this dissertation was to design a mechanically-tunable hydrogel system with the ability to control the presentation of mechanical signals in terms of magnitude, spatial and temporal profiles, as well as context (2D vs. 3D). The implications of this work extend not only to further understanding fundamental stem cell biology, but also to reinforce the incorporation of matrix mechanics as an important design variable for future tissue engineering strategies.

In order to accomplish this goal, a sequentially crosslinked hydrogel system based on the naturally-derived polymer hyaluronic acid (HA) was developed (Chapter 4). After demonstrating initial mechanosensitive human mesenchymal stem cell behavior on uniform, synthetic poly(ethylene glycol) diacrylate hydrogels, two sequential crosslinking systems were investigated for their potential to present controlled mechanical signals to

hMSCs in terms of spatial and temporal mechanical properties. The first system involved the formation of an interpenetrating network of calcium-crosslinked alginate and radically polymerized PEGDA. While this system demonstrated a wide range in mechanics (from ~2-85 kPa), as well as the ability to spatially control mechanics, the inability of this hydrogel to adequately support uniform cell attachment and survival necessitated development of an alternate mechanically-tunable system. Chemically modifying HA with a reactive methacrylate functionality (i.e., methacrylated HA, MeHA) allowed formation of hydrogels *via* two distinct mechanisms: 1) Michael Addition ('Addition') using a dithiol crosslinker, and 2) Radical polymerization ('Radical') using UV light in the presence of a photoinitiator. Using this system, MeHA could be initially 'Addition' crosslinked by consuming a fraction of the methacrylates followed by secondary 'Radical' crosslinking in order to further consume unreacted methacrylates. Utilization of UV light in the secondary crosslinking process afforded spatial and temporal control of crosslinking density, and thus hydrogel modulus. This system confirmed our Specific Aim 1 hypothesis as it demonstrated a wide range in elastic moduli (~3-100 kPa), spatial and temporal control of mechanics, and adequately supported cell attachment and survival.

Chapter 5 first demonstrated the ability of sequentially crosslinked MeHA hydrogels to control hMSC behavior on 2D thin films with uniform, as well as spatially and temporally modulated mechanics in standard growth medium. As expected, hMSCs exhibited a general trend of increased spreading with increasing mechanics, as well as proliferated at a significantly higher rate on stiffer hydrogels (~100 kPa) compared to softer hydrogels (~3 kPa). These trends observed on uniform hydrogels were conserved

in hydrogels with spatially controlled mechanics as the local mechanics were shown to direct the local cell behavior. Specifically, on hydrogels with photopatterned stripes of soft and stiff regions, hMSCs remained rounded on the softer (-UV) stripes while cells on the stiffer (+UV) stripes became highly spread. Likewise, on hydrogels with a gradient in mechanics, the local cell morphology was shown to steadily increase along the length of the gradient in accordance with the increase in local mechanics (from ~6-90 kPa). Finally, hMSCs were shown to respond to dynamic mechanics as stiffening the hydrogel from ~5 to 33 kPa resulted in hMSCs (which were initially rounded) adopting a more spread morphology characteristic of cells cultured on static hydrogels of the same mechanics (~33 kPa).

In Chapter 6, the effects of spatially controlled mechanics on hMSC differentiation were determined in a well-established adipogenic-osteogenic inductive medium system. Stem cell differentiation was found to be dependent on hydrogel mechanics as adipogenesis and osteogenesis were promoted on softer (~2 kPa) and stiffer (~30 kPa) hydrogels, respectively. The effects of spatially controlled mechanics on hMSC differentiation in this bipotential inductive system were also investigated for both photopatterned stripes and a gradient in mechanics. Similar to Chapter 5, the differentiation of hMSCs was shown to depend on the local mechanics as cells on the softer stripes (~2 kPa) favored adipogenesis, while cells on the stiffer stripes (~30 kPa) favored osteogenesis. This trend was also demonstrated in a gradient manner, as the ratio of osteogenesis:adipogenesis increased with increasing mechanics along the gradient. The results shown in Chapters 5 and 6 thus confirm the hypothesis outlined in Specific

Aim 2: stem cell behavior is dependent on the local hydrogel mechanics in uniform, patterned, and gradient hydrogels.

Chapter 7 presents a departure from the 2D hydrogel systems in Chapter 5 and 6 and introduces controlled mechanics in a non-porous system using MeHA. Varying the ratio of low- and high-modified MeHA polymers resulted in a range of mechanics (~4-25 kPa). hMSC morphology was highly dependent on the crosslinking density as only cells in the softest ~4.2 kPa hydrogels could adopt a spread morphology, while cells in more densely crosslinked hydrogels were restricted to a rounded morphology. Expression of differentiation markers was also dependent on mechanics as there was greater upregulation of genes associated with a 'rounded' lineage (chondrogenic and adipogenic) in hydrogels above the softest group as the cells maintained a rounded morphology throughout the culture period. Similarly, the threshold response was observed in terms of secretion as hMSCs in ~4.2 kPa hydrogels showed maximal expression of angiogenic and cytokine factors at day 7 and 14. While this system did not afford the ability to spatially and temporally control mechanics (due to radical-only crosslinking), it highlights the importance of contextual presentation of mechanics (3D non-porous) on hMSC responses.

In Chapter 8, the sequential crosslinking system was translated into a 3D macroporous system in order to investigate the effects of spatially and temporally controlled mechanics on hMSCs in a 3D porous context. Porous hydrogels with spatially and temporally controlled mechanics were successfully created by performing the addition crosslinking around a degradable PMMA microsphere template and controlling the location and timing of UV exposure. Using this system, we successfully showed that

hMSC morphology, proliferation, and differentiation exhibit mechanically-dependent responses. Above ~1.5 kPa kPa, hMSCs adopted a highly spread morphology, significantly increased in cell number over the culture period and possessed distinct differentiation marker signatures when compared to the hMSCs in the 1.5 kPa condition. Secretion of factors was also shown to be mechanosensitive as higher secretion levels were apparent for stiffer hydrogels (~3.8 and 7.4 kPa) at an early time point (day 2) while by day 14, greater secretion was observed in the softer hydrogels (~1.5 and 2.6 kPa). Furthermore, upon stiffening of hydrogels from ~2.6 to 12.4 kPa at two time points (day 2 and day 7), noticeable decreases in secretion were observed at both day 7 and day 14. The timing of stiffening was found to be important as there was a greater reduction in secretion at day 14 for hydrogels that were stiffened at an earlier time point (day 2) as compared to those hydrogels stiffened at a later time point (day 7). Notably, these results were found to be independent of other cell responses as cell morphology, proliferation, and differentiation marker expression were similar for all static (unstiffened) and dynamic (stiffened) conditions. The work outlined in Chapters 7 and 8 therefore demonstrate the importance of context (non-porous vs. porous) and spatial and temporal presentation of mechanics in 3D on hMSC behavior.

## 9.2 Limitations and Future Directions

### *9.2.1 Overall limitations*

The majority of this work presents mechanically-controlled environments that do not fully mimic native tissue microenvironments in terms of their network structure (mesh size), degradability, and fibrous architecture. While attempts were made to

translate the 2D sequentially crosslinked system into a more biologically relevant 3D context, the non-porous and porous hydrogel systems do not fully recapitulate the complexities in native tissue. Furthermore, the cell adhesive ligand used in this system (RGD) is a simplified analog for entire proteins, such as fibronectin and vitronectin, which may not elicit the appropriate response due to the lack of synergy-binding sequences, as well as the geometric orientation of the binding site.[1, 2] Therefore, further investigation into stem cell mechanosensing in more biologically relevant contexts that incorporate fibrous architecture and more complex chemical signals are necessary to better understand the effect of mechanics on stem cell behavior. Finally, the use of purely elastic materials (such as the hydrogels used in these studies) to mimic native tissue moduli has limitations as native tissues possess viscoelastic properties such as strain stiffening.[3, 4]

### *9.2.2 Specific Aim 1: Develop sequentially crosslinked hydrogel systems with both spatially and temporally controlled mechanics.*

#### *9.2.2.1 Limitations*

In order to modulate mechanics, crosslinking density was varied by adjusting the amount and type of 'addition' and 'radical' crosslinking. However, as the MeHA hydrogels exhibited pronounced differences in swelling, there is a possibility that differences in local hydrogel structure such as ligand and HA density could contribute to the observed stem cell responses. Differences in crosslinking affect mesh size and could result in differences in ligand accessibility for different mechanics. RGD ligand density

was varied in Chapter 5 in order to determine if the increased swelling in softer hydrogels affected stem cell spreading due to a possible 'dilution' of the RGD ligand as compared to the less swelled stiffer hydrogels. Variations in RGD density were found to not affect stem cell morphology even when increased to five times the amount used throughout the studies. The effect of different modification efficiencies (% methacrylation) and macromer concentration (% HA) should also be considered in the future as small functional groups can affect cell behavior[5], as well as HA itself, which is involved in natural processes.[6, 7]

*9.2.2.2 Future Work*

In order to better understand the sequential crosslinking system, a more thorough characterization of parameters involved in the synthesis and crosslinking steps is necessary. Specifically, a high modification MeHA (~100% methacrylated) was used for all studies and other lower modification macromers could be investigated to determine if the addition of a methacrylate to the HA backbone results in a biological response or alters the recognition of HA functionality. Quantification of the methacrylate consumption in 'addition' and 'radical' crosslinking steps would also provide further insight into the crosslinking kinetics and extent of reaction. Due to the functional versatility of the methacrylate, the MeHA hydrogel system could be modified to include different monothiolated functional groups, as well as dithiol crosslinkers with altered degradability (hydrolytic or MMP-sensitive) and/or biological responses.

*9.2.3 Specific Aim 2: Spatially and temporally control human mesenchymal stem cell (hMSC) behavior on sequentially crosslinked hyaluronic acid hydrogels.*

*9.2.3.1 Limitations*

A notable limitation associated with this hydrogel system is the effect of differential swelling in patterned hydrogels. Specifically, at the interface of soft and stiff regions there was an observed height difference as the increased swelling in the soft regions resulted in microscale topographical features. However, at early and later timepoints cells were found at positions along this interface indicating that this surface-induced topography did not serve as an effective 'barrier' to cell migration. For gradient hydrogels, this was less of a concern as the differences in swelling occurred over a greater length scale and thus no topographical features were observed.

*9.2.3.2 Future Work*

Further insight into stem cell mechanosensing could be gained by monitoring cell migration in response to spatially controlled mechanics in both static and dynamic settings. For example, cells seeded on a uniformly soft substrate could be dynamically exposed to a gradient in mechanics at different time points in order to evaluate cell plasticity and motility after temporally-controlled exposure to mechanical signals. These temporal responses to mechanical gradients could prove useful for investigating stem cell homing to pathologically stiff tissues such as cardiac scar tissue and tumors.[9, 10]

Determining the machinery involved in the mechanosensing response would also be useful for understanding how hMSCs respond to spatial and temporal mechanics. Inhibition of factors associated with mechanosensing (such as NMMII and ROCK) could elucidate the importance of tension-mediated matrix sensing in these complex

environments. Furthermore, local 'stiffening' of the hydrogel *in situ* (using multiphoton microscopy) could allow for microscale investigation of focal adhesion formation as well as the temporal evolution of specific cell adhesion complexes in response to dynamic mechanics.

### *9.2.4 Specific Aim 3: Investigate hMSC response to 3D presentation of mechanical signals in hyaluronic acid hydrogels.*

#### *9.2.4.1 Limitations*

As mentioned above, the most significant limitation of this aim is the inability to fully recapitulate the native architecture of complex 3D tissues. The non-porous system, while relatively simple to vary the mechanics, results in somewhat confounding variables in terms of presentation of mechanical signals and cell morphology restrictions. In this 3D contextual presentation, the importance of cell morphology appears to hold precedence over the magnitude of mechanical signals as the threshold response in morphology, differentiation, and secretion could be directly correlated with the ability of a cell to spread within the hydrogel. While matrix degradability could be incorporated into this scheme, this would result in changes in mechanics and it would therefore be difficult to determine whether the observed effects were a result of the matrix mechanics or due to differences in traction generation and cell spreading caused by local degradation of the matrix.

For the porous system, while the presentation of mechanical signals did not result in restricted morphologies (governed by the crosslinking density), the porous architecture

resulted in an effective 3D presentation of a 2D surface. Furthermore, as cells began to exert tension and proliferate to fill the pores, differences in cell-cell and cell-scaffold contact were apparent. Mechanical signals in this porous context therefore appear to direct an initial response in hMSCs that then result in differential cell-cell and cell-scaffold interactions that then contribute to the long-term responses such as differentiation and secretion of factors. However, it should be noted that even after 7 days, when cells had proliferated and significantly increased cell-cell contact, that there was an observed response to matrix stiffening (in terms of factor secretion), which indicates that cells were still able to effectively sense and respond to the dynamic mechanics of the porous scaffold.

*9.2.4.2 Future work*

Further investigations into 3D presentation of mechanical signals is necessary in order to understand the relative importance of matrix mechanics and cell interactions affected by these different hydrogel systems. Although a diversion from the mechanics theme of this dissertation, using the non-porous MeHA system in Chapter 7 to investigate the effects of 3D restriction of cell morphology could be useful for understanding cell fate decisions. In systems that utilize bipotential induction media, this could be particularly interesting as both adipogenic-osteogenic[8] and chondrogenic-myogenic[11] conditions exist that involve cell types with distinct rounded (adipogenic and chondrogenic) and spread (osteogenic and myogenic) morphologies. Sophisticated methods to characterize traction force generation in 3D[12] could be used in these studies to

further understand how hMSCs effectively 'probe' their surroundings and respond to distinct mechanical signals.

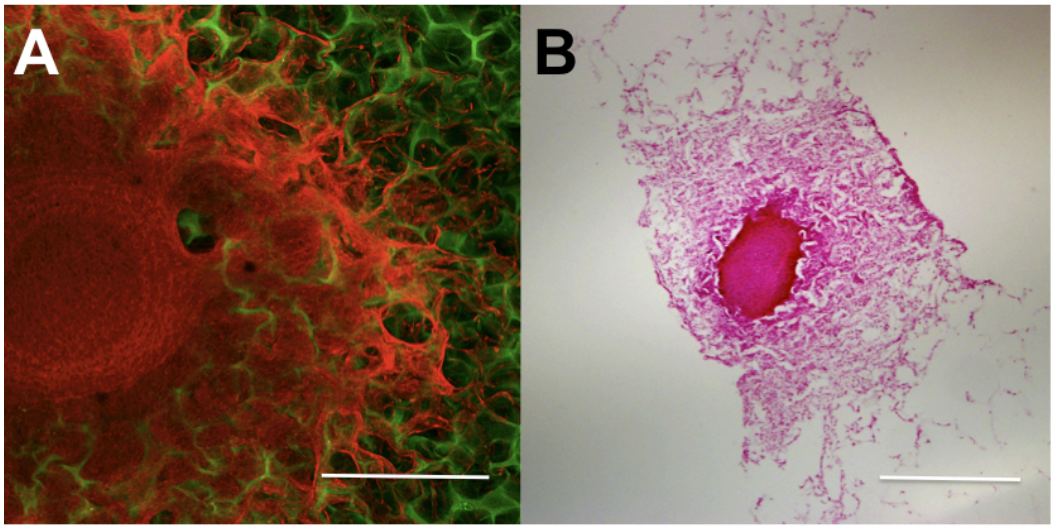


**Figure 9.1** Aortic Arch day 7 infiltration into macroporous MeHA hydrogel. A) Confocal z-stack showing radial outgrowth of arch (phalloidin, red) seeded atop macroporous hydrogel (FITC, green). Scale bar = 1 mm (B) Hematoxylin and Eosin staining of aortic arch outgrowth into macroporous hydrogel (top surface of hydrogel is to the left). Scale bar = 1 mm

The porous hydrogel system could be further investigated in terms of temporal presentation of local changes in mechanics in order to monitor potential migratory behavior of stem cells. It could also be utilized as a model tissue infiltration assay as cell aggregates (such as embryoid or mesenchymal spheroids) or small tissue equivalents (such as aortic arches) could be seeded atop the porous hydrogel and the effects of distinct spatial and temporal mechanical signals on infiltration could be determined. **Figure 9.1** shows initial evidence that macroporous hydrogels promote a high degree of infiltration both across the surface and throughout the porous architecture. Finally, due to

the high porosity and incorporation of HA, this porous hydrogel could be investigated as a tissue engineering strategy in order to serve as a cell-delivery vehicle or to promote *in vivo* repair and recruitment of regenerating tissue.

### 9.3 Conclusions and Innovation

In summary, this work introduces a unique method for controlling the presentation of mechanical signals to adult stem cells in a uniform, as well as spatial and temporal manner. Due to the synthetic versatility of HA and the ability to modify the crosslinking parameters associated with the sequential crosslinking process, thorough characterization of stem cell responses to complex mechanical environments was possible. Specifically, stem cell morphology and differentiation are dependent on local mechanics on both 2-D films and when interacting with the surfaces of pores in 3-D macroporous substrates. This work also highlights the importance of the contextual presentation of mechanical signals to cells as distinct morphology, proliferation, differentiation, and secretion profiles were observed in 2-D and 3-D non-porous and porous systems using the same base hyaluronic acid-based material.

The major innovations of this work stem from the ability of the sequentially crosslinked system to present mechanics in a variety of contexts (2D and 3D porous/non-porous), as well as in distinct spatial and temporal presentations. In 2D, local mechanics were shown to directly control hMSC morphology, proliferation, and differentiation in uniform, patterned, and gradient systems. Furthermore, multi-lineage commitment (adipogenesis and osteogenesis) from a single cell population was achieved by spatially controlling mechanics in a single hydrogel in order to create distinct differentiation

patterns. Finally, the presentation of mechanics in 3D using porous and non-porous hydrogel systems emphasized the importance of the context, location, and timing of mechanical signals perceived by hMSCs. In non-porous hydrogels, hMSC morphology, proliferation, differentiation, and secretion were dictated by the mechanics and the ability of cells to spread within the 3D network. In porous hydrogels, the mechanical signals directed cell-cell and cell-scaffold interactions, which resulted in threshold morphology, proliferation, and differentiation responses. Secretion of angiogenic and cytokine factors was significantly affected by hydrogel mechanics in uniform hydrogels with distinct temporal secretion profiles observed for soft and stiff hydrogels. Furthermore, in porous hydrogels with dynamic mechanics, hMSCs were shown to be sensitive to changes in mechanics by altering their secretory profile while maintaining similar morphology, proliferation, and differentiation expression responses.

The implications of this research extend not only to the field of tissue engineering, but also mechanobiology in the context of native tissue development and pathologies with distinct mechanical profiles. In order to design biomaterials that elicit desired stem cell responses, the properties of the microenvironment must be optimized to facilitate proper tissue integration and regeneration, and the findings of this dissertation implicate mechanics as a critical determinant of stem cell behavior. Therefore, future tissue regeneration therapies should consider mechanics as a design variable particularly in terms of the magnitude, context, and spatiotemporal presentation of the mechanical signals. Sequentially crosslinked hydrogels with spatial and temporally controlled mechanics also provides a model system for investigating cell responses to microenvironments that mimic the complex mechanical properties present during

embryonic development, as well as with pathological conditions such as tumor progression and myocardial infarction. This biomimetic system represents a novel *in vitro* system that could vastly improve our understanding of tissue maturation as well as the progression of diseases with complex mechanical microenvironments.

**REFERENCES:**


1. M. Kato and M. Mrksich. Using model substrates to study the dependence of focal adhesion formation on the affinity of integrin-ligand complexes, *Biochemistry*, 2004, **43**, 2699-2707.
2. M. M. Martino, M. Mochizuki, D. A. Rothenfluh, S. A. Rempel, J. A. Hubbell and T. H. Barker. Controlling integrin specificity and stem cell differentiation in 2D and 3D environments through regulation of fibronectin domain stability, *Biomaterials*, 2009, **30**, 1089-1097.
3. P. A. Janmey, J. P. Winer and J. W. Weisel. Fibrin gels and their clinical and bioengineering applications, *Journal of the Royal Society, Interface / the Royal Society*, 2009, **6**, 1-10.
4. C. Storm, J. J. Pastore, F. C. MacKintosh, T. C. Lubensky and P. A. Janmey. Nonlinear elasticity in biological gels, *Nature*, 2005, **435**, 191-194.
5. D. S. W. Benoit, M. P. Schwartz, A. R. Durney and K. S. Anseth. Small functional groups for controlled differentiation of hydrogel-encapsulated human mesenchymal stem cells, *Nature materials*, 2008, **7**, 816-823.
6. C. Chung and J. A. Burdick. Influence of three-dimensional hyaluronic Acid microenvironments on mesenchymal stem cell chondrogenesis, *Tissue Engineering Part A*, 2009, **15**, 243-254.
7. I. Erickson, A. Huang, C. Chung, R. Li, J. Burdick and R. Mauck. Differential Maturation and Structure-Function Relationships in MSC- and Chondrocyte-Seeded Hydrogels, *Tissue Engineering Part A*, 2009.

8. R. McBeath, D. M. Pirone, C. M. Nelson, K. Bhadriraju and C. S. Chen. Cell shape, cytoskeletal tension, and RhoA regulate stem cell lineage commitment, *Dev Cell*, 2004, **6**, 483-495.

9. M. F. Berry, A. J. Engler, Y. J. Woo, T. J. Pirolli, L. T. Bish, V. Jayasankar, K. J. Morine, T. J. Gardner, D. E. Discher and H. L. Sweeney. Mesenchymal stem cell injection after myocardial infarction improves myocardial compliance, *Am J Physiol Heart Circ Physiol*, 2006, **290**, H2196-2203.

10. K. R. Levental, H. Yu, L. Kass, J. N. Lakins, M. Egeblad, J. T. Erler, S. F. T. Fong, K. Csiszar, A. Giaccia, W. Weninger, M. Yamauchi, D. L. Gasser and V. M. Weaver. Matrix crosslinking forces tumor progression by enhancing integrin signaling, *Cell*, 2009, **139**, 891-906.

11. L. Gao, R. McBeath and C. S. Chen. Stem cell shape regulates a chondrogenic versus myogenic fate through Rac1 and N-cadherin, *Stem Cells*, 2010, **28**, 564-572.

12. W. R. Legant, J. S. Miller, B. L. Blakely, D. M. Cohen, G. M. Genin and C. S. Chen. Measurement of mechanical tractions exerted by cells in three-dimensional matrices, *Nat Methods*, 2010, **7**, 969-971.